UNIVERSITAT DE BARCELONA

A multiplexed diagnostic approach for cardiovascular disease biomarkers

Glòria Colom Sanmartí

Glòria Colom Sanmartí

Tesi Doctoral

2015

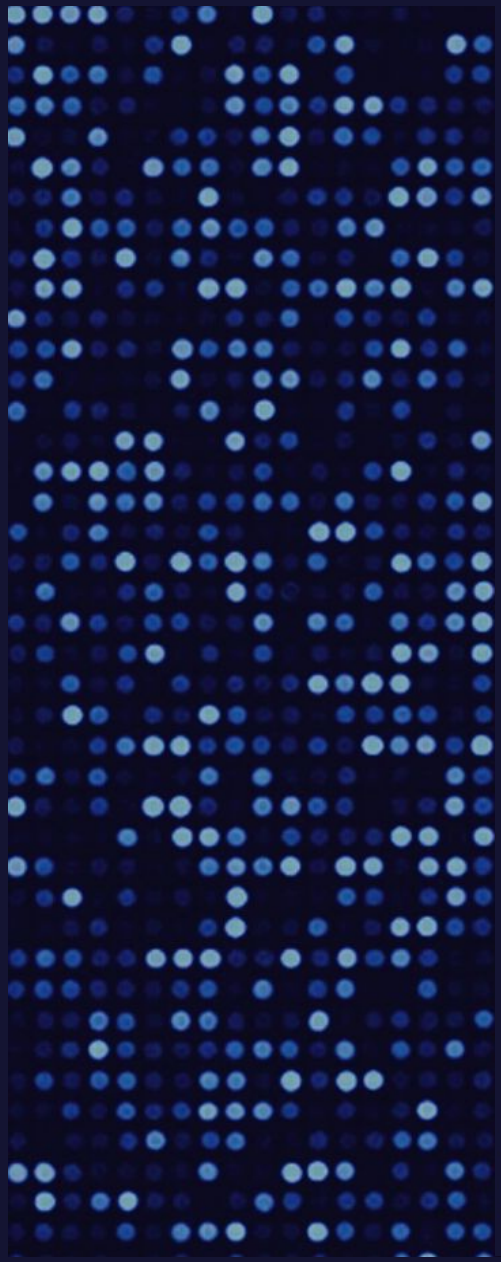

A MULTIPLEXED IMMUNOCHEMICAL DIAGNOSTIC APPROACH FOR CARDIOVASCULAR DISEASE BIOMARKERS

Glòria Colom Sanmartí

Universitat de Barcelona

CSIC
Consejo Superior de Investigaciones Científicas

Universitat de Barcelona, Facultat de Química, Departament de Química Orgànica

Consejo Superior de Investigaciones Científicas

Institut de Química Avançada de Catalunya

Nanobiotechnology for Diagnostics group

Centro de Investigación Biomédica en Red en Bioingeniería, Biomateriales y Nanomedicina

A MULTIPLEXED IMMUNOCHEMICAL DIAGNOSTIC APPROACH FOR CARDIOVASCULAR DISEASE BIOMARKERS

Memòria per optar al grau de Doctor per la Universitat de Barcelona presentada per:

Glòria Colom Sanmartí

Barcelona, octubre de 2015

Universitat de Barcelona

Facultat de Química – Departament de Química Orgànica
Programa de doctorat de Química Orgànica

A MULTIPLEXED IMMUNOCHEMICAL DIAGNOSTIC APPROACH FOR CARDIOVASCULAR DISEASE BIOMARKERS

Memòria per optar al grau de Doctor per la Universitat de Barcelona
presentada per:

Glòria Colom Sanmartí

Directors:

Prof. Mª Pilar Marco Colás
Professora d'Investigació
Dept. de Nanotecnologia
Química y Biomolecular
Nb4D group, IQAC-CSIC

Dr. J. Pablo Salvador Vico
Investigador associat
Àrea de Nanomedicina

Nb4D group, CIBER-BBN

Tutor:

Prof. Pedro Romea García
Professor titular
Departament de Química Orgànica
Facultat de Química
Universitat de Barcelona

AGRAÏMENTS

- A la Pilar i al Pablo, per donar-me l'oportunitat de poder realitzar la tesi doctoral al grup Nb4D. A l'AGAUR per la beca FI concedida, a l'IQAC i a la UB.

- A tota la resta de membres del grup Nb4D. A la Carme i a l'Àlex, per la seva paciència, ajuda i coneixements transmesos.

- A tot el grup de Florència. Al Francesco i a l'Ambra, per acollir-me i fer-me sentir com a casa.

- Als amics de Cervera i als de la universitat, pel vostre interès, estimació i els bons moments que passem junts.

- Als meus pares, avis i, especialment, a la Berta i al David. Perquè tenir-vos al meu costat és el que em fa sentir plenament feliç.

TABLE OF CONTENTS

1 GENERAL INTRODUCTION

1.1 CARDIOVASCULAR DISEASES

According to World Health Organization (WHO) [1], cardiovascular diseases (CVDs) are a group of disorders of the heart and blood vessels and they include:

- Coronary heart disease: affects the blood vessels supplying the heart muscle
- Cerebrovascular disease: affects the blood vessels supplying the brain
- Peripheral arterial disease: affects the blood vessels supplying the arms and legs
- Rheumatic heart disease: damage to the heart muscle and heart valves from rheumatic fever (caused by streptococcal bacteria)
- Congenital heart disease: caused by malformations of heart structure existing at birth
- Deep vein thrombosis and pulmonary embolism: Blood clots in the leg veins, which can dislodge and move to the heart and lungs.

All of them are caused by atherosclerosis, an accumulation of fatty deposits on the inner walls of the blood vessels, except rheumatic and congenital heart diseases, that in the first case as result of a damage of the heart muscle and heart valves from rheumatic fever, following a streptococcal pharyngitis/tonsillitis, while the second case are malformations of heart structures present at births like holes in the septum of the heart, abnormal valves or abnormalities in heart chambers.

Myocardial infarctions, commonly called heart attacks, and strokes are acute events consequence of a blockage that prevents blood from flowing to the heart or brain respectively. Atherosclerosis is the most common reason for this, although strokes can also be caused by bleeding from a blood vessel in the brain or from blood clots [2].

Factors that promote the process of atherosclerosis are known as risk factors and include behavioral risk factors such as tobacco use, physical inactivity, unhealthy diet rich in salt, fat and/or calories and harmful use of alcohol; and metabolic risk factors consequence of the previous ones [3]. Raised of blood pressure (hypertension), of blood sugar (diabetes), of blood lipids (cholesterol), overweight and obesity are examples of metabolic risk factors. Often, there are

no symptoms regarding CVDs. A heart attack or stroke is most of the times the first warning of such diseases.

CVDs are included within the noncommunicable diseases (NCDs) group, which are non infectious and non transmissible among people by definition and are compared to communicable, maternal, perinatal and nutritional conditions group and injuries group in order to classify all diseases. They remain the biggest cause of deaths worldwide.

In 2012, a total of 56 million deaths occurred in the world; 38 million were due to NCDs, principally cardiovascular diseases (17.5 million, 31% of all global deaths), cancer and chronic respiratory diseases. Of these deaths, 7.4 million people died of coronary heart disease and 6.7 million from stroke. Moreover, nearly three quarters of these NCD deaths (28 million) occurred in low- and middle-income countries.

The leading causes of NCD deaths in 2012 were cardiovascular diseases (17.5 million deaths or 46.2% of NCD deaths); cancers (8.2 million, or 21.7% of NCD deaths); and respiratory diseases, including asthma and chronic obstructive pulmonary disease (COPD), (4.0 million, or 10.7% of NCD deaths). Diabetes caused an additional 1.5 million deaths (4.0% of NCD deaths) (see Figure 1.1). Thus, these four major NCDs were responsible for 82% of NCD deaths [4].

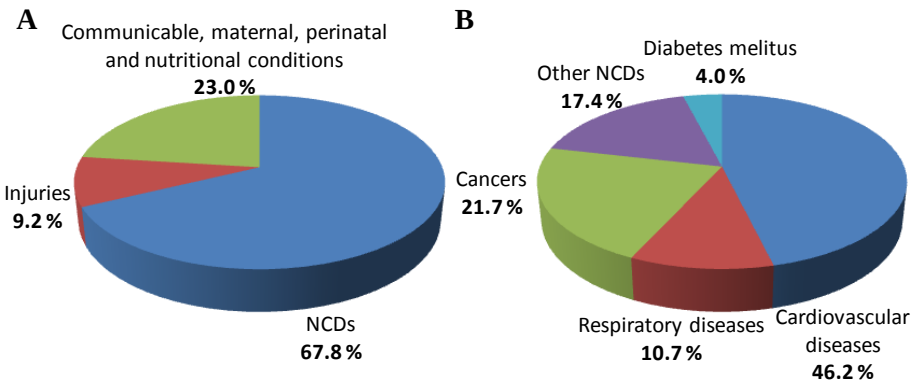

Figure 1.1. A) Distribution of major causes of death and B) distribution of global NCD by cause of death, males and females in 2012. Adapted from [4].

In the future, the total annual number of NCD deaths is projected to increase to 52 million by 2030. Annual cardiovascular disease mortality is projected to

increase from 17.5 million in 2012 to 22.2 million in 2030, and annual cancer deaths from 8.2 million to 12.6 million. These increases will occur despite projected decreases in NCD death rates.

1.2 CVDS SCENARIO

Due to the relevance of CVDs, there is a great need of tests that would help clinicians in the early assessment of those with chest discomfort and inconclusive electrocardiography.

On one hand, admission of patients to emergency departments (ED) with low probability of acute coronary syndrome (ACS) evolves to excessive hospital costs, but on the other hand, it is known that inappropriate discharge of patient has been estimated to occur in 2-5% of patients representing the most common cause of malpractice for ED physicians [5]. The protocol of admission starts with the entrance of a patient suffering from chest pain on the emergency unit. After a first evaluation by means of clinical history and physical examination, an electrocardiogram (ECG) is performed. If the signal is clearly ST segment elevation myocardial infarction (STEMI), the patient is admitted. If the signal is not concluding (non-ST segment elevation acute coronary syndromes, NSTEACS), a biomarker/s detection test is ordered in order to clarify if the patient should be admitted or not. Therefore, appropriate tools are needed for optimal risk stratification and cardiovascular biomarkers tests are addressed to do so.

1.3 CARDIOVASCULAR BIOMARKERS

Atherosclerosis is one of the main pathological processes that lead to most CVDs as it has been mentioned in the previous section. It is an inflammatory process affecting medium- and large-sized blood vessels through the cardiovascular system. When the lining (endothelium) of these blood vessels is exposed to increasing levels of low-density lipoprotein cholesterol (LDL cholesterol) and fatty substances it becomes permeable to lymphocytes and

monocytes. Then, these kinds of cells migrate into the deep layers of the wall of the blood vessel.

A series of reactions occur, attracting LDL cholesterol particles to the site. These particles are engulfed by monocytes, which are then transformed into macrophages (foam cells). Smooth muscle cells migrate to the site from deeper layers of the vessel wall (the media). Later, a fibrous cap consisting of smooth muscle and collagen is formed. At the same time, the macrophages involved in the original reaction begin to die, resulting in the formation of a necrotic core covered by the fibrous cap (see Figure 1.2). These lesions (**atheromatous plaques**) enlarge as cells and lipids accumulate in them and the plaque begins to bulge into the vessel lumen. When the process continues, there is thinning of the fibrous cap accompanied by fissuring of the endothelial surface of the plaque, which may rupture. With the **rupture of the plaque**, lipid fragments and cellular debris are released into the vessel lumen. These are exposed to thrombogenic agents on the endothelial surface, resulting in the formation of a **thrombus**. This thrombus evolves to a reduction of blood flow (cardiac ischemia) restricting the supply of oxygen to the myocardium. While ischemia is a reversible process, the irreversible damage is called necrosis. When this myocardial **ischemia** is continued it is named acute coronary syndrome (ACS) which ranges from unstable angina (UA) associated with reversible injury to **myocardial infarction (MI)** with large areas of irreversible damage (**necrosis**). Finally, if the thrombus is large enough, and a coronary blood vessel or a cerebral blood vessel is blocked, this results in a **heart attack** or stroke [2, 6].

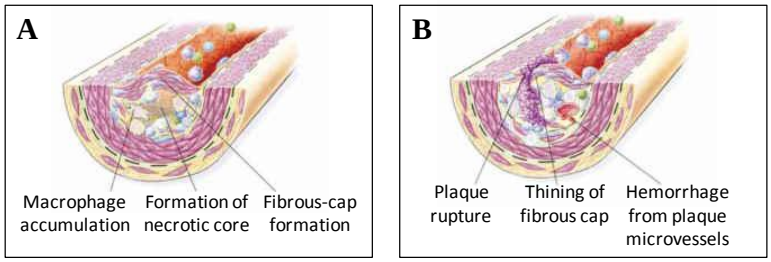

Figure 1.2. A) Fibrous cap formation and the necrotic core and B) the ruptured plaque. Adapted from [2].

In spite of the success of the already available tests these are mainly addressed to detect markers from the necrosis or even later steps after the thrombus (cTnI, CK-MB, myoglobin and natriuretic peptides). For this reason there is an

intensive search of additional cardiac markers for early diagnosis acute myocardial infarction (AMI) and assess prognostic. Moreover, these new biomarkers could help to perform a more correct risk stratification of the patients monitoring the progress of the disease and taking therapeutic decision (see Figure 1.3). These cardiac markers are biological analytes that can be detected in the bloodstream at particular levels during CVD or after myocardial damage.

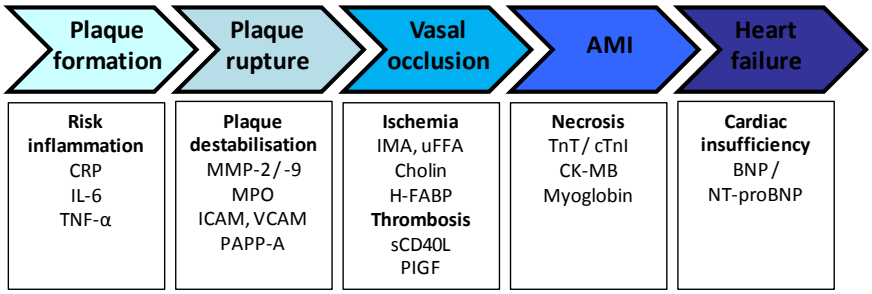

Figure 1.3. The entire pathophysiology of acute coronary syndrome (ACS). This flowchart depicts candidate markers related to earlier aspects of atherogenesis which may provide independent information in the diagnosis of AMI. *CRP* C-reactive protein, *IL-6* interleukin-6, *TNFα* tumor necrosis factor α, *MMP-2/-9* matrix metalloproteinases 2 and 9, *MPO* myeloperoxidase, *ICAM* intracellular cell adhesion molecules, *VCAM* vascular cell adhesion molecules, *PAPP-A* pregnancy-associated plasma protein A, *IMA* ischemia-modified albumin, *uFFA* unbound free fatty acids, *H-FABP* heart-type-isoform fatty acid binding protein, *sCD40L* soluble CD40 ligand, *PlGF* placental growth factor, *TnT* troponin T, *cTnI* cardiac troponin I, *CK-MB* creatine kinase MB isoenzyme, *BNP* brain natriuretic peptide, *NT-proBNP* N-terminal pro-brain natriuretic peptide [5].

Thus, additional biomarkers reflecting earlier stages of the disease like independent components of myocardial ischemia, of inflammatory activity and plaque stability, vascular and intracellular cell adhesion molecules or markers indicating activated platelets are expected to be very useful and are actually being studied.

1.4 IN-VITRO DIAGNOSTICS

Most of the current tests for cardiac markers used for in-vitro diagnostics of CVDs are based on immunoassays, which are antibody-based analytical methods.

1.4.1 ANTIBODY-BASED ANALYTICAL METHODS

Molecular recognition mechanisms play an important role in most biological processes; examples of this are the enzyme-substrate, receptor-effector and antibody-antigen (Ab-Ag) bindings. All of them are based on the lock and key model where both the receptor and the substrate possess specific interactions and complementary geometric shapes that fit into one another. In this case, the binding is noncovalent involving hydrogen bonding, metal interactions, hydrophobic forces, van der Waals forces, π-π interactions and/or electrostatic effects. The specificity of this selective molecular recognition phenomenon has been used for the detection and quantification of different kinds of analytes such as metabolites, drugs and biomarkers between others, using most of the times samples with very small amounts of the target analyte. The systems based on the antibody recognition have been currently the ones giving better results, providing well established and widely used immunochemical techniques not only in the clinical field, but also in environmental and alimentary areas.

Regarding in-vitro diagnostic addressed to CVD, the natural recognition receptors and, particularly, antibodies are employed in most cases. Also in the current thesis, this kind of biomolecules has been produced in order to develop the analytical methods for the detection and quantification of the selected cardiac markers.

The key element of the immunochemical techniques is the antibody and they are based on the affinity reaction of the antibody (Ab) for the antigen (Ag). This is a reversible reaction in which the affinity or an equilibrium constant (K_a) can be defined.

$$Ab + Ag \rightleftharpoons Ab\text{-}Ag$$

$$K_a = ([Ab\text{-}Ag])/([Ab]\cdot[Ag])$$

In occasions, K_a can reach extremely high values (10^{-10} M^{-1}). This high degree of affinity has allowed these techniques to be potential tools for the detection of analytes in very low concentrations (trace levels) requiring low sample volumes, from mL to µL. Different antibody-based methods have been

developed based on this reaction, ones like analytical methods and others like sample treatment to isolate the analyte from complex matrixes (e.g.: immunoaffinity chromatography).

1.4.1.1 Antibody

Antibodies are globular proteins produced by the immune system to neutralize foreign agents (antigens, Ag). There are five different families of immunoglobulins (IgG, IgM, IgA, IgD and IgE) that differ in charge, dimensions, amino acids sequence as well as in the number and type of bound carbohydrates. Depending on the family, the effect caused when joined to certain proteins is different. In the serum of mammals, IgG is the most abundant type and also the most employed in immunochemical applications. The immunoglobulins G (IgG) have a molecular weight around 150 KDa and their dimensions are 12x15x5 nm. Their structure is composed of two heavy (H; MW ~50 KDa) and two light (L; MW ~25 KDa) identical polypeptide chains interconnected by disulfide bonds (see Figure 1.4).

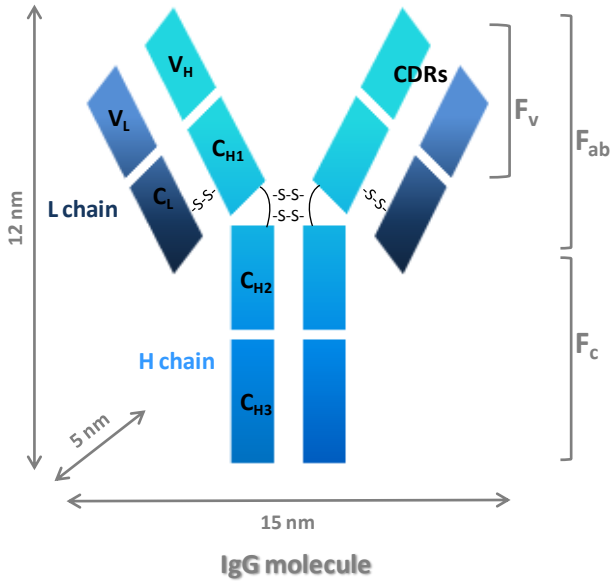

Figure 1.4. Schematic antibody structure and dimensions. Constant domains: CL; CH1, CH2 and CH3. Variable domains: VL and VH. Antigen binding site: CDR (hypervariable regions). Disulfide bond: -S-S-.

The global structure has constant and variable regions in regard to amino acids sequences. The Fc (fragment crystallisable) region is the constant region formed by two heavy chains and has the ability to bind to various cell receptors to regulate the immune response. On the other hand, the Fab fragment (antibody binding fraction) is composed of one constant and one variable domain from each heavy (C_{H1}, V_H) and light chain (C_L, V_L). The most important parts of the antibody are those which recognize the antigen epitope, being shaped at the amino terminal end of the antibody monomer by the variable domains (F_v) from the heavy and light chains.

The antibody production for insulin determination was the first approach in the development of immunochemical techniques as an analytical method [7]. Since then, a great advance has been produced in this field thanks to the progress in molecular biology and genetic engineering thus allowing the production of more specific antibodies for a wide variety of substances in larger amounts with less cost. Nowadays, depending on the technique followed for their production is possible to obtain and work with three different kinds of antibodies: polyclonal (PAbs), monoclonal (MAbs) and recombinant antibodies (RAbs). While big molecules can stimulate the immune system of the host animals by themselves, for the smallest ones (MW <1000 Da) a hapten is required to be designed and synthesized, that is similar to the target analyte, but with a spacer arm provided of a chemical functional group in order to be covalently bound to a bigger protein to initiate the immune response [8].

- Polyclonal antibodies (PAbs)

They are directly obtained from the serum of the immunized animal and sometimes purification is needed previously to be used. This serum contains a family of antibodies from distinct cellular clones that recognize the global structure of the immunization hapten, where each one shows a major or minor specificity for different epitopes or antigenic parts of the molecule. Rabbit is the most used animal for the production of PAbs, although in the cases where a greater volume of serum is needed, goat, pig, sheep or even horse are employed. The production of PAbs is simple, but for small molecules the design and synthesis of the hapten is a crucial step in the procedure and a limiting factor regarding the time needed for the development of an immunochemical

technique. The most important disadvantage for PAbs is the variability observed between animals.

- Monoclonal antibodies (MAbs)

They are obtained through the fusion of cells which are responsible for the antibody production (B cells) and are located in the spleen of the immunized animal (normally mice from BALB/C line) with tumor cells derived from myeloma cells [9]. In this case, following a long and laborious screening procedure, a unique IgG is isolated coming from an immortalized clone of B cells. Although this technology can provide unlimited amounts of antibody with the same affinity for the antigen, it is normally more expensive compared to the production of PAbs and, for small molecules, MAbs sometimes show worse affinity and stability than PAbs.

- Recombinant antibodies (RAbs)

These antibodies are the result of the rapid progress in recombinant DNA technologies which has allowed developing a great variety of antibody libraries. While for PAbs and MAbs, the specificity and affinity is the consequence of the immunization and the protocol followed, for RAbs this aspect is partly solved with the generation of small fragments of antibody that simulate the in-vitro immune response. The procedure involves the following steps: 1) preparation of antibody libraries, usually through mRNA isolation, 2) cloning genes in a bacterial plasmidic vector, 3) expression in bacteria and co-infection with viruses, providing antibody fragments (Fv fragments), 4) screening depending on the specificity for the antigen [10]. The greatest advantage of this technology is the ability to design polypeptide structures from antibodies and modify already available fragments in order to improve the antibody affinity. In spite of this, the sensitivities achieved with PAbs and MAbs have not yet been reached with RAbs.

1.4.1.2 Immunoassays

Immunoassays (IAs) are based on the quantification of the Ab-Ag complex through labels. The label may consist of radioisotopes (radioimmunoassay,

RIA), an enzyme (enzyme immunoassay, EIA), fluorophores (fluoroimmunoassay, FIA), chemiluminescent reagents (chemiluminescence immunoassay, CLIA) or magnetic markers (magnetic immunoassay, MIA). RIA has been the first immunoassay used, although it has been replaced by others safer for the operator and less damaging for the environment. EIAs are the most used ones and they offer the possibility to increase the detectability through the enzyme amplification.

In FIA, the molecule (label) is excited to provide an emission spectrum which give the final signal at a determined wavelength, in CLIA, the chemical reaction gives a product electronically excited that emits light when returns to the normal state and finally, in EIA, the enzyme often catalyses a reaction with a final colored product (colorimetric method). In regard to immunoassays for cardiovascular biomarkers, a lot of FIAs have been developed. These FIAs utilized the unique chemical properties of lanthanide chelates in concern with time-resolved fluorescence (TRF) detection to create assays that offer advantages over traditional methods, such as high sensitivity, wide dynamic range and superior stability. Apart from this, the lanthanide chemistry allows the elimination of concerns regarding enzyme quality or degradation, being extremely stable and allowing for delayed signal detection.

Most common IAs require the use of a solid support, like microtiter plates, tubes, microspheres or magnetic particles, to immobilize one of the immunoreagents before the analysis process. This configuration is known as heterogeneous format. On the contrary, when all the elements of the immunoassay are in solution it is known as homogeneous format and it is normally more exposed to matrix interferences.

One of the most popular immunoassay due to its speed is the *test strip*, where the immunoreagents are immobilized in a membrane providing an optical response through enzyme labels or gold particles. Another widely used enzyme immunoassay is the ELISA (enzyme-linked immunosorbent assay), which employs microplates where the antigen or antibody are immobilized depending on the format and horseradish peroxidase (HRP) and alkaline phosphatase are the most common labels. ELISAs have been developed in this thesis (chapter 3, 4 and 5) for the determination of several cardiovascular biomarkers, using HRP as a label and 3,3’,5,5’-tetramethylbenzidine (TMB) as a substrate.

The quantification of small molecules involves a competition step, where the free analyte and the antigen (competitor) establish a competition for the antibody, these last two in fixed amounts. At the end of the reaction the amount of analyte can be indirectly determined measuring the labelled antigen or antibody. The competition step is not needed with the determination of large substances, then the sandwich format is employed (see Figure 1.5).

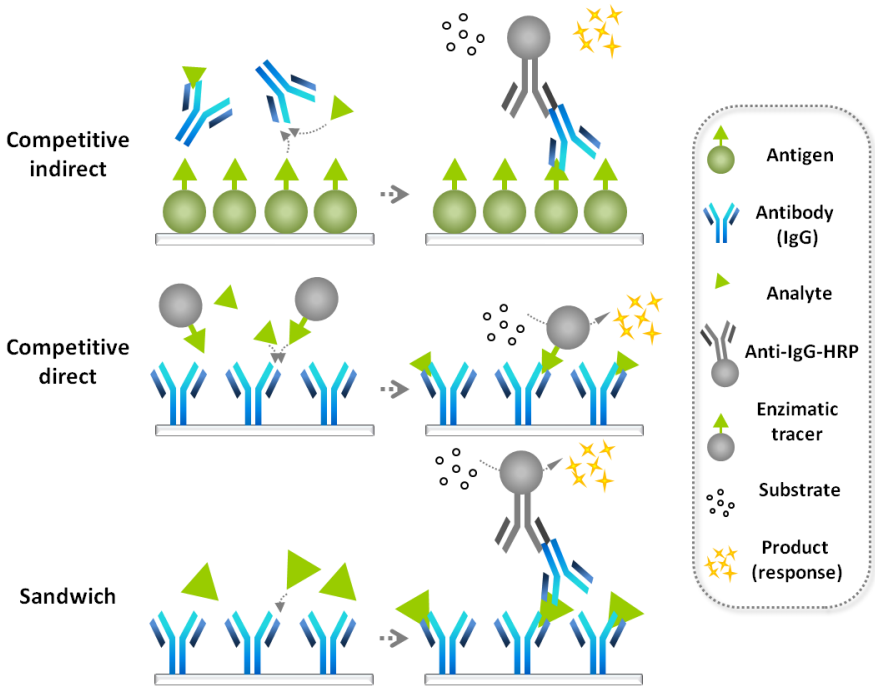

Figure 1.5. Schematic view of ELISA formats used for the detection of low and high molecular weight analytes.

In the indirect format a second antibody labelled with an enzyme (anti-IgG-HRP) is needed for the measurement. In this case, the equilibrium is established between the antigen or competitor immobilized by adsorption in a pre-treated plate, the analyte and the antibodies that are in solution. In contrast, in the direct format the equilibrium is between the antibody immobilized, the analyte and the enzyme tracer in solution (see Figure 1.5). Therefore, for a direct format, a second antibody is not required. In both cases, TMB was used as substrate in the enzymatic reaction and absorbance was measured at a wavelength of 450 nm.

Calibration curves for competitive ELISA normally fits a nonlinear equation between the signal and the analyte concentration. Generally, the response shows a sigmoidal relationship with the concentration, providing in this way different parameters to characterize the immunoassay. IC50 is the concentration in which the signal is 50 % inhibited, IC90 is the concentration in which the signal is 10 % inhibited and can be employed as a limit of detection (LOD), IC20 and IC80 define the linear or working range of the assay, Abs_{max} and Abs_{min} when there is no analyte (maximum absorbance) and the background of the assay when the signal is totally inhibited (minimum absorbance) and the slope, the slope of the tangent line on the inflection point. Figure 1.6 shows a representative curve.

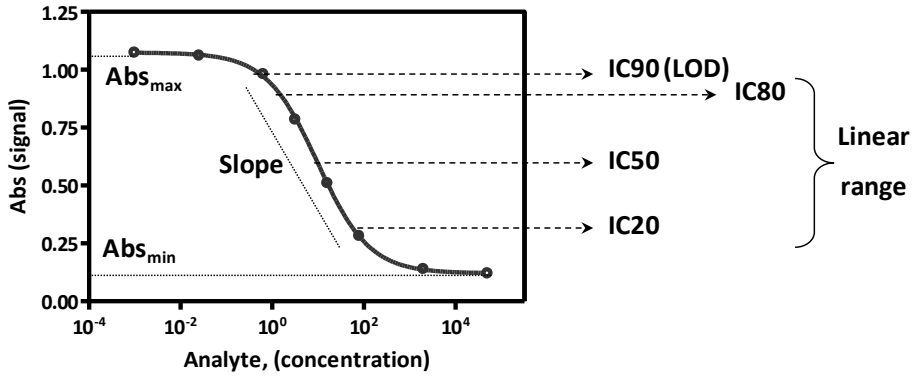

Figure 1.6. Sigmoidal calibration curve generated for a competitive format and the corresponding parameters.

In the sandwich format, once the capture antibody has been immobilized, the addition of the analyte solution is done. Later, the detection antibody and a second antibody labelled with an enzyme (anti-IgG-HRP) are needed for the measurement. Like in competitive direct indirect format, if the detection antibodies were labelled, the addition of a secondary antibody would not be necessary. In this format, the analyte must have two different binding epitopes. Moreover, its dimensions have to be great enough to allow the interaction with two antibodies without steric hindrance. The incubation of the analyte with the detection antibody previous to the addition is only recommended if capture and detection antibodies are recognizing different epitopes of the analyte (e.g.:

two different monoclonal antibodies), otherwise epitopes can be blocked when added to the plate and the final response decreased.

Calibration curves for sandwich ELISA can be fitted in several ways. Although they can fit a linear regression, in this thesis data have been adjusted to a four-parameter logistic equation (sigmoidal fitting) also employed in competitive formats to relate the analyte concentration to the corresponding response. Thus, IC50 is the concentration in which the signal is 50 % of the maximum signal, IC10 is defined as a limit of detection (LOD), IC20 and IC80 define de linear or working range of the assay, Abs_{max} and Abs_{min} when there is the highest concentration of analyte (maximum absorbance) and the background of the assay when there is no analyte (minimum absorbance) and the slope, the slope of the tangent line on the inflection point. Figure 1.7 shows a representative curve.

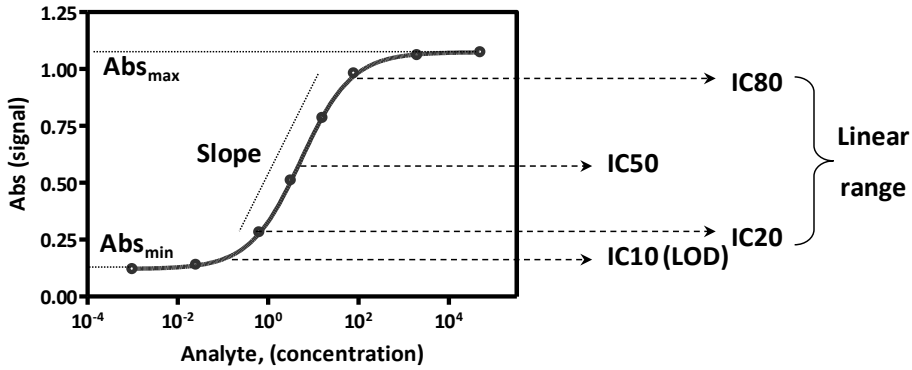

Figure 1.7. Sigmoidal calibration curve generated for a sandwich format and the corresponding parameters.

1.4.1.3 Biosensors

Biosensors are an alternative to the diagnostic which can also use antibodies (immunosensors). They are miniaturized devices with a biological receptor (bioreceptor) in contact with a transducer that will convert the biorecognition event into a measurable signal that allow detection or quantification of the analyte. The signal can be amplified and processed. The ideal sensor is this one that can provide response on-site, in real time, in a direct and selective way

when it is in contact with the sample and with the corresponding dimensions to make it portable [11]. They can be classified depending on the bioreceptor or the transducer (see Figure 1.8).

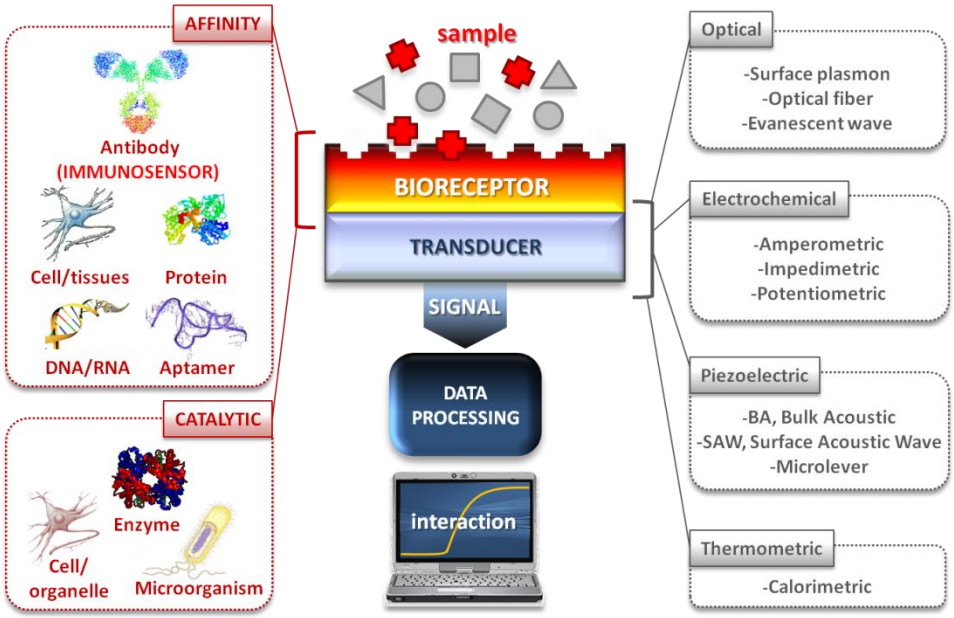

Figure 1.8. Components of a biosensor and their classification based on the bioreceptor and transducer.

In catalytic biosensors the formation or inhibition of a particular product can be related to the presence of the analyte. In most cases enzymes are used, either isolated [12, 13] or as part of cells, tissues or microorganisms [14]. The most common example is the glucose sensor for diabetes which measures the glucose thanks to an oxidase enzyme. On the other hand, in affinity biosensors the formation of the analyte-receptor complex is detected in a direct or indirect way. Aptamers and antibodies are between the bioreceptors used on affinity biosensors.

The immunosensors monitor the formation of the Ab-Ag complex to detect the presence of the analyte. Similarly to immunoassays, usually, the quantification of small molecules involves a competition step (direct or indirect) while this is not required for the determination of large molecules. These sensors show nearly unlimited specificities and the advantage to not need labels depending

on the transducer system. Based on the transducer system, immunosensors can be:

- Electrochemical

The molecular recognition on the electrode surface provides electric signal changes which are monitored. The potential difference, impedance, conductivity or current can be measured with potentiometric, impedimetric or amperometric sensors, respectively. A redox label, for example an enzyme, is needed for the amperometric sensors.

- Piezoelectric

The frequency changes caused by the Ab-Ag recognition are measured by piezoelectric materials already functionalized with a bioreceptor. In this group, there are the BAW (Bulk Acoustic Wave), also known as quartz crystal microbalances (QCM), and SAW (Surface Acoustic Wave) sensors. Microbalances or cantilevers are also involved in these mass sensors, which are based on the flexion frequency changes.

- Optical

They measure the changes in the light properties, consequence of the molecular recognition Ab-Ag. The most important ones are those based on the evanescent wave and on the surface plasmon. The first ones look at the changes in the radiation that is circulating in an optical guide previously functionalized with an antibody or antigen. Through internal reflections, the radiation creates an evanescent wave that can penetrate to the surface at a determined distance (aprox 100 nm). The possibility to use fluorescent labels evolves to TIRF (total internal reflection fluorescence) immunosensors with improved sensitivities. The second ones are based on the variation of the reflected light properties by a gold surface where the antibody or antigen is immobilized on top of a nobel metal surface, and it binds its counter-partner. Under the action of the light at certain critical angle, the electrons of the surface start to oscilate generating an electromagnetic field on the surface (plasmon), with a penetration deep of about 100-150 nm. This absorbance of the energy of the light induces a minimum (or absorption band) in the

reflectance spectra. The position of this minimum depends on the refraction index nearly the interfase.

More detailed information on transducer principles, methods and examples of all these types of immunosensors can be found in recent reviews [15-18].

One of the key steps in the development of an immunosensor is the immobilization of the bioreceptor (antibody or antigen) on the transducer to achieve a biofunctional, biocompatible, stable and homogeneous surface. This immobilization can be done by adsorption or through a covalent binding using different kind of linkers and chemistries (see section 7.1.4).

1.4.1.4 Advantages and disadvantages of antibody-based analytical methods

In general, the antibody-based analytical methods are characterized for their simplicity, speed and generally for their sensitivity and specificity. Once antibodies are produced, immunochemical techniques are unexpensive and allow the analysis of a great number of samples in a short time. On the contrary, it is necessary to evaluate potential non-specific effects caused by complex real samples on the final quantification because they can provide under or overestimation and consequentely false positive or negative results. The contribution to the final response can come from specific signals due to the presence of compounds structurally related to the analyte and also recognized by the antibody (cross-reactivity phenomenon) or from non-specific signals (matrix effect). These last ones can be caused by physico-chemical parameters of the sample (pH, conductivity, etc.) or non-specific interactions of the immunoreagents with other matrix components. Nevertheless, false negatives results are not very common in immunochemical techniques, therefore they can be used as fast screening tools and substitute or complement conventional analytical techniques.

1.4.2 ACTUAL DIAGNOSTIC TOOLS FOR CARDIOVASCULAR DISEASES

Nowadays, there are many tests for cardiovascular biomarkers available in the market. These tests used for in-vitro diagnostics of CVDs can be bench top analyzers (BTA) in central laboratory testing or point-of-care (POC) devices. Both types can be based on different immunochemical strategies including immunoassays (ELISA, FIA, CLIA or RIA) or immunosensors (optical, electrochemical, piezoelectric or thermometric). A great number of POC devices are based on lateral flow immunocromatography (LFIC) also called test strips. In this case, the support is a nitrocellulose membrane where the capture antibody or antigen is immobilized; the analyte travels along the membrane through capillarity until arriving to the detection zone (test line). The most frequently used label are gold nanoparticles which can be easily visualized, although there have also been developed LFIC based on agglutination using latex particles, on fluorescence with immunoliposomes or fluorescent particles. POC devices and their advantages are also explained in chapter 7.

In the following table, there is a summary of some diagnostic tools for CVDs commercially available (see Table 1.1). There it can be observed that most of them share a short assay time, except for the ELISA (Percipio Bioscience), and short sample volumes, reaching excellent limits of detection.

Table 1.1. Characteristics of some commercial tests for cardiac markers.

Test name (analyte), immunoassay method	Company	POCT/ BTA	LOD/LOQ (pg mL^{-1})	Sample volume (µL)	t_{assay} (min)
Elecsys® proBNP, ECLIA	Roche	BTA	LOQ: 5	20	18
Cardiac® myoglobin / CK-MB / cTnT / D-dimer / NT-proBNP, Immunocromatography	Roche	POCT	LOQ: $3{\cdot}10^4$ / $1{\cdot}10^3$ / 100 / $1{\cdot}10^5$ / 60	150	8 / 12 / 12 / 8 / 12
Triage® cTnI / CK-MB / Myoglobin / BNP / D-dimer, Immunocromatographic fluorescent assay	Biosite	POCT	LOD: 50 / $1{\cdot}10^3$ / $5{\cdot}10^3$ / 5 / $1{\cdot}10^5$	250	20
ADVIA® Centaur® BNP / CK-MB / Myoglobin / cTnI, CLIA	Siemens	BTA	LOD: 2 / 180 / $3{\cdot}10^3$ / 8	100 / 100 / - / 100	18

H-FABP / CRP / cTnI / MPO / CK-MB ELISA	Percipio Bioscience	BTA	LOD: - / $1 \cdot 10^5$ / 480[a] / $2.5 \cdot 10^4$ / $2.5 \cdot 10^3$	100 / 5 / 100 / 5 / 20	80 / 65 / 110 / 200 / 80
PATHFAST® cTnI / NT-proBNP / D-dimer / CRP / Myoglobin / CK-MB mass, CLIA	Mitsubishi Chemical	BTA	LOQ: 1 / 15/ $5 \cdot 10^3$ / $5 \cdot 10^4$ / $5 \cdot 10^3$ / $2 \cdot 10^3$	100	15

LOD: limit of detection, LOQ: limit of quantification, ECLIA: electrochemiluminescent assay, CK-MB: creatine kinase MB, MPO: myeloperoxidase. [a]It does not achieve the cut-off recommended (0.06 ng mL^{-1}, 99th percentile cut-off concentrations established by ESC/ACC/AHA in the studied population [19]).

Additional information regarding commercial assays for brain natriuretic peptides and troponins can be found in chapter 3 and 4 respectively.

As can be observed in the above table, there are plenty of tests for cardiac markers but multiplexation is still something scarce. Usually, the same company has tests for different analytes without multiplexing capabilities. Multidetection of different markers from different stages of the disease would allow more precise risk stratification and therefore it is the main aim of this thesis. Apart from this, cTnI, CK-MB and myoglobin are detected by most commercial tests and sometimes additional markers are also incorporated such as CRP, D-dimer, brain natriuretic peptides (BNP or NT-proBNP but not both at the same time) and, exceptionally, H-FABP or myeloperoxidase. The targets selected for this thesis are described in the following sections and they are particularly representative from different stages of cardiovascular disease.

1.5 CLINICAL RELEVANCE OF POTENTIAL BIOMARKERS

1.5.1 KINETIC RELEASE OF CARDIOVASCULAR BIOMARKERS

An ideal cardiac biomarker should be highly specific for the cardiac tissue and absent on non cardiac tissue. Moreover, it should be easily accessible through non extremely invasive methodologies to obtain the sample, have fast kinetics of release and clearance from the injured tissue and at the same time high stability and long plasma half-life. For this last matter, peak levels should ideally be reached relatively quick and kept in circulation for few hours. Although the

ideal marker has not yet been discovered, cTnI fulfills quite well with the requirements and for this reason is known as the preferred and "golden" biomarker for ACS.

At the same time, the kinetics of release of each biomarker must have a relationship with the corresponding injury. Consequently, each biomarker has its own profile of release and with this its first detection, peak and normalization of protein concentration as it is shown in Table 1.2.

Table 1.2. First detection, peak and normalization of protein plasma concentration during ACS [6, 20].

Marker	First detection	Peak	Normalization
CRP	4-6 h	50 h	NA
H-FABP	2-3 h	8-10 h	18-30 h
cTnI	3-6 h	24-48 h	5-10 days
TnT	3-6 h	24-48 h	5-14 days
CK-MB	3-12 h	24 h	48-72 h
Myoglobin	2 h	4-12 h	24 h
BNP	early	20 h-5 days	<30 days to NA

NA: not available

As it can be observed in the table, while myoglobin and H-FABP can be detected 2 h after the onset of symptoms, troponins offer the widest diagnostic window from 4 h to 14 days. In conclusion and despite the different temporal profile of the biomarkers, blood samples for determination of biomarkers changes should be taken when the patient presents and later during the course of the disease, depending on the profile of each molecule.

1.5.2 CLINICAL STUDIES

In the search of novel biomarkers or the optimal combination of the known ones, the primary objective becomes early diagnosis allowing monitoring and appropriate treatment in patients suspected of having ACS, as well as the prevention of adverse outcomes. From a public health viewpoint, preventative care must focus on minimizing the development of CVD and the conditions leading to ACS and its more severe consequences including heart failure (HF). Only few cardiac biomarker tests are routinely used by physicians. The current

biomarker test of choice for detecting heart damage is troponin and the current biomarker test for HF is BNP. Other cardiac biomarkers are less specific for the heart and may be elevated in skeletal muscle injury, liver disease or kidney disease. Many other potential cardiac biomarkers are being investigated, but their clinical benefit on a large scale population still has to be established. Today, BNP and/or NT-proBNP and troponins (cTnI and/or TnT) are currently used in daily practices for cardiac diseases. Both were subjects to guidelines from the National Academy of Clinical Biochemistry (NACB, 2007 and 2009) [21, 22] and from the European Heart Journal and ACC/AHA (2008 and 2013) [23, 24].

Troponins as well as brain natruiretic peptides are characteristic from late diagnosis stage and do not give any kind of information before AMI. The measurement of cardiac troponins first became available in the early 1990s. It is the first fully cardio-specific biomarker and for that reason has supplanted creatine kinase-MB (CK-MB) as the biomarker of choice for the evaluation of patients with possible AMI. Troponins were substantially more sensitive than CK-MB [25] and, at the time of the first troponin assays, many situations where cardiac injury was present began to be defined [26]. Similarly, HF therapy guided by NT-proBNP has been proposed to improve outcome compared with conventional therapy in patients with chronic HF in some studies [27, 28].

For other cardiac biomarkers, clinical evidence are not yet established at a level leading to recommended practices from health organizations. However, despite the absence of health authority recommendations, some biomarkers appear to bring clinical interests in one or many step of the disease life cycle:

- diagnosis and/or
- prognosis and/or
- predictive interest for HF or AMI
- as a disease/treatment companion biomarker

Clinical research is under analyzing and/or clinical trials under course. Due to the absence of written international recommendations, these biomarkers can be classified as “emerging biomarkers”. However, for most of the emerging biomarkers, kits are already marketed.

Although up to know, only troponin has been used to direct therapeutic intervention and none of the new prognostic biomarkers have been tested and proven to alter the outcome of this intervention, several studies point to the benefits of a multimarker approach incorporating combinations of particular biomarkers and clinical scores to increase the prognostic accuracy [19, 29-33]. Thus, it has been reported that H-FABP and copeptin in combination with cardiac troponin help diagnose AMI [34]. Cameron et al. reported the results of using CRP, CK-MB, troponin, NT-proBNP and myoglobin to evaluate the prognosis after AMI or ACS in the early hours following symptoms [30]. Hence, an elevated NT-proBNP has been well validated to predict death and HF following AMI. Similarly, high-sensitivity CRP has also been reported to be useful to predict death following an ACS, in addition to predict risk of coronary disease in an apparently healthy population, which would allow clinicians to initiate early preventative treatment. Certain studies point also to the strong value of Cys C as predictor of death risk from cardiovascular events in elderly persons, even though this biomarker is known in clinical practice as an indicator of renal failure. In this way, on a cohort study with 1135 participants, Zethelius et al. demonstrated that a combination of biomarkers that reflect myocardial cell damage (cTnI), left ventricular dysfunction (NT-proBNP), renal failure (Cys C) and inflammation (CRP) improved risk stratification in elderly patients [33].

Clinical studies are ongoing and it is difficult at the present moment to identify the best combination of biomarkers to assist clinicians in their diagnostic. Hence, certain biomarkers seem to have an improved prediction of outcome in AMI, but up to now, none have been demonstrated to alter the outcome of a particular therapy or management strategy. It is necessary to continue investigation, in this respect through randomised trials addressing this translational gap to facilitate tailored treatment following an acute coronary event. However, it seems quite clear the improved effect of using distinct biomarkers on patient stratification and prognosis. Accordingly, from these studies and considering the availability of the corresponding immunoreagents, it was possible to identify **CRP, Cys C, Lp(a)** and **H-FABP** together with **cTnI** and **NT-proBNP** as prioritary biomarkers to be included in a multiplexed platform.

These biomarkers belong to different chemical entities and also are indicative of different stages of the progression of the disease. cTnI is a biomarker of myocardial necrosis. Both, CRP and Lp(a) may appear increased at the earlier

stages of the disease (inflammation, plaque formation/destabilization), but high CRP levels are also observed after AMI. Similarly for H-FABP, which levels may appear increased earlier shortly before AMI, at vassal occlusion, but also during and after such event. Finally, NT-proBNP appears as clear indicator of the risk of HF, helping thus to the prognostic.

Lp(a), Cys C and H-FABP are potential biomarkers for early diagnosis of AMI. Lp(a) is a lipoprotein involved in some arteriosclerotic disorders including myocardial infarction. H-FABP is a cytosolic protein present in the heart, expressed mainly in the heart tissue. Cys C is a biomarker for kidney malfunction and related with several cardiovascular diseases such as AMI, stroke or HF.

The biomarker for which the largest body of data exists is CRP, an acute-phase reactant of hepatic origin. Multiple epidemiological reports have been published, all generally supporting an association between CRP concentrations and future cardiovascular risk, although estimates of effect vary. Despite the robust statistical association between CRP and cardiovascular events, evidence from multiple studies indicates that CRP measurements provide only modest improvements in predictive accuracy. In spite of this, CRP indicates the risk of a first acute atherothrombotic event and the destabilization of vulnerable plaque.

Cys C seems to be less influenced by age, gender and muscle mass compared to serum creatinine [26]. Sarnak et al. and Shlipak et al. affirmed in their studies that Cys C is useful for prognostic in HF [35, 36], while in Jernberg's work its usefulness for ACS prognostication is suggested [37]. Hence, it would make sense as it has already been accepted that renal function is a critical determinant of prognosis. Lipoprotein subclasses have been shown to be related to the development of the initial coronary heart disease, although most results in the corresponding studies do not show additional benefit in the risk evaluation for primary prevention [22].

H-FABP allows a possible early detection of AMI in subjects at risk, such as HF patients and patients with previous first AMI episode, who present chest pain (early diagnosis). In such cases, H-FABP is used to confirm or exclude a diagnosis of AMI and for monitoring recurrent infarctions. As an example, thirty patients suspected of AMI presented to the emergency department within 12

hours after onset. There were 59.1% of patients with positive H-FABP within 6 hours after onset, while there were only 18.2% with positive cTnI. Results indicated the diagnostic power of H-FABP for AMI was significantly higher than that of cTnI [38]. Thus, the combination of H-FABP and cTnI was found to have the higher diagnostic accuracy (91%) among different cardiac markers and the other combinations. It gave the highest sensitivity (96%) and a comparable specificity (84%) to cTnI alone. A cardiac panel consisting of H-FABP and troponin is recommended (diagnosis of AMI) [39]. Apart from this, H-FABP might be a useful biomarker for risk stratification of normotensive patients with acute pulmonary embolism and for diagnosis for lung dysfunction (prognosis) [40]. Moreover, it is possible use in severe chronic HF patients presenting chest pain and patients with previous first AMI episode has been evidenced as a disease monitoring.

The existence of CardioDetect highlights the effectiveness of this protein in improving treatment that will reduce patient morbidity and mortality and prevent unnecessary hospital stays for non-AMI patients.

Early detection (acute phase) of CVD is focusing on elevated levels of the above mentioned biomarkers. There is a special time frame for all these molecules to achieve adequate measurement. Correct results of biochemical measurements will determine the therapy of each patient and may help to survive the disease.

1.6 RELEVANT BIOMARKER TARGETS

Based on the clinical relevance on the entire patophysiology of ACS and the availability of immunoreagents, C-reactive protein, cystatin C, heart fatty acid binding protein, lipoprotein (a), cardiac troponin I and brain natriuretic peptides are between the most relevant biomarkers.

1.6.1 C-REACTIVE PROTEIN (CRP)

C-reactive protein is one of the markers for **inflammatory diseases** (early diagnosis). CRP was the first acute-phase protein to be described, it was

discovered by Tillett and Francis in 1930 as a substance in the serum of patients with acute inflammation that reacted with the C polysaccharide of pneumococcus [41]. The human CRP molecules is composed of five identical subunits (23 kDa), each containing 206 amino acid residues, not covalently associated in an annular configuration with cyclic pentameric symmetry [42]. Each subunit has a concave face in which the ligand-binding site, containing two calcium atoms, is located; the specificity of the binding site is for ligands containing phosphocholine (see Figure 1.9).

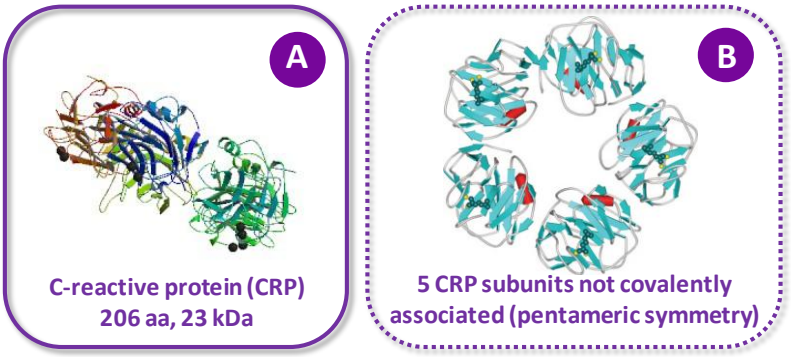

Figure 1.9. A) Human C-reactive protein. Protein chains are colored from the N-terminal to the C-terminal using a rainbow (spectral) color gradient (image from Protein Data Bank, 1GNH). B) Ribbon diagram of x-ray crystal structure of CRP-phosphocoline complex [43].

The capacity of the human CRP to activate complement and to stimulate tissue-factor production suggests that CRP may have both pro-inflammatory and pro-coagulant effects. Even if it was not considered a useful clinical parameter for many years because of its unspecificity, nowadays it is measured as a sensitive systemic marker of inflammation, infection and tissue damage and moreover it has emerged as an interesting novel and potentially clinically useful marker for increased cardiovascular risk [44]. Following an acute-phase stimulus, the circulating concentration of human CRP rises from normal levels of about 1000–10000 ng mL^{-1} up to 20000–40000 ng mL^{-1} for a viral infection or even up to about 500000 ng mL^{-1} in case of a bacterial infection, and may do so within 24–48 h. In clinical practice CRP is routinely measured via enzyme-linked immunosorbent assay (ELISA) [45] and the results are generally supplied by central laboratories.

Regarding the CRP role in the risk assessment for cardiovascular diseases, CRP concentrations of < 1000 ng mL^{-1} are classified as a low risk level, moderate for 1000-3000 ng mL^{-1} and high risk for concentrations > 3000 ng mL^{-1} [22].

1.6.2 CYSTATIN C (CYS C)

Cystatin C is a cytoplasmatic protein inhibiting cysteine proteases in the bloodstream. It contains 120 amino acid residues and has a MW of 13.4 kDa (see Figure 1.10).

Since Cys C is produced at a constant rate by almost all nucleated cell types and it is eliminated from serum by glomerular filtration thus resulting a constant serum level of Cys C; it is known as a well-described serum marker of renal failure. Compared to creatinine-based equations to estimate glomerular filtration rate (GFR), Cys C measurement does not depend on the age, sex, race and lean muscle mass while creatinine does. On the other hand, this protein is becoming acknowledged as a marker of risk of death from cardiovascular complications as Shlipak et al. affirm in their studies [35, 46].

Cys C concentration in plasma or serum from healthy individuals ranges around 800-1200 ng mL^{-1} depending on measurement methods. Increased levels are associated to kidney function (reduction in GFR), renal disorders and risk of death and cardiovascular events in elderly persons (≥ 1290 ng mL^{-1}) [35].

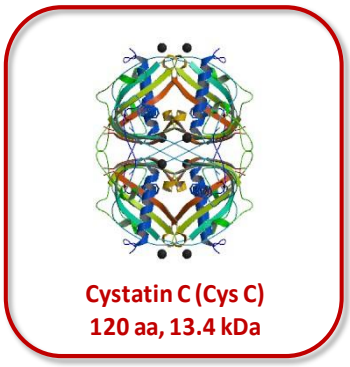

Figure 1.10. Cys C. Protein chains are colored from the N-terminal to the C-terminal using a rainbow (spectral) color gradient (image from Protein Data Bank, 1G96).

1.6.3 HEART FATTY ACID BINDING PROTEIN (H-FABP)

Fatty acid binding protein (FABP) is a cytosolic protein responsible for the transport and deposition of fatty acids inside the cell. There are nine different FABP isoforms depending on the different tissue types that are expressed in. For instance, cardiac isoform (H-FABP) is mainly expressed in the heart and it is in lower concentrations in skeletal muscles. H-FABP consists on a 132 amino acid residues protein with a MW of 14.7 kDa (see Figure 1.11), it is released after cardiomyocyte damage within 6 hours.

H-FABP is rapidly released after **infarction (AMI)** and thus has been proposed as an alternative to myoglobin that although performing better still lacks of cardiac specificity. Because H-FABP concentration in skeletal muscle is lower, recent studies demonstrated that its measurement can be useful for the early detection of minor myocardial events such as unstable angina and it reaches its upper reference limit sooner than myoglobin or troponin [28], switching clinical studies form myoglobin to H-FABP can improve the early AMI diagnosis. A cut-off value of 5.8 ng mL^{-1} is used to define abnormality based on the 99^{th} percentile cut-off concentrations established by ESC/ACC/AHA in the studied population [19].

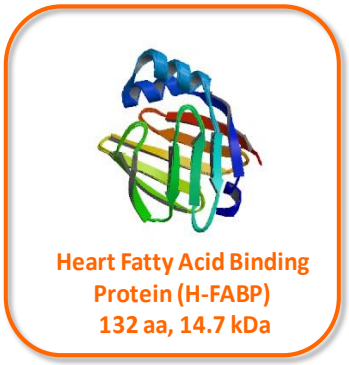

Figure 1.11. H-FABP. Protein chains are colored from the N-terminal to the C-terminal using a rainbow (spectral) color gradient (image from Protein Data Bank, 1G5W).

1.6.4 LIPOPROTEIN (a) (LP(a))

Lp(a) is a lipoprotein consisting a core of low density lipoprotein (LDL) involved by two proteins linked covalently by disulfide bond called apolipoprotein B (apoB) and a glycoprotein apolipoprotein (a) (apo(a)). This last one is a homologue of plasminogen, containing multiples copies of plasminogen kringle 4, a single copy of plasminogen single 5 and an inactive protease domain. The number of kringle 4 domains can vary from 12 to 51 giving rise to 34 different-sized apo(a) isoforms. Moreover, within the repeated kringle 4 domain exists 10 distinct types each present in single copy except for kringle 4 type 2 which exists in varying manner (see Figure 1.12). Assembly of Lp(a) is complex and requires multiple apo(a)-apoB interactions for the efficient association, which involves firstly initial non-covalent interactions between lysine residues in apoB and lysine binding domains in apo(a) followed by the formation of a disulphide bond between apo(a)-Cys_{4057} and apoB-Cys_{4326} (N, N-terminus; C, C-terminus).

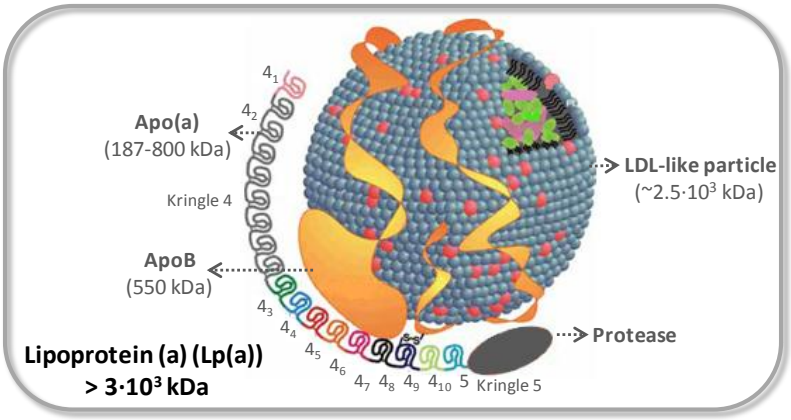

Figure 1.12. Model of lipoprotein (a) assembly. ApoB consists of 4536 aa and has a molecular mass of 550 kDa and apo(a) molecular mass ranges between 187 and 800 Da [47]. Figure adapted from [48].

Lp(a) is the unique lipoprotein emerged as an independent risk factor for developing vascular diseases. It has high affinity for arterial wall due to apo(a) affinity for extracellular matrix proteins and thus displays many athero-thrombogenic properties **(plaque formation)**. Many clinical studies have shown the relation between elevated levels of Lp(a) and high risk for developing cardiovascular diseases (see section 1.5.2). The commonly cited cut-off value for Lp(a) becoming a risk factor is $5 \cdot 10^5$ ng mL^{-1}. This value is approximated

since there exists a great genetic individual. Although further standardization is still needed for Lp(a) analysis, a standardized international reference material has been developed and is accepted by the WHO Expert Committee on Biological Standardization and the IFCC. A desirable level below the 80th percentile is recommended (less than ~50 mg dL^{-1}) [48, 49].

There are already a lot of immunoassay for Lp(a) determination, although there is still the need of a common representative calibrator and the problem when using antibodies that have epitopes within the repetitive kringle 4 type 2. Marcovina et al. have documented the impact of apo(a) size on Lp(a) measurements using two ELISA assays with antibodies recognizing kringle 4 type 2 in one, and kringle 4 type 9 in the other [50].

While ELISA assays for CRP, CysC and H-FABP determination were developed in chapter 5 of this thesis first and then moved to the microarray, Lp(a) immunoassays was directly developed on the fluorescent microarray (chapter 6). Firstly, the assay was developed individually and then attempts to involve it in the multiplexed assay were carried out.

1.6.5 CARDIAC TROPONIN I (CTNI)

From all the most important cardiovascular biomarkers, cTnI is the one circulating in the blood of a healthy patient at the lowest concentration, followed by brain natriuretic peptides. Therefore, for the detection of cTnI, high sensitive analytical techniques are needed.

cTnI is considered to be the most sensitive and significantly more specific marker in the diagnosis of **myocardial infarction** compared to those such as CK-MB or myoglobin. As a consequence, it is known as the *golden marker*. This protein, with 210 aa and a MW of 24 kDa contains two serines in the 22 and 23 positions that can be phosphorylated in vivo by protein kinase A. In this way, four forms of protein (one dephosphorylated, two monophosphorylated and one bisphosphorylated) can coexist. Although latest findings affirms that a significant part of cTnI released into patient's blood is phosphorylated, this process changes cTnI conformation and modifies the interaction with other troponins or the corresponding antibodies [51].

While for cTnI only one tissue-specific isoform of TnI is described for cardiac muscle (cTnI) and is only expressed in myocardium, for troponin T there are several cardiac specific isoforms described in the literature (cTnT) and are also expressed in skeletal tissue of patients with chronic skeletal muscle injuries. On the other hand, for troponin C no cardiac specific isoform is known and the one expressed in cardiac muscle is an isoform typical for slow skeletal muscle. All three troponins have two isoforms for skeletal muscles, slow skeletal and fast skeletal isoform (skTn, fkTn) [52, 53].

cTnI is released in the blood of the patient in the form of binary complex with TnC or ternary complex with cTnT and TnC (see Figure 1.13) [54]. Each subunit is responsible for a part of troponin complex function. TnT is a tropomyosin-binding subunit which regulates the interaction of troponin complex with thin filaments; TnI inhibits ATP-ase activity of acto-myosin and TnC is a calcium-binding subunit, playing the main role in calcium dependent regulation of muscle contraction [55]. Inside this complex, the strongest interaction is for cTnI-TnC binary complex especially in the presence of calcium ion (Ca^{2+}) (K_a=1.5·10^{-8} M^{-1}) [56]. When TnC forms a complex with cTnI, this last one changes the conformation and shields part of its surface, thus affecting on the interaction with antibodies.

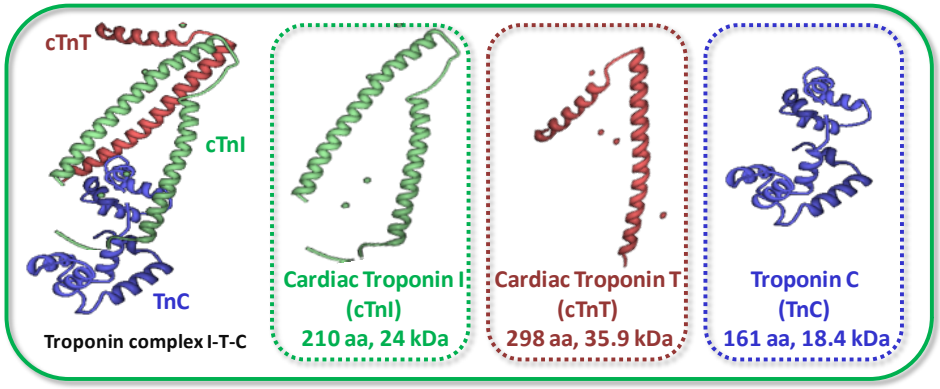

Figure 1.13. Troponin complex I-T-C based on three subunits-cardiac troponin I, cardiac troponin T and troponin C.

cTnI is more unstable in its free form than in cTnI-TnC or cTnI-cTnT-TnC complex. Consequently, TnC has been used sometimes as a stabilizer material

of cTnI in water solutions, because TnC protects cTnI from protease cleavage in forming cTnI-TnC complex [57]. Thus, these two complexes are preferable as materials for standard and calibrator preparation. Troponin I-T-C complex from Hytest (Turku, Finland) has been chosen by AACC cTnI Standardization Subcommitee for international reference material and it is the one that has been used in this thesis (see chapter 3 and 6). This standard reference material (SRM® 2921) is available from National Institute of Standards and Technology.

The cut-off level of cTnI is 0.06 ng mL^{-1}, which is the 99^{th} percentile cut-off concentrations established by ESC/ACC/AHA in the studied population [19]. Consequently, the immunoassay for cTnI detection has to achieve a LOD lower than 0.06 ng mL^{-1}, which is a real challenge. Apart from this, other interference can exist during the assay development, such as phosphorylation and other posttranslational modifications, proteolysis, complex formation with TnC and cross-reactivity with skeletal isoforms [58]. Thus, antibodies used in the assay have to recognize different cTnI forms presented in blood with same efficiency which evolves to the need to look for an optimal immunogen design and antibody selection. All this problematic is better explained in chapter 3.

1.6.6 BRAIN NATRIURETIC PEPTIDES

Brain natiuretic peptide (BNP) is a peptide hormone that belongs to a family of structurally similar peptide hormones like atrial natriuretic peptide (ANP), C-type natriuretic peptide (CNP) and urodilatin. All of them have a 17 aa ring structure with a disulfide bond between two cysteine residues which is the part that binds to specific receptors, showing a high homology between the different natriuretic peptides (11 out of 17 are identical). The two terminal parts show a high degree of variability among them. ANP and BNP are synthesized and secreted mainly by cardiomyocytes, although ANP is produced in the atria while BNP in the ventricles particularly in patients with chronic cardiac diseases [59]. By contrast, CNP expression is mainly found in vascular endothelial cells, neurons and Leydig cells in the testicles. The receptors of these hormones have a broad distribution, apart from the vasculature and kidneys they are present in the adipose tissue, liver, pancreas and brain [60].

BNP is the product of a proteolytic process of preproBNP, which is composed of 134 aa and is synthesized in cardiac myocytes. Once signal peptide (aa 1-26) is removed, it results the proBNP molecule with 108 aa which is processed by a convertase-dependent cleavage rising NT-proBNP (aa 1-76) and BNP (aa 77-108). The two last peptides as well as their precursor are circulating in the bloodstream (see Figure 1.14).

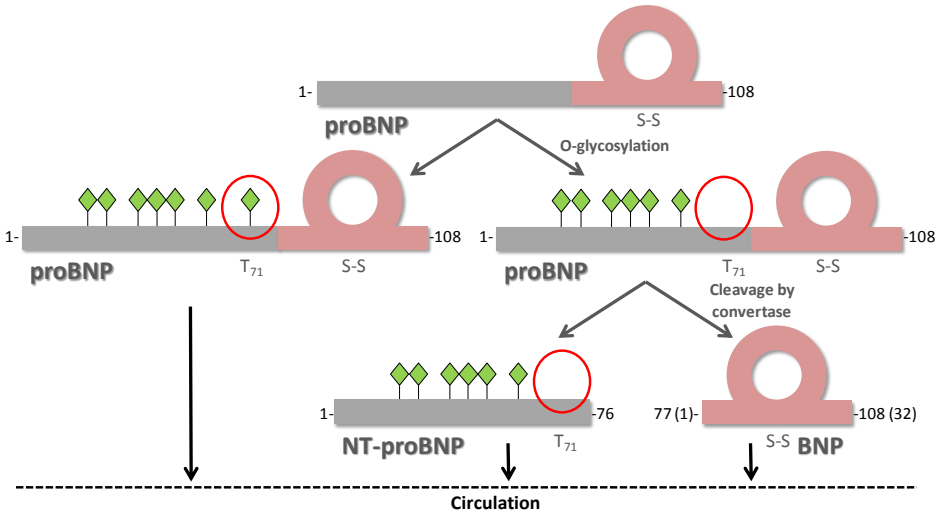

Figure 1.14. Schematic representation of proBNP processing.

As it can be observed in the above picture, proBNP is an O-glycosylated protein with seven O-glycosylation sites: T_{36}, S_{37}, S_{44}, T_{48}, S_{53}, T_{58} and T_{71} [61]. Glycosylation of the region near the proBNP cleavage site, especially threonine 71 (T_{71}) is crucial for its processing. Therefore, proBNP molecules in human blood are glycosylated in T_{71}, whereas in NT-proBNP this aa is not glycosylated. NT-proBNP glycosylation varies from patient to patient, as well as the ratio proBNP/BNP although proBNP is the predominant form in patients suffering from heart failure (HF) [62, 63].

For several years, two proprotein convertases, furin and corin, have been discussed in the literature as possible candidates for proBNP cleavage but this question still remains unanswered. Regarding furin, the presence of arginine residues at the P1 and P4 positions (i.e., number of residues N-terminal of the cleavage site) is the requisite condition for substrate recognition and proBNP has the corresponding at R_{73} and R_{76} [64]. R_{73} is one aa residue separated from

T_{71}, thus glycosylation of this last aa hampers furin-mediated cleavage of proBNP. On the other hand, corin is also proposed as a BNP convertase although Tonne et al. suggested that it may not process intracellular proBNP [65].

BNP peptide mediates a variety of biological effects when interacting with the natriuretic peptide receptor type A (NPR-A) causing intracellular cyclic guanosine monophosphate (cGMP) production. BNP physiological effects comprise natriuresis/dieresis, peripheral vasodilatation and inhibition of the rennin-angiotensin-aldosterone system (RAAS) and the sympathetic nervous system (SNS). This peptide is cleared from plasma by binding to natriuretic peptide receptor type C (NPR-C) and through proteolysis by neutral endopeptidases (see Figure 1.15). Oppositely, NT-proBNP is mainly cleared by renal excretion. Due to the biological activity of BNP, its half life is 20 min whereas for NT-proBNP is 120 min. This explains the fact that NT-proBNP basal levels are approximately six times higher compared to BNP values, although both are released in equimolar proportions [66].

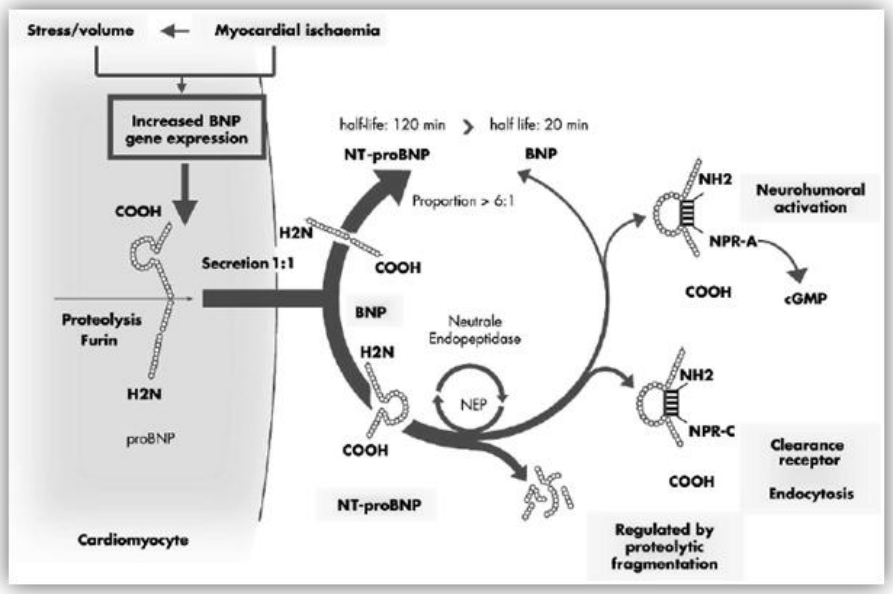

Figure 1.15. Schematic illustration of BNP and NT-proBNP synthesis, release and receptor interaction. Figure copied from [66].

ProBNP synthesis increases in response to cardiac wall stretch, which results in increased of BNP, NT-proBNP and itself in blood. Elevated level of both peptides have been described for patients with different cardiac pathologies and all three are well established cardiovascular biomarkers for prognosis and diagnosis of **heart failure (HF)** as it has already been mentioned in section 1.5.2 of this same chapter. European Society of Cardiology (ESC) guidelines recommend 0.4 ng mL^{-1} for NT-proBNP and 0.1 ng mL^{-1} for BNP as cut points [23].

In chapter 4, the development of antibodies and immunochemical techniques for brain natriuretic peptides will be deeply described. It will be important to consider then that glycosylation sites negatively affect antibodies access and recognition. Thus, not glycosylated epitopes of these peptides are highly recommended for their immunoassays development.

1.7 REGULATION AND GUIDELINES

In order to succeed in the adequate measurement of the cardiac markers chosen and the correct interpretation of the results provided by their corresponding tests, the regulation established by the following guidelines (Table 1.3) and the analytical parameters explained underneath need to be considered and fulfilled.

Table 1.3. Regulation of different aspects related to the assay development for cardiovascular biomarkers determination and their application.

Scientific bodies	Regulation	Ref.
ESC, ACC 2000 ESC, ACC 2002 ESC, ACC, AHA, WHF 2007	Redefinition of MI	[67], [68], [69]
ACC and AHA 2002	Management of patients with UA and non-ST-segment elevation MI	[70]
NACB 2007	Clinical characteristics and utilization of biochemical markers in ACS (chapter 1)	[21, 71]
NACB and IFCC Committee 2007	Analytical issues for biochemical markers of ACS (chapter 2)	[21, 72]

NACB and IFCC Committee 2007	Clinical utilization of cardiac biomarker testing in HF (chapter 3)	[21]
NACB and IFCC Committee 2007	Analytical issues for biomarkers of HF (chapter 4)	[21, 73]
NACB and IFCC Committee 2007	Point of care testing, oversight and administration of cardiac biomarkers for ACS (chapter 5)	[21]
NACB 2007	Use of cTn and BNP or NT-proBNP peptide for etiologies other than ACS and HF (chapter 6)	[21]
ESC 2008	Diagnosis and treatment of acute and chronic HF	[23]
NACB 2009	Emerging biomarkers for primary prevention of CVD	[22]
ACC and AHA 2013	Guideline for the management of HF	[24]

Relevant parameters such as turnaround time (TAT) and cut-off levels must be taken into account in the design and development of diagnostic tools addressed to CVDs.

- TURNAROUND TIME (TAT)

TAT is the total amount of time required for the realization of the cardiac test, from the patient arrival to the final result obtaintion. Accordingly to the above guidelines, the results from cardiac marker test should be available within 30 min ("vein-to-brain" time) to start with the therapy in 60-90 min ("door-to-needle" time) after the patient present at the ED.

- CUT-OFF LEVELS

For each cardiac biomarker, reference decision limits should be established in order to differentiate those suffering from a heart disease from those that are healthy. The cut-off value of an assay is then defined as the decision limit based on a population of normal, healthy individuals without a known history of heart disease (reference population).

The scientific committees of ESC/ACC and NACB/IFCC proposed an uniform cut-off criteria in which the 99th percentile of a reference population had to be used as the cut-off point for detection of cardiac injury and that the imprecision at the this point had to have a coefficient of variation (CV) of 10% or less.

Table 1.4 shows the blood levels expected in healthy people and the expected concentrations in the case of CVD above the defined cut-off for the cardiovascular biomarkers chosen in this thesis.

Table 1.4. Basal levels and CVD levels above the cut-off for the different cardiovascular biomarkers chosen.

Biomarker	Basal levels, ng mL^{-1}	CVD levels, ng mL^{-1}
CRP[a]	<1000 low risk	1000-3000 average risk >3000 high risk ≥10000 very high risk
Cys C[b]	~800-1200	≥1290
Lp(a)[c]	$<14 \cdot 10^5$	$>5 \cdot 10^5$
H-FABP[d]	≤ 5.8	>5.8
cTnI[d]	≤ 0.06	>0.06
NT-proBNP[e]	<0.4	>0.4

Data information was obtained from: [a]NACB [22], [b][35], [c] Approximate levels since there exists a great genetic individual. Although further standardization is still needed for Lp(a) analysis, a standardized international reference material has been developed and is accepted by the WHO Expert Committee on Biological Standardization and the IFCC. A desirable level below the 80th percentile is recommended (less than ~50 mg dL^{-1}) [48], [d]99th percentile cut-off concentrations established by ESC/ACC/AHA in the studied population [19], [e]ESC guidelines [23].

2 CONTEXT SCENARIO, OBJECTIVES AND STRUCTURE OF THIS THESIS

2.1 CONTEXT SCENARIO

The present doctoral thesis has been carried out in the framework of three different research projects:

1) Cajal4EU project (Chip architectures by joint associated labs for European diagnostics). *ENIAC (European Nanoelectronics Initiative Advisory Council) Joint Undertaking Action. Subprogramme: Nanoelectronics for Health and Wellness. Programa Nacional de Internacionalización de la I+D. Subprograma de Fomento de la Cooperación Científica Internacional (FCCI) Plan E – Tipo ENIAC. ENIAC-120215.*

This project was addressed to the development of nanoelectronics-based biosensor technology platforms enabling in-vitro diagnostic test manufacturers to rapidly build a variety of new multi-parameter test applications in a robust, user-friendly and cost-effective way. The first prototypes were developed to target diagnostic cases within the area of infectious diseases and cardiovascular diseases. Therefore, the main results of this project were the different technologies developed; sensor technology including bio-chemical functionalization, microfluidics and related hardware and software drivers. The integrated technology aimed to be a generic system solution to be tested in demonstrators to proof integration, cost efficiency and biological application relevance. This project has been performed in close collaboration with end-users and medical companies to realize a valuable impact on the European society and economy.

2) Nanocardiococo project. Nanotecnología para cardiología y pneumococo. *MICINN, Subdirección General de Estrategias de Colaboración Público-Privada IPT-2011-1337-010000.*

Its objective was based on the optimization and development of the functional characteristics of two biosensors, one directed to infectious diseases especially to pneumococo (pneumosensor) and another addressed to cardiovascular diseases. The first one was related to the diagnosis in real time with a microchip for risk episodes, and the second

more preventative and personalized based on obesity indices. In regard to infectious diseases, pneumococcus (Staphylococcus pneumococcus) was selected as a model since it is a bacterium which causes a variety of infectious processes, from pneumonia to meningitis, otitis and sinusitis between others.

3) OligoCODEs project. Universal diagnostic platforms based on oligonucleotide codified nanoparticles and DNA microarray sensor devices. *MINECO, Dirección General de Investigación Científica y Técnica, Subdirección General de Proyectos de I+D. MAT2011-29335-C03-01. MAT2012-38573-C02-01.*

The fundamental of the OligoCODEs approach is the capability to translate any type of biomolecular interaction into a PCR-less DNA amplification process that is finally detected on a DNA-microarray biosensor platform. With the proposed approach, nucleic acids, proteins, peptides or small organic molecules biomarkers could be detected using the same chip and sensor technology, independently from the different chemical nature of the biomarker targets. The technology and tools developed are based on the use of oligonucleotide codified biohybrid gold nanoparticles (oligo(BR)AuNP), biofunctionalized magnetic particles and DNA microarrays on electrochemical sensor transducers. As proof-of-concept the project was focused on the detection of cancer and cardiovascular biomarkers.

In all of them the specific tasks which is part of this thesis was in the area of cardiovascular diseases regarding the production of antibodies and the necessary immunoreagents and bioconjugates for biosensors development, together with the development of immunochemical protocols.

Apart from this, OligoCODEs platform is currently being developed in our group and the final version could be an alternative to adapt the multidetection of several cardiac biomarkers already developed on a fluorescent microarray (see chapter 6). The simultaneous detection of target analytes of different chemical nature and present at very different concentration ranges has been the main challenges. The OligoCODEs platform aims at providing an alternative to these limitations. Thus, by changing the number of oligonucleotide molecules of the

biofunctionalized gold nanoparticles codifying each analyte, it could be possible to modulate the amplification of the signal, and therefore the reaching the necessary detectability.

Finally, preliminary studies addressed to develop a multiplexed optical immunosensor were performed within the frame of collaboration with the Chemical and Biochemical Optical sensor group in the Instituto di Fisica Applicata "Nello Carrara" in Florence (Italy). The investigation was made during a 3-month pre-doctoral stage in such institute under the supervision of Dra. Ambra Giannetti. The objective was to transfer the multiplexed assay from the fluorescent microarray developed in this thesis to an optical immunosensor to be used as a point-of-care (POC) device, which was automated, more portable and suitable for clinical applications.

2.2 OBJECTIVES AND STRUCTURE OF THIS THESIS

The final objective of this thesis has been developing a multiplexed platform able to detect cardiovascular biomarkers involved in the different stages of the disease (see the target selection in section 1.5.2 and 1.6). For this purpose the cut-off levels established for each of them by the different guidelines has to be taken into account. Particularly, antibodies for troponins and brain natriuretic peptides have been produced in this thesis, while other immunoreagents were provided by Audit Diagnostics (Cork, Ireland), a partner from Cajal4EU project, or from other commercial sources. ELISA was used to characterize all immunoreagents, optimize assays, discover the problems and difficulties and investigate the most appropriate solutions before integrating them on a fluorescent microarray chip.

The specific objectives addressed were:

1. Selection of the most relevant target markers

This objective required an exhaustive revision of the literature to get knowledge on the most relevant steps of the disease, the biomarkers involved and the clinical value of them. Moreover, it also claimed to identify the tests

nowadays available in the market and to know their performance in clinical samples. Some of the information collected has already been disclosed in the Introduction chapter and will be described in more detail in the following chapters for some of the most important targets. As results of this literature search, cTnI, brain natriuretic peptides, CRP, Cys C, H-FABP and Lp(a) were identified as relevant targets to develop a multiplexed device. cTnI is the most specific cardiac marker and therefore it is known as the "golden" biomarker. Brain natriuretic peptides, particularly BNP and NT-proBNP, provide information regarding heart failure, which is the last stage after the myocardial infarction. Other not so much specific biomarkers such as CRP, Cys C and Lp(a) start to be altered in earlier steps of the disease. H-FABP levels rise 30 min after chest pain and it has been pointed as an excellent biomarker for diagnosis and long term prognostic if used in combination with troponin.

2. Establishment of immunochemical assays for cardiovascular biomarkers

The aim here was to establish the immunochemical conditions to detect the selected biomarkers and to characterize their performance in clinical samples in terms of sensitivity, specificity as well as other analytical parameters (robustness, accuracy, precision, etc.). For this purpose it was necessary to have access to specific antibodies against the selected markers. In this context, and because of their relevance, we addressed production of antibodies against troponins and the natriuretic peptides. Antibodies against CRP, Cys C and Lp(a) were available from Audit Diagnostics, another partner from the Cajal4EU consortium, while H-FABP was obtained from commercial sources (Randox Laboratories). Thus, the objectives addressed were:

2.1. Development of antibodies against troponins
2.2. Development of antibodies against natriuretic peptides
2.3. Establishment of immunochemical assays for the biomarker targets selected
2.4. Implementation of the immunochemical assays developed to the analysis of clinical samples

3. Development of a multiplexed assay for multidetection

With the immunochemical analytical conditions established and knowing the performance of the immunoreagents, next step consisted on their implementation on a multiplexed platform (chapter 6). For this purpose, we selected the development of a fluorescent microarray. Thus, the multiplexed format would allow the simultaneously determination of several cardiovascular biomarkers, in this case CRP, Cys C, H-FABP, Lp(a), cTnI and NT-proBNP, from the same sample. Thus, specific objectives addressed here were:

3.1. Investigation of the potential cross-reactivities and cooperative phenomena between the different immunoreagents
3.2. Development and analytical characterization of the multiplexed fluorescent microarray
3.3. Implementation of the fluorescent microarray chip to the analysis of human plasma and serum

4. Development of a point-of-care (POC) device

In order to reduce analysis time, facilitate the use and improve portability, a POC device (immunosensor) was developed. This objective was addressed in the context of collaboration between Chemical and Biochemical Optical sensor group at the Instituto di Fisica Applicata “Nello Carrara” in Florence (Italy) within a 3-month pre-doctoral stage. The sensor used was an evanescent wave optical sensor based on the fluorescence anisotropy. As proof of concept, the potentiality of this device as POC was assessed for CRP detection and NT-proBNP detection as individual assays (chapter 7).

As a summary, the structure of the present thesis including the content of each chapter is shown in Figure 2.1. Chapter 8 contains description of the experimental part; while chapter 9, 10 and 11 contain the conclusions and contributions of this thesis, a summary (in catalan language) and the bibliography, respectively. Finally, chapter 12 has the acronyms and the table of figures and tables detailed.

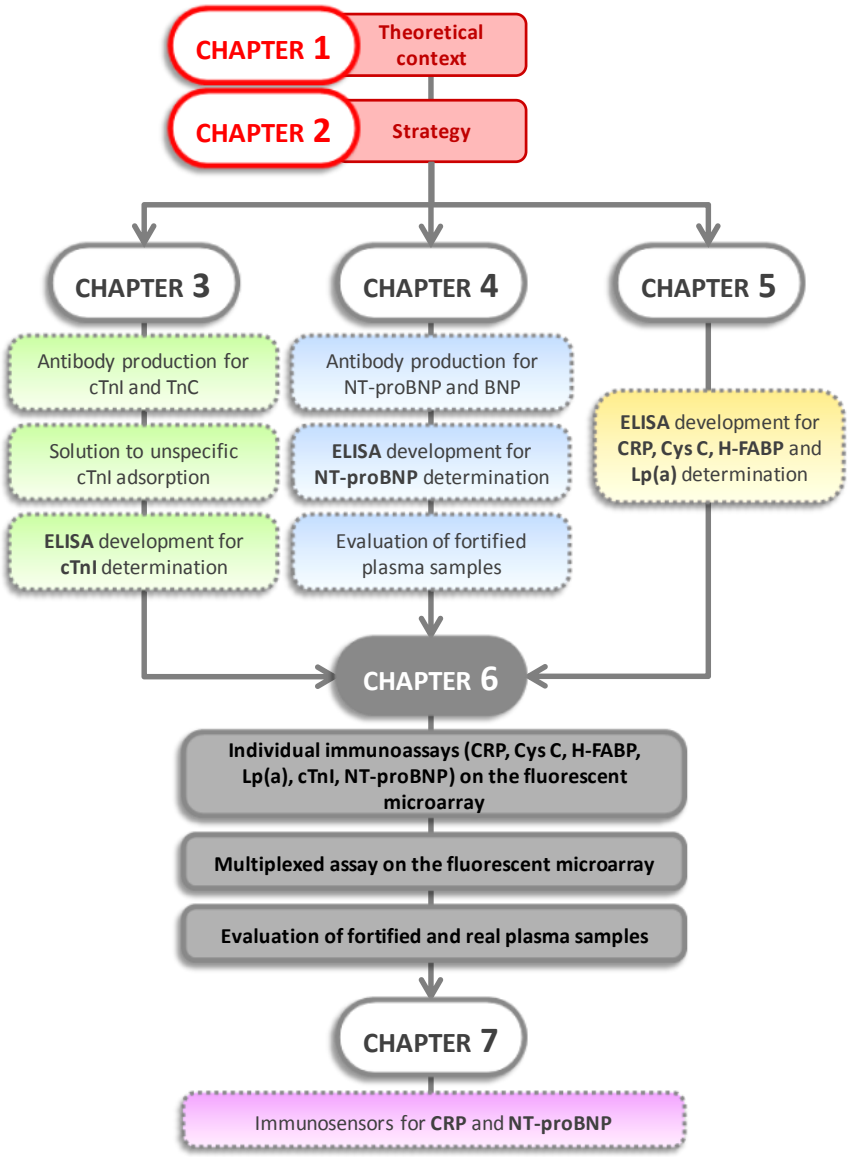

Figure 2.1. The structure of this thesis related to the different chapters and the parts included in each one.

3 DEVELOPMENT OF ANTIBODIES AND IMMUNOCHEMICAL TECHNIQUES FOR TROPONINS

3.1 INTRODUCTION

Troponin is a protein complex in the myofilaments of striated muscles playing an essential role in the calcium regulation of cardiac and skeletal muscle contraction. It consists of three subunits, troponin I, C and T, that have evolved into muscle type-specific isoforms as it has already been detailed in chapter 1 (section 1.6.5).

In this chapter, we describe the scientific efforts made to address immunochemical detection of the cardiac troponin I subunit (cTnI) which can be found circulating in the bloodstream alone or mainly as binary (cTnI-TnC) and ternary (cTnI-TnC-cTnT) complexes. TnC interacts with cTnI and the strength of this interaction is sharply increased in the presence of Ca^{2+} [74]. When developing antibodies against proteins such as cTnI it is very important to take into consideration all the potential interfering aspects that may influence further detection of the biomarker. Thus, aspects such as proteolytic degradation of the cTnI molecule, oxidation, reduction, phosphorylation, complex formation with TnC or cTnT, or the presence of heparin in the samples should be taken into account. For this purpose, a deep knowledge of the chemical structure and function of cTnI was considered essential.

The primary structure of cTnI can be divided into six segments: the cardiac specific N-terminal extension ($cTnI_{1-30}$) that contains protein kinase A (PKA) phosphorylation sites $Ser_{23/24}$; the N-terminal region ($cTnI_{34-71}$) that binds the C-domain of TnC and contains two protein kinase C (PKC) phosphorylated serines; the TnT binding region ($cTnI_{80-136}$); the inhibitory peptide ($cTnI_{128-147}$) that interacts with TnC and actin-tropomyosin; the switch or triggering region ($cTnI_{147-163}$) that binds the N-domain of TnC; and the C-terminal region ($cTnI_{164-210}$) that binds actin-tropomyosin (see Figure 3.1). There are also skeletal muscle troponins. The main difference between the cardiac and the two skeletal muscle TnI isoforms is the N-terminal extension which does not have binding sites for other thin filament proteins, but it is a regulatory structure that modulates the overall molecular conformation and the interaction of cTnI with the other Tn subunits [75]. Thus, the N-terminal segment of cTnI has a potential use in improving the specific detection of AMI and the N- and C- terminal extremities were found to be the strongest antigenic regions [76].

Phosphorylation of cTnI in the complex with the N-terminal fragment of TnC also results in a significant decrease in the affinity of Ca^{2+} [74].

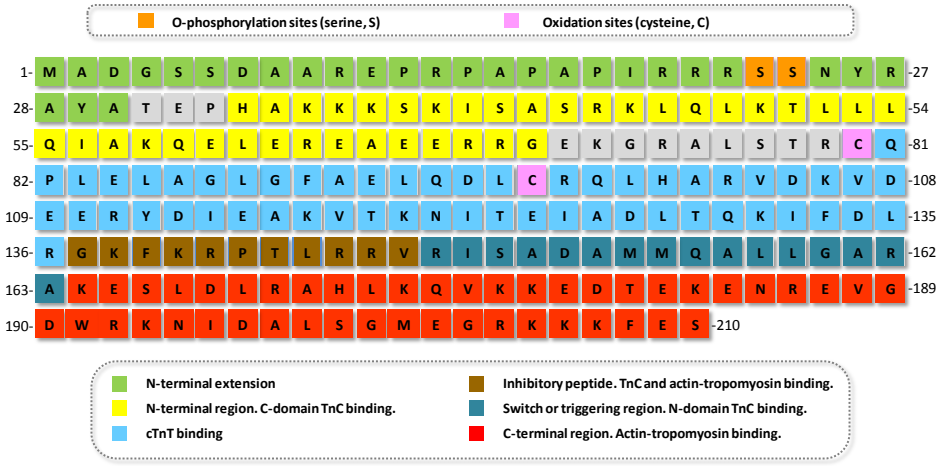

Figure 3.1. Scheme of cTnI primary structure and its division in six determined segments. Aa 30-110 is considered the most stable part due to its protection by TnC.

The post-translational modifications involved in cTnI are: cleavage of the primary structure (proteolytic modification) [77] and aa side chain modifications such as phosphorylation. This last one is regulated by protein kinase A and C (PKA and PKC) and PKA substrate are two adjacent serine residues, $Ser_{23/24}$, in the N-terminal extension and it mainly affects the overall Ca^{2+} sensitivity of force development and weakens the interaction between the region next to the phosphorylation sites and TnC. In like manner, proteolytic degradation provides a rapid mechanism to alter protein functions, the following ones have been found during myocardial adaptation to stress conditions but they do not affect the association with other subunits.

- C-terminal truncation: A proteolytic truncation of the last 19 aa at the C-terminus was found during myocardial ischemia and reperfusion injury. This fragment is an allosteric element that participates in the Ca^{2+} regulation of troponin. It is highly conserved among the muscle type-specific isoforms. Therefore, any detection of this C-terminal fragment needs to be validated for its tissue source for differential diagnosis of AMI from skeletal muscle injury or disease.
- Selective removal of the N-terminal extension: A proteolytic N-terminal truncation of cTnI (aa 1-30) is found in normal cardiac muscle with

significantly increased levels during hemodynamic adaptation. This selective removal is an effective regulation of cardiac function under physiological and pathological stress conditions. Although is the most heart specific portion of cTnI, its detection may reflect not only acute damage of cardiac muscle, but also chronic adaptations.

Apart from the phosphorylation that can cause structural and conformational changes that can significantly affect the binding of some antibodies to cTnI and the proteolytic modification, the two cysteine residues in positions 80 and 97 (see Figure 3.1) can form a disulfide bond allowing cTnI to be found in oxidized and reduced forms, again affecting the antigen recognition. Because the cTnI molecule has a high positive charge (pI 9.87) it will attract negatively charged molecules such as heparin, which in turn can also interfere with the antibody-antigen recognition. The use of EDTA as an anticoagulant influences the association of the ITC complex, because EDTA can cause partial unfolding of the calcium-dependent troponin complex.

In addition, other interfering factors (probably anti-cTnI autoantibodies) bind to the central region of the cTnI molecule, aa 87-91 appear particularly susceptible, and the presence of heterophilic antibodies and human autoantibodies together with fibrin strands due to incomplete clotting can interfere and cause false positive results. Moreover, some of the regions on the stable part of the molecule appear to contain sites of interaction with cTnT and TnC [78, 79].

As a consequence of all these possible modifications and interferences, some companies have switched to a dual capture and/or detection antibody assay format to optimize analytical sensitivity. It is important to consider all the characteristics mentioned above in the design and development of cTnI immunoassays, although it also represents a great challenge.

Over the years the analytical sensitivity of cTnI assays has been improved and a new generation of assays, high-sensitivity (hs) cTnI assays, have been introduced into routine clinical practice. They permit measurement of cTnI with <10% imprecision at the 99^{th} percentile reference value (defined as the recommended upper reference limit; the analytical limit of detection is in the single digit range of ng L^{-1}). Thus, hs-cTnI assays are believed to improve both early diagnosis and short and long-term risk stratification. Despite all this, at

least two measurements of hs-cTnI test results to verify a kinetic pattern are required and samples should be obtained at the time of presentation and 3h after admission when using these hs assays. It is important to take into account that cTn is a marker of myocardial necrosis but not a specific marker of AMI. AMI should only be diagnosed when there is a rise and/or fall of cTn together with characteristic symptoms and/or ECG or imaging evidence of acute myocardial ischemia.

3.1.1 IMMUNOASSAYS IN THE LITERATURE

Assays for the detection of cTnI circulating in the bloodstream have already been developed and published in the literature, all of them in a sandwich format. Until now, a large number of assays have been published and just some of them are summarized in the following table (Table 3.1).

Table 3.1. Characteristics of different cTnI immunoassays reported in the literature

	Capture antibody (recognized aa)	Detection antibody (recognized aa)	Sample	LOD (ng mL^{-1})	Working range (ng mL^{-1})	t_{assay} (min)	Ref.
FIA	MAb_1-biotin, MAb_3-biotin (35-55,20-35)	MAb_2-Eu^{3+}, MAb_4-Eu^{3+} (80-95,185-200)	Serum, EDTA plasma	0.02	-	125	[78]
	2 MAb (41-49,110-x)	MAb (110-x)	Serum	-	-	-	[79]
	MAb-biotin[a] (free cTnI:C-terminal) (total cTnI:34-37)	MAb-Eu^{3+a} (free cTnI:56-61) (total cTnI:C-terminal)	Serum	-	-	63	[54]
	MAb-biotin[b] (aa central region)	MAb-Eu^{3+b} (N-terminus aa, C-terminus aa and 41-49-central region)	Serum	0.1	0.3-100	63	[57]
	MAb: cFab (190-196)	MAb-(NP-Eu^{3+}) (41-49)	Plasma	$4.1 \cdot 10^{-4}$	0-10	75	[80]

ELISA	MAb: 91-94	MAb-HRP:31-34 MAb-HRP: 15-26	Plasma	$7 \cdot 10^{-3}$	-	135	[81]
	MAb	MAb-biotin (+ Avidin-AP)	Serum	1.9	-	195	[82]
	Goat anti-cTnI Ab	MAb_1 MAb_2	Serum	0.1	-	115	[83]

[a]Two different MAbs combinations were used for the detection of free TnI and for measurement of total TnI in the presence of EDTA. [b]Two different combinations were used for the detection of cTnI using antibodies against the stable part (aa 30-110) or the C- and N-terminal regions. NP-Eu^{3+}: europium (III)-chelate doped Fluoro-Max^{TM} polystyrene nanoparticles, AP: alkaline phosphatase.

On the basis of what has been found in the literature, antibodies against the N- and C-terminal regions have shown good performance measuring cTnI probably due to its antigenicity and because the N-terminus is the most specific part; however, both parts are very susceptible to degradation. On the other side, cTnI assays that use antibodies against epitopes situated in the central, more stable part of cTnI, give falsely low cTnI concentrations in samples containing the interfering factor. Therefore, it has been proposed that a combination with N- and C-terminal antibodies ("interference-free") and antibodies against mid-fragment would provide the best alternative together with better recoveries and less false positive samples [78]. Le Moal et al. demonstrated that the combination based on a MAb against the mid-fragment (central part) as a capture and the mixture of two antibodies, one against the mid-fragment and another against the N-terminal part, as detection MAbs, provided the best clinical sensitivity compared with other combinations employing the same and other MAbs [81]. Moreover, according to Hyytiä et al., removal of Fc-part of capture antibodies in cTnI immunoassays was clearly the most effective way to decrease non-specific binding, improving the detection limit and reducing reagent consumption [80].

While Le Moal et al. [81] were employing ELISA in their study, Eriksson et al. [78] and Katukha et al. [54, 57] employed FIA.

To sum up, FIA assays detailed on the above table have better limits of detection and shorter assay time. For instance, Bodor's assay does not achieve the LOD required [82]. Because cTnI can be found isolated or inside a

binary/ternary complex, the accessibility of some epitopes is not the same in all cases [84]. Thus, it has been seen that a combination of N- and C-terminal antibodies and antibodies against mid-fragment would be the solution. Finally, special control experiments should be performed to exclude probable effects of EDTA on the detection systems, since EDTA chelates Ca^{2+} and this has an effect in the complex formation.

3.1.2 COMMERCIAL IMMUNOASSAYS

Immunological assays for cTnI are commercially available on many different analytical platforms. While advanced detection platforms have very much improved the sensitivity and efficiency of diagnostic troponin assays in the recent years, challenges remain regarding the cardiac specificity and interpretation of results for the nature of myocardial injuries.

The first commercial immunoassay for cTnI was a double monoclonal antibody-based immunoenzymometric assay offered by Sanofi Pasteur [85] and applied to aid in the diagnosis of myocardial injury. The diagnostics business of “Sanofi Diagnostics Pasteur” along with its Access immunoassay analyzer system was later acquired by Beckman Coulter. The first cTnI assay run on an automated analyzer was also a monoclonal antibody-based assay developed by Baxter Stratus for clinical applications [86]. The Baxter Diagnostics division was acquired by Dade and subsequently Dade Behring was acquired by Siemens. Besides Stratus, Siemens also owns Dimension Vista (acquired from Dade Behring), ADVIA Centaur (acquired from Bayer Diagnostics) and Immulite (acquired from DPC: Diagnostic Products Corporation).

Diagnostic products from different original manufacturers employ a range of different technologies, formats and combinations of monoclonal and/or polyclonal antibodies (MAbs, PAbs). Unfortunately, there is a lack of standardization of the measurements which leads to significant differences in results obtained between cTnI assays when measuring the same samples. Variations between 20- to 40-fold or more have been reported among the first generation cTnI assays [87]. This variation was later reduced [88] but still there are important discussions in this respect. It exists a huge amount of literature reporting comparison and performance of the different tests that can be found

in the market and also the risk of overusing those tests [89-93]. Interpretation of the results is difficult and should take into account also the clinical history of the patient, but the method used for the measurement of the biomarker also has an influence.

Assays for cTnI could be two-site, three-site, or four-site immunoassays, depending on the number of capture and detection antibodies used. The capture antibody is immobilized on a solid phase and can specifically bind the troponin present in the sample. The captured troponin is then sandwiched and bound by a second antibody and in some assays a third or fourth antibody that is coupled to an indicator molecule. The assays vary from each other depending on which immunoassay technology chosen, the types of antibody used, the epitopes to which they bind, the indicator molecules used and how signals from those molecules are converted to a numerical value. For instance, enzyme systems are used to tag the detection antibody which amplifies the reaction and generates optical density (OD) reading signals. The most frequently used enzyme systems include horseradish peroxidase (HRP) (Ortho VITROS cTnI) and alkaline phosphatase (AP) (cTnI assays on Abbott AxSYM, Abbot i-STAT, Beckman Coulter Access, bioMerieux Vidas, Mitsubishi PATHFAST, Siemens Dimension RxL, Siemens Stratus CS, Tosoh ST AIA-PACK, Siemens Stratus CS and Tosoh ST AIA-PACK).

Another strategy is to use fluorescence or gold nanoparticles, which are utilized by some point-of-care assays. Many of these assays use magnetic or paramagnetic nanoparticles to serve as a solid phase for capture, which facilitates washing and enhances sensitivity. Other “labels” or “tags” on the detection antibody for cTn assays include fluorescent organic molecules (Alere Triage, Response Biomedical RAMP), europium (Radiometer AQT90 FLEX), chemiluminophore acridinium (Abbott Architect, Siemens Centaur) and electrochemiluminophore ruthenium (Roche Elecsys, Roche Cobas e system). All these assays are summarized in Table 3.2, where they are divided in three groups: the “high-sensitivity” assays which are the newest generation, the “contemporary assays” which are the improved or updated versions of the first version assays and the point-of-care devices.

Table 3.2. Comparison of test principles and analytical performance of high-sensitivity, contemporary and point-of–care (POC) cTnI assays.

Assay	Test principle, components	LOD (pg mL^{-1})	99th percentile (pg mL^{-1})
High-sensitivity assays (in various stages of clinical evaluation and regulatory clearance processes)			
Abbott Architect hs-cTnI	CLIA, MP	1.1-1.9	16-26.2
Beckman Coulter Access2 / UniCel DxI AccuTnI+3 hs-cTnI	CLIA, paramagnetic particle	2-3	8.6-32
Siemens Dimension Vista hs-cTnI	LOCI	0.5-0.8	9-58
Singulex Erenna hs-cTnI	Quantitative FIA, paramagnetic MP and microplate	0.09-0.2	10-40
Contemporary assays			
Abbott Architect STAT cTnI	CLIA, paramagnetic MP and acridinium detection	9-10	12-40
Abbott AxSYM ADV cTnI (2nd generation)	Fluorescent MEIA, three-step assays	<10-20	34-40
Beckman Coulter Access (2nd generation) cTnI, Access 2 modified-sensitive cTnI	CLIA, two-site immunoenzymatic sandwich assay	<10-10 2.5	40 56
Mitsubishi Kagaku Iatron P cTnI PATHFAST	CLIA, immunoenzymatic with Magtration® Technology	8-20	29
Ortho-Clinical Vitros ECi / ECiQ Troponin I ES	Immunometric immunoassay, Intellicheck® Technology	<10-12	19-34
Roche Elecsys cTnI / cobas e601 cTnI	ECLIA, two-step sandwich assay, streptavidin MP, ruthenium label	160	160-184
Siemens Centaur cTnI Ultra	CLIA, three-site sandwich immunoassay	<6-6	12-40

Siemens Dimension Vista cTnI / Dimension EXL 200 cTnI, Siemens Dimension RxL cTnI	LOCI	15-17 40	21-56 70
Siemens Immulite 1000 Turbo / Immulite 2000 XPi cTnI / Immulite 2500 STAT	CLIA	100	200-392
Tosoh AIA-Pack cTnI (2nd generation)	FIA, individual test cups base on the AIA-Pack technology	60	60
POC devices			
Abbott i-STAT cTnI	ELISA, AP cleaves the substrate to produce amperometric signal	20	39-80
Alere Triage cTnI / Triage SOB, Alere Triage revised cTnI, Alere Triage Cardio3	FIA	50-190 10 10	40-190 12-56 20-22
BioMerieux Vidas cTnI Ultra	ELFA	<10	<10
Radiometere AQT90 Flex Troponin I	Time-resolved FIA, europium chelate as fluorescent label	9-9.5	23
Response Biomedical RAMP® Troponin I	Quantitative immunochomatrographic FIA	30-200	<10-100
Siemens Stratus CS cTnI	FIA, AP	<18-30	40-200

CLIA: chemiluminescent immunoassay, MP: microparticles, LOCI: luminescent oxygen channelling immunoassay, this technology is explained in section 4.1.2 (chapter 4), FIA: fluorescent immunoassay, MEIA: microparticle enzyme immunoassay, ECLIA: electrochemiluminescent assay, ELFA: enzyme-linked fluorescent immunoassay. This overview of test principles and selected analytical characteristics of cTnI assays was summarized based on manufacturer's product information, FDA 510k database, (IFCC 2012), and additional literature references [94-96]. LOD and 99th percentile concentration values were collected from recent studies and reported as a range. Table adapted from [97] (not yet published).

In the above table, it can be observed that high sensitivity assays show improved sensitivity at very low troponin concentrations what can improve both early detection and risk stratification. Therefore, clinical interpretation also needs to take the improvement into consideration and, importantly, cTnI values from one assay cannot be interchanged with other assay.

In addition to the different technologies used by different manufacturers, the variable antibody reactivity towards different cTnI forms and differences in the reference materials used in the assay calibration may also contribute to differences in cTnI assay results. The more frequently selected epitopes in the previous cTnI assays include the following aa sequences: 24-40, 41-49, 87-91 and 136-149. As an example, in Figure 3.2, sequences chosen for different Abbott platforms are represented.

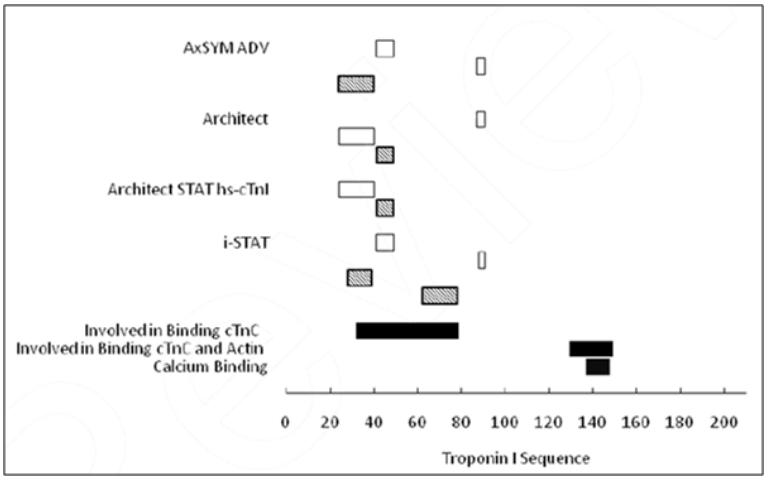

Figure 3.2. Aa sequence positions for different epitopes recognized by the MAbs (white bars) and detection MAbs (slashed bars) used in different Abbott cTnI assays. The aa sequence corresponding to the epitope recognized by the MAb is as follows: AxSYM (capture 41-49, 87-91; detection 24-40); Architect (capture 24-40, 87-91; detection 41-49); Architect STAT hs-cTn (capture 24-40; detection 41-49), i-STAT (capture 41-49, 88-91; detection 28-39, 62-78). The sequence information was obtained from the Uniprot database which shows the amino acid sequences from calcium binding, for binding cTnC, and for binding cTnC and actin (solid black bars). Figure copied from [97] (not yet published).

3.1.3 OBJECTIVES AND SPECIFIC TASKS

A great number of immunoassays for the determination of cTnI have been developed and published in the literature. However, the aim of the current thesis is the development of a platform for the multidetection of different cardiovascular biomarkers involving also cTnI. Thus, there is the need to develop an immunoassay for cTnI achieving one of the greatest challenges, the high sensitivity required. For this purpose, we addressed development of antibodies and the development of an ELISA for the determination of cTnI, also known as the "golden" cardiovascular biomarker. Since the interest was focused to detect isolated and complexed cTnI, antibodies for TnC were also produced.

In order to accomplish such aim, specific objectives were planned for each target.

- Design and synthesis of appropriate haptens
- Production of antibodies
- Development and optimization of the microplate-based ELISA

Two different antibody productions were done (1st and 2nd generation), in the first one, the native protein was used as immunogen, on the second one, we addressed the production of antibodies against particular 10-15 aa sequences of the protein, selected taking into account the above mentioned properties of the molecule. In this thesis, we will only describe the development of the ELISA that uses the 1st generation antibodies. The second generation of antibodies were designed and produced as consequence of the results obtained with this ELISA, but their further screening, evaluation and their employment for a new and improved ELISA assay has been performed by Àlex Hernandez within the context of his PhD thesis.

3.2 ANTIBODY PRODUCTION FOR NATIVE CTNI AND TNC: 1ST GENERATION

Native cTnI and TnC were used to first immunize white New-Zealand rabbits to obtain polyclonal antibodies. Two rabbits were used for each immunogen and the antisera produced were called As 220 and 221 for cTnI and As 222 and 223 for TnC. The evolution of the antibody titer was assessed by non-competitive indirect ELISA (see procedures in section 8.1.2).

While for cTnI a good antibody titer evolution was observed, no response was obtained for TnC. Although the molecular weight is high enough (18416 g mol^{-1}), the 3rd immunization was performed with TnC coupled to horseshoe crab hemocyanin (HCH).

Molecules with a low molecular weight (MW <2000 g mol^{-1}) are not able to stimulate the immune system of the host animal by themselves [98, 99]. For this reason, it is necessary to covalently couple these molecules properly functionalized (haptens) to a bigger protein in order to get immunogenic bioconjugates. HCH was chosen to prepare the immunogen since it is a protein with a high molecular weight (3300 kg mol^{-1}), based on 48 units linked as eight hexamers in which each unit has 628 aa and a MW of 72.6 kg mol^{-1}. This circumstance added to the fact that it is isolated from arthropods which are phylogenetically far away from mammals, provides to this protein with high antigenic properties when used to immunize rabbits. A drawback of using this protein is the difficulties to characterize the bioconjugates formed. Thus, HCH is a huge protein and this makes determination of the number accessible lysine amino acid residues for bioconjugation not easy. In the same way, accurate quantification on the number of hapten molecules attached is a challenge. For this reason, bovine serum albumin (BSA) was conjugated in parallel to HCH. BSA is a protein with lower molecular weight (66 kg mol^{-1}) and whose total number of lysines is known (59 residues), from which 30-35 are accessible [100]. The BSA conjugates synthesized in parallel will be used as bioconjugation control but also used as immunoreagents during ELISA development.

In order to choose the optimal cross-linker, a chain of methylene groups with a final functional group (amino, carboxyl, hydroxyl, sulfhydryl, etc.) to allow the coupling would be the ideal one. The final conditions of the coupling reaction

must be those in which the organic solvent does not exceed 10% of the total volume in the protein solution, thus avoiding the denaturalization of the protein.

In this case, bioconjugate was prepared employing dimethyl pimelimidate dihydrochloride (DMP·2 HCl) as cross-linker to obtain TnC-DMP-HCH. In parallel, the TnC-DMP-BSA bioconjugate was also prepared which thus to test antibody titer and for characterization.

DMP·2 HCl is a homobifunctional reagent with two imidoester groups that allows amino-amino coupling generating stable amidine linkages. The 7-atom bridge obtained with DMP is positively charged at pH 7.5 (physiological pH) due to the protonated amidine bonds and pH 8-9 must be used to be reacted with amine-containing molecules (Figure 3.3) [101]. The reaction could not be completely controlled and a mixture of bioconjugates was probably obtained, this time including protein-protein or peptide-peptide oligomers. MALDI-TOF-MS analysis of the BSA conjugate could not be recorded and it was characterized through SDS-PAGE. In this way it was possible to observe different bands that migrated differently. These results confirmed that the bioconjugation had occurred but it was impossible to quantify the number of TnC molecules attached to the protein.

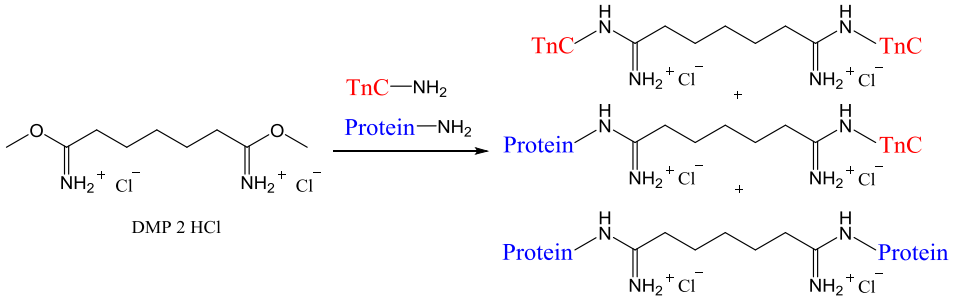

Figure 3.3. DMP reacted with HCH or BSA ("Protein" colored in blue) and TnC (colored in red) to form amidine bonds. Different products are possible due to the self-polymerization.

Antibody titer was followed by coating the microplates with cTnI for As 220 and As 221 and with TnC-DMP-BSA for As 222 and 223. As it can be observed in Figure 3.4, specific antibodies for cTnI were detected from the very beginning with a good evolution of the titer although a slight decrease of the response was observed at the end, probably due to the maturation process [102] which

usually means that although the amount of antibodies does not increase there is an enrichment of those antibodies produced by the more specific clones. It can be also observed that As 220 presented higher response compared to 221 which would allow a greater dilution when developing the sandwich immunoassay.

For TnC, specific antibodies could not be obtained neither when native TnC was immunized (2nd bleed) nor when using the conjugate TnC-DMP-HCH (3rd bleed). These results prompted us to perform MALDI-TOF-MS of commercial TnC acquired for this purpose, being possible to observe two peaks, one with a molecular weight corresponding to the desired protein (peak at m/z 18568.32) and another with a lower MW corresponding to some kind of impurity or a fragment of the whole TnC (peak at m/z 16893.82). The supplier could not give any explanation for these results and ensured that the protein they served was pure. This fact does not explain the lack of immunoresponse. A possible hypothesis could be related to the homology with proteins of host animal, but this fact has not been probed. A clear rational reason explaining this behavior has not been found until the moment.

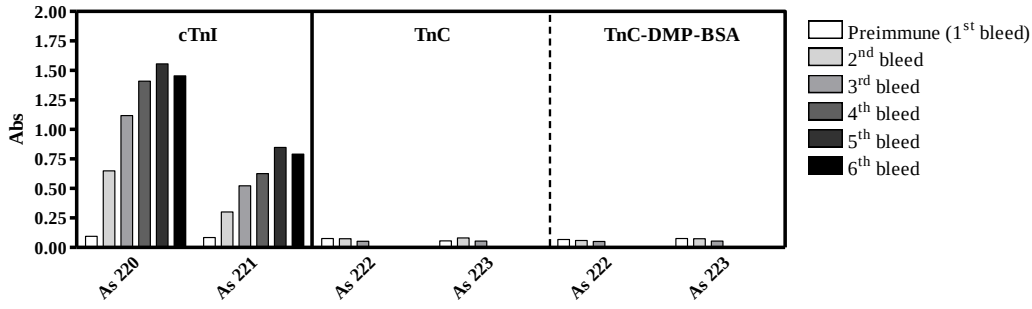

Figure 3.4. Antibody titer to evaluate the response of the antisera produced. For cTnI (1 µg mL^{-1}), As 220 and 221 were 1/32000 diluted and for TnC and TnC-DMP-BSA (1 µg mL^{-1}), As 222 and 223 were 1/1000 diluted.

3.3 ESTABLISHMENT OF THE IMMUNOCHEMICAL ASSAY FOR CTNI: APPROACHING PROBLEMS RELATED FROM THE UNSPECIFIC ADSORPTION OF CTNI

Appropriate concentrations of the capture and detection antibody were established after the corresponding checkerboard titration ELISA experiments (see section 8.2.1). The experiments were done in absence ([cTnI]=0 ng mL^{-1}) and presence of the analyte ([cTnI]=1000 and 10 ng mL^{-1}). In this case, it was necessary to label the antibodies with biotin in order to use horseradish peroxidase (HRP) labelled streptavidin (streptavidin-HRP) to generate the signal. Here, the biotinylation is important because both antibodies, capture and detection, are produced in rabbit and an anti-rabbit IgG could recognize both of them. The procedure followed for the antibody biotinylation is described in section 8.1.3.

The first problem observed was the non-specific signal probably due to the non-specific adsorption of the cardiac troponin I (cTnI) to the microplate surface or even to the antibody. Thus, great efforts were invested to solve this issue in collaboration with Àlex Hernández from the Nb4D group, who joined this research line after the production of the antibodies. It is worth mentioning that the tendency of cTnI to non-specifically bind surfaces and biomolecules has already been discussed by many authors [80, 83, 103] and that such problem has even been admitted by highly specialized suppliers such as Hytest (Turku, Finland), one of the main providers of immunoreagents and standards for cardiac markers. Such supplier recommended using the Tn I-T-C complex to avoid such problem. However, due to the high cost of such reagent and to the fact that many research papers were using cTnI without apparently any problem, we decided to pursuit with the use of such troponin unit. Therefore, as you will see in the next pages, many experiments are still done with cTnI while others are performed with Tn I-T-C complex.

All experiments are performed as schematized in Figure 3.5. As 220 purified by ammonium sulfate precipitation (Ab 220) was used as capture antibody once immobilized on the Immulon™ 2HB microplates. As 221 was also purified using the same methodology and labelled with biotin to be used as detection antibody. Finally, commercial streptavidin-HRP was added to catalyze the redox

reaction of TMB and H_2O_2 (substrate solution) and acquire the absorbance signal. All the experimental procedures related to the purification and biotin labelling of the antibodies are described in section 8.1.2 and 8.1.3.

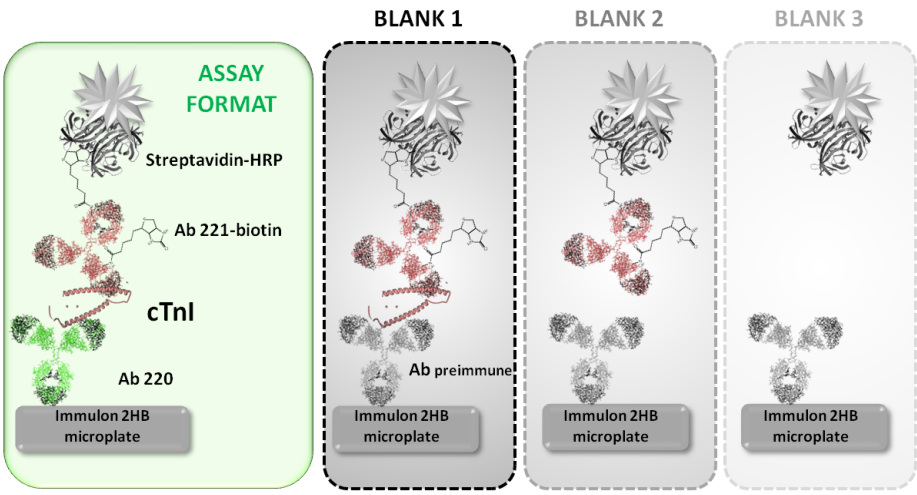

Figure 3.5. Schematic representation of the assay format for cTnI detection and the three blanks realized with different additives added in the analyte step to solve the non-specific adsorption. In all three blanks a preimmune antibody is used for the microplate coating.

On a first series of experiments and exhaustive study in which different microplate brands and types were tested, Immulon™ 2HB (Thermo Fisher Scientific) was selected because of the lower non-specific signal, even if this effect was not completely eliminated by just using such microplates. Immulon™ 2HB plates are described by its commercial source to have a high binding surface, thus providing increased binding of hydrophilic proteins and complexes. NUNC® MaxiSorp™ plates, the most common plates used in our group for ELISAs, have a particular surface treatment that confers high affinity to molecules with mixed hydrophilic/hydrophobic domains. It has been described that troponin I is a polar protein with an excess of positively charged residues and its calculated pI is approximately 9.9 [74].

Next series of experiments, addressed to minimize the adsorption of the cTnI on the surfaces, were based on the effect of additives in the assay buffer. Thus, different additives such as BSA, polyethylene glycol (PEG), gelatin, polyvinylpyrrolidone (PVP), milk, polyvinyl alcohol (PVA) and casein were added to the assay buffer (at 2% of the final volume in PBST). It is known that PEG is

normally added to block hydrophobic interactions, while casein and milk are used to block hydrophilic and ionic interactions and PVP for anionic interactions.

The experiments were performed assessing the signal of the sandwich assay using three different concentrations of cTnI (1000, 10 and 0 ng mL^{-1}). Moreover, three different blanks were always introduced using a preimmune antibody as capture antibody on the Immulon 2HB microplates:

I. Blank 1: everything was performed as in the normal experiments except for the fact that the capture antibody was not specific.
II. Blank 2: NO cTnI, only PBST buffer was added at the step were the analyte had to be added.
III. Blank 3: NO analyte and NO detection antibody, only the corresponding buffers with the same incubation times.

In this way, non-specific adsorptions of all reagents employed in the assay were checked. The results of these series of experiments are shown in Figure 3.6.

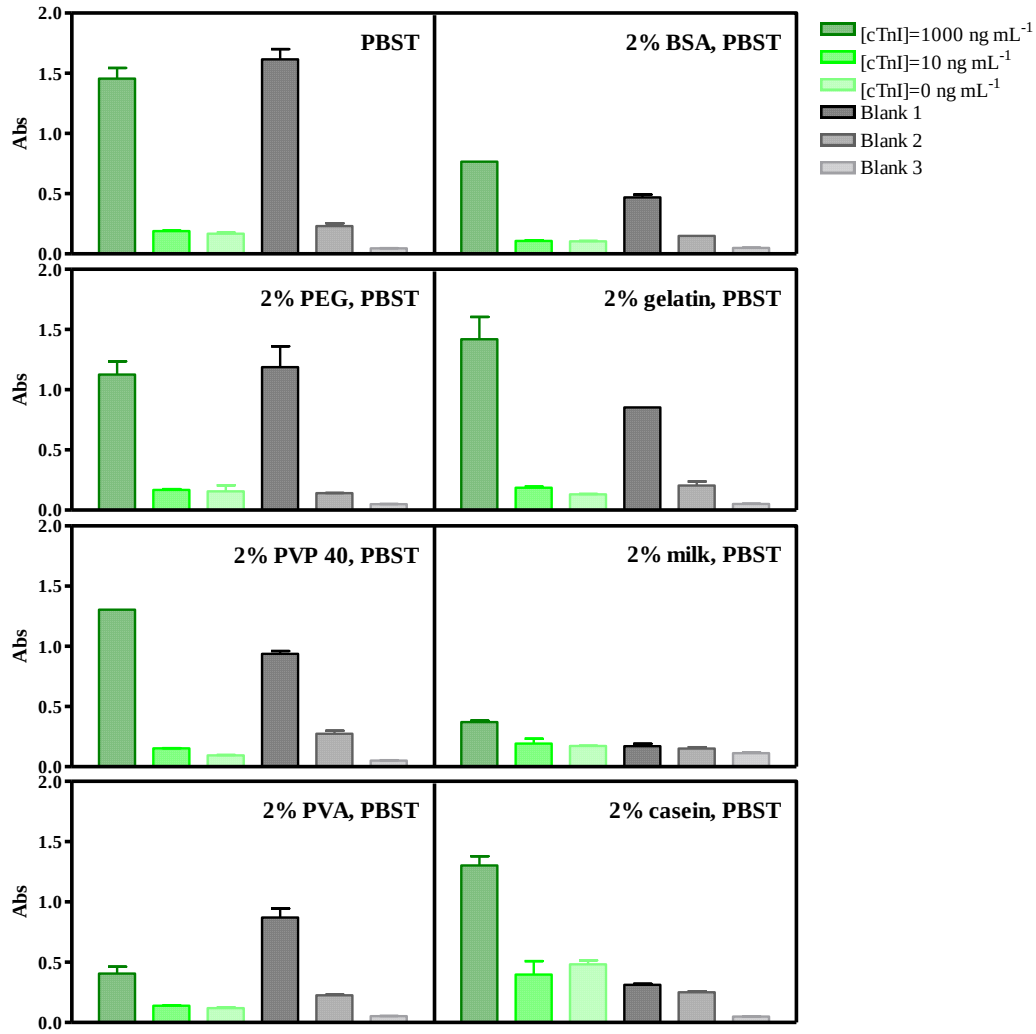

Figure 3.6. Results obtained when using different additives in the analyte step. In all cases, three different concentrations of cTnI (1000, 10 and 0 ng mL^{-1}) are tested together with the three blanks shown in Figure 3.5. In Blank 1, cTnI was added at 1000 ng mL^{-1} and in all cases capture and detection antibody were added at 1 µg mL^{-1}. The standard deviation shown is the result of analysis made one day using two well replicates.

When cTnI is added dissolved in PBST without the presence of any additive, the signal corresponding to the maximum concentration of cTnI is approximately the same than Blank 1. It means that all cTnI added is non-specifically bound on the plate. From all the additives tested, only gelatin, PVP and casein succeeded on reducing the non-specific signal. PEG did not produce any significant effect,

while BSA and even more milk inhibited the specific and non-specific signals in almost a similar extent. PVA produced the opposite effect increasing the signal of the Blank 1 and reducing the specific signal at 1000 ng mL^{-1} of cTnI.

From the three additives that succeeded on reducing the non-specific signal, casein achieved the higher difference between the specific signal at [cTnI]=1000 ng mL^{-1} and that recorded on microplate wells coated with the preimmune antibody. Although the background could not be completely removed, this option was chosen to go on with the development of the assay. As it can be observed in the graph, the background signal observed is on the same order that recorded in the absence of cTnI, therefore it could be due to the non-specific adsorption of the biotin labelled antibody used as a detection antibody. It should be noticed that the use of casein as blocking agent has also been reported by other authors to reduce the non-specific adsorptions of this protein [80, 83, 103]. Further experiments were addressed to find out the best percentage of casein to be employed (seeFigure 3.7).

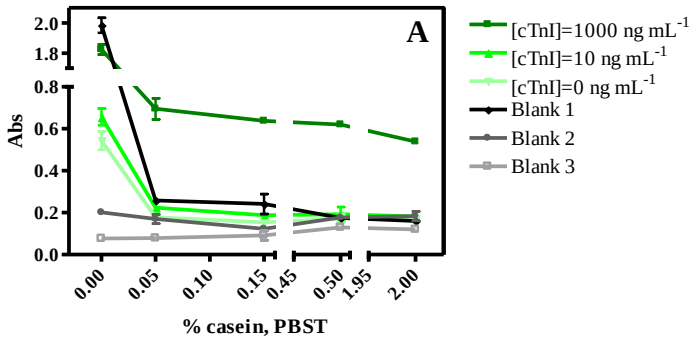

B

% casein, PBST	0	0.05	0.15	0.5	2
[cTnI]=1000 ng mL^{-1} (S)	1.83	0.70	0.64	0.62	0.54
[cTnI]=0 ng mL^{-1} (N)	0.54	0.18	0.15	0.17	0.17
S/N ratio	3.35	3.91	4.16	3.60	3.12

Figure 3.7. A) Results obtained when using different percentages of casein as additive in the analyte step. In all cases, three different concentrations of cTnI (1000, 10 and 0 ng mL^{-1}) are tested together with the three blanks shown in the first figure of this section (see Figure 3.5). B) Signal-to-noise ratio calculation for each percentage of casein. In Blank 1, cTnI was added at 1000 ng mL^{-1} and in all cases capture and detection antibody were added at 1 µg mL^{-1}. The standard deviation shown is the result of analysis made one day using two well replicates.

As it can be observed in the above figure, 0.15% casein in PBST is the percentage in which the best signal-to-noise ratio is obtained, therefore this concentration value was used for further experiments.

Once the optimal buffer was decided, it was employed to confirm the difference between both different kinds of microplates. Figure 3.8 shows comparison of the performance between MaxiSorp™ and Immulon™ 2HB microplates using cTnI and Tn I-T-C complex.

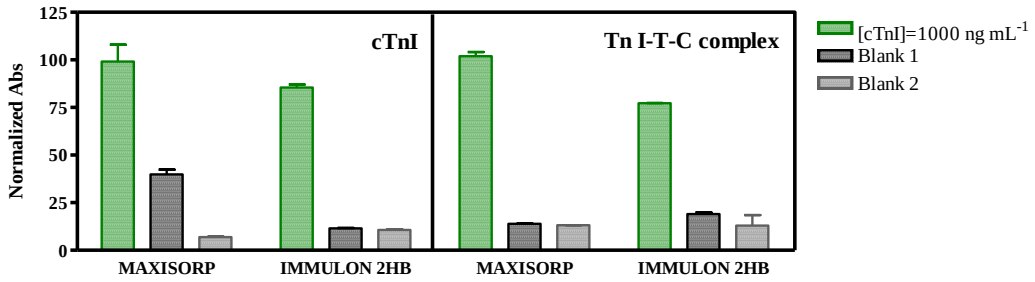

Figure 3.8. Comparison of the signal obtained using the assay format shown in Figure 3.5 with cTnI and Tn I-T-C complex and employing in both cases Maxisorp and Immulon 2HB microplates. In all cases, the analyte at 1000 ng mL^{-1} and blank 1 and 2 are tested. In Blank 1, cTnI was added at 1000 ng mL^{-1} and in all cases capture and detection antibody were added at 2 and 4 µg mL^{-1} respectively. The standard deviation shown is the result of analysis made one day using two well replicates. The analysis for each analyte was performed in two different days and different plates.

As can be observed in the above figure, for cTnI, Immulon™ 2HB microplates provides better signal-to-noise ratio. In contrast, for the ternary complex the differences are not so evident, although apparently the signal-to-noise ratio is slightly better on the MaxiSorp™ plates.

Since in spite of the efforts non-specific signals were not completely removed, on some experiments performed in this chapter and also in chapter 6, the troponin I-T-C complex was also used following the recommendations from Hytest (Turku, Finland). The I-T-C complex from this supplier has been chosen by AACC cTnI Standardization Subcommitee for international reference material. This standard reference material (SRM® 2921) is available from National Institute of Standards and Technology. Troponin I-T-C complex was from human heart tissue and purified in mild conditions without urea treatment. In this way, it reflected the real form of human cTnI in serum of AMI patients and had higher stability when diluted in human serum in comparison

with purified cTnI. The concentrations corresponding to the lots used of this standard material for this thesis were 1.5 mg mL^{-1} for troponin I, 1.42 mg mL^{-1} for troponin T and 1.39 mg mL^{-1} for troponin C and were determined by gel-scanning (Enhanced Laser Densitometer). The ratio of the components in complex I/T/C was 1/0.61/1.20. Thus, all calculations done during the thesis were realized taking into account the concentration of cTnI in the complex, in this case 1.5 mg mL^{-1}.

3.4 SANDWICH ELISA FOR CTNI DETERMINATION

Attending to the above considerations, different strategies have been studied to deal with the best combination and the best sensitivity. In Figure 3.9, there is a summary of these strategies and the immunoreagents and calibrators employed on each of them. Although Immulon™ 2HB has shown to perform better, MaxiSorp™ plates have also been used in some experiments. Figure 3.10 shows the calibration curves obtained for each strategy and Table 3.3, the parameters defining each assay.

First strategy investigated employed the antibodies initially produced (1st generation). Unfortunately, in spite of the great efforts made varying a great number of conditions the LOD accomplished (16.4 ng mL^{-1}) was much below of the cut-off established for cTnI (0.06 ng mL^{-1}), already in buffer, and the situation could be worse when trying to implement this assay to the analysis of plasma or serum samples, since probably those would have to be diluted to minimize non-specific interferences.

At the light of these discouraging results, we acquired from commercial sources (Life Diagnostics) a monoclonal antibody and a goat polyclonal anti-cTnI antibody with the aim to test our conditions with other immunoreagents. According to the supplier, the monoclonal antibody had been purified by protein A agarose chromatography while the goat polyclonal antibody produced immunizing highly purified human cTnI as we did, had been purified by affinity against the cTnI peptide fragment comprised from aa 16 to aa 26 (H_2N-PAPIRRRSSNY-COOH). We selected antibodies produced in different species in order to develop sandwich assays without the need to label the

antibodies with biotin. In such way, HRP labelled secondary anti-IgG antibodies (anti-rabbit IgG or anti-mouse IgG) could be used to generate the signal.

Thus, in strategies B, C and D the commercial antibodies were used to establish sandwich assays in combination with the antibodies produced in our laboratory (B: MAb/As221; C: goat PAb/MAb; D: goat PAb/As220). These combinations and the most appropriate concentrations of the immunoreagents involved were selected as result of the checkerboard titrations ELISA experiments performed with all the potential antibody arrangements, in the presence and absence of cTnI or Tn I-T-C complex.

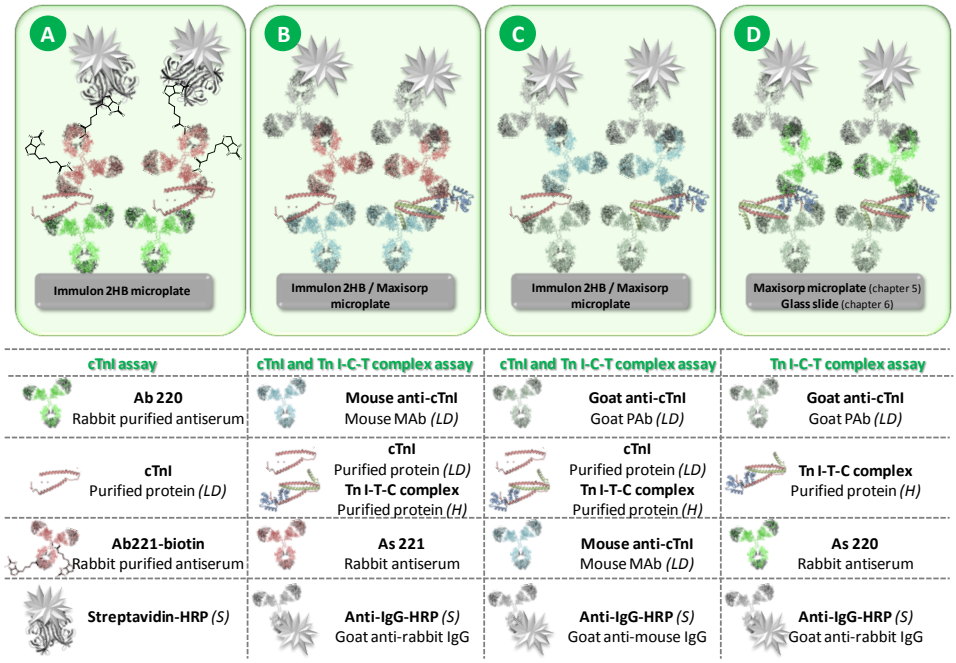

Figure 3.9. Schematic representation of the different strategies used for cTnI and Tn I-T-C detection. Brief description of the immunoreagents used in each strategy and their commercial source. LD: Life Diagnostics, H: Hytest, S: Sigma-Aldrich.

As it can be observed in Figure 3.10 and in Table 3.3, the combination of commercial MAb with in-house produced As 221 (strategy B) improved detectability, but this was even better when using the goat anti-cTnI antibody with the same MAb (strategy C). Thus, using such combination the LOD achieved for cTnI was 0.8 ng mL^{-1}, still more than one order of magnitude lower than the cut-off level (0.06 ng mL^{-1}) and for the I-T-C complex the LOD was 2.9

ng mL^{-1}. When the detection antibody was As 220 (strategy D) the LOD worsened slightly down to 4.3 ng mL^{-1}.

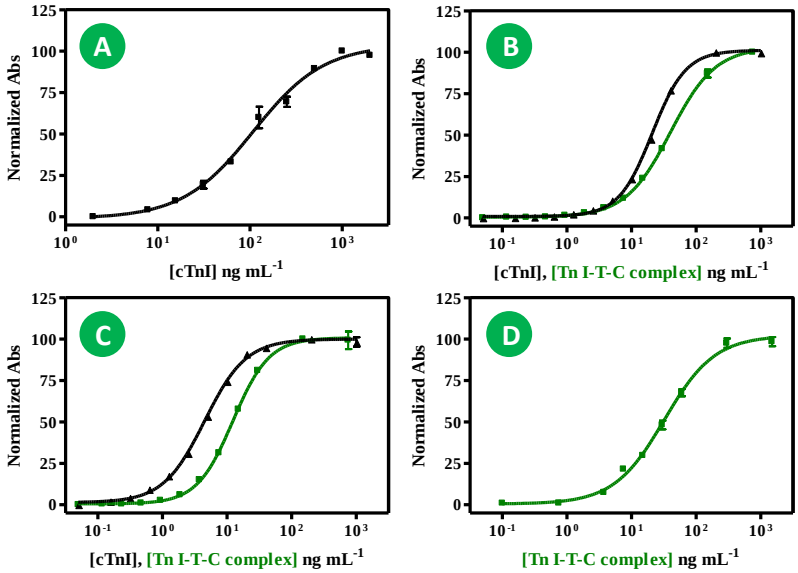

Figure 3.10. Calibration curves for the four different strategies employing the different calibrators and immunoreagent combinations. A, B, C) Each curve was tested once using two replicates on the assay. D) The curve was tested three times (interday and intraday) using at least two replicates on every assay.

Table 3.3. ELISA features for the four different strategies.

	A	B		C		D
	cTnI[a]	cTnI[a]	Tn I-T-C complex[a]	cTnI[a]	Tn I-T-C complex[a]	Tn I-T-C complex[b]
Capture Ab	Ab220	MAb		Goat PAb		Goat PAb
Detection Ab	Ab221-B	As221		MAb		As220
Abs_{max}	103.90	101.2	103.00	100.00	100.80	102.03
Abs_{min}	-1.08	0.89	0.45	1.32	0.52	0.71
Slope	1.13	1.68	1.25	1.36	1.55	1.14
R^2	0.99	1.00	1.00	1.00	1.00	0.98
IC50, ng mL^{-1}	107.90	20.93	40.16	4.51	12.39	33.09
Working range, ng mL^{-1}	31.91-316.99	8.83-46.00	12.60-108.61	1.54-12.41	4.96-29.37	9.10-101.62
LOD, ng mL^{-1}	16.38	5.29	6.48	0.80	2.90	4.29

[a]Each curve was tested once using two replicates on the assay. [b]The curve was tested three times (interday and intraday) using at least two replicates on every assay. All calculations regarding the troponin complex are based on the data that the stock solution contains 1.5 mg mL^{-1} of cTnI.

As result of these studies it seems clear that in any case we were able to reach the desired detectability, neither with the antibodies produced in-house nor with the commercial antibodies or a combination of commercial and in-house produced antibodies. At this stage, we started to reconsider the suitability of the immunogen used. Thus, although antibodies against whole cTnI have been reported or can be found commercially available, it could be that those have to be purified by immunoaffinity to isolate the polyclonal antibody fractions that recognize epitopes that are not blocked by the interaction with the other troponin units of the complex, which are not phosphorylated or bound to autoantibodies or heparin (see above in the introduction section). Alternatively, a new generation of antibodies could be produced against well-designed immunogens consisting on selected peptide sequences not affected by all these potential interferences. Both approaches required the design and synthesis of appropriate peptide sequences.

With this scenario we decided to approach the production of a second generation of antibodies produced against selected peptide epitopes (see next section, section 3.5). On the meanwhile, we would pursuit with the experiments addressed to develop a multiplexed microarray platform (chapter 6) since strategy D based on the use of one of our in-house produced antibodies (As 220) and the goat PAb. This combination, even if not optimum would allow performing a feasibility study of the multiplexed platform at a reasonable cost.

3.5 HAPTEN DESIGN TO PRODUCE A 2ND GENERATION OF ANTIBODIES AGAINST SELECTED PEPTIDE EPITOPES

In regard to what has been explained in section 3.1.1 and 3.1.2, some immunoassays developed for the determination of human cardiac troponin I have employed antibodies against N- and C-terminal regions and also against the mid-fragment (aa 30-110). In general, the most common epitopes employed are: aa 24-40 (N-terminus), 41-49 and 87-91 (mid-fragment) and 185-200 (C-terminus).

The N-terminal extension is a unique structure of cardiac TnI and ideal target for diagnostic of cardiac muscle diseases due to its high specificity in respect to the skeletal troponin. However, phosphorylation of cTnI by PKA at Ser_{23-24} could affect the affinity of antibodies recognizing this region. Both, the N- and C-terminal antibodies could be good alternatives for measuring cTnI due to its antigenicity and specificity, but both parts are very susceptible to degradation. On the other hand, cTnI assays that use antibodies against epitopes situated in the central more stable moiety of cTnI give falsely low cTnI concentrations in samples containing the interfering factor. For this reason, a combination with N- and C-terminal antibodies ("interference-free") with antibodies against mid-fragment has often been selected as the best option to accomplish better selectivity and accuracy. This option has been followed by some authors and by those hs commercial assays (see Table 3.1 and Figure 3.2).

Apart from the information coming from the assays already developed and published in the literature or even commercialized, studies were performed to predict epitopes B from cTnI and TnC. An epitope B is a structural characteristic of a protein which is accessible and recognized by lymphocytes B. There are several data bases to predict them, but in most cases they only refer to lineal epitopes and not discontinuous or conformational ones which represent 90% of the total existent epitopes and are found more or less near the tridimensional conformation of the protein, able to be detected by antibodies. Based on the known cTnI and TnC sequences, there are the following algorithms that allow their structural prediction:

- Algorithms of hydrophobicity/hydrophilicity profiles. They are based on weighted matrixes that assign a hydrophobicity value to each protein residue. Therefore, those hydrophilic residues are potentially relevant to be detected by an antibody.
- Algorithms for protein flexibility prediction. They look for aa which have tendency to be localized in the badly structured regions or in turns which do not have secondary structure and are stabilized by hydrogen bonds. The flexibility of these regions is associated with the hydrophilicity.
- Algorithms for secondary structure prediction. They predict the secondary structure, together with the information of which are the more structured regions and where are the alpha helices and beta sheets.

- Algorithms for antigenicity prediction. One of the oldest prediction programs is called Hoop & Woods. It is based on a matrix associated to the frequency at which aa are localized in the epitope regions. In spite of this, if all the above algorithms provide concordance in their results, there is already evidence in which will be the most antigenic regions.

All these predictive algorithms were applied for cTnI and TnC, individually. Results regarding cTnI are shown in Figure 3.11, although it is known that epitopes B prediction methods have a relatively low reliability.

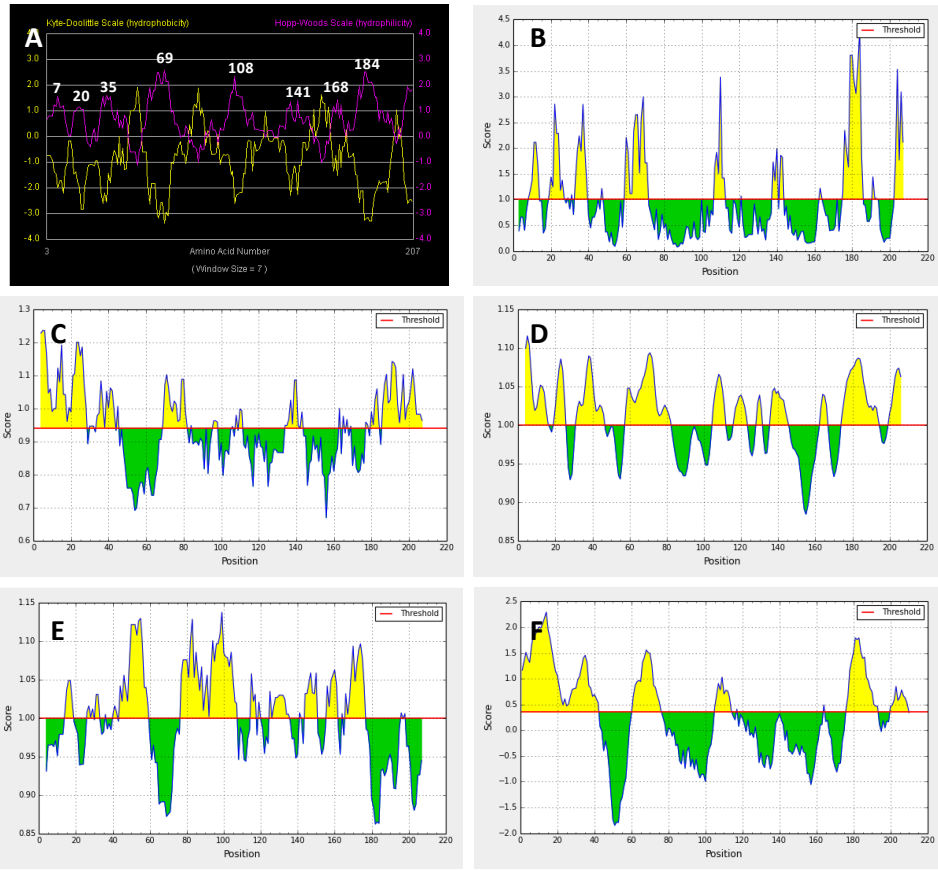

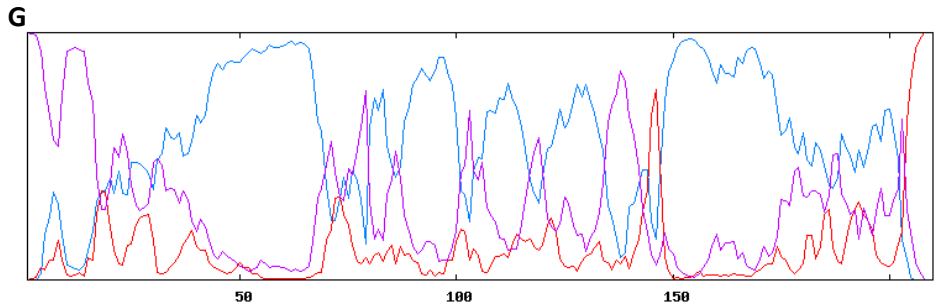

Figure 3.11. A) Kyte-Doolittle (in yellow) is a widely applied scale for delineating hydrophobic character of a protein. Regions with values above 0 are hydrophobic in character. Hopp-Woods scale (in purple) was designed for predicting potentially antigenic regions of polypeptides. Values greater than 0 are hydrophilic and thus likely to be exposed on the surface of a folded protein. B) Emini surface accessibility prediction, C) Chou & Fasman beta-turn prediction (flexible regions), D) Karplus & Schulz flexibility prediction, E) Kolaskar & Tongaonkar antigenicity prediction, F) Bepipred linear epitope prediction, prediction tool that combines the hydrophilicity scale of Parker and the occult models of Markov and G) GOR IV secondary structure prediction method (blue: alpha helix, purple: random coil, red: extended strand) [104-106]

Moreover, a simulation of troponin I ternary complex with TnC and cTnT was realized as well in order to see the more suitable epitopes to be used for the production of antibodies (see Figure 3.12) since this material is recommended to be used as a calibrator and it is known that cTnI is mostly circulating in the bloodstream in this form.

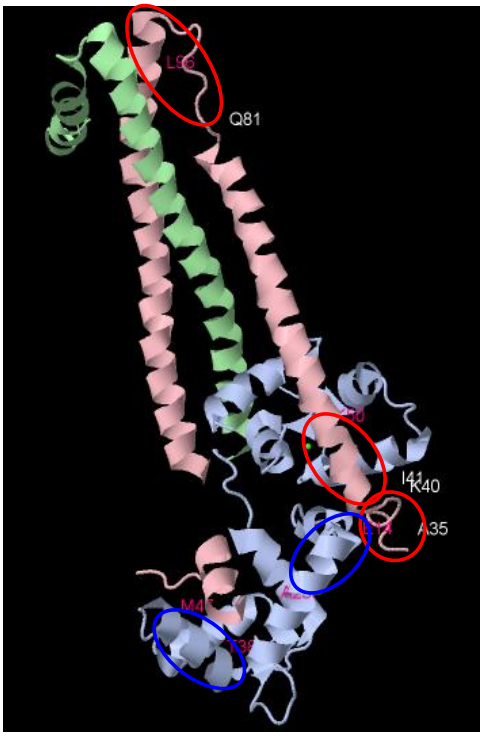

Figure 3.12. Crystal structure of the 46 kDa domain of human cardiac troponin in the Ca^{2+} saturated form (1J1D). Image from Jmol, Protein Data Bank (PDB). In red, cTnI fragments selected for antibody production from already published and commercialized assays; in blue, TnC epitopes were selected looking at the most exposed ones. C-terminal region of cTnI was not crystallized and therefore not shown in this image.

Since the information coming from the different algorithms was not conclusive at all, the epitopes chosen and employed in most published and commercialized assays were selected to produce the antibodies of this thesis. These epitopes were also confirmed on the above picture to be exposed although affected by some of the post-translational modifications such as phosphorylation and proteolytic degradation.

Thus, four peptide epitopes were selected for cTnI and the following haptens were proposed, all of them with an additional cysteine (Cys) residue for bioconjugation to a biomacromolecule that would made them immunogenic (see Figure 3.13 for the peptide sequences).

- **Hapten TI1** (18 aa): contained the aa 24-40 sequence, starting with the S_{24} which is the serine (Ser) that can be phosphorylated and, previously

to this Ser, a Cys residue was added. In this way potential variabilities due to phosphorylation would be minimized due to the proximity of the protein used for bioconjugation.

- **Hapten TI2** (11 aa): contained aa 41-50 peptide sequence with a Cys added to the C-terminus instead of the N-terminus.
- **Hapten TI3** (17 aa): contained the aa 81-96 sequence with a Cys at the N-terminal part. This fragment was localized between both Cys residues (C_{80} and C_{97}) that can be oxidized forming a disulfide bond. Thus, the presence of these residues was avoided in the hapten. The additional Cys residue for conjugation was placed at the N-terminal part.
- **Hapten TI4** (15 aa): containing the aa 188-202 peptide sequence also with a Cys at the N-terminal part.

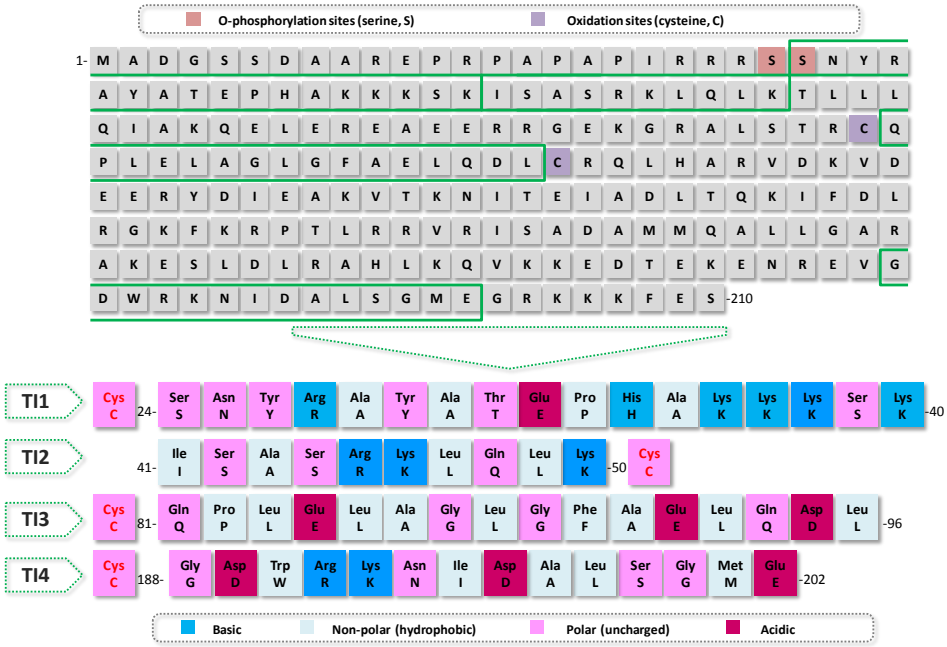

Figure 3.13. Scheme of cTnI sequences chosen for the immunogen preparation with their properties. In red, the cysteine (Cys) added in order to perform the coupling to a protein.

In the same way two peptide sequences were also selected for TnC. In this manner, antibodies for TnC could be used in the assays as capture or detection antibodies allowing detection of cTnI in the binary and ternary complexes. The two peptides selected for TnC contained the aa 14-23 and aa 38-47 sequences, both with additional Cys residues in the C-terminus. These peptides were called

TC1 and TC2 respectively and had each of them a total of 11 aa (see Figure 3.14 for the aa sequences).

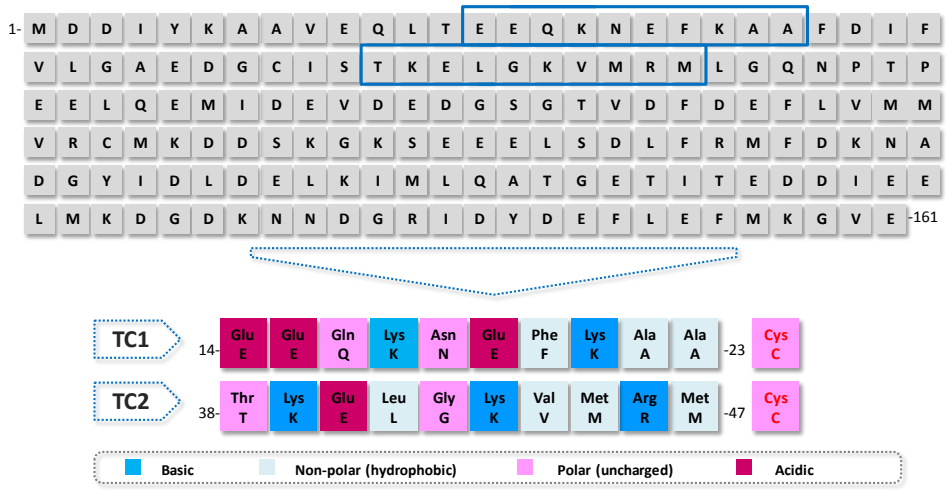

Figure 3.14. Scheme of TnC sequences chosen for the immunogen preparation with their properties. In red, the cysteine (Cys) added in order to perform the coupling to a protein.

The additional Cys residue was selected because of its thiol group which allowed performing orthogonal chemistry with appropriate cross-linkers avoiding interferences from other chemical groups of the protein. Neither amino, carboxyl nor halogen groups were suitable because of their complementary chemistry with several functional groups present in the peptide sequence. Moreover, in this way, the whole peptide sequence was exposed to the immune system once conjugated. Additionally, the location of the Cys at the N- or C-terminal regions allowed directing recognition of the most interesting regions of the peptide sequence.

3.5.1 HAPTEN SYNTHESIS

Haptens for cTnI (TI1, TI2, TI3 and TI4) and for TnC (TC1 and TC2) described above were synthesized by the Unitat de Química Combinatòria (UQC, PCB) under the responsibility of Dr. Míriam Royo in the context of collaboration within the Nanocardiococo project.

3.5.2 HAPTEN CONJUGATION

Peptides TI1, TI2, TI3 and TI4 for cTnI and TC1 and TC2 for TnC were coupled to HCH and BSA using the N-succinimidyl iodoacetate (SIA) cross-linker (see Figure 3.15).

SIA is a heterobifunctional linker containing amine-reactive and sulfhydryl-reactive ends. Conjugations done with such a linker usually proceed by a two-step protocol. At first, its N-hydroxysuccinimide (NHS) ester end, the most labile functionality reacts with the protein amino groups of the lysine residues to create an iodoacetyl-activated intermediate. This iodoacetyl protein derivative is stable enough in aqueous solution to purify it by dialysis or size exclusion chromatography, to remove the excess of SIA and other reaction by-products. The only caution that must be taken is to protect iodoacetyl derivative from light, which can generate iodine and reduce the reactivity of such intermediate. In the second step, the iodoacetyl-derivatized protein is made to react with sulfhydryl-containing peptide, which through a SN2 reaction with the iodine group forms a thioether bond. The relative reactivity of α-haloacetates toward different functional groups is sulfhydryl > imidazolyl > thioether > amine. In like manner, the relative reactivity of halo derivatives such as haloacetamides is I > Br > Cl > F, with fluorine being almost unreactive. In conclusion, it can be affirmed that iodoacetamide intermediate has the highest reactivity toward sulfhydryl cysteine residues contained in the peptide sequence and are directed specifically for –SH modification. If iodoacetate is present in limiting quantities (relative to the number of sulfhydryl groups present) and a slightly alkaline pH, cysteine modification will be the exclusive reaction. At the end, blocking of the remaining iodoacetyl sites with the addition of cysteine is highly recommended.

Although other side reactions may occur, this orthogonal coupling approach is quite selective. For instance, sulfhydryl groups may also form thiol ester linkages, although they are not as stable as the amides.

Although the size of the SIA cross-linker is very small, it avoids introduction of additional non desired antigenic determinants in the bioconjugate, as occurred with other more frequently used cross-linkers bearing maleimide groups such as MBS (m-maleimidobenzoyl-*N*-hydroxysuccinimide ester) or SMCC

(succinimidyl-4(*N*-maleimidomethyl)cyclohexane-1-carboxylate). Thus, in such way it was ensured that antibodies produced were not able to recognize other conjugates prepared through the same chemistry.

In this way, the protein was first derivatized with SIA by reacting the amino group of the lysine residues to the active acid and subsequently the iodoacetylated proteins were reacted with the peptide (see Figure 3.15).

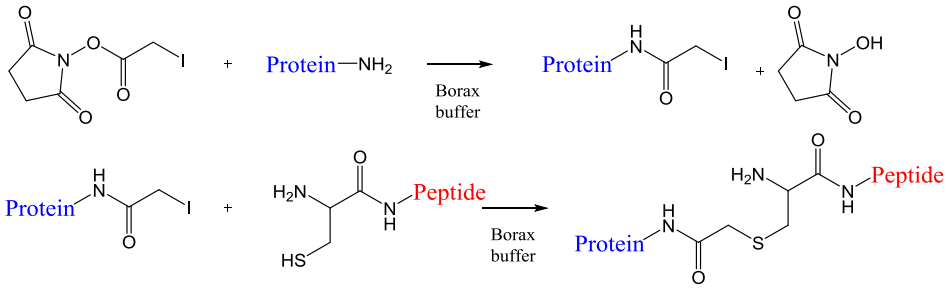

Figure 3.15. Chemical reaction that took place when coupling the peptides (TI1-TI4 and TC1-TC2) to a protein such as BSA and HCH through SIA linker.

Although it has often been claimed that for antibody production the optimal length of the spacer arm between the protein and the hapten should be about 3-6 atoms length [107, 108], in many occasions shorter spacer arms have also provided good results [109, 110]. Another property that a good spacer should fulfil is low antigenicity, which is usually accomplished using linkers with no or very few functional groups or heteroatoms along its chain. SIA cross-linker fulfilled these requirements.

Hence, using such chemistry, 12 bioconjugates were obtained (6 for HCH and 6 for BSA). Characterization of these bioconjugates was achieved by MALDI-TOF-MS and all hapten densities obtained are summarized in section 8.1.1.

3.6 ANTIBODY PRODUCTION FOR CTNI AND TNC FRAGMENTS: 2ND GENERATION

TI1-TI4- and TC1-TC2-CH_2CO-HCH bioconjugates were used to immunize three white New-Zealand rabbits with each of them, employing the same

immunization protocol as for the 1st generation of antibodies described in the experimental section (chapter 8). The evolution of the antibody titer was assessed in a non-competitive ELISA, measuring the absorbance related to the binding of serial dilutions of each antiserum to microtiter plates coated with their corresponding peptide-BSA conjugate. The results of such studies are shown in Figure 3.16 and Figure 3.17.

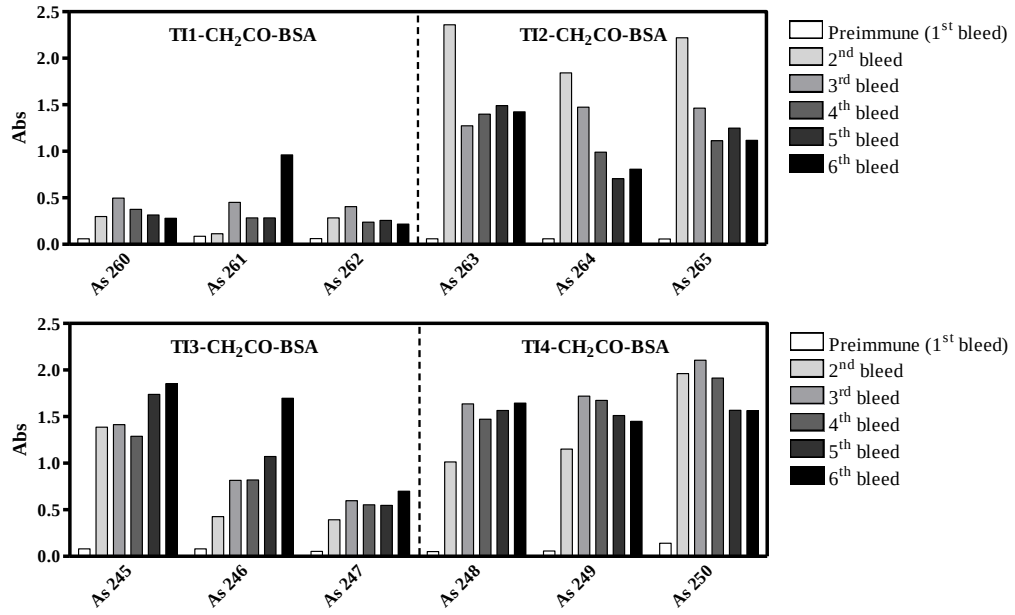

Figure 3.16. Antibody titer to evaluate the response of the antisera produced for four cTnI fragments. Peptide-CH_2CO-BSA conjugates were immobilized at 1 μg mL^{-1} and all antisera 1/32000 diluted.

As it can be observed, good antibody titer for all cTnI peptide bioconjugates were obtained, although certain animal variability was observed in some cases. The antisera produced against TI1 fragment which corresponds to the amino acid sequence Cys(aa 24-40) showed the lowest response although the results shown in Figure 3.16 correspond to dilution of the antisera 1/32000 which means that in spite of this the response was good.

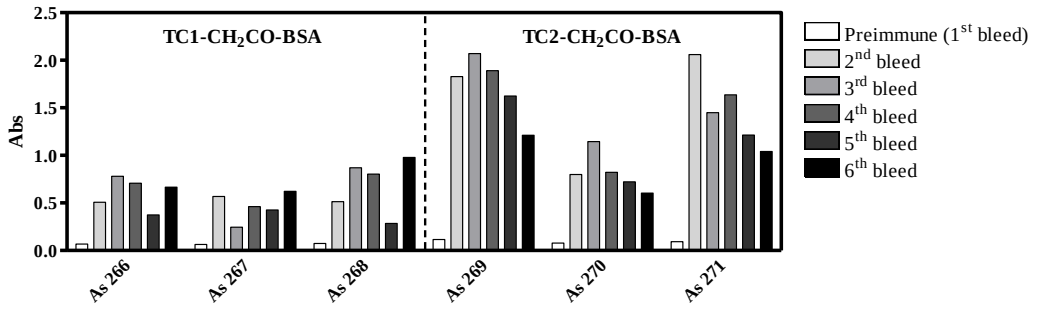

Figure 3.17. Antibody titer to evaluate the response of the antisera produced for two TnC fragments. Conjugates were immobilized at 1 μg mL^{-1} and all antisera were 1/32000 diluted.

Regarding TnC, the antisera produced against the TC1 peptide fragment, corresponding to the amino acid sequence (aa 14-23)Cys showed lower titer than the antisera against TC2, but the response was good enough considering the dilution employed.

3.7 ESTABLISHMENT OF IMMUNOCHEMICAL ASSAYS USING THE 2ND GENERATION OF ANTIBODIES

The screening of this 2nd generation antibodies and the establishment of the corresponding assays has been the object of part the PhD thesis of Àlex Hernández, therefore will not be included in this thesis. However at the time of approaching the establishment of a multiplexed platform (chapter 6) no assay showing better features than those obtained using commercial antibodies or combination between commercial and the 1st generation of antibodies reported above (Figure 3.10 and Table 3.3) could have been established. For this reason, strategy D (see Figure 3.9) was used for multidetection experiments in chapter 6.

4 DEVELOPMENT OF ANTIBODIES AND IMMUNOCHEMICAL TECHNIQUES FOR BRAIN NATRIURETIC PEPTIDES

4.1 INTRODUCTION

Brain natriuretic peptide (BNP) and N-terminal pro brain natriuretic peptide (NT-proBNP), both cleavage products of the precursor proBNP (aa 1-108) (see Figure 4.1), are established cardiovascular biomarkers for prognosis and diagnosis of heart failure (HF) [111]. Also, it was demonstrated that proBNP concentrations are significantly and highly correlated to BNP and NT-proBNP in patients with systolic HF and that the precursor is the major immunoreactive form in human blood and circulates in patients with HF [112].

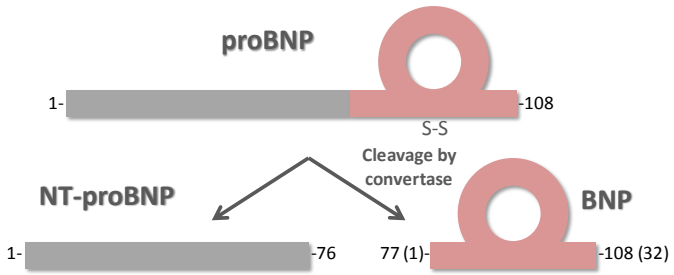

Figure 4.1. Schematic representation of proBNP processing. ProBNP is processed by a convertase to form BNP (32 aa) and N-terminal part of the proBNP called NT-proBNP (76 aa).

The European Society of Cardiology (ESC) guidelines for diagnosis and treatment of acute and chronic HF affirms that there is no definitive cut-off value recognized for NT-proBNP and BNP because changes in left-ventricular (LV) filling pressures may not be reflected by rapid changes in these peptides with relative long half-lives. In spite of this, they recommend 0.4 ng mL^{-1} for NT-proBNP and 0.1 ng mL^{-1} for BNP as cut points. Then, concentration of BNP in healthy individuals is less than 0.1 ng mL^{-1} but it increases from 0.1 to 0.4 ng mL^{-1} for patients diagnosed of congestive HF and to more than 0.4 ng mL^{-1} for patients diagnosed with sever cardiac HF. NT-proBNP shows higher circulating levels, thus under 0.4 ng mL^{-1} is defined as unlikely chronic HF, between 0.4 and 2 ng mL^{-1} comprises the uncertain diagnosis and over 2 ng mL^{-1} the patient is classified as a likely chronic HF [23]. Similarly, the Roche package insert for NT-proBNP kit, that is somehow the commercial assay most used as a validation method, indicates that the most appropriate cut-off for HF is 0.125 ng mL^{-1} for patients <75 years, and 0.450 ng mL^{-1} for patients >75 years of age. McUllogh et al. also showed in a prospective study of BNP as a diagnostic test, that using a

cut-off point of 0.1 ng mL^{-1}, BNP had a sensitivity of 90% and specificity of 73% [113, 114].

4.1.1 IMMUNOASSAYS IN THE LITERATURE

Assays for the detection of the two cleavage products and the precursor that is also circulating in the bloodstream have already been developed and published in the literature. Until now, a large number of methods such as enzyme-linked immunosorbent assay (ELISA), radioimmunoassay (RIA), fluorescent immunoassay (FIA) and chemiluminescent immunoassay (CLIA) have been developed for the determination of BNP, NT-proBNP and their precursor in human serum or plasma (Table 4.1). The differences between these immunoassay methods are explained in section 1.4.1.2.

Table 4.1. Analytical characteristics of different brain natriuretic peptides immunoassays reported in the literature.

	$Analyte_{aa}$ (calibration curve)	**Reagents**	**Sample**	**LOD (ng mL^{-1})**	**Working range (ng mL^{-1})**	**t_{assay} (min)**	**Ref.**
ELISA	BNP	MAb_1-biotin MAb_2-HRP MP-streptavidin	Serum	0.01	x-1	30	[115]
	proBNP	MAb(BNP) PAb(proBNP)-HRP	Plasma	0.01	0.15-10	300	[116]
	BNP	Ab_1 Ab_2-HRP	-	-	$1{\cdot}10^{-4}$–0.1	15	[117]
RIA	NT-proXNP[a] ($NT\text{-}proBNP_{1\text{-}37}$-$NT\text{-}proANP_{29\text{-}98}$)	NT-proXNP-$Na^{125}I$ PAb(NT-proBNP) PAb(NT-proANP)	Plasma, serum	80 pM[b]	150–7300 pM[b]	960	[118]
	$proBNP_{1\text{-}10}$-Tyr	$proBNP_{1\text{-}10}$-[^{125}I]Tyr PAb	Plasma	0.2 pM[b]	0–250 pM[b]	7210	[119]
	$proBNP_{1\text{-}21}$	$proBNP_{1\text{-}13}$-[^{125}I]Tyr PAb	Plasma	1) 158 pM[b] 2) 5.2 pM[b]	- 2) 10–625 pM[b]	2760 1440	[120, 121]

	$proBNP_{1-21}$ $proBNP_{62-76}$	$proBNP_{1-13}$-[^{125}I]Tyr, [^{125}I]$proBNP_{62-76}$ PAb_1, PAb_2	Plasma	5.2 pM[b] 4.5 pM[b]	10–625 pM[b] -	1440 2760	[122]
	$NT\text{-}proBNP_{1-23}$	- PAb	Plasma	1 pM[b]	-	-	[123]
FIA	BNP	MAb_1-biotin MAb_2-Eu^{3+}	Plasma	$4\cdot10^{-4}$ (BNP)	-	30	[124]
FIA	proBNP	MAb_1-biotin MAb_2-Eu^{3+}	Plasma	$3\cdot10^{-3}$ (proBNP)	-	30	[124]
FIA	NT-proBNP	MAb_1-biotin MAb_2-Eu^{3+}	Plasma	0.01	0.015-100	40	[62]
FIA	BNP proBNP	$MAb(BNP)_1$ $MAb(Ab\text{-}BNP)_2$-Eu^{3+}	Plasma	$4\cdot10^{-4}$ (BNP)	$0.23–17.6\cdot10^{-3}$ pM[a]	30	[125]
CLIA	BNP	MAb_1-biotin MAb_2-HRP MP-streptavidin	Serum	0.02	0.02-1	25	[126]
CLIA	NT-proBNP	$NT\text{-}proBNP_{65-76}$-AE PAb MP-Anti-IgG	Plasma	$1.3\cdot10^{-9}$	-	1440	[127]
CLIA	BNP + proBNP	MAb_1-biotin $MAb(Fab')_2$-AP $MAb(Fab')_3$-AP	Plasma	BNP: $6.93\cdot10^{-5}$ proBNP: $4.76\cdot10^{-4}$	$6.93\cdot10^{-4}$-0.87 $4.76\cdot10^{-3}$-2.98	420	[128]
CLIA	BNP	Ab_1, Ab_2-AP	-	$1\cdot10^{-3}$	$1\cdot10^{-3}$-10	-	[129]

MP: magnetic particle, PS: polystyrene beads, AE: acridinium ester, AP: alkaline phosphatase. [a]NT-proXNP is a hybrid recombinant peptide containing NT-proBNP (aa 1-37) and NT-proANP (aa 29-98) in its sequence. [b]Exact quantitation of NT-proBNP is not possible without a purified standard of $proBNP_{1-76}$ and thus results are expressed in equivalents of the purified standard used in the calibration curve. Some of these immunoassays detect different peptide fragments coming from proBNP processing.

Accordingly to what is detailed on the above table, the most used assay format for brain natriuretic peptides determination is the sandwich format. All RIAs which were the first assays published for these analytes together with the CLIA developed by Hughes et al. [127] employed a competitive format. In all these cases polyclonal antibodies (PAbs) were used while different ^{125}I labelled and enzyme labelled peptides were used as competitors in the case of RIAs and CLIAs respectively, whereas for sandwich assays monoclonal antibodies (MAbs)

were used as capture antibodies and MAbs and in few cases PAbs as detection antibodies.

All RIAs used a tracer responsible of the competition and the final response based on a radioiodinated peptide fragment. Normally, this peptide was the same employed as immunogen. The calibration curve of these immunoassays was made using a fragment of the target analyte as standard instead of the whole molecule. For this reason, results such as LOD and working range values are expressed with pM units instead of ng mL^{-1}. The time (min) invested to run these assays was much longer than other immunochemical assay formats, which represents a considerable disadvantage in addition to the radioactive residues generated. Moreover, often, plasma samples had to be treated using reverse phase extraction cartridges (i.e. Sep-pak® C18 Millipore-Waters, Milford, MA, USA) [128] to avoid matrix interferences. On the other hand, while performance of most CLIAs, FIAs and ELISAs took shorter time than RIAs, CLIAs and FIAs obtained the best LOD values. The characteristics of each of these immunoassay methods as well as the differences between them are described in section 1.4.1.2.

As observed in the table, magnetic beads or other kind of particles are used in several of the immunoassays reported with the purpose to enhance the sensitivity of the assays, to get more rapid reactions kinetics as they were in suspension and to avoid or minimize matrix effects. Magnetoimmunoassays facilitate the analysis of complex samples diminishing sample preparation prior the analysis thanks to the possibility to separate the interferences with a magnet. With the aim to achieve higher sensitivities, most assays add an amplification step such as biotin-streptavidin strategy [62, 115, 124, 126, 128].

Regarding antibody production, a peptide fragment conjugated to a carrier protein is normally used for immunization. For instance and related to NT-proBNP, aa 65-76 were used for polyclonal antibody production by Hughes et al. [127] and aa 1-23 by Campbell et al. [123], while for proBNP a fragment containing aa 1-10 was selected by Goetze and co-workers [119] and aa 1-13 and later aa 62-76 were the choices from Hunt et al. [120-122]. Other immunoassays developed and summarized in Table 4.1 employed commercial monoclonal antibodies mostly from Hytest, which were produced in Balb/c mice immunized with synthetic peptides corresponding to different regions of

NT-proBNP like aa 13-20 [62, 124, 128] and aa 63-71 [62] conjugated with a carrier protein. For BNP, MAbs from this commercial source were obtained immunizing synthetic BNP peptide fragments like aa 11-22 [124, 125], aa 26-32 [124] and others [115, 126] conjugated to a protein. The most problematic aspect shared between all these assays is the cross-reactivity of the precursor proBNP when the measurement of the processing products is desired or viceversa, although when proBNP measurement is the objective an antibody for BNP and another for NT-proBNP have been used in the same assay [124].

A novelty was introduced by Ala-Kopsala et al. [118] using a hybrid recombinant peptide called NT-proXNP, which contained the NT-proBNP (aa 1-37) and NT-proANP (aa 29-98) peptide sequences, with the objective to detect simultaneously NT-proBNP and NT-proANP. This last peptide together with the bioactive atrial natriuretic peptide (ANP) comes from their precursor proANP. ANP and BNP are cardiac natriuretic hormones, share a similar structural conformation and have a similar processing, although it is generally thought that ANP is preferentially produced in the atria while BNP is produced in the ventricles, particularly in patients with chronic cardiac disease. Increased plasma concentrations of peptides from proANP are then good markers of acute overload and rapid hemodynamic changes (e.g., tachycardia), whereas proBNP-derived peptides seem to be better markers of ventricular overload (e.g. aortic stenosis) [59, 118] (see section 1.6.6 for more details). The assay mentioned employed NT-proXNP as a calibrator and as tracer once radioiodinated. Antiserum was produced immunizing a fusion protein (NT-proANP$_{1\text{-}98}$-NT-proBNP$_{1\text{-}76}$) and finally recognizing NT-proBNP (aa 10-29) and NT-proANP (aa 46-79). Results correlated well with both independent assays and with the arithmetic sum of both peptides, thus providing an assay with increased diagnostic and prognostic power. Also in Giuliani's work [116], it is reported the first antibody specific for proBNP$_{1\text{-}108}$ and with this, an immunoassay that specifically measured this peptide in plasma. The obtained monoclonal antibody recognized the cleavage site of proBNP, an epitope present only in the precursor (see Figure 4.1), and therefore, for the first time it was possible to quantify proBNP without cross-reactivity with the cleavage products, BNP and NT-proBNP. Finally, a "single-epitope sandwich assay" for quantifying BNP and proBNP in human blood was reported by Tamm et al. [125], in which the capture antibody recognized BNP (aa 11-22), whereas the

detection antibody was specific to the immune complex capture antibody-BNP. The assay did not recognize the individual components of the complex.

4.1.2 COMMERCIAL IMMUNOASSAYS

Apart from the immunoassays for brain natriuretic peptides that have been reported in the literature, in most cases, researchers and clinicians use commercial immunoreagents or kits already implemented in the clinical practice (see Table 4.2). The Elecsys® proBNP system (Roche) appears as the most reliable system in the market according to different studies [130, 131], and therefore is used as reference method to compare performance of other NT-proBNP assays [113, 132-136]. A biotinylated capture antibody (1), a fluorescent ruthenium derivative-labelled antibody (2) and NT-proBNP form a complex that binds to streptavidin coated microparticles. The assay is run in 18 min and shows a linear range of $5 \cdot 10^{-3}$-35 ng mL^{-1}.

Other used systems are the Dade Behring Stratus® CS Acute Care™ Diagnostic System (Dade Behring, Siemens), the Dade Behring NT-proBNP (PBNP®) on Dimension RxL® (Dade Behring, Siemens), the LOCI® technology on the Dimension® Vista™ System (Siemens Diagnostics) or in the AlphaLISA® format (Perkin Elmer), the PATHFAST® system (Mitsubishi Chemical) and the competitive BNP fragment EIA assay (Biomedica immunoassays), between others. Apart from these tests used in bench top analyzers (BTA), there are point-of-care tests (POCT) like Cardiac® proBNP (Roche) based on an immunochromatographic principle. Apart from their advantages regarding smaller size and faster results, they normally provide assays with worse sensitivity compared to those ones using a BTA [114].

The Dade Behring Stratus® CS Acute Care™ Diagnostic System is a two site immunoassay system in which the capture and detection antibodies are covalently linked to Starburst® (Dendritech, Inc., Midland MI) dendrimer and alkaline phosphatase (AP), respectively. With the addition of the substrate, bound labelled antibody generates a fluorogenic product. Quantitative results from whole blood are obtained in 15 min. The quantitation range is 0–20000 pg mL^{-1} and the limit of detection is 5 pg mL^{-1} [137]. In PBNP®, the same antibodies

and calibrator materials from Elecsys® proBNP are used, although the assay format and the method are different (see Table 4.2) [136].

The LOCI® technology (Luminescent Oxygen Channeling Assay) is a homogeneous assay approach based on paired synthetic beads. It is also known as ALPHA (Amplified Luminescence Proximity Homogeneous Assay) and it was first described by Ullmann et al. [138] and further on implemented to the detection of a variety of analytes. Dade Behring Diagnostic Inc. (San Jose, CA, USA) was one of the first companies to implement this technology in the clinical diagnostic field. This company was acquired by Siemens AG (Germany) which nowadays has incorporated this approach on their Dimension® (Vista® and ELX™) automated laboratory analyzers. The LOCI® technology utilizes paired synthetic beads (the Chemibead and the Sensibead). The Chemibead with a chemiluminiscent dye is biofunctionalized with a first NT-proBNP specific antibody. The Sensibead, that contains a photosensitive dye, is coated with streptavidin and is used to capture a second antibody biotinylated reagent. When this complex is exposed to light at 680 nm, the photosensitive dye releases singlet oxygen which rapidly diffuses to and is absorbed by the Chemibead, causing a chemiluminescent reaction which is measured by spectrophotometry (see Figure 4.2). For NT-proBNP, this assay has a LOD of 5 pg mL^{-1} and takes 8 min. Based on the same principle cTnI, CK-MB and MYO can also be measured [133, 139].

This same strategy is incorporated in AlphaLISA® in a plate format [140].

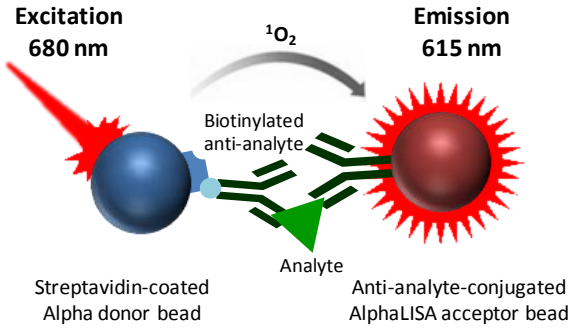

Figure 4.2. Scheme of the fundamental of the LOCI® (or ALPHA) technology. A biotinylated antibody to the analyte (i.e. NT-proBNP) binds to the streptavidin-coated Sensibeads (donor beads) and a second specific antibody is directly conjugated to Chemibead (acceptor beads). In the presence of the analyte, the two beads come into close proximity. The excitation of the donor beads at 680 nm generates singlet oxygen molecules that trigger a series of chemical reactions in the acceptor beads resulting in a sharp peak of light emission at 615 nm (figure copied from [140]).

PATHFAST® is a system based on a benchtop chemiluminescent enzyme immunoassay (CLEIA) analyzer and it has its single-use reagent cartridges for cTnI, MYO, CK-MB and NT-proBNP. The system adopted highly sensitive CLEIA using CDP-Star/Sapphire-II (Applied Biosystems) as substrate and Magtration® technology [141], a method of operating magnetic particles by which efficient bound/free separation can be performed in a disposable pipette tip with a small volume of washing buffers [134]. CDP-Star® is a 1,2-dioxetane chemiluminescent substrate, while Sapphire-II™ is a polymeric enhancer that provides high signal-to-noise ratios. It is known that the choice of an optimal substrate/enhancer formulation depends on the instrumentation being used (spectral sensitivity), the type of microplate being used and the desired signal intensity. The light emission mechanism of this substrate with AP is shown in Figure 4.3. In this case, the maximum of the light emission is at 461 nm.

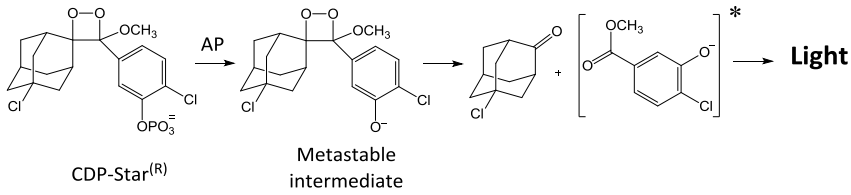

Figure 4.3. Light emission of mechanism of CDP-Star® substrate.

The BNP fragment EIA assay from Biomedica immunoassays is a competitive direct ELISA assay and uses a polyclonal sheep antibody directed against aa 8-29 of proBNP as capture antibody and a NT-proBNP fragment (aa 8-29) labelled with HRP as enzymatic tracer. The calibrator is the whole synthetic NT-proBNP (aa 1-76) and TMB and hydrogen peroxide are employed as substrate solution [142].

All these examples of commercial tests are summarized in Table 4.2.

Table 4.2. Immunoreagents and characteristics of some commercial immunoassays.

Test name, immunoassay method	Company	POCT/BTA (Bench Top Analyzer)	LOD/LOQ (pg mL^{-1})	Capture antibody (recognized aa)	Detection antibody (recognized aa)
NT-proBNP immunoassays					
Elecsys® proBNP, ECLIA [136]	Roche	BTA	5 (LOQ)	PAb_1(1-21)-biotin	PAb_2(39-50)-Ru derivative
Cardiac® proBNP, Immunocromatographic assay [114]	Roche	POCT	60 (LOQ)	-	-
Dade Behring Stratus® CS acute Care™ Diagnostic System, CLIA [137]	Dade Behring (Siemens)	BTA	5 (LOD)	MAb_1-dendrimer	MAb_2-AP
Dade Behring NT-proBNP (PBNP®) on Dimension RxL® in StreamLab® work-cell, CLIA [136]	Dade Behring (Siemens)	BTA	10 (LOQ)	PAb_1(1-21)-chromium dioxide particles	PAb_2(39-50)-AP
BNP fragment EIA, ELISA [142]	Biomedica immunoassays	BTA (plate)	1436 (LOD)	PAb(8-29)	NT-proBNP(8-29)-HRP
AlphaLISA® (LOCI® technology), CLIA [135, 140]	Perkin Elmer	BTA (plate)	16 (LOD)	MAb_1(1-12)-biotin (Streptavidin-donor bead-photosensitive dye)	Acceptor bead-MAb_2(63-76)-chemiluminescent dye
LOCI® on Dimension® Vista™ System, CLIA(Siemens Diagnostics) [133, 139]	Siemens Diagnostics	BTA	5 (LOD)	Ab_1-biotin (Streptavidin-donor bead-photosensitive dye)	Acceptor bead-Ab_2-chemiluminescent dye
PATHFAST®, CLEIA [134]	Mitsubishi Chemical	BTA	12 (LOQ)	Ab_1-MP	Ab_2-AP
BNP immunoassays					
Shionoria BNP, IRMA [143, 144]	Shionogi & Co	BTA	2.5 (LOD)	MAb_1(14-21)-bead	MAb_2(27-32)-^{125}I
Triage® BNP, Immunocromatographic fluorescent assay [113, 114]	Biosite	POCT	5 (LOD)	-	-

ADVIA® Centaur® BNP, CLIA [143]	Bayer (Siemens)	BTA	2 (LOD)	MAb_1(27-32)-biotin, Streptavidin-MP	$MAb(F(ab')_2)_2$(14-21)-AE
AxSYM® BNP, MEIA (FIA) [145]	Abbott	BTA	15 (LOD)	MAb-microparticle	MAb-AP
ST-AIA-PACK® BNP, MEIA (FIA) [146]	TOSOH Corporation	BTA	5.4 (LOD)	MAb_1(14-21)-MP	MAb_2(27-32)-AP

POCT: Point-of-care testing, ECLIA: electrochemiluminescent assay, CLEIA: chemiluminescent enzyme immunoassay, IRMA: immunoradiometric assay, MEIA: microparticle enzyme immunoassay. AlphaLISA was developed for the quantification of NT-proBNP in saliva, while all other in serum/plasma samples. Biomedica assay is based on a competitive format, while others are based on sandwich format.

It must be noticed, that clinical studies revealed some discrepancies between the results obtained with the different tests and also between those tests using the same immunoreagents. As an example greater imprecision was found for the PBNP® on Dimension RxL® compared to the values stated by the Elecsys® proBNP, even if the two methods use the same polyclonal antibodies and calibrators. This fact does not seem to guarantee an agreement between them indicating that the detection principle may play an important role [136]. While the Elecsys system uses a Rhutenium fluorescent derivative, the Dimension RxL system uses antibody coated chromium dioxide particles and a second antibody labelled with alkaline phosphatase that catalizes the formation of a chemiluminescent product. The linear range accomplished in this case is 10-30000 pg mL^{-1}, with a limit of quantitation an order of magnitude worse than for the Elecsys test. In like manner, a large mean difference of 52% was found between the BNP fragment EIA assay (Biomedica immunoassays) and the Elecsys® proBNP test using lithium heparin treated plasma [142]. In this case, the detection principle is different as well as the assay format and the immunoreagents used. Moreover, the first assay from Biomedica does not achieve the required NT-proBNP cut-off, its limit of detection is 1436 pg mL^{-1} and basal levels are below 400 pg mL^{-1}.

Regarding BNP commercial immunoassays, the ADVIA® Centaur® BNP assay (Bayer ADVIA Centaur) is and automated random access immunoassay system from Siemens Medical Solutions Diagnostics. Bayer HealthCare's Diagnostic Division is now a division of Siemens. This assay is a fully automated sandwich immunoassay using direct chemiluminescent technology, which uses constant amounts of two monoclonal antibodies. The first antibody is an acridinium ester labelled monoclonal mouse anti-human BNP $F(ab')_2$ fragment specific to the ring structure of BNP. The second antibody attached to the solid phase is a biotinylated monoclonal mouse anti-human antibody specific to the C-terminal portion of BNP, which is coupled to streptavidin magnetic particles. On the other side, the AxSYM® BNP assay (Abbott Laboratories, Abbott Park IL) is a 2-site microparticle enzyme immunoassay that uses a monoclonal anti-BNP antibody coated on the microparticles and a monoclonal anti-BNP alkaline phosphatase (AP) conjugate. The substrate, 4-methylumbelliferyl phosphate is added and the enzymatic conjugate catalyzes the removal of a phosphate group yielding the fluorescent product 4-methylumbelliferone. In a similar manner, the ST-AIA®-PACK BNP is a two-site immunoenzymometric assay that

uses two monoclonal antibodies that are the same ones employed in ADVIA® Centaur® BNP and supplied by the Shionogi's Diagnostic Division. The capture antibody is immobilized on magnetic beads, while the detection antibody is labelled with AP. The magnetic beads are washed to remove unbound enzyme-labelled antibody and are then incubated also with the fluorogenic substrate 4-methyllumbelliferyl-phosphate. Finally, Shionoria BNP (Shionogi & Co) is a solid-phase immunoradiometric assay kit that uses the two different MAbs that recognize the C-terminal region and the intramolecular ring structure of BNP, one coated to a bead and the other radioiodinated with ^{125}I. The assay sensitivity is about 2.5 pg mL^{-1} and the working range 5-2000 pg mL^{-1}.

Results obtained with AxSYM® BNP were also significantly different compared to the others and better agreement between Shionoria BNP and ADVIA® Centaur® BNP methods was found [130]. Similarly, ST-AIA-PACK® BNP presents BNP values that are about the half compared to other very popular BNP immunoassays such as the MEIA from Abbott performed on ARCHITECT analyzer and Triage® BNP for UniCell DxI platform and similar to those found using the ADVIA® Centaur® BNP. ST-AIA-PACK® BNP, ADVIA® Centaur® BNP, AxSYM® BNP and Shionoria BNP use the same antibodies and standard materials supplied by Shionogi's Diagnostic Division and directed to the C-terminal part (aa 27-32) and to the intramolecular ring (aa 14-21) [146].

Nowadays, technological advances allow the development of novel point-of-care tests (POCTs) that shorten the time to clinical decision-making, which improves medical outcome and lowers the cost. In this particular case, the NT-proBNP point-of-care test (POCT) (Cardiac® proBNP) allows biochemical detection of HF with satisfactory predictive values and is equivalent to BNP POCT (Triage® BNP). Their analytical ranges are 60-30000 pg mL^{-1} and 5–1300 pg mL^{-1} respectively and have demonstrated to give excellent predictive values for the detection of symptomatic or congestive HF [114]. Another POC device for BNP measurement is the i-STAT® (Abbott), whereas Cobas® h232 (Roche) and RAMP® 200 (Response Biomedical) are addressed to NT-proBNP determination [147].

Although theoretically most commercial immunoassays methods should be able to differentiate between healthy individuals and patients with severe heart failure, there has been reported important differences in performance which

affect their analytical features and reliability. Thus, there exists variation on the concentration values measured, decision levels and cut-off definition among the most commonly used commercial methods for BNP and NT-proBNP. Diagnostic accuracy can strongly depend on patient selection and on the cardiac natriuretic peptide assayed, as well as on the analytical performance and diagnostic accuracy of the immunoassay chosen.

4.1.3 MATRIX OF INTEREST

The most suitable matrices in which these peptides can be measured are human serum or plasma. While NT-proBNP assays can be performed in serum, as well as EDTA or heparinized plasma, for BNP measurements the use of EDTA plasma is highly recommended [131]. This is a consequence of the greater biological variation of BNP caused by its fast degradation in vivo and in vitro. Thus, the use of EDTA or other inhibitors of plasma proteases minimize its degradation in vitro. Another aspect that must be taken into consideration is the cross-reactivity caused by their precursor (proBNP) and other related peptides produced from BNP or NT-proBNP, due to proteolytic cleavages and other posttranslational modifications such as N- and C-terminal trimmings. Due to individual variation of the precursor and processing products among patients, the measurement of a single peptide may not be sufficiently reliable to diagnose the disease.

Saliva and urine have also been used for the evaluation of brain natriuretic peptides. Human saliva contains approximately 20% of the proteins that are present in the blood and has advantages derived from the fact that is a non-invasive, simple and safe sample collection biological fluid. However, some studies pointed out the need of more sensitive assays and a better definition of the recommended cut-off values. Thus, on a study addressed to measure NT-proBNP in saliva using the AlphaLISA® immunoassay it was shown that the NT-proBNP levels of some HF patients were below the LOD of the immunoassay (16 pg mL^{-1}) and there was no a strong correlation with the plasma NT-proBNP concentrations [135]. In regard to urine matrix, while some studies indicate a good diagnostic value of HF [148, 149], others suggest the need to confirm the positive cases with plasma as a cost-effective strategy [150]. In addition, urinary BNP levels were also assessed using the microparticle enzyme immunoassay

(MEIA) from Abbott [151], confirming its applicability in clinical diagnosis and prognosis of HF and a similar accuracy to plasma BNP. On the other hand, Michielsen et al. [152] evaluated the NT-proBNP Roche immunoassay in urine samples and concluded that serum is more reliable. Low recoveries, great variability within and between individuals and other factors such as the renal function that can influence the results obtained with urine were between the problems encountered.

4.1.4 CRITICAL OVERVIEW OF THE EXISTING IMMUNOCHEMICAL APPROACHES FOR NATRIURETIC PEPTIDES

Although several immunoassays for the determination of BNP, NT-proBNP and proBNP have been developed and published in the literature, there are still some aspects to be improved. At the same time and in order to have useful information for the diagnosis of HF, it would be ideal to have a multiplexed assay detecting simultaneously and on a reliable manner all of them. A key aspect is to reduce the cross-reactivity existing between the BNP and the proBNP in most of the immunochemical assays, and the potential interferences of the processing peptides derived.

Considering that BNP is rapidly cleared from plasma due to its bioactive behavior and that it shares the exact sequence with proBNP, the production of specific antibodies for BNP is a great challenge. On the other hand, it has been reported that an individual assay for NT-proBNP determination already would give suitable information to assess HF risk, due to their longer half-life in blood, and the fact that it may be possible avoiding or controlling somehow the interference caused by the precursor employing an appropriate hapten. Hence, the NT-proBNP sequence does not have the glycosilated threonine 71 (Thr 71), while the precursor does (see Figure 1.14 in Chapter 1). However, the measurement of BNP and/or proBNP would provide additional information to the data obtained with NT-proBNP, thus allowing a better confirmation of the final result and conclusion.

As it has been explained along section 4.1, most immunoassays for the determination of BNP, NT-proBNP and proBNP are normally sandwich assays, except for the RIAs, the CLIA developed by Hughes et al. [127] and the BNP

fragment EIA assay (Biomedica immunoassay). The competitive format compared to the sandwich format does not require using two different antibodies. Also, in the case of using an indirect competitive format, in which a bioconjugate is immobilized on the surface, eliminates the risk of losing antibody activity due to immobilization. Moreover, in most of the immunoassays published MAbs are used instead of PAbs. The first ones are characterized for their homogeneity and consistency. Thus, small changes of an epitope can considerable affect their recognition. Otherwise, PAbs are heterogeneous and any change of the epitope is less probable to be relevant. They can be generated with less time, less cost and less technical skills than the ones required for MAbs production. Furthermore, PAbs usually have better specificity than MAbs since they are produced by a great number of B cell clones producing antibodies to different epitopes of the immunogen, making polyclonal sera a quasi optimum pool of different antibodies with unique and diverse specificities [153] versus a single antigen. The immunochemical response will be the addition of the response provided by this pool of antibodies.

4.1.5 OBJECTIVES AND SPECIFIC TASKS

With this scenario, the objective addressed has been the development of an ELISA for the determination of brain natriuretic peptides, particularly, NT-proBNP, BNP and proBNP keeping in mind the need to improve performance and selectivity in respect to the proBNP precursor. In order to accomplish this aim, the following specific objectives were proposed.

- Design and synthesis of appropriate haptens brain natriuretic peptides
- Production of antibodies
- Development and optimization of the microplate-based ELISAs
- Evaluation of the ELISA performance

Initially, immunizing haptens were designed for all three peptides, NT-proBNP, BNP and proBNP, as described in section 4.2. However, as it will be explained below, a series of difficulties were found which impede to pursuit in the direction to obtain immunochemical assays for both, BNP and proBNP.

Therefore, most of the work described in this chapter is focused on the immunochemical determination of NT-proBNP.

4.2 PREPARATION OF IMMUNOGENS

4.2.1 HAPTEN DESIGN AND SYNTHESIS

All the work related to the synthesis of haptens for NT-proBNP (NB1), BNP (BNP1) and proBNP was performed by the Unitat de Química Combinatòria (UQC, PCB) under the responsibility of Dr. Míriam Royo in the context of collaboration within the Nanocardiococo project.

Hapten design was realized for all three natriuretic peptides because of the potential clinical relevance of measuring the three targets to improve stratification and prognostic. NT-proBNP is being contemplated as the biomarker providing more specific and useful information for HF. Producing antibodies against it appears to be more straightforward than for BNP or proBNP. Thus, cross-reactivity caused by the precursor can be minimized by hapten design selecting an appropriate peptide epitope that is only present in NT-proBNP. In contrast, BNP and proBNP share the exact 32 aa sequence. BNP is easily degradable in its N- and C-terminal regions, binds to different receptors and its half-life is shorter than NT-proBNP [66]. The proBNP:BNP ratio in plasma of HF patients varies from patient to patient being the precursor always the predominant form [62]. In spite of these particularities, clinicians claim that their measurement would provide additional information and confirmation to the result obtained with NT-proBNP.

NT-proBNP

The criteria and arguments followed to design a hapten for NT-proBNP were:

I. avoiding glycosylated sequences, since it has been demonstrated that o-glycosylation negatively affects the recognition of some antibodies and the degree of glycosylation varies between patients [62]

II. accessibility for antibody recognition, thus, it is known that the central part of the molecule (aa 28-56) is rarely accessible while regions 13-27 and 61-76 are well recognized for antibodies [63]

III. previous reports showed that antibodies raised against the N-terminal region (aa 1-12) of the molecule were not able to detect endogenous NT-proBNP due to its proteolytic degradation, which is greater in this area [63]

IV. in contrast to proBNP, NT-proBNP is not glycosylated in the threonine 71 (T_{71}), whereas both are glycosylated in the following threonine and serine amino acids: T_{36}, S_{37}, S_{44}, T_{48}, S_{53} and T_{58} (Figure 4.4). Therefore the use of this peptide sequence as immunizing hapten could provide additional selectivity in respect to proBNP. T_{71} is apparently involved in the metabolic processing of proBNP and its glycosylation significantly hampers the furin cleavage of proBNP in vitro. Processing of the precursor is better explained in section 1.6.6.

Although most assays published for NT-proBNP employed antibodies directed to the mid-fragment of the molecule and to the N-terminus (see Table 4.3), based on these arguments, the fragment chosen in this work for raising antibodies is the peptide sequence contained between aa 63 and aa 76 (NB1, see Figure 4.4). Moreover, it is worth noting that Semenov et al. [64] demonstrated that proBNP molecule was almost not recognized by monoclonal antibodies specific towards the 61-76 region which were produced immunizing a synthetic peptide conjugated with a carrier protein. Thus, the peptide chosen starts at aa 63 until aa 76, from now and on it will be called NB1. Seferian et al. [62] used MAbs recognizing the aa 63-71 region, but we extended our peptide to aa 76 since we wanted to make sure of the recognition of aa 71, that would provide selectivity to the antibodies raised. In this direction, also Hughes et al. [127] employed a synthetic peptide containing aa 65-76 as immunogen hapten and AlphaLISA® assay (Perkin Elmer) contains an anti-NT-proBNP MAb recognizing aa 63-76.

Table 4.3. NT-proBNP epitopes recognized by antibodies used for the development of NT-proBNP immunoassays. These immunoassays are published and/or commercially available.

Recognized epitopes (aa-aa)	Capture antibody	Detection antibody	Assay format (method)	Ref.
	PAb: 10-29	-	Competitive (RIA)	[118]
	PAb: 1-23	-	Competitive (RIA)	[123]
	MAb: 63-71	MAb: 13-20	Sandwich (FIA)	[62]
	PAb: 65-76	-	Competitive (CLIA)	[127]
	PAb: 1-21	PAb: 39-50	Sandwich (Elecsys® proBNP, Roche)	[136, 142]
	PAb: 1-21	PAb: 39-50	Sandwich (PBNP® Dimension RxL, Siemens)	[136]
	MAb: -	MAb: -	Sandwich (Dade Behring Stratus® CS acute Care™ Diagnostic System, Siemens)	[137]
	MAb: 1-12	MAb: 63-76	Sandwich (AlphaLISA®, Perkin Elmer)	[135]
	PAb: 8-29	-	Competitive (BNP fragment EIA assay, Biomedica immunoassays)	[142]

As discussed in the previous chapter, due to the high number of functional groups suitable for conjugation along the NB1 sequence, further bioconjugation of this hapten had to employ an orthogonal chemistry. Thus, NB1 was synthesized with a cysteine at the N-terminus in order to use its thiol group for the covalent coupling to HCH and BSA using a cross-linker such as SIA.

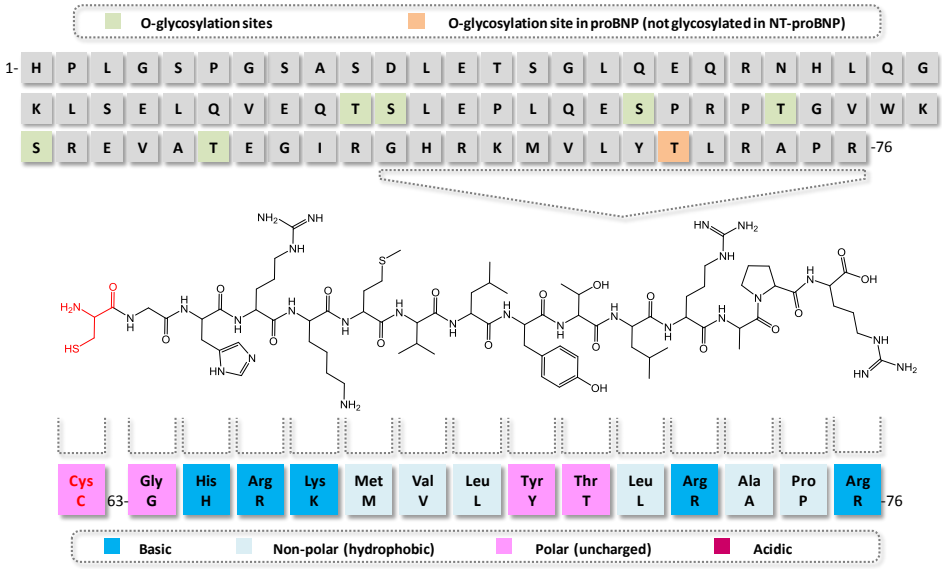

Figure 4.4. Scheme of NT-proBNP sequence (aa 1-76) and the fragment chosen (aa 63-76) for the immunogen (NB1) preparation with their properties. In red, the cysteine (Cys) added in order to perform the coupling to a protein.

BNP

The hapten designed for BNP immunization was based on its entire sequence with the addition of a lysine at the N-terminus with an azide group in the variable chain instead of an amino group (BNP1, see Figure 4.5) to perform orthogonal chemistry through a 1,3-cilcoaddition reaction with an alkinylated protein (*Click* reaction) [154] used to enhance immunogenicity.

Previously, we proposed a hapten with Cys at the N-terminus but its synthesis posed too many problems due to the competition of the thiol group from the N-terminal Cys with the disulfide bridge (S-S bond), forming the characteristic loop.

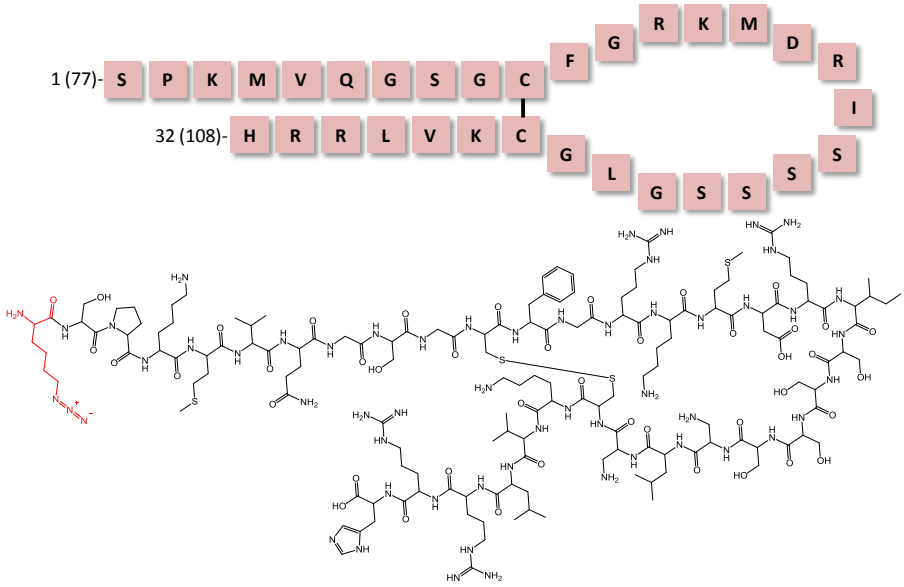

Figure 4.5. Scheme of BNP1 sequence (aa 1-32 = 77-108) for the immunogen preparation. In red, the lysine added in order to perform the coupling to a protein through a Click reaction.

proBNP

For proBNP it was proposed raising antibodies against the cleavage site since it is an epitope that only exists in proBNP and not in BNP neither in NT-proBNP [116]. Thus, in this case, the hapten was based in a sequence that contained the last seven aa from NT-proBNP sequence followed by sixteen more that belonged to BNP (aa 70-92). In this case, at the C-terminus, a cysteine was added to perform orthogonal chemistry during the conjugation to the protein and half of the BNP loop was simulated by a poly(ethylene glycol) diamine with three glycol units (see Figure 4.6) with the aim to increase the affinity versus the proBNP. The presence of a loop was necessary to adopt the original conformation. The use of a hydrophilic PEG chain to accomplish this geometry ensured the lack of immunogeneicity of this newly introduced structure. Placing the Cys at the C-terminus maximized recognition of the aa sequence that contained the more specific part in respect to BNP and NT-proBNP and minimized recognition of the moiety which is more similar to BNP.

The synthesis of the proBNP hapten raised many difficulties. At the time of finishing this PhD thesis, the proposed hapten was still being synthesized and

new strategies were being searched. The difficulties came mainly from how PEG chain was introduced and how it was cycled.

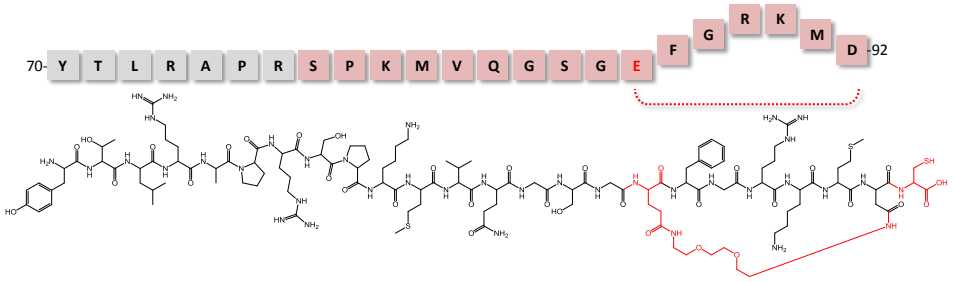

Figure 4.6. Design of the hapten for proBNP detection. In red, the cysteine added in order to perform the coupling to a protein, the glutamic acid (E) added instead of a cysteine to create the loop with the addition of PEG (n=3) diamine.

4.2.2 PREPARATION OF NB1 BIOCONJUGATES

As it has already been explained in section 3.2, molecules with a low molecular weight (MW <2000 g mol^{-1}) need to be properly functionalized (haptens) and covalently coupled to a bigger protein to stimulate the immune system of the host animal. In this case, the NB1 (aa 63-76, MW 1801.19 g mol^{-1}) and BNP1 (MW 3618.21 g mol^{-1}) were coupled to HCH (immunogen) and also to BSA as bioconjugation control and as immunoreagent during indirect ELISA development.

4.2.2.1 Preparation of the NB1-CH_2CO-HCH and NB1-CH_2CO-BSA bioconjugates

NB1 hapten was conjugated to HCH and BSA using SIA as cross-linker to ensure an orthogonal chemistry between the iodoacetylated protein (reaction intermediate) and the sulfhydryl group from the NB1 cysteine (see Figure 4.7). According to MALDI-TOF-MS analysis, the hapten density of the NB1-CH_2CO-BSA bioconjugate was around 17, a value that supported the use of the corresponding HCH bioconjugate for antibody production.

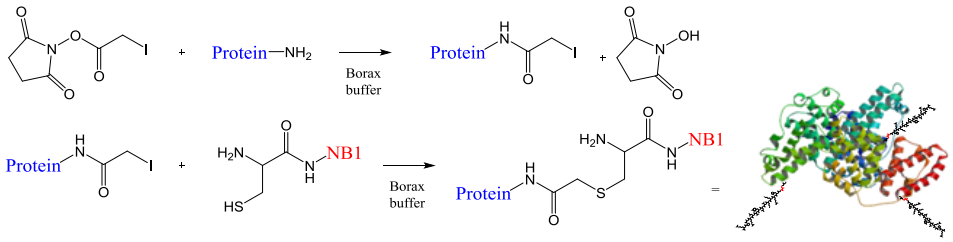

Figure 4.7. Chemical reaction that took place when coupling the peptide NB1 to a protein such as BSA and HCH through SIA linker.

4.2.2.2 Preparation of the NB1 bioconjugates based on the use of heterologous cross-linkers

Two other bioconjugate heterologous competitors were prepared using orthogonal chemistry with the same cysteine modified NB1 peptide, but using different cross-linkers, particularly sulfosuccinimidyl 4-(N-maleimidomethyl)cyclohexane-1-carboxylate (sulfo-SMCC) and N-succinimidyl 3-maleimidopropionate (SMP) instead of SIA (see Figure 4.8). The corresponding bioconjugates NB1-SMCC-BSA and NB1-SMP-BSA were obtained with a hapten density of 3 in both cases. The heterology here was only due to the cross-linker used and thus exposure of the hapten to antibody recognition did not differ as much except from the potential hindering effect of the protein in the NB1-CH_2CO-BSA bioconjugate, due to the short length.

Similarly to SIA, SMP and sulfo-SMCC are two heterobifunctional linkers and the conjugation in which are used proceed by a two-step protocol. The difference with SIA is that SMP and sulfo-SMCC contain a maleimide group instead of an iodo group that when introduced as a spacer can be antigenic. The reaction procedure is very similar, except for the fact that on the second step, the maleimide reacts with sulfhydryl group at pH 6.5-7.5 (see Figure 4.9). At more alkaline pH, amines could also start reacting and hydrolysis of the maleimido to give an open maleamic acid form may occur [101].

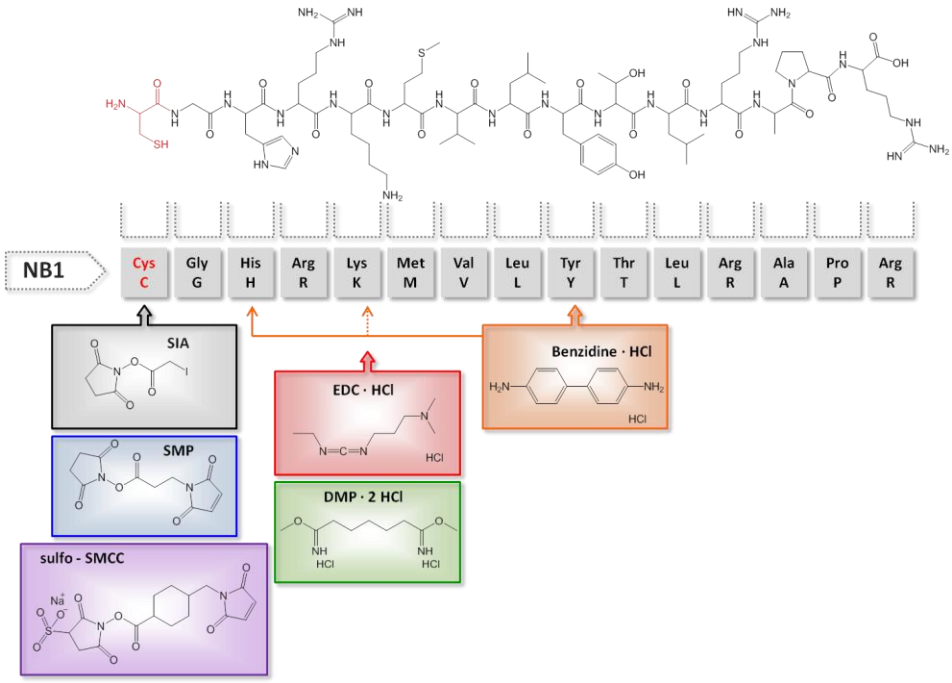

Figure 4.8. Schematic representation of the heterology based on cross-linker and position. Other amino groups apart from the Lys one can also react with EDC·HCl and DMP·2 HCl. Moreover, other nucleophilic groups apart from amino groups can take part in the conjugation procedure using EDC·HCl.

Finally, an HRP enzyme tracer was also prepared to be use as competitor on the indirect format. HRP is an enzyme with about two free lysine groups accessible for bioconjugation [155, 156] and for this reason, we decided for enhance the conjugation yield employing higher molar ratios than for the preparation of the BSA bioconjugates. Thus, NB1-SMCC-HRP in this case a 4:4:1 peptide:linker:Lys molar ratio was employed using sulfo-SMCC as a cross-linker. The chemical reaction that took place is shown in Figure 4.9, while the chemical procedure is detailed in section 8.1.1.

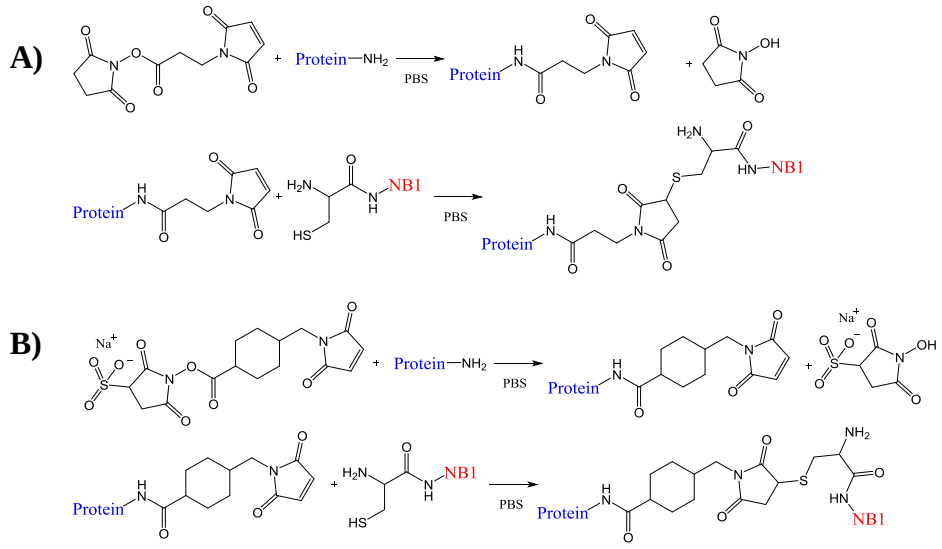

Figure 4.9. Chemical reaction that took place when coupling the peptide NB1 to BSA through A) SMP and B) SMCC linker.

4.2.2.3 Preparation of the NB1 bioconjugates based on location heterology

More heterologous competitors were obtained by reacting the peptide to the protein using other nucleophilic groups like amino groups of the lysine residues (see Figure 4.8). For this purpose two chemical strategies were employed. The first one, was just based on the use of a water soluble carbodiimide (N-(3-dimethylaminopropyl)-N'-ethylcarbodiimide hydrochloride, EDC·HCl) to link the carboxyl groups of the protein to the amino groups of the peptide. EDC as well as other N-substituted carbodiimides can react with carboxylic acids from the protein to first yield o-acylisourea, a highly reactive intermediate, which can later react with nucleophile species such as a primary amine to form an amide bond (see Figure 4.10). When working with proteins and peptides, EDC-mediated amide bond formation effectively occurs at pH 4.5-7.5. In spite of this, carbodiimide reaction successfully occurs up to at least pH 7.5 without significant loss of yield. No aspartic or glutamic acid amino acids were present in the peptide sequence; therefore reaction would exclusively take place through its amino groups as shown in Figure 4.10. We could not control the peptide Lys amino acid residue or the protein carboxy amino acid reacting, so

we assumed that a stochastic mixture of bioconjugates would be obtained using this approach. When wondering to couple a peptide to a protein using this cross-linker, other side reactions can occur since other nucleophiles are also reactive and also self-polymerization can happen due to the abundance of amines and carboxylates in both species. For instance, sulfhydryl groups may attack to form thiol ester linkages, although they are not as stable as the ones formed by an amine. Also oxygen atoms such as those from water molecules can attack and tyrosine residues can react as well with EDC, most likely through the phenolate ionized form.

MALDI-TOF-MS analysis of these conjugates, once purified, revealed a single peak with a mass of 68835 g mol^{-1}, which indicated that the average bioconjugates formed had a hapten density of 1.

The second strategy consisted on using dimethyl pimelimidate dihydrochloride (DMP·2 HCl) as cross-linker, which is a homobifunctional reagent with two imidoester groups that allows amino-amino coupling generating stable amidine linkages. The 7-atom bridge obtained with DMP is positively charged at pH 7.5 (physiological pH) due to the protonated amidine bonds and pH 8-9 must be used to be reacted with amine-containing molecules (see Figure 4.10) [101]. As before, the reaction could not be completely controlled and a mixture of bioconjugates was probably obtained, this time including protein-protein or peptide-peptide oligomers. MALDI-TOF-MS analysis of these conjugates once purified revealed a single peak with a mass of 70508 g mol^{-1} which indicated that the average bioconjugates formed had a hapten density of 1.

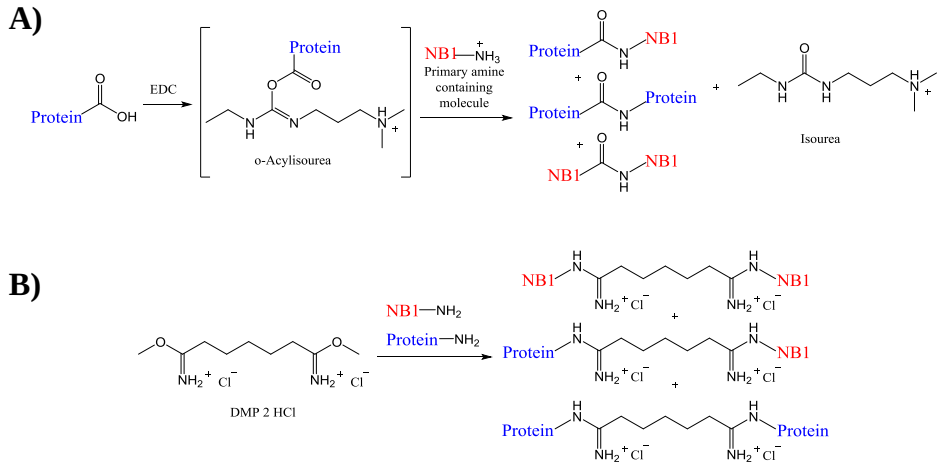

Figure 4.10. A) EDC reacted with carboxylic acids to create an active-ester intermediate. After a nucleophilic attack done by an amine, an amide bond was formed and the reaction gave isourea as a by-product. Different products can be yield due to the self-polymerization and the attack of different nucleophilic groups. These last ones are not represented in the figure. B) DMP reacted with BSA and NB1 to form amidine bonds. Different products are possible due to the self-polymerization.

Finally, a third strategy was investigated which consisted on employing a homobifunctional diazo cross-linker, the bis-diazotized benzidine (BDB), which is able to react on a non-selective manner by primary amino reaction (Lys) and aromatic addition (His and Tyr) as it can be observed in Figure 4.11.

The diazonium-reactive groups generated by treating benzidine with sodium nitrite ($NaNO_2$) under acidic conditions, reacted with active hydrogens on aromatic rings to give covalent diazo bonds. In this case, the BDB obtained was used in a one-step conjugation reaction wherein both the BSA and the NB1 peptide were cross-linked immediately after it was diazotized. At basic pH (pH 8-9), phenolic side chains of tyrosine residues and the imidazole rings of histidines are particularly reactive, although primary amines from Lys can also react. The mechanism of such a reaction is based on an electrophilic attack of the diazonium group toward the electron rich points. Although phenolic compounds can be modified at positions ortho and para to the aromatic hydroxyl group, in this case for tyrosine, only the ortho modification is available. The highly reactive and unstable bis-diazotized benzidine (BDB) compound could also react attacking the electron rich nitrogen of the imidazole ring. The reaction to obtain BDB gave a yellow product which turned to brown

when it was conjugated. It is known that these diazo linkages are reversible by addition of 0.1 M sodium dithionite in 0.2 M sodium borate, pH 9. After the cleavage, the color of the complex is lost [101]. Using this procedure a bioconjugate with a hapten density of 8 was obtained according to MALDI-TOF-MS analysis.

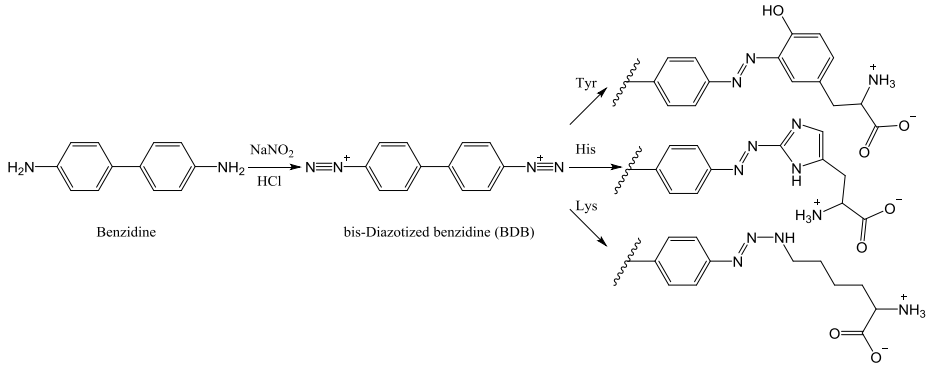

Figure 4.11. Benzidine was diazotized with sodium nitrite and HCl for reaction with tyrosine, histidine or lysine side-chain groups from BSA and NB1 peptide. Particularly reactive are the phenolic side chains of tyrosine residues and the imidazole rings of histidine groups.

With all this battery of antigens, it was possible to assess the effect of the heterology based on the coupling position using different nucleophilic functional groups along NB1 sequence: a sulfhydryl group, amino groups, a phenolic group and an imidazole group, but also the heterology based on the cross-linkers able to react with each of these functional groups.

4.2.3 PREPARATION OF BNP BIOCONJUGATES

4.2.3.1 Preparation of the BNP1-T(4)$(CH_2)_2$CO-HCH,BNP1-T(4)$(CH_2)_2$CO-BSA and BNP1-T(4)$(CH_2)_2$CO-OVA bioconjugates

The hapten BNP1 with an azido functional group (MW 3618.21 g mol^{-1}) was coupled to HCH, BSA and ovalbumin (OVA) through a 1,3-cicloaddition (*Click* reaction) [154]. The coupling was achieved assessing the formation of 1,2,3-triazole which in this case, and at the opposite of NB1, it means the introduction of an antigenic group.

Click chemistry refers to the reaction between an azido functional group added in the peptide sequence and an alkyne introduced in the protein to form a [3+2] cycloaddition product, a 5-membered trizaole ring (see Figure 4.12). The advantage of such synthetic approach is that both functional groups employed, the azido and the alkyne, are not reactive with any other functional group and free of side reactions. Such orthogonality provides extreme selectivity for the conjugation procedure. Thus, the protein was previously derivatized with an alkyne group which was introduced in the protein using 4-pentinoic acid through the active ester method (DCC, NHS).

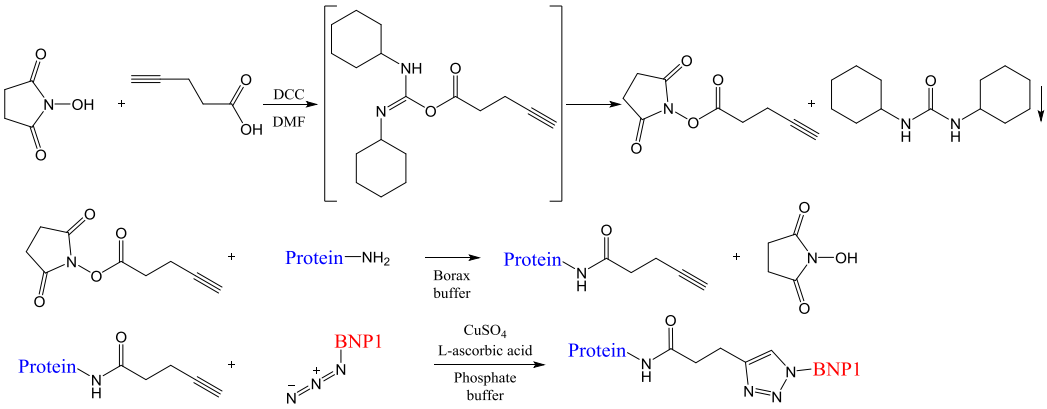

Figure 4.12. Click reaction performed for HCH, BSA and OVA (protein) conjugation to BNP1 peptide.

This 1,3-dipolar cycloaddition reaction is accelerated in the presence of Cu(I) to get good yields even at room temperature and ambient pressures. The Cu(I) is generally generated in situ by the reduction of $CuSO_4$ salt by ascorbic acid. The amount of Cu(II) and ascorbic acid is typically at a concentration of at least 0.1 mM $CuSO_4$ and 0.2 mM ascorbic acid. The triazole ring generated by the reaction in the final product is a very stable linkage and not likely to be hydrolyzed or any kind of other reaction that could cleave the linkage. For protein conjugations, the labelling reaction is done on azide targets at very low concentration levels and for long times [101].

As for NB1, the bioconjugates were purified by dialysis and characterized. The alkyne density of the first conjugate obtained was assessed by MALDI-TOF-MS by comparing the molecular weight of the bioconjugates with that intact protein, reaching an alkyne density of 5 for BSA. Unfortunately it was not

possible to characterize by MALDI-TOF-MS the other bioconjugates since they could not be ionized. However, their biofunctionality was confirmed on a non-competitive indirect ELISA by measuring the binding of serial dilutions of a commercial BNP MAb to microtiter plates coated with BNP1-T(4)$(CH_2)_2$CO-BSA, BNP1-T(4)$(CH_2)_2$CO-OVA and BNP1-T(4)$(CH_2)_2$CO-HCH. The assay procedure is explained in detail in section 8.1.2. The good signal obtained in all cases (Abs_{max} 1.39 at [BNP1-T(4)$(CH_2)_2$CO-BSA]=1 μg mL^{-1} and [MAb 50E1]=0.03 μg mL^{-1}, Abs_{max} 1.27 at [BNP1-T(4)$(CH_2)_2$CO-OVA]=1 μg mL^{-1} and [MAb 50E1]=2 μg mL^{-1} and Abs_{max} 1.31 at [BNP1-T(4)$(CH_2)_2$CO-OVA]=1 μg mL^{-1} and [MAb 50E1]=2 μg mL^{-1}) supported the idea that the conjugations had taken place and therefore the corresponding HCH bioconjugates for antibody production.

4.2.3.2 Preparation of the BNP-EDC-BSA and BNP-EDC-OVA as heterologous bioconjugates

Two heterologous competitors were obtained by reacting the whole peptide BNP without any additional amino acid residue to two different proteins: ovalbumin (OVA) and BSA, using other nucleophilic groups like amino groups of the lysine residues or the N-terminal amino group.

With this aim, EDC was used as a cross-linker to link the carboxyl groups of the protein to the amino groups of the peptide. Chemical strategy has already been explained in section 4.2.2.3 for NB1 peptide and the procedure is detailed in section 8.1.1.

MALDI-TOF-MS analysis of these two conjugates, once purified, revealed that the average bioconjugates formed had a hapten density of 1.

4.3 ANTIBODY PRODUCTION FOR AN NT-PROBNP FRAGMENT: 1ST GENERATION

The NB1-CH_2CO-HCH bioconjugate was used to raise antibodies immunizing three white New-Zealand rabbits as described in section 8.1.20. The obtained

antisera (As) were named As 251, 252 and 253 and their antibody titers were evaluated on a non-competitive ELISA (see Figure 4.13).

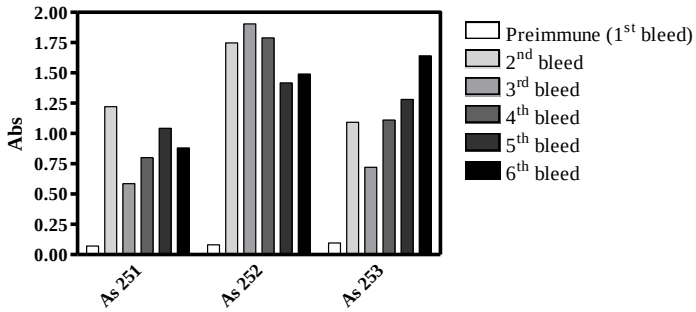

Figure 4.13. Antibody titer to evaluate the response of the antisera produced. Coating antigen NB1-CH_2CO-BSA was used at 1 μg mL^{-1} and the corresponding As 1/16000 diluted.

As it can be observed in Figure 4.13, after the third immunization (3rd bleed) there was a slight decrease of the antibody response in two of the rabbits, but further inoculations succeeded on increasing the title, which remained almost constant after six inoculations. Because of the maturation process [102], although As 251 had less signal in its final bleed compared to As 252 and As 253, this does not mean that its performance under competitive conditions has necessarily to be worse.

4.4 A COMPETITIVE ELISA FOR NT-PROBNP DETERMINATION

4.4.1 INDIRECT AND DIRECT FORMAT

The idea of developing a competitive ELISA for NT-proBNP was mainly based on the experience of our research group on this kind of immunochemical formats and on the fact that just one antibody, and not two different antibodies as in the sandwich format, was necessary. The production of polyclonal antibodies instead of monoclonal was decided, because they are less costly and easier to obtain and by the fact that polyclonal antibodies are a pool of different antibodies recognizing different epitopes of the same hapten. This is important

knowing that peptides are degradable and can suffer posttranslational modifications and/or enzymatic cleavages, which evolves to the presence of material smaller in size circulating in the blood. NT-proBNP standard used in the following experiments was provided by Hytest (Turku, Finland) and it was a recombinant peptide produced in Escherichia coli and contained additional methionine residue at the N-terminus in comparison with native NT-proBNP. It was purified by immunoaffinity followed by ion-exchange chromatography.

Both, indirect and direct ELISA configurations were assessed in order to find out the more suitable format and immunoreagents combination. Both formats are explained and schematized in section 1.4.1.2. On the indirect format, the homologous and heterologous bioconjugates described above were used to coat the microplates, whereas for the direct format NB1-SMCC-HRP was used as tracer.

On a first instance only the homologous conjugates were available and thus used to establish the indirect competitive assay. For the direct format NB1-SMCC-HRP was used. Firstly, appropriate concentrations of the immunoreagents were chosen from two-dimensional checkerboard titration experiments (2D) and further on these concentrations were used to establish the corresponding competitive assays (see Figure 4.14 and Table 4.4). Experimental procedures for 2D and competitive assays are described in section 8.2.2.

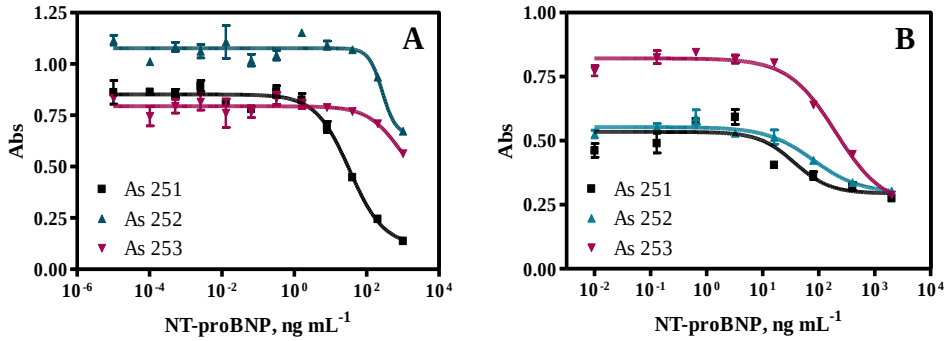

Figure 4.14. Calibration curves for the different combinations and assay formats: A) indirect format using the homologous NB1-CH_2CO-BSA as competitor and B) direct format using the heterologous NB1-SMCC-HRP as competitor. The standard deviation shown is the result of analysis made one day using two (indirect format) and three (direct format) well replicates.

Table 4.4. Immunoassay features for the different combinations and assay formats.

	Indirect format			Direct format		
	As 251	**As 252**	**As 253**	**As 251**	**As 252**	**As 253**
Abs_{max}	0.85	1.08	0.79	0.53	0.55	0.82
Abs_{min}	0.11	0.66	0.37	0.29	0.30	0.24
IC50, ng mL^{-1}	34.03	270.40	837.70	36.93	79.93	202.50
Slope	-0.92	-2.34	-0.96	-1.37	-1.04	-1.02
R^2	0.98	0.85	0.72	0.79	0.91	0.98

Calibration curves were performed using two (indirect format) and three (direct format) well replicates.

Although competitive assays could be obtained with all the antisera and in both formats, the direct assays showed higher background and worse detectability. The selection of the best antisera/competitor combination was based on the immunoassay features, choosing that one with the highest Abs_{max}/Abs_{min} ratio, lowest IC50 value, a slope between -0.7 and -1.2 and a coefficient of regression (R^2) higher than 0.90. Thus, the combination using the antigen NB1-CH_2CO-BSA and As 251 in the indirect format was selected for further investigation. It is worth noting that the indirect (antigen coating) format provides some advantages compared to the direct (antibody coating) format. Hence, using a second antibody that recognizes several epitopes of the first one, may allow enhancing the signal and increasing the detectability (lower LOD). Moreover, the antibody is always in solution avoiding potential denaturation due to surface immobilization. Another advantage can be the potential greatest robustness of the indirect format in front composition of the analyzed matrix, since the enzyme is never in contact with the sample, at the opposite of the direct format [157]. Thus the anti-IgG-HRP in the indirect format is always dissolved in buffer and added on a second step. However there are also some disadvantages such as the fact that in the indirect format there is one more incubation step compared to the direct one when the antibody is not labelled and a secondary antibody labelled with HRP is needed.

In regard to what it has been published in the literature, this assay is the only one detecting NT-proBNP in a competitive indirect format. The Biomedica BNP fragment EIA test and the assay developed by Hughes et al. [127] employed a competitive direct format. The difference between them lies in the recognized epitopes by the antibody used. While the antibody here described was produced against the aa 63-76, the antibody employed in the ELISA

commercialized by Biomedica recognized the aa 8-29 epitope [142] and Hughes and co-workers used an antibody recognizing aa 65-76 in their CLIA. The fragment aa 8-29 is near the mid-fragment region affected by glycosylation but not in the extreme of the N-terminus (1-12 epitope) which seems to be easily degradable [63].

4.4.2 ASSAY OPTIMIZATION

The clinical cut-off value for NT-proBNP analysis in blood samples is 0.4 ng mL^{-1}, while under the standard conditions the IC50 was 34 ng mL^{-1} and the detectability reached by the As 251/NB1-CH_2CO-BSA ELISA was 1.26 ng mL^{-1}. Own to the need to reach a highest detectability, additional efforts were addressed to modify the immunoassay conditions. On a first instance, the number of peptide molecules bound to the protein was decreased. It has been described that bioconjugates of lower hapten density usually favour competition of the target analyte increasing the assay detectability [158-160]. Moreover, reducing the hapten density could favour getting a more soluble antigen.

4.4.2.1 Effect of the hapten density (δ)

Two additional NB1-CH_2CO-BSA bioconjugates were prepared using different peptide:SIA:Lys molar ratios (0.2:2:1 and 0.1:2:1) accomplishing bioconjugates with hapten densities of 5 and 3, respectively, much lower than the one initially employed (17). As expected, reduction of the hapten density allowed to reach assays with a better IC50 values of 11.64 and 7.77 ng mL^{-1} and LOD of 0.72 and 0.77 ng mL^{-1} for δ=5 and δ=3 respectively (see Figure 4.15), much more close to the cut-off level, but in buffer. Although between them, these values are not very different, the bioconjugate (δ=3) was totally soluble, while we had certain difficulties to dissolve the two others. Thus, the NB1-CH_2CO-BSA (δ=3) bioconjugate was chosen for the following studies.

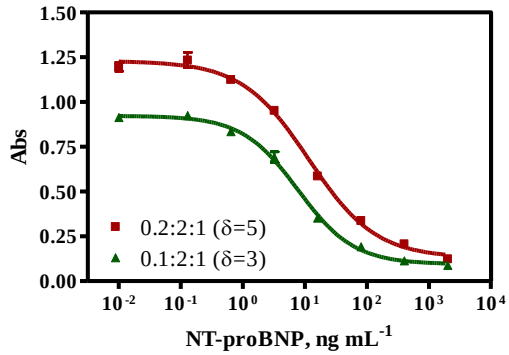

Figure 4.15. Calibration curves and immunoassay features for the two different bioconjugates. The standard deviation shown is the result of analysis made one day using three well replicates.

Table 4.5. Immunoassay features for the two different bioconjugates.

	δ=5	**δ=3**
Abs_{max}	1.23	0.92
Abs_{min}	0.13	0.10
Slope	-0.81	-0.96
R^2	0.99	0.99
IC50, ng mL^{-1}	11.64	7.77
Working range, ng mL^{-1}	2.04-66.37	1.83-33.89
LOD, ng mL^{-1}	0.72	0.77

Calibration curves were performed one day using three well replicates.

In spite of the increase of the detectability compared to the first bioconjugate obtained (δ=17), considering that the assay had to perform in complex samples such as serum or plasma, a further improvement was required. Thus, the most usual method to eliminate matrix interferences in immunoassay is dilution of the sample, which is a simple method but at the same time it has a direct effect on the assay detectability. With this objective in mind, we decided to investigate the effect of increasing competitor heterology in respect of the immunogen.

4.4.2.2 Heterology studies

Optimum chemical, geometrical and electronical features of competitor haptens are not completely defined. Up to know, usually the competitor

bioconjugate is selected based on exhaustive screenings of different biomolecules for which reason a wide battery of competitors are often prepared [100, 161]. The introduction of certain structural differences in the competitors compared to immunizing haptens sometimes has been found to conveniently increase detectability based on the so called heterology principle (see Figure 4.16) [8]. Thus, Ballesteros et al., showed how detectability requirements of competitive immunoassays can be modulated by selecting the appropriate chemical structure of the competitor hapten [162], and some other authors have corroborated this fact ([163-165]). Thus, under heterology conditions, the affinity of the antibody versus the competitor is lower than for the analyte, and this is more able to displace the equilibrium from antibody-competitor to analyte-antibody complex formation (see Figure 4.16). Consequently, the ability of an antibody to be bound to the analyte in the presence of the competitor will define the detectability of such assay.

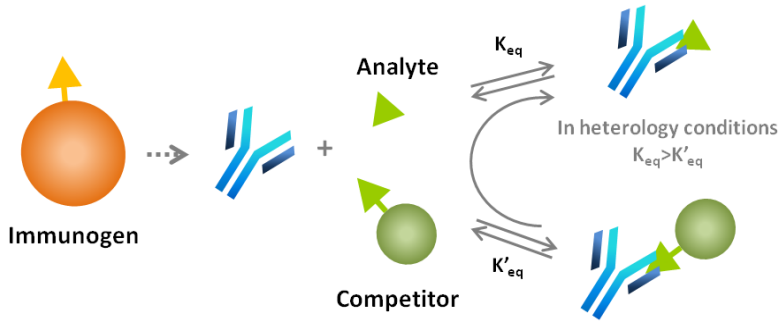

Figure 4.16. Schematic representation of the heterology principle. Antibody affinity for the competitor is lower compared to the analyte and the equilibrium is displaced to the antibody-analyte complex formation due to the major similarity between the immunogen and the analyte.

Heterology can be introduced in different ways: using a cross-linker or a conjugation procedure different from that used in the immunogen (different in length, size or chemical structure), adding the linker in a different position along the hapten structure, changing the chemical structure of the hapten or just employing a fragment from the corresponding structure. All different kinds of heterology were evaluated with the aim of improving detectability using the bioconjugates prepared as described above in section 4.2.2.2 and 4.2.2.3. The preparation and characterization of all antigens here mentioned is accurately described in section 8.1.1.

Heterologous bioconjugates were evaluated, by first selecting the appropriate concentrations through two-dimensional checkerboard titration experiments, and subsequently establishing the corresponding competitive ELISAs under standard conditions. Figure 4.17 and Table 4.6 show the calibration curves and immunoassay features obtained when using these competitors in comparison to the homologous NB1-CH_2CO-BSA bioconjugate and as it can be observed no significant improvement in the detectability was observed. In respect to the cross-linker heterology SIA and SMP bioconjugates behaved very similar. Regarding those bioconjugates with location heterology, those linked through the peptide lysine residues (DMP and EDC) also showed very similar features to the homologous bioconjugate, being EDC slightly better. Finally, the one prepared through Tyr amino acid showed the worse detectability.

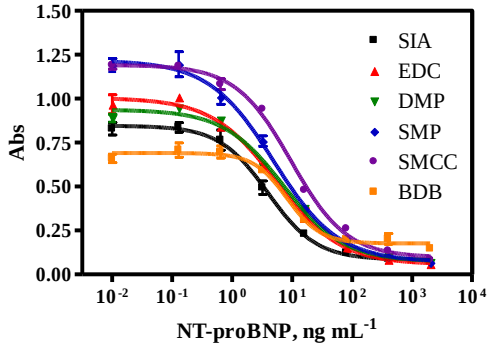

Figure 4.17. Calibration curves for the different competitors with As 251. Curves were performed in one day and each concentration was tested using two well replicates.

Table 4.6. Immunoassay features for the different competitors with As 251.

	Heterologous cross-linkers			**Location heterology**		
	SIA (δ=3)	**SMP** (δ=3)	**SMCC** (δ=3)	**EDC** (δ=1)	**DMP** (δ=1)	**BDB** (δ=8)
Abs_{max}	0.85	1.22	1.19	1.00	0.94	0.69
Abs_{min}	0.08	0.07	0.10	0.06	0.07	0.18
Slope	-1.07	-0.81	-0.94	-0.81	-0.87	-1.55
R^2	0.99	0.99	1.00	0.99	0.99	0.98
IC50, ng mL^{-1}	3.94	4.92	9.64	5.39	7.19	8.22
Working range, ng mL^{-1}	1.16–15.65	1.00–28.69	2.26–44.86	0.94–28.59	1.38–36.28	3.15–23.88
LOD, ng mL^{-1}	0.57	0.41	0.96	0.33	0.51	1.64

Calibration curves were performed in one day and each concentration was tested using two well replicates.

The same studies were performed with As 252 and As 253, but the detectability continued being worse than that reached with As 251. At the light of these results, we decided to increase even more the heterology by modifying the chemical structure of the peptide (hapten heterology).

4.4.2.2.1 Hapten heterology

The hapten heterology was evaluated using the peptides (shown in Figure 4.18) with increased degree of heterology. Thus, NB2 had the same sequence than the immunizing hapten NB1, but the cysteine (Cys) was at the C-terminus, instead of at the N-terminus. In fact, the heterology of that hapten could be considered like the highest degree of linker location heterology, since in such case, although the sequence is the same, the peptide moiety more exposed to the recognition of the antibody is the opposite to that exposed to the immunosystem by the immunizing peptide NB1. NB3 is shorter peptide sequence comprising the amino acids of the C-terminus and with a Cys used for orthogonal bioconjugation placed at the C-terminus, as NB2. Finally, NB4 has the same short peptide sequence but with the Cys at the other end. NB3, would thus be, theoretically, the most heterologous hapten.

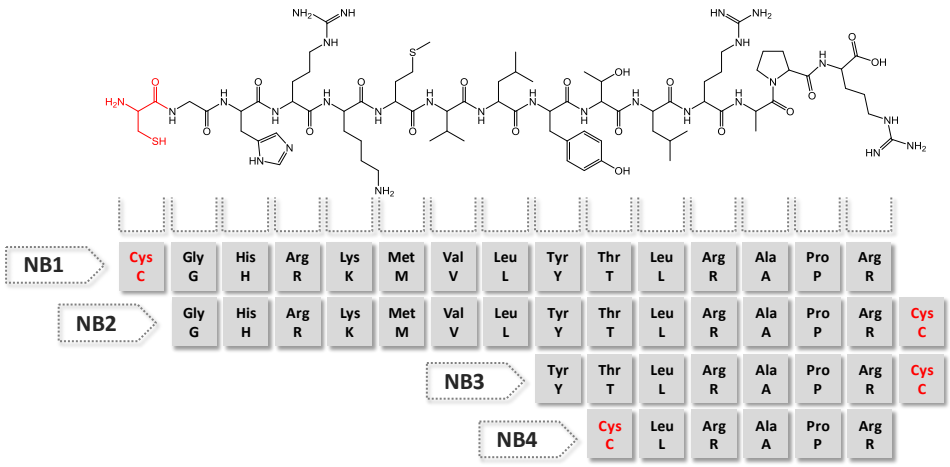

Figure 4.18. Schematic representation of the heterology based on the peptide sequence and position.

As before, these peptides were synthesized by the Unitat de Química Combinatòria (UQC, PRB) under the responsibility of Dr. Míriam Royo. All peptides were conjugated to BSA through the SIA linker using the thiol group

from the corresponding Cys. The chemical reaction procedure followed for the preparation of such competitors was the same used for the immunogen and it is explained in section 4.2.2.1 (Figure 4.7), while the experimental protocol is described in section 8.1.1. After their preparation, all conjugates were purified and characterized by MALDI-TOF-MS and tested by ELISA. The hapten densities achieved were 3, 3, 3 and 4 for NB1, NB2, NB3 and NB4, respectively.

Competitive ELISAs were established for all these antibody/bioconjugate combinations providing acceptable absorbance signals at zero concentration of the target analyte. A side from NB1-CH_2CO-BSA, the homologous bioconjugate already evaluated, NB2-CH_2CO-BSA was the best recognized by all three antisera raised, even though the peptide was linked at the opposite position. This point to the fact that the antisera raised against NB1 has produced polyclonal antibodies also against the area close to the protein attachment point, which is in NB2 more exposed to recognition. Because of the same reason, probably was NB4-CH_2CO-BSA better recognized than NB3-CH_2CO-BSA, since higher hapten density (4 instead of 3) does not justify such difference. From all antibodies tested, As251 was the one providing the lowest signal, while As 252 and As 253 behaved different depending on the bioconjugate (see Figure 4.19, graph A).

From all the antisera/bioconjugate combinations tested, only As 251/NB2-CH_2CO-BSA gave a usable immunoassay in terms of detectability (see Figure 4.19, graph B). The other bioconjugates provided competitive assays with very high LOD values and therefore not suitable for our purposes, considering the cut-off value that we had to reach. After variation of some experimental conditions, both As 251/NB1-CH_2CO-SIA and As 251/NB2-CH_2CO-BSA showed very similar analytical features regarding the assay parameters as it can be observed in Figure 4.19, graph C, being the detectability in the same order (see table D).

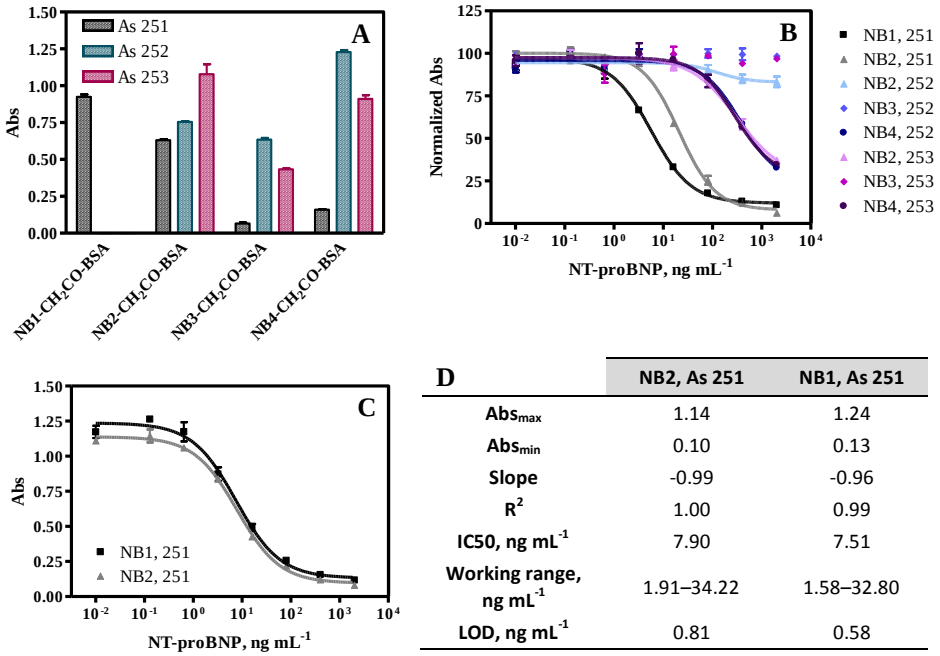

D	NB2, As 251	NB1, As 251
Abs_{max}	1.14	1.24
Abs_{min}	0.10	0.13
Slope	-0.99	-0.96
R^2	1.00	0.99
IC50, ng mL^{-1}	7.90	7.51
Working range, ng mL^{-1}	1.91–34.22	1.58–32.80
LOD, ng mL^{-1}	0.81	0.58

Figure 4.19. Graphs and table showing data obtained with the different combinations, NB(1,2,3,4)-CH_2CO-BSA and As 251, 252, 253. NB1 was already assayed with As 252 and 253 in section 4.3 and 4.4.1. A) Response evaluation at 1 µg mL^{-1} NB-CH_2CO-BSA and As 1/2000 diluted, B) competitive indirect ELISA using the combinations in A, except those in which the signal was too low (NB3-CH_2CO-BSA and NB4-CH_2CO-BSA with As 251), C) competitive indirect ELISA for the best two combinations and D) immunoassay features for these last combinations. Data presented correspond to the average of at least two well replicates.

Thus, the results obtained seem to indicate that the best bioconjugate competitor should keep a certain degree of homology to the immunizing hapten to provide the necessary detectability. Thus, the most heterologous bioconjugates (NB3- and NB4-CH_2CO-BSA) gave very poor assays, while the bioconjugates keeping all the peptide sequence (NB1 and NB2) provided assays with similar response independently from the bioconjugation procedure used or the position of the linker (see Figure 4.17).

4.4.2.3 Optimization of physicochemical parameters

At this point we decided to use As 251/NB1-CH_2CO-BSA for further studies focused on the effect of different physicochemical parameters of the competitive step (pH, ionic strength, etc.) on the immunoassay performance and to acquire knowledge regarding behavior in different media. Thus, changes

in physico-chemical features or composition of the immunoreaction media can affect not only the interactions analyte-antibody and antibody-antigen but also the properties of the biomolecules involved (bioconjugate and antibody conformation, activity of the enzyme tracers, etc.). The bonding forces driving formation of immunocomplexes are hydrophobic, Van der Waals, and electrostatic interactions and hydrogen bonds. Physico-chemical parameters such as the pH and the ionic strength of the media, or the incubation time and temperature may affect these interactions, similarly for additives present in the assay buffers such as detergents or blocking agents.

As stated before, assessment of the immunoreagents has been performed under what we know as "standard conditions" (30 min incubation times, PBST: 0.01 M phosphate buffer 0.8% saline solution (~16 mS cm^{-1}), pH 7.5; with 0.05% Tween 20 and without a previous incubation analyte–antibody and without the use of any blocking agent), however such conditions may be investigated in more detail in order to achieve optimum performance.

Percentage of Tween 20, ionic strength and presence of additives in the competition buffer were evaluated in this order. Moreover, pH, preincubation and competition time together with the temperature were further studied. All experiments were performed building calibration curves under different conditions with at least two-well replicates for each concentration.

The presence of a detergent like Tween 20 in the buffer provides better solubility and decreases unspecific adsorptions. In spite of this, it is described that better LOD is achieved decreasing the concentration of detergents for hydrophobic compounds [166-168], what underlines the hypothesis proposed by some authors [169]. This hypothesis explains that hydrophobic interactions can be established between the analyte and the detergent which would make difficult the specific interaction with the antibody. In this case, from 0.2 to 0.05% Tween 20, the IC50 value increased but then it decreased until 0% when the slope got worse. Percentage of Tween was again assessed starting from 0.05% to 0%, observing that detectability improved when the percentage decreased, but at 0.001 and 0% also the slope was significantly worse as previously noticed. Thus, a Tween 20 percentage of 0.005% was considered to be the most appropriate (Figure 4.20).

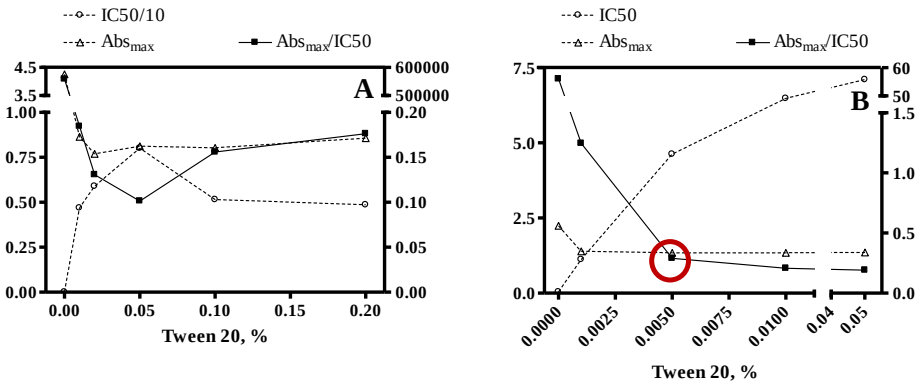

Figure 4.20. Effect of Tween 20 percentage in the competition buffer. Right axis shows Abs$_{max}$/IC50 ratio, while the left axis shows IC50/10 or IC50 and Abs$_{max}$ values. In A) the percentage of Tween 20 goes from 0 to 0.2% and in B) the region comprised from 0 to 0.05% is deeply studied.

To study if the ionic strength had some effect in the interaction between the analyte and the antibody, phosphate buffer solutions (0.01 M PB) were prepared with different concentrations of NaCl and KCl in order to have a range of conductivities of 2, 5, 9, 16, 29 and 52 mS cm^{-1} (corresponding to 0, 0.2, 0.4, 0.8, 1.6, 3.2% NaCl respectively). Each one was adjusted to pH 7.5 and the percentage of Tween previously selected was added. Results are shown in Figure 4.21 were it can be observed that detectability improved when the conductivity decreased obtaining the best value at 2 mS cm^{-1} (0% NaCl) but an increase in the background noise of the assay was also observed in these conditions (data not shown). It has been described that polar substances are better detected on low conductivity media, and on the contrary, for non-polar substances for which the interactions are mainly hydrophobic [169, 170].

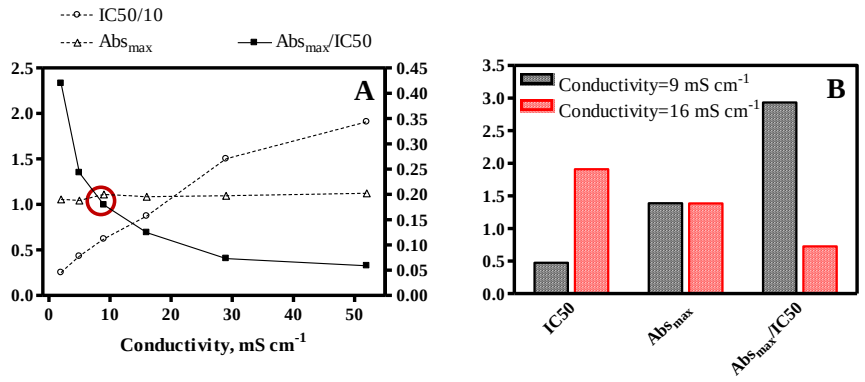

Figure 4.21. Effect of the conductivity in the competition buffer. Right axis shows Abs_{max}/IC50 ratio in A), while the left axis shows IC50 and Abs_{max} values. In A) the conductivity was studied adding 0.05% Tween 20 in the competition buffer and the same result was confirmed in B) using 0.005% Tween 20, which was the percentage finally chosen.

Plasma has an ionic strength similar to 0.8% saline solution (~16 mS cm^{-1}) and it may be 1/2 diluted during the competitive step when adding the antiserum, therefore a conductivity of around 9 mS cm^{-1} corresponding to a 0.4% saline solution was initially selected as a compromise to improve detectability without increasing too much the background noise, while mimicking the expected conditions when measuring plasma samples. Nevertheless, the effect of some blocking agents was also investigated in order to be able to work in lower conductivity media to improve detectability. Solutions of 2% polyethylene glycol (PEG), 2% polyvinylpyrrolidone (PVP) and 2% milk in PBT (standard PBST with the absence of salts, 0% NaCl) were assayed as additives in the assay buffer (Figure 4.22). For PVP and milk a decrease in background was observed, but it was accompanied by a significant increase in IC50 and decrease in Abs_{max} compared to PBT. With the addition of PEG, an increase of IC50 and Abs_{max} was observed as well as an increase of background noise. In conclusion, the addition of additives in a buffer without salts did not improve the results obtained previously.

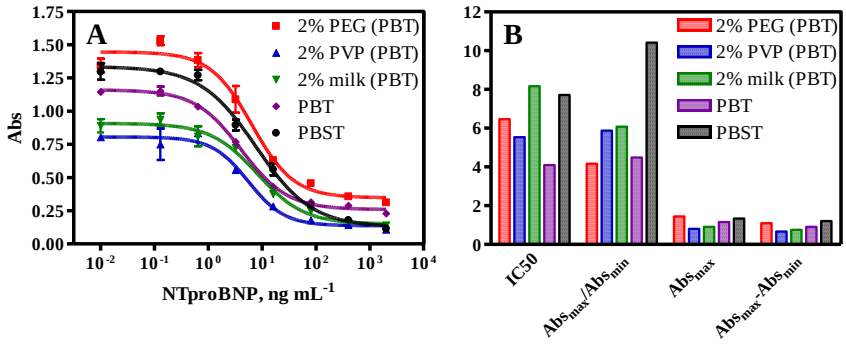

Figure 4.22. Effect of the additives in the competition buffer containing 0.05% Tween 20. In A) calibration curves for the different buffers are represented. In B) it is shown the corresponding IC50, Abs_{max}/Abs_{min} ratio, Abs_{max} and Abs_{max}-Abs_{min}. PBST is the standard PBST with a conductivity of 16 mS cm^{-1} (0.8% NaCl) and PBT is PBST with the absence of salts (0% NaCl).

As it can be observed in Figure 4.23 the assay tolerated a wide interval of pH values, from 6.5 to 9.5. Below pH 5.5 the IC50 considerably increased, similarly for the background noise (data not shown). Since no significant variations were observed within the 6.5 to 9.5 pH interval, the value was maintained at 7.5 on the subsequent experiments.

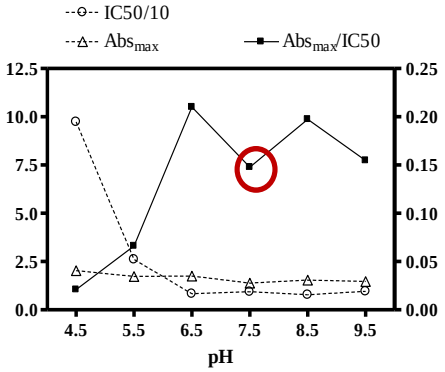

Figure 4.23. Effect of pH in the competition buffer with 0.05% Tween 20 and a conductivity of 9 mS cm^{-1} (0.4% NaCl). Right axis shows Abs_{max}/IC50 ratio, while the left axis shows IC50/10 and Abs_{max} values.

In some occasions, it has been described that the detectability of an immunoassay can be improved by preincubating the analyte with antibody before the competitive step [171]. For the NT-proBNP immunochemical system, this parameter was investigated and the results are shown in Figure 4.24 (graph

A), where it can be seen that preincubation notably influenced the detectability of the assay. Just with 15 min of preincubation, a great improvement in IC50 was observed, which did not get better with the time (similar results were seen after 30, 45 and 60 min of preincubation).

Similarly to the preincubation time, the time required for an effective competition between the analyte and competitor for the antibody binding sites, can be an important factor. This parameter together with the temperature in the competitive step, were assessed and results can be observed in Figure 4.24. Incubation periods greater than 30 min decreased assay detectability and this effect was much more evident when no preincubation was performed (see Figure 4.24, graphs B and C). On the other hand, detectability slightly increased if incubation time during competition was decreased (see Figure 4.24, graph E), however this effect was not observed if performing the incubation at 40°C. In contrast, temperature significantly improved detectability, particularly when a preincubation step was included in the immunochemical protocol (see Figure 4.24, graph D) step worked well although it did not make a lot of difference in terms of Abs_{max}/IC50 compared to the competitive step at room temperature (RT). In order to save antiserum and be able to dilute it from 1/5000 to 1/10000 to decrease Abs_{max}, competitive step at 40°C was set.

Finally, the acetonitrile was also investigated, with the aim to potentially improve peptide solubility, and perhaps to enhance detectability, however as it can be observed in Figure 4.24 (graph F), the assay did not tolerate the organic solvent and the signal was almost inhibited above 20% acetonitrile (ACN). Acetonitrile was the only organic solvent studied because the peptide was completely soluble in it and it was also employed during the HPLC purification of the NT-proBNP immunogen fragment.

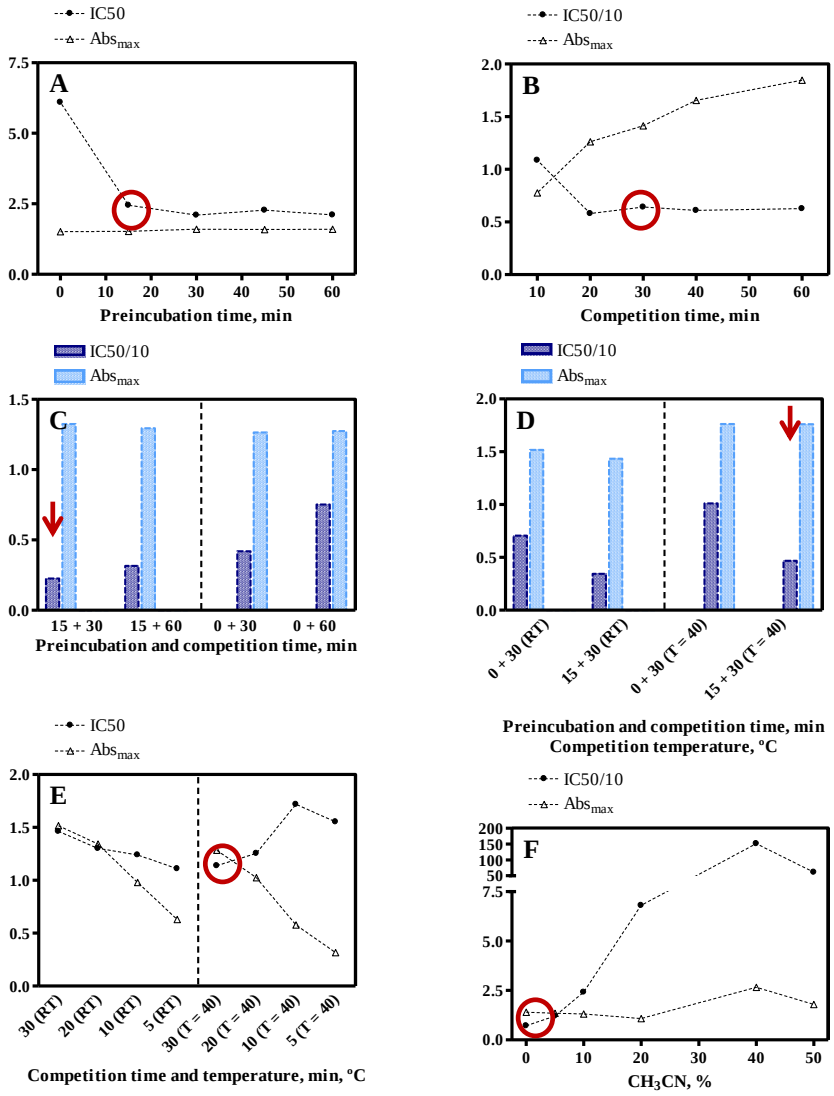

Figure 4.24. A) Effect of analyte-antibody preincubation time previous the competitive step, B) effect of the competition time with a preincubation for 15 min at RT. In C) both effects were joined together, but antibody dilution was optimized for 60 min competitive step. In the three cases calibration curves were performed with 0.05% Tween20 and a conductivity of 9 mS cm^{-1} in the competition buffer. D) and E) Effect of the preincubation time, competition time and temperature in the competitive step, F) effect of the percentage of organic solvent (ACN) that can be tolerated by the assay. In D), E) and F) calibration curves were performed with 0.005% Tween 20 and a conductivity of 9 mS cm^{-1} in the competition buffer.

According to these studies, an immunoassay protocol was set up which conditions are summarized in Table 4.7. From the initial conditions, As 251 final

dilution was changed from 1/5000 to 1/10000, 0.8% NaCl in the competition buffer to 0.4% and 0.05% Tween 20 to 0.005%, an analyte-As 251 preincubation step (15 min at RT) was added before the competition and the competition was performed at 40ºC instead of at RT. With these final conditions, detectability improved from 0.58 ng mL^{-1} (see Figure 4.19) to 0.15 ng mL^{-1} (see Figure 4.27) with an Abs_{max} of 1.24 and 0.93 respectively.

Table 4.7. Assay features for the optimized ELISA NB1-CH_2CO-BSA/As 251 in buffer.

	NB1-CH_2CO-BSA/As 251
	Buffer
NB1-CH_2CO-BSA, µg mL^{-1}	0.125
As 251, final dilution	1/10000
Competition buffer	0.01 M phosphate buffer pH 7.5, 0.4% NaCl, 0.005% Tween 20
Preincubation step	RT, 15 min
Competition step	40°C, 30 min

4.4.3 IMPLEMENTATION OF THE NT-PROBNP ELISA TO THE ANALYSIS OF PLASMA SAMPLES

With these results, we moved forward with the intention to assess performance of the assay in biological samples. Even if we would have desired to improve detectability the LOD was close to the cut-off level. Since whole blood is a complex sample, we decided to start our studies with plasma. Plasma is normally extracted from blood by centrifugation in the presence of anti-coagulant agents, such as sodium and lithium heparin, EDTA and its potassium salt (K_2EDTA), oxalate and citrate. About 55% of blood is plasma while the other 45% are red blood cells (RBD or erythrocytes), platelets (thrombocytes) and white blood cells (leukocytes), present on a 600:40:1 ratio, respectively (see Figure 4.25). Once the blood is centrifuged, the cell fraction is also known as *buffy coat*. It has around 50-70 mg mL^{-1} of proteins and approximately 70% of them are albumins (35-50 mg mL^{-1}) and 10% immunoglobulins (IgG) (5-7 mg mL^{-1}) [172]. Plasma contains fibrinogen and other coagulation factors, while coagulated blood yields serum without fibrinogen although some coagulation factors remain. Both, plasma and serum contain addition all proteins not used

in coagulation, electrolytes, antibodies, antigens, hormones and any other exogenous substances such as drugs and microorganisms.

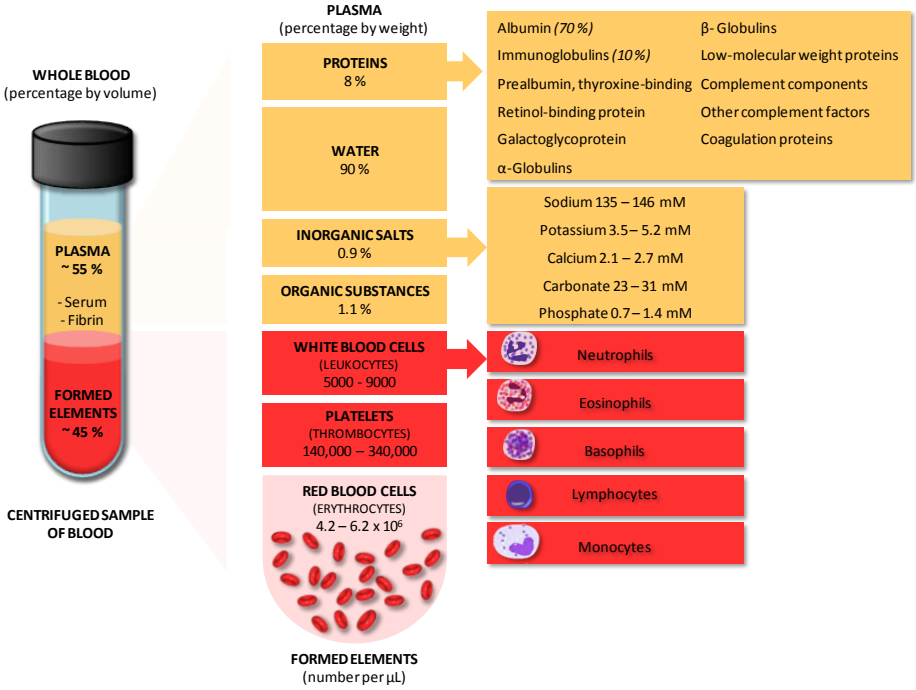

Figure 4.25. Schematic representation of whole blood composition. Adapted from [173].

Assessment of ELISA performance was initially made using human plasma provided by Banc de Sang i Teixits de Catalunya (plasma BST) obtained by pooling expired (not suitable for transfusion) blood samples of healthy donors, and stored frozen in aliquots. However, on the later steps of the evaluation, plasma free of brain natriuretic peptides (BNP and NT-proBNP free plasma) was obtained from commercial sources. According to the supplier it was pooled plasma purified by immunoaffinity chromatography, which bead was BrCN-activated Sepharose CL 4B prepared by coupling anti-BNP and anti-NT-proBNP monoclonal antibodies with different epitope specificity.

Standard curves were first prepared in buffer and plasma BST and run in the ELISA to compare the parallelism (see Figure 4.26). The physicochemical conditions employed for the achievement of these calibration curves were not the final ones established in Table 4.7 since curves were performed earlier. For the assay in buffer, the analyte and antiserum were both diluted in the same

buffer (0.01 M phosphate buffer in a 0.4% saline solution, 0.05% Tween 20, pH 7.5), while in plasma assay the analyte was diluted in the corresponding plasma and the antiserum in buffer (0.01 M phosphate buffer solution without salt, 0.1% Tween 20, pH 7.5). For both assays, the competition step was done during 30 min at RT with a previous preincubation during 15 min at RT.

Plasma BST produced considerable undesired matrix effect (red curve) when using the same conditions established for buffer (black curve). Therefore, we re-adjusted the immunoreagents concentrations by running checkerboard titration experiments in plasma BST undiluted at RT (see Table 4.8). Under these conditions the assay (green curve) was able to reach a good detectability (IC50=2.59 ng mL^{-1} and LOD=0.13 ng mL^{-1}) below the cut-off level (see Table 1.4, chapter 1). However, it should be noticed that the slope had decreased significantly.

At this point we realized that the plasma BST could have basal levels of brain natriuretic peptides which could contribute to the signal and the detectability observed. Therefore we implemented these conditions to the analysis of BNP and NT-proBNP free plasma (blue curve). In such case, the slope increased and the detectability was, as expected, slightly worse.

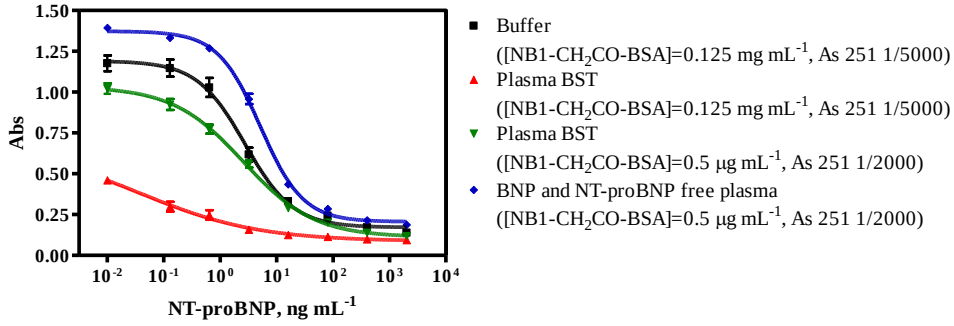

Figure 4.26. Matrix effect caused by human plasma and BNP and NT-proBNP free human plasma. Calibration curve in buffer (black curve) was assayed six times in four different days, curve in plasma (red curve) was performed once, curve in plasma with the immunoreagent concentrations re-adjusted (green curve) was performed five times in three different days and BNP and NT-proBNP free plasma curve (blue curve) was assessed once. In all cases, each concentration was tested using two well replicates every time.

Table 4.8. Immunoassay features for the ELISA in buffer, plasma BST and BNP and NT-proBNP human plasma.

	Buffer	Plasma BST	Plasma BST	BNP and NT-proBNP free plasma
[NB1-CH_2CO-BSA] µg mL^{-1}	0.125	0.125	0.5	0.5
As 251	1/5000	1/5000	1/2000	1/2000
Abs_{max}	1.19	0.68	1.03	1.37
Abs_{min}	0.17	0.09	0.11	0.21
Slope	-1.02	-0.41	-0.69	-1.15
R^2	0.92	0.98	0.97	1.00
IC50, ng mL^{-1}	2.77	0.23	2.59	5.16
Working range, ng mL^{-1}	0.79–13.02	0.03–3.32	0.38–18.48	1.44–18.11
LOD, ng mL^{-1}	0.38	0.02	0.13	0.65

Calibration curve in buffer (black curve) was assayed six times in four different days, curve in plasma (red curve) was performed once, curve in plasma with the immunoreagent concentrations re-adjusted (green curve) was performed five times in three different days and BNP and NT-proBNP free plasma curve (blue curve) was assessed once. In all cases, each concentration was tested using two well replicates every time.

As it can be observed in Figure 4.26 and Table 4.8 there is, in fact, significant differences between the response of both plasma samples using the same immunoreagents conditions. In addition to the NT-proBNP basal levels of the plasma BST, it could be that the way these plasma samples were obtained from human blood (separation process, anti-coagulant used, etc.) or the additional purification BNP and NT-proBNP free plasma suffered would influence. For the case of plasma BST it was not possible to obtain all the necessary information regarding how this blood was obtained or the plasma prepared and which additives (i.e. anticoagulants) were used. On the other hand, assuming that plasma BST contains the reported basal NT-proBNP levels (0.4 ng mL^{-1}), this value does not justify the decrease in the maximum absorbance in respect to the BNP and NT-proBNP free plasma curve since the LOD is higher than the cut-off level.

As result of the optimization of the assay in buffer described above (see section 4.4.2.3), it was decided to run the competitive step for 30 min at T=40°C, with a previous preincubation with the analyte and the antibody during 15 min at room temperature and employing a competition buffer composed by 0.01 M

phosphate buffer in 0.4% saline solution with 0.005% Tween 20, pH 7.5. These conditions were now implemented for the BNP and NT-proBNP free plasma samples (see Table 4.9).

Table 4.9. Assay features for the optimized ELISA NB1-CH_2CO-BSA/As 251.

	NB1-CH_2CO-BSA/As 251	
	Buffer	BNP and NT-proBNP free plasma
[NB1-CH_2CO-BSA]	0.125 µg mL^{-1}	0.5 µg mL^{-1}
As 251, final dilution	1/10000	1/4000
Competition buffer	0.01 M phosphate buffer pH 7.5, 0.4% NaCl, 0.005% Tween 20	1:1 Plasma:Assay buffer (Assay buffer: 0.01 M phosphate buffer pH 7.5, 0% NaCl, 0.01% Tween 20)
Preincubation step	RT, 15 min	RT, 15 min
Competition step	40°C, 30 min	40°C, 30 min

The results obtained are shown in Figure 4.27 and Table 4.10.

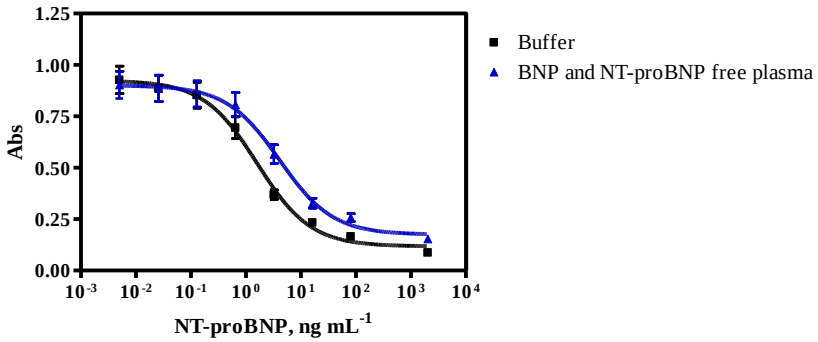

Figure 4.27. Calibration curves for the evaluation of NT-proBNP in buffer and human plasma. Each curve was tested in four days using three well replicates on every assay (n = 12).

Table 4.10. ELISA features for the evaluation of NT-proBNP in buffer and human plasma.

	Buffer		BNP and NT-proBNP free plasma	
	Mean±SD	**CV (%)**	**Mean±SD**	**CV (%)**
Abs_{max}	0.93±0.25	26.86	0.9±0.3	27.6
Abs_{min}	0.12±0.03	21.15	0.2±0.1	26.0
Slope	-0.9±0.1	13.1	-0.92±0.07	7.36
R^2	0.990±0.001	0.118	0.990±0.002	0.228
IC50, ng mL^{-1}	1.6±0.4	24.0	4±2	41
Working range, ng mL^{-1}	0.4±0.1-10±2	31.9, 21	1.0±0.4-23±10	39.5, 41
LOD, ng mL^{-1}	0.15±0.05	36.04	0.4±0.2	39.0

Each curve was tested in four days using three well replicates on every assay (n = 12).

As it can be observed, the assay shows acceptable parameters regarding Abs_{max}, slope and the LOD is just at the cut-off level. The variation on the assay conditions had a significant influence on the detectability. Although we had not accomplished the goal to obtain an assay with a LOD below the cut-off, at this point we consider these features sufficient to continue with our studies. Thus, in fact, as described in the introduction, the levels between 0.4 and 2 ng mL^{-1} indicate unlikely chronic HF (uncertain diagnosis) and over 2 ng mL^{-1} would indicate HF. With the actual features the assay developed should be able to distinguish between these two groups.

4.4.4 EVALUATION OF THE NT-PROBNP ELISA PERFORMANCE IN PLASMA SAMPLES

The accuracy of the As 251/NB1-CH_2CO-BSA NT-proBNP ELISA was assessed by measuring 8 fortified samples, prepared in buffer and BNP and NT-proBNP free plasma, during 4 different days. On each assay the samples were measured using three well replicates. The results obtained are shown in Figure 4.28. As it can be observed, there is a good correlation found between the measured and the fortified concentration values. Results obtained matched very well the fortified values. A slope near 1 was obtained (1.06 for buffer and 0.91 for plasma) with a coefficient of correlation of 0.978 and 0.933, respectively.

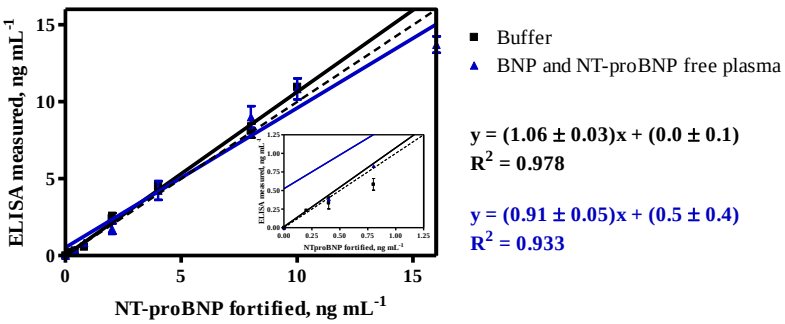

Figure 4.28. Correlation between the fortified and measured concentration values. The dotted line corresponds to a perfect correlation (slope=1).

In the following table (Table 4.11), the coefficient of variation (CV) for each sample is calculated. The CV obtained is the inter-day variation between four days, using three well replicates each day.

Table 4.11. Mean, standard deviation and coefficient of variation obtained for each sample measured in 4 different days.

	Buffer		BNP and NT-proBNP free plasma	
NT-proBNP, ng mL^{-1}	**Mean±SD**	**CV (%)**	**Mean±SD**	**CV (%)**
16	[a]	[a]	14±1	7.9
10	11.0[b]	[b]	11±1	12.5
8	8.1±0.8	9.6	9±1	15.6
4	4.6±0.5	11.5	4±1	29.0
2	2.4±0.7	28.0	1.7±0.7	38.6
0.8	0.6±0.2	26.9	0.6±0.3	42.2
0.4	0.3±0.2	48.0	0.4[c]	[c]
0.2	0.23±0.03	13.27	0[d]	0[d]
0	0	0	0	0

[a]Sample detected all 4 days but it was out of the corresponding working ranges (not able to be quantified), [b]detected every day but once could be quantified, thus there is nor SD neither CV (%) values, [c]detected one day and could also be quantified, [d]sample not detected.

Although in general CV (%) values around 15-20% are acceptable for screening bioanalytical assays, National Academy of Clinical Biochemistry (NACB) and the International Federation of Clinical Chemistry and Laboratory Medicine (IFCC) committee for standardization of markers of cardiac damage laboratory medicine practice guidelines recommends that assays for BNP and NT-proBNP should have a total imprecision (%CV) of ≤15%.

Although in buffer the NT-proBNP ELISA is reaching a LOD of 0.15±0.05 ng mL^{-1}, suitable for measuring this biomarker at the cut point and basal levels, in plasma, LOD of 0.4±0.2 ng mL^{-1} allows to detect and in some cases quantify unlikely chronic HF (0.4 – 2 ng mL^{-1}) and always quantify low level of patient that could be suffering from heart failure (over 2 ng mL^{-1}).

At this point, the way to increase the assay detectability was discussed, considering the interest of start measuring NT-proBNP already in the range from 0.1 to 0.4 ng mL^{-1}, which when levels start raise at the very beginning of the disease. One of the hypotheses was that the cross-linker SIA employed on the immunogen could have provided a too short spacer arm, and that part of the peptide structure could be hindered by the HCH protein due to this fact. Even though the experiments done with the NB2 heterologous competitor was against this hypothesis, we decided to produce a second generation of antibodies but using a longer spacer arm expecting to improve the recognition.

4.5 ANTIBODY PRODUCTION FOR NT-PROBNP FRAGMENT: 2ND GENERATION

The same peptide NB1 was then coupled to HCH using the SMCC linker. While with the SIA linker the final conjugate had a spacer arm of 1.5 Å, with SMCC linker the distance between the peptide and the carrier protein increased to 8.3 Å (Figure 4.29). We assumed that in this way the peptide would be more exposed and less hindered by the protein compared to the first case. The only drawback was the introduction of additional antigenic groups (cyclohexyl and maleimide groups) that could evolve antibodies able to recognize other potential bioconjugate competitors prepared with such linker or any other molecule containing this group.

This type of bioconjugation has already been explained in section 4.2.2.2 and the experimental protocol followed is described in section 8.1.1.

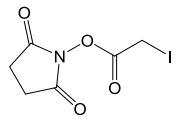	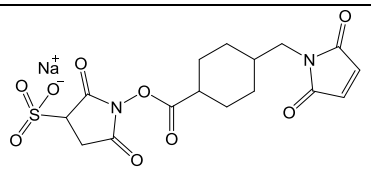
N-Succinimidyl iodoacetate (SIA) MW = 283.02 g mol^{-1} Spacer arm = 1.5 Å	**3-Sulfo-N-hydroxysuccinimidyl-4-(N-maleimidomethyl)cyclohexane-1-carboxylate sodium salt (sulfo-SMCC)** MW = 436.37 g mol^{-1} Spacer arm = 8.3 Å (9 atoms)

Figure 4.29. Chemical structure, nomenclature, molecular weight and length of the final spacer arm for the two linkers used in both NB1 conjugations to HCH.

Using NB1-SMCC-HCH for inoculating white New Zealand rabbits, three antisera were obtained named As 321, 322 and 323. These antibodies were evaluated as described in section 8.1.2 and the conditions studied to establish competitive indirect ELISAs under homologous and heterologous conditions using the homologous (NB1-SMCC-BSA) and heterologous (NB1-CH_2CO-BSA, δ=3) as competitors, respectively. Figure 4.30 shows the calibration curves obtained on the first screening in comparison to the As 251/NB1-CH_2CO-BSA immunoassay established before, as reference. It is worth noticing that all assays were run under standard conditions.

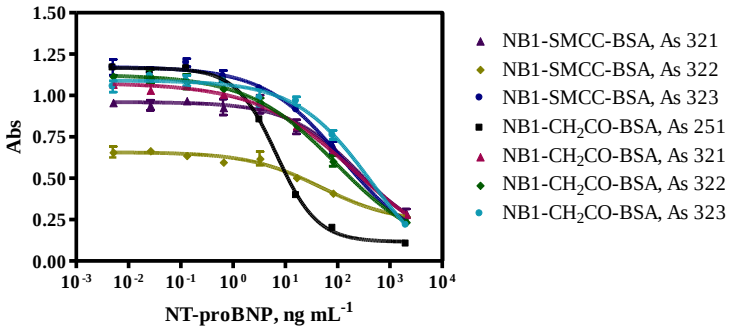

Figure 4.30. Calibration curves and immunoassay features for the different combinations. These assays were run under standard conditions. Curves were performed in one day and each concentration was tested using three well replicates.

Table 4.12. Immunoassay features for the different combinations.

	NB1-SMCC-BSA			NB1-CH_2CO-BSA			
	As 321	**As 322**	**As 323**	**As 251**	**As 321**	**As 322**	**As 323**
Abs_{max}	0.96	0.66	1.17	1.17	1.08	1.13	1.09
Abs_{min}	0.12	0.23	0.06	0.12	-0.00	0.05	-0.13
IC50, ng mL^{-1}	243.60	48.83	123.20	6.82	219.20	92.77	438.00
Slope	-0.65	-0.62	-0.58	-1.11	-0.46	-0.51	-0.60
R^2	0.94	0.93	0.98	1.00	0.99	0.98	0.97

Curves were performed in one day and each concentration was tested using three well replicates.

The parameters shown in the above Table 4.12 demonstrate that the antibodies produced using the SMCC linker do not improve the assay detectability. We should admit that further work could have been done for optimization including the evaluation of additional competitors prepared, as it has been described above, but at this point, we decided to move forward in our investigation using the As 251/NB1-CH_2CO-BSA NT-proBNP ELISA.

4.6 ANTIBODY PRODUCTION FOR BNP

The BNP1-T(4)$(CH_2)_2CO$-HCH bioconjugate described in section 4.2.3 was used to raise monoclonal antibodies for BNP immunizing four mice as described in section 8.1.2. Preimmune (first bleed), second and third bleeds were obtained for the four mice and evaluated on a non-competitive ELISA (see Figure 4.31) using in parallel BNP1-T(4)$(CH_2)_2CO$-BSA and BNP1-EDC-BSA as coating antigens.

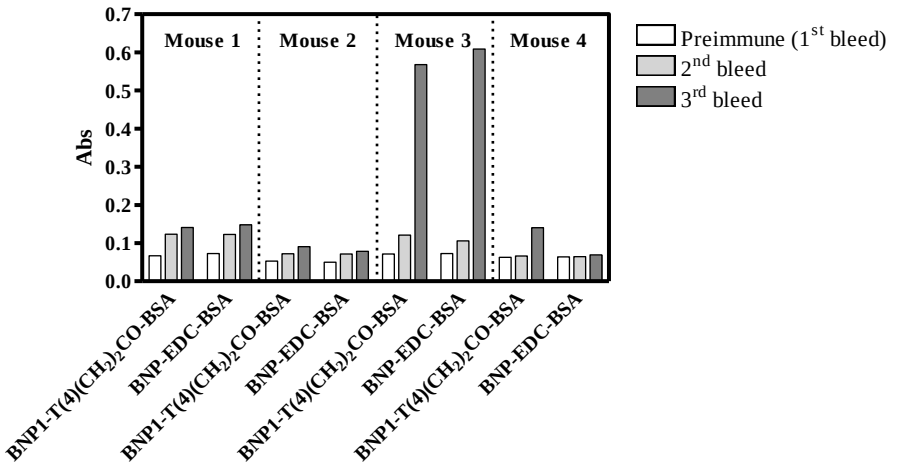

Figure 4.31. Antibody titer to evaluate the response of the antisera produced. Coating antigens BNP1-T(4)$(CH_2)_2$CO-BSA and BNP-EDC-BSA were used at 1 μg mL^{-1} and the corresponding As 1/1000 diluted.

As it can be observed in Figure 4.31, surprisingly, no antibody specific response was observed for any mouse except for the third bleed of Mouse 3. Although the response was not very high having into account that both coating antigens and As were considerably concentrated, the corresponding fusion and the first screening were carried. Unfortunately, no positive clones were obtained.

Between the potential reasons, there could be the low solubility observed for the HCH immunogen. For this reason, a new immunogen was prepared using the same molar ratios, but taking care of aspects such as avoiding freezing and thawing steps. Again, it was not possible to characterize by MALDI-TOF-MS the final bioconjugate since it could not be ionized. However, its biofunctionality was confirmed on a non-competitive indirect ELISA by measuring the binding of serial dilutions of commercial BNP MAbs (see Figure 4.32 for a determined MAbs concentration).

Four more mice were immunized and the antibody titers in the preimmune (first) and second bleeds were assessed on a non-competitive ELISA (see Figure 4.32) using in parallel homologous (BNP1-T(4)$(CH_2)_2$CO-BSA and BNP1-T(4)$(CH_2)_2$CO-HCH) and heterologous (BNP-EDC-BSA) bioconjugates coating antigens. At the same time, the response of two commercial MAbs (24C5 and

50E1) was assessed with the same three coated antigens. According to the supplier (Hytest, Turku, Finland), both antibodies were purified by affinity chromatography against protein A, and MAb 24C5 was obtained by immunizing with the aa 11-22 peptide sequence while MAb 50E1 was produced with the whole synthetic BNP molecule but recognized mainly aa 26-32 which is the C-terminal part.

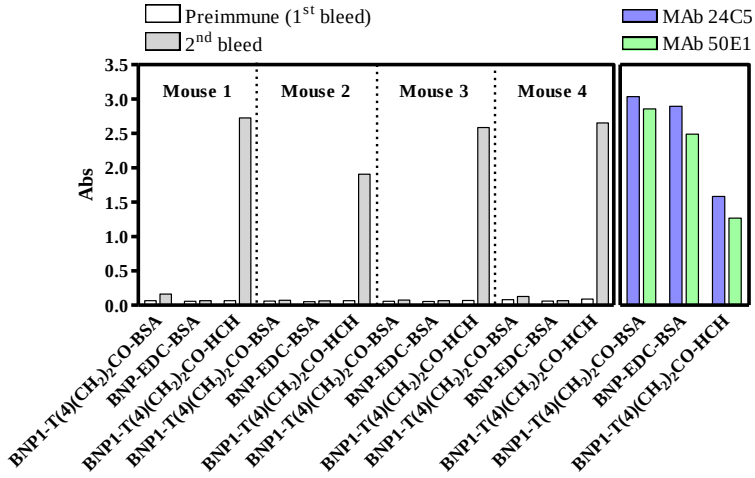

Figure 4.32. Antibody titer to evaluate the response of the antisera produced. Coating antigens BNP1-T(4)$(CH_2)_2$CO-BSA, BNP-EDC-BSA and BNP1-T(4)$(CH_2)_2$CO-HCH were used at 1 μg mL^{-1} and the corresponding As 1/1000 diluted. Two MAbs (24C5 and 50E1 at 2 μg mL^{-1}) from Hytest were evaluated using these same coating antigens at 1 μg mL^{-1}.

While the antisera produced could only recognize the protein from the immunogen, 24C5 and 50E1 antibodies were able to recognize all three different coating antigens. This fact confirms the bioactivity of our bioconjugates however does not explain the lack of antibody response of the mice we immunized.

More efforts were still addressed to the antibody production trying to use the BNP1-T(4)$(CH_2)_2$CO-BSA conjugate instead of the HCH conjugate for immunization of the same mice and preparing additional homologous BNP1-T(4)$(CH_2)_2$CO-OVA and heterologous BNP-EDC-OVA bioconjugates using OVA as protein. Figure 4.33 shows the response of the preimmune (first bleed) and fourth bleed against all these conjugates. As it can be observed, the antisera produced recognized now also the BSA immunogen, the 4th bleed of all four mice could recognize the BNP1-T(4)$(CH_2)_2$CO-BSA and HCH immunogens, but

could not recognize the OVA conjugate (BNP1-T(4)$(CH_2)_2$CO-OVA). In contrast, commercial MAbs were able to recognize all four different coating antigens.

These results point to the fact that the antibodies had only been produced against the protein and it is against the possibility that antibodies would have been produced mainly against a sub product of the Click reaction.

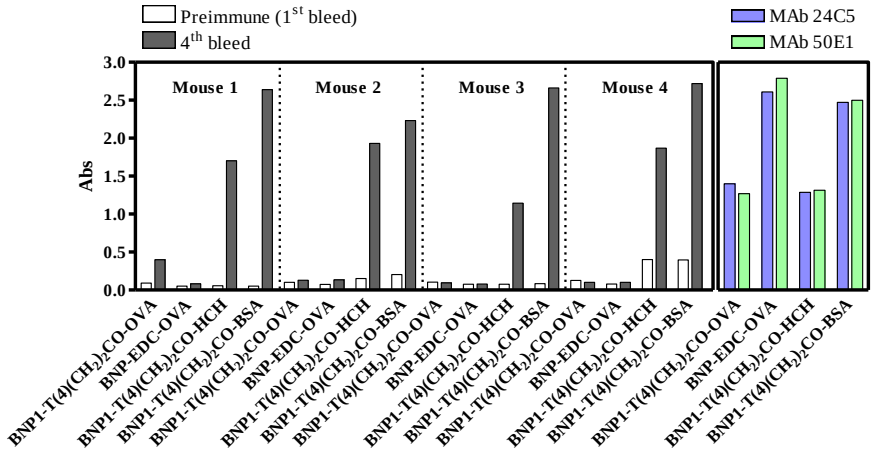

Figure 4.33. Antibody titer to evaluate the response of the antisera produced. Coating antigens BNP1-T(4)$(CH_2)_2$CO-OVA, BNP-EDC-OVA, BNP1-T(4)$(CH_2)_2$CO-HCH and BNP1-T(4)$(CH_2)_2$CO-BSA were used at 1 µg mL^{-1} and the corresponding As 1/1000 diluted. Two MAbs (24C5 and 50E1 at 2 µg mL^{-1}) from Hytest were evaluated using these same coating antigens at 1 µg mL^{-1}.

Finally, it was attempted to produce polyclonal antibodies with two white New Zealand rabbits using the BNP1-T(4)$(CH_2)_2$CO-BSA bioconjugate described in section 4.2.3.1. Preimmune (first bleed), second, fourth, fifth and final bleeds were obtained for the two rabbits and evaluated on a non-competitive ELISA (see Figure 4.34) using BNP1-T(4)$(CH_2)_2$CO-OVA as coating antigen. As it can be observed in Figure 4.34, in this case a positive response was obtained being the As 329 the one that provide higher antibody titer, even if the dilution of the antiserum was not so high as with other immunogens used in this thesis.

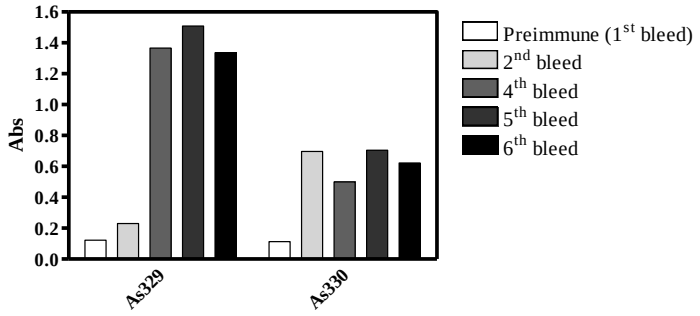

Figure 4.34. Antibody titer to evaluate the response of the polyclonal antisera produced. Coating antigen BNP1-T(4)$(CH_2)_2$CO-OVA used at 1 µg mL^{-1} and As 329 and As 330 1/8000 and 1/2000 respectively diluted.

Figure 4.35 shows the calibration curves obtained with this antiserum and using two different combinations with the commercial MAbs.

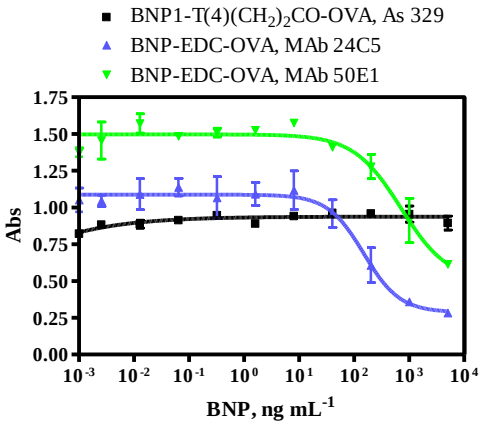

	As 329	MAb 24C5	MAb 50E1
Abs_{max}	0.94	1.09	1.50
Abs_{min}	0.02	0.29	0.49
IC50, ng mL^{-1}	$8 \cdot 10^{-6}$	149.0	708.9
Slope	0.43	1.32	1.01
R^2	0.49	0.91	0.91

Figure 4.35. Calibration curves and immunoassay features for the different combinations in an indirect competitive format using As 329 and commercial MAb 24C5 and 50E1 (BNP1-T(4)$(CH_2)_2$CO-OVA, As 329; BNP-EDC-OVA, MAb 24C5 and BNP-EDC-OVA, MAb 50E1).

As it can be observed above, in spite of the successful production of a specific polyclonal antiserum, it was not possible to establish any usable competitive immunoassay if we consider that the cut-off for BNP assays is at 0.1 ng mL^{-1} [23].

At the time of writing this thesis we had not found any explanation for the failure of the BNP1-triazol conjugates to produce antibodies against BNP. For the case of the mice antibodies seemed to only recognize the protein (HCH or

BSA). Even of the potential immunogenic properties of the triazol group, this was not recognized as it can be seen in Figure 4.33 by the lack of response against the corresponding OVA conjugate. A failure in the bioconjugation or the lack of immunogenicity of the designed hapten was also discharged since the bioconjugates are recognized by the commercial MAbs (24C5 and 50E1). Moreover, a potential degradation after emulsification with the Freud's adjuvant or inside the host animal would be difficult to explain from the chemical point of view, but also because when rabbits were immunized it was possible to observe a response. Future work could be addressed in the optimization of the competitive assay trying different formats and increasing the heterology like it was done with the NT-proBNP immunoassay.

4.7 DISCUSSION

Polyclonal antibodies for NT-proBNP were produced in this chapter and with them an indirect competitive ELISA was developed achieving the established cut-off in buffer and allowing working very near the cut-off with plasma samples.

When this ELISA is compared to other ELISAs already published or even available in the market we could say that we have been able to develop for the first time a competitive indirect immunoassay with detectability at the cut-off level in plasma. The BNP fragment EIA (Biomedica immunoassays) is the only ELISA available for NT-proBNP. It is a direct competitive ELISA employing a polyclonal antibody for the NT-proBNP fragment (aa 8-29) as a capture antibody, this same fragment labelled with HRP as enzymatic tracer and TMB and H_2O_2 in the substrate solution [142]. The Biomedica assay reaches a LOD of 1.4 ng mL^{-1}, far from the cut-off which is at 0.4 ng mL^{-1}. Thus, in that respect our ELISA is superior since the LOD is already at the cut-off level. There are other ELISAs published in the literature but they are addressed to BNP or proBNP detection, using all of them a sandwich format.

Regarding other competitive assays, there is a direct competitive CLIA for NT-proBNP published in the literature that achieves a great LOD ($1.3 \cdot 10^{-9}$ ng mL^{-1}) but with a long assay time including an overnight antibody-antigen

preincubation. In this assay, a polyclonal antibody produced for aa 65-76 was bound to magnetic particles with anti-IgG antibodies previously attached. Then, NT-proBNP fragment (aa 65-76) labelled with acridinium ester is the responsible for the chemiluminescent detection [127].

Apart from these two cases, there are other assays for NT-proBNP detection but not using the ELISA method neither a competitive format. For instance, Seferian et al. developed a FIA employing two different MAbs, one labelled with biotin and the other with europium thus reaching a LOD of 0.01 ng mL^{-1} [62]. All commercial assays employ a sandwich format a part from the explained above, achieve excellent LOD and are performed in less than 1h. Most of them are based on the chemiluminescent principle [133-137, 139, 140]. This indicates that changing to a sandwich format or even changing the immunoassay principle to CLIA with the most suitable label and enhancer could be ideas to improve LOD and performance of the assay developed in this chapter.

In conclusion, the ELISA for NT-proBNP detection and quantification is the best ELISA assay developed for this analyte and allow affirming that the strategy followed for the PAb production was a good one.

5 INDIVIDUAL IMMUNOASSAYS FOR CRP, CYS C H-FABP AND LP(a) DETERMINATION

5.1 INTRODUCTION

In the current chapter we will describe the development of immunochemical assays for CRP, Cys C, Lp(a) and H-FABP cardiovascular biomarkers, using immunoreagents from commercial sources (Audit Diagnostics, a partner of the Cajal4EU project, and Randox) to further on implement them on the multiplexed microarray platform (chapter 6). A key element on the multiplexed platform is to accomplish that all assays perform with the best features under the same conditions (buffer composition, incubation times, etc.). Thus, in here, we will also describe performance of the cTnI and NT-proBNP immunochemical assays under the same conditions as the other assays.

5.2 DESCRIPTION OF ANALYTES, IMMUNOREAGENTS AND ASSAY FORMATS

Due to the different chemical nature (proteins and peptides) of the biomarkers selected, different immunochemical configurations can be used. The most common format for the detection of proteins such as CRP, Cys C, Lp(a), H-FABP and cTnI is in a sandwich format, and on the key issues is the selection of the most suitable pair of antibodies recognizing different epitopes located at distant positions of the protein. Peptides with a MW above 10000 g mol^{-1} are often detected on sandwich formats but, if the MW is below 10000 g mol^{-1}, the most appropriate is to use a competitive format.

The corresponding assay formats for CRP, Cys C and Lp(a) are shcematized in Figure 5.1, while those for H-FABP, Tn I-T-C complex and NT-proBNP are shown in Figure 5.2.

CRP, Cys C and Lp(a) standards and the corresponding antibodies were provided by Audit Diagnostics, a partner involved in Cajal4EU project. The CRP calibrator was obtained from pooled human whole blood. The two antibodies for CRP (AbCRP1 and AbCRP2) were polyclonal antibodies (PAbs) produced in goats immunizing purified human CRP. They were different as they were from different suppliers but later acquired by Audit Diagnostics and, thus, different immunogens were used. The antisera had been purified by solid-phase

adsorption, fractionated and passed over a diethylaminoethanol (DEAE) resin to isolate the immunoglobulins G (IgG) fraction. AbCRP1 was a defibrinated and delipidated antibody. The antibody for Cys C was also a purified Ig fraction obtained from goat PAb using purified human Cys C as immunogen. Lp(a) calibrator was an apolipoprotein B-100 disulphide-linked to the large glycoprotein apolipoprotein(a). Lp(a) PAbs (AbLp(a)1, AbLp(a)3) were from goat immunized with a chemically synthesized epitope sequence of the human apolipoprotein (a) (monospecific). They were defibrinated, delipidated and affinity purified by using solid-phase to which Lp(a) antigenic components were bound. Defibrinated blood is plasma which has anticoagulant present during collection and hence needs a chemical treatment to remove fibrin and to form clotting and, consequently, serum. Delipidated serum is devoid of lipid components of blood.

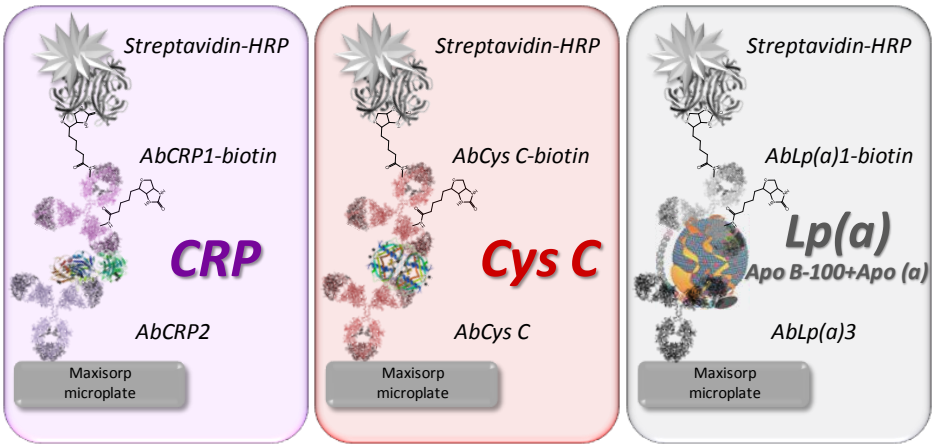

Figure 5.1. Schematic representation of the different assay formats and immunoreagents used for CRP, Cys C and Lp(a) detection.

Randox was chosen as commercial source for the H-FABP pair of antibodies. One of them as the Ig fraction of a PAb developed in sheep by immunizing recombinant human H-FABP, whereas the second one was a MAb also from sheep (clone 3, C3) purified through protein A affinity chromatography. Sheep monoclonal antibodies (MAbs) were created using similar methods as those used to create mouse ones with the particularity that a sheep hetero-myeloma fusion partner is used to immortalize sheep B cells. According to the supplier, sheep MAbs compared to mouse MAbs are almost always of a higher affinity which can be very convenient to develop assays for analytes at very low

concentrations (10^{-10} to 10^{-14} M). Moreover, apparently sheep MAbs recognize a much broader range of epitopes. As summary, sheep MAbs are characterized by the following features:

- Ability to remain bound to their target (affinity) is commonly 100-fold greater than mouse antibodies
- Greater ability to bind where the target analytes are present but at very low concentrations
- Ability to recognize "difficult" targets where rodent antibody technologies failed (broader epitope recognition)
- Ability to discriminate between closely related molecules
- Can be humanized without affecting the antibody affinity

The H-FABP calibrator was purchased from Life Diagnostics and was obtained from human cardiac tissue and purified using a combination of gel filtration and ion-exchange chromatography. The calibrators and immunoreagents used for cTnI and NT-proBNP are described in chapter 3 and 4, respectively.

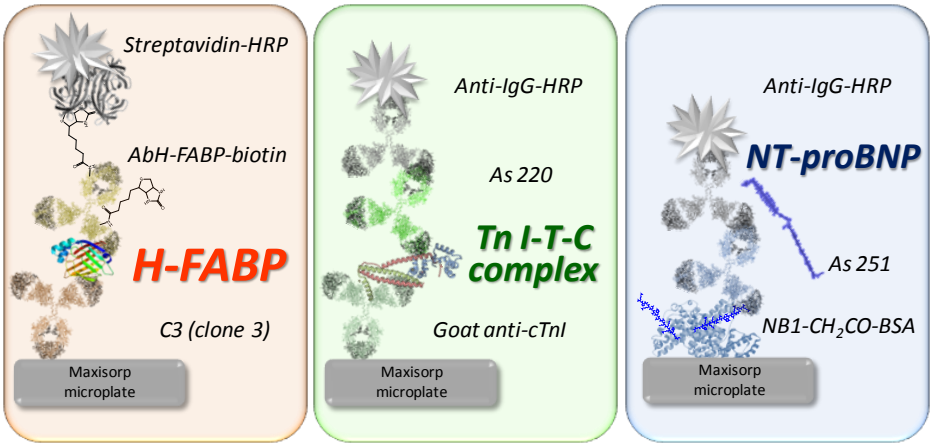

Figure 5.2. Schematic representation of the different assay formats and immunoreagents used for H-FABP, cTnI and NT-proBNP detection.

HRP labelling of the detection antibodies was initially attempted but we observed that the background noise of the assays increased if the antibodies had been purified only by ammonium sulphate precipitation. It was possible to demonstrate that such background noise was due to unspecific adsorption of the labelled antibodies to the surface, effect which was even greater on the microarray glass surfaces (data not shown). For this reason, we decided to use

anti-rabbit IgG-HRP for the cTnI and NT-proBNP assays, while in CRP, Cys C, Lp(a) and H-FABP assays the antibodies (goat and sheep) were biotinylated in order to use streptavidin-HRP to generate the signal. Anti-goat IgG-HRP or anti-sheep IgG-HRP could not be used in this case since both capture and detection antibodies were from the same animal. The procedure followed for the antibody labelling with biotin is described in section 8.1.3. All reagents together with its commercial source and assay formats used in the development of each ELISA assay are summarized in Table 5.1.

Table 5.1. Reagents and assay format for the ELISA development of each biomarker.

Biomarker	Assay format	Biorecognition elements (providers)		Analyte (provider)	Signal
		Capture Ab	Detection Ab		
CRP	Sandwich	Goat PAb (AD): AbCRP2	Goat PAb (AD)-biotin: AbCRP1-biotin	Serum based CRP (AD)	Streptavidin-HRP
Cys C		Goat PAb (AD): AbCys C	Goat PA (AD)-biotin: AbCys C-biotin	Serum based Cys C (AD)	
Lp(a)		Goat PAb (AD): AbLp(a)3	Goat PAb (AD)-biotin: AbLp(a)1-biotin	Serum based Apo B-100+apo (a) (AD)	
H-FABP		Sheep MAb (R): C3	Sheep PAb (R)-biotin: AbH-FABP-biotin	Human cardiac H-FABP (LD)	
cTnI		Goat PAb (LD): Goat anti-cTnI	Rabbit PAb As 220	Human cardiac Tn I-T-C complex (H)	Anti-IgG-HRP
NT-proBNP	Competitive	Coating antigen: NB1-CH_2CO-BSA	Rabbit PAb As 251	Recombinant NT-proBNP, aa 1-76 (H)	

AD: Audit Diagnostics, R: Randox, LD: Life Diagnostics, H: Hytest.

5.3 SANDWICH ELISA ASSAYS FOR CRP, CYS C AND H-FABP DETERMINATION

The ELISAs were developed taking into consideration the conditions established for cTnI and NT-proBNP assays. Thus, the blocking buffer (0.15% casein in PBST)

used to reduce the unspecific adsorption observed for troponin I and its tertiary complex was now used for the incubation steps of the distinct analytes. Moreover, since the sandwich assays (CRP, Cys C, Lp(a), H-FABP and cTnI) have an additional step (detection antibody) in respect to the competitive immunoassay (NT-proBNP), on the last one, an additional incubation step with PBST during 30 min was introduced before the anti-IgG-HRP addition. This was done to simulate the addition of detection antibodies required in sandwich assays and compare all performances to those that will further take place on the microarray. Calibration curves and ELISA features are shown in Figure 5.3 and Table 5.2.

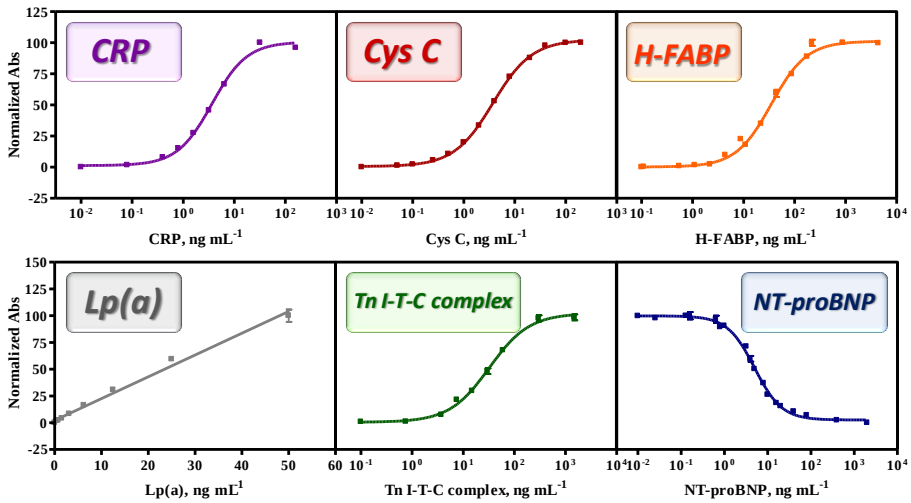

Figure 5.3. Calibration curves for each analyte: CRP, Cys C, Lp(a), H-FABP, Tn I-T-C complex and NT-proBNP, using the blocking buffer in the analyte step for all cases. CRP, Cys C and NT-proBNP calibration curves were performed four times during two/three different days using at least two replicates on every assay. H-FABP and Tn I-T-C complex calibration curves were performed three times on two/three different days using at least two replicates on every assay. Lp(a) calibration curve was performed once using two well replicates and fitted to a linear equation.

Table 5.2. ELISA features and defined cut-off for each biomarker.

	CRP[a]	Cys C[a]	H-FABP[b]	Lp(a)[c]	Tn I-T-C complex[b]	NT-proBNP[a]
Abs_{max}	101±2	102.6±0.6	103±3	105.8	102±2	100.1±0.7
Abs_{min}	1.3±0.3	0.5±0.2	-0.3±0.3	-0.04	0.7±1.1	2.5±0.9
Slope	1.27±0.06	1.12±0.03	1.26±0.02	2.04±0.06	1.14±0.07	-1.4±0.2
R^2	0.995±0.002	0.999±0.002	0.997±0.004	0.988	0.98±0.01	0.995±0.002
IC50, ng mL^{-1}	3.7±0.2	3.8±0.2	33±7	-	33±8	5.0±0.4
Working range, ng mL^{-1}	10.6±0.4-1.16±0.02	11.6±0.8-1.05±0.03	92±29-11±2	50-3.4	102±21-9±1	1.9±0.3-15±1
LOD, ng mL^{-1}	0.6±0.02	0.50±0.02	5.8±1.3	0.5	4.3±0.1	1.1±0.2
Cut-off, ng mL^{-1}	1000-3000[d] >3000[e] ≥10000[f]	>1290	>5.8	>$5{\cdot}10^5$	>0.06	>0.4

[a]The assay was performed four times during two/three different days using at least two replicates on every assay. [b]The assay was performed three times on two/three different days using at least two replicates on every assay. [c]The calibration curve was performed once in PBST using two well replicates and fitted to a linear equation (y=(2.05±0.05)x+(1.9±0.9)). LOD and LOQ were calculated with the average of the six blanks summed to 3 and 10 times their standard deviation, respectively. [d]average risk, [e]high risk, [f]very high risk.

Six reference immunochemical assays have been developed based on sandwich and competitive formats but with procedures that are compatible between them for the implementation on the multiplexed microarray platform. Table 5.2 shows the detectability achieved by these assays in comparison to the basal human blood levels of these biomarkers and the recommended cut-off points. As it can be observed, the LOD achieved was enough for CRP, Cys C, Lp(a) and H-FABP assays. However, under these conditions the cTnI and NT-proBNP assays did not reach the necessary detectability. In chapter 4 we demonstrated that NT-proBNP assay was able to detect 0.15 ng mL^{-1} in buffer and 0.4 ng mL^{-1} in BNP and NT-proBNP free plasma. The main differences between the protocol used then and here are shown in Table 5.3. Conditions regarding cTnI assay were exactly the same ones established in chapter 3.

Table 5.3. Differences in the assay features for the ELISA NB1-CH2CO-BSA/As 251.

	NB1-CH_2CO-BSA/As 251	
	Optimized conditions (chapter 4)	Conditions employed in this chapter
[NB1-CH_2CO-BSA]	0.125 µg mL^{-1}	0.125 µg mL^{-1}
As 251, final dilution	1/10000	1/2000
Competition buffer	0.01 M phosphate buffer pH 7.5, 0.4% NaCl, 0.005% Tween 20	0.15% casein in PBST PBST: 0.01 M phosphate buffer pH 7.5, 0.8% NaCl, 0.05% Tween 20
Preincubation step	RT, 15 min	RT, 15 min
Competition step	40°C, 30 min	RT, 30 min
Detection Ab step	-	PBST, 30 min
Anti-IgG-HRP	1/6000 in PBST, 30 min	1/6000 in PBST, 30 min

Since the use of the blocking buffer is needed to avoid the unspecific adsorption of troponin I as it was explained in section 3.3, all calibration curves were performed in this buffer during the analyte incubation. This explains the worsening of the LOD obtained for NT-proBNP assay compared to that reported in chapter 4 when using the optimized conditions. Since troponin I is the golden cardiovascular biomarker due to its highest cardiospecificity and consequently to its clinical relevance, inclusion of this biomarker in the multiplexed platform was considered mandatory even if the detectability achieved was not enough. Therefore, we decided to continue using the blocking buffer even if this caused a decrease in the NT-proBNP detectability. As it has been explained in chapter 3, the blocking buffer was necessary to avoid non-specific adsorptions of the cTnI. As it can be seen in Figure 3.6 (section 3.3), in the absence of a blocking agent the non-specific signal was on the same order than the specific signal, and the assay was completely useless.

With these results we decided to move forward toward the implementation of all these immunochemical assays on a fluorescent multiplexed microarray platform. Since, as it has been mentioned in section 4.1 that greater limits of detection for NT-proBNP were achieved with fluorescent immunoassays [124, 125] using europium as a fluorescent label, we had some expectations of being able to increase the assay detectability.

6 MULTIDETECTION OF CARDIOVASCULAR BIOMARKERS THROUGH A FLUORESCENT MICROARRAY

6.1 INTRODUCTION

High throughput screening (HTS) capabilities and multiplexation are important and desirable features in diagnostics in order to improve efficiency and to obtain greater amount of information at the same time. Thanks to the advances in manufacturing and miniaturization during the last decades it has been possible to develop high-density microarrays that provide maximum information from small sample volumes, with just one measurement and the best possible detectability. Microarrays allow multidetection of a high number of analytes through site-encoded codification on very small chip surfaces. This has been particularly possible for DNA microarrays addressed to be used in gene expression studies. Protein microarrays present a variety of limitations mainly related to the great diversity of chemical structures and functions, which has prevented reaching the same advance. Nevertheless, being miniaturized solid phase assays, microarrays are contemplated of diagnostic tools with high potential to be able to provide the maximum information with the minimum sample quantity and the less reagent consumption. Because of all these reasons, development of a fluorescent microarray chip was proposed to accomplish simultaneous multidetection of the selected cardiovascular biomarkers (CRP, Cys C, Lp(a), H-FABP, cTnI and NT-proBNP) in plasma or serum samples.

6.1.1 PROTEIN MICROARRAYS

An array is a tidy arrangement of bioreagents, samples, etc. on a solid surface. The microarray concept was introduced by Ekins and collaborators at the end of 1980s [174, 175]. The important revolution in diagnostic has been for the DNA microarrays due to their major stability compared to proteins and the elevated specificity of the hybridization process that takes place between two single complementary DNA strands (ssDNA) [176, 177]. However, there are great expectations regarding the potential of protein microarrays to study protein-protein interactions, to quantify different proteins expressed in a cell, characterize enzymes, etc. In diagnostics, often the proteins immobilized through different chemical strategies in defined zones (spots) are antibodies or antigens deposited on the surface using a *spotter*, although a variety of novel

fabrication approaches have been developed, particular for DNA microarrays for which it has been possible to standardize procedures to manufacture them on a high scale. Typically, the readout is fluorescent using appropriate labels, although microarrays have also been reported making use of many other optical or electrochemical sensor transducing principles [178, 179].

Material: Glass surfaces are the most employed for microarrays due to their high chemical and physical resistance. Chemically, glass is inert, able to resist high temperatures and maintain their properties when it is in touch with water. Physically, it has a low intrinsic fluorescence and high transmission. Moreover, it is easy to obtain, its surface is normally flat with few wrinkles, rigid, transparent and without pores, allowing to a more favourable kinetic reaction. Apart from glass, also silicone, polymeric (polymers like polydimethylsiloxane (PDMS), poly(methyl methacrylate) (PMMA) or polycarbonate (PC) immobilized on glass surfaces), gold surfaces, etc. are used for the same purpose [180]. As more hydrophobic is the surface, smaller is the size of the formed spots because the dispensed sample is normally hydrophilic. In this chapter, glass slides were chosen as solid surfaces to carry out the multiplexed microarray. When fluorescent readout is used, glass is the most frequently used material, in which we will mainly focus in this chapter.

Microarray biofunctionalization: This is a crucial step which must provide a stable, homogeneous and bioactive surface and avoid the undesired non-specific adsorptions. Such a step can significantly influence on the selectivity, sensitivity and detectability of the immunosensor. Protein immobilization can be accomplished mainly through three different strategies:

- **Passive adsorption**: The adsorption of the biomolecule onto the surface is done through electrostatic and hydrophobic interactions by only depositing the antibody or antigen on the material surface.
- **Affinity binding**: Avidin-biotin is one of the strongest non covalent interactions that exist with a dissociation constant of $K_D \approx 10^{-15}$ mol/L. Avidin/streptavidin/neutravidin adsorption on solid surfaces is based on the hydrogen bonds formation, electrostatic interactions, Van der Waals bonds and hydrophobic interactions. Nevertheless, this is a costly method because it requires high quantities of avidin to cover the surface and, moreover, avidin is susceptible to be desorbed with the presence of

acid and basic solutions with high ionic strength but also high temperatures. Streptavidin with an isoelectric point (pI) of 5 is more used than avidin with a pI at 10.5 in order to avoid non-specific interactions with other proteins [181].

- **Covalent binding**: The surface must be activated with the introduction of a functional group that will react with another functional group from the biomolecule. This kind of binding guarantees more reproducibility and stability and consequently was selected for the purpose of this chapter. In order to obtain the protein microarray, the derivatization of the selected support was needed thus introducing functional groups on the surface. It exist a great variety of silanizing agents which from one end are covalently attached to the surface and from the other end they provide a functional group able to bind molecules (see Figure 6.1).

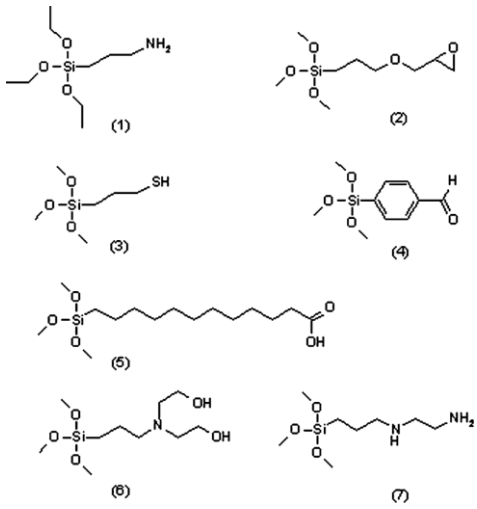

Figure 6.1. Commonly applied silanes in glass modification: (1) 3-aminopropyltriethoxysilane; (2) glycidopropyltrimethoxysilane; (3) 3-mercaptopropyl-triethoxysilane; (4) 4-trimethoxysilyl-benzaldehyde; (5) triethoxysilane undecanoic acid; (6) bis (hydroxyethyl) aminopropyltriethoxy-silane; (7) 3-(2-aminoethylamino) propyltrimethoxysilane [182].

Also, surfaces can be divided in three sub-groups [183]:

A. **Flat bi-dimensional (2D) glass surfaces**, which can be activated with epoxy silanes, amino silanes and heterobifunctional reagents such as glutaraldehyde or phenyl isothiocyanate giving functional groups like amines, aldehydes, epoxy or carboxylic esters (see Figure 6.2; A and B). In such surfaces, the immobilization can be done through electrostatic

interactions or through covalent binding. If the evaporation of nanodrops is fast the tri-dimensional structure of the proteins can be affected.

B. **Tri-dimensional structures (3D)** making use of polymers such as hydrogels, polyacrilamide [184, 185], agarose [186] and nitrocellulose [187] membranes (see Figure 6.2; C and D). In this case, the binding of the proteins is mainly by physical adsorption. It has been claimed that these type of surfaces respect better the tri-dimensional structures. These surfaces provide efficient immobilization of a greater number of molecules compared to 2D surfaces, although changes in signal intensity have also been observed with the time [188].

C. **2D/3D Surfaces**, these are kind of mixed surfaces in which the 2D flat surfaces has been derivatized with biomolecules such as dendrimers or neutravidin/streptavidin. Although these molecules do not present a real 3D visible structure, the surfaces cannot either be considered 2D because they present a supramolecular structure. Several published works discuss the advantages and limitations of these different surfaces for protein microarray development [188-190].

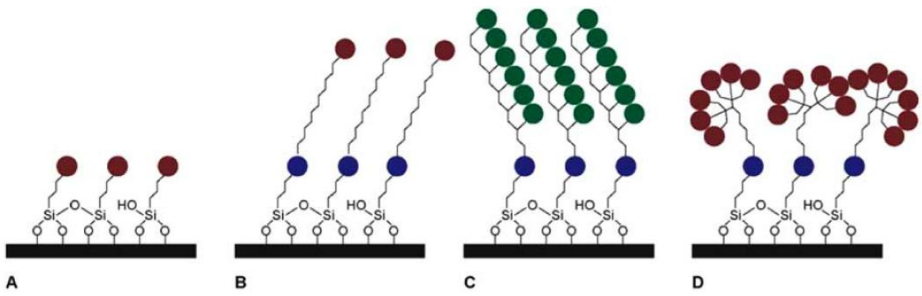

Figure 6.2. Molecular architecture of chemical surface coating. Red, blue and green balls represent different functional groups [183].

Equally important, the buffer (printing buffer) used for protein immobilization with the *spotter* is also a crucial factor. Different compositions and additives have been proposed to obtain reproducible and homogeneous spots [191]. Thus, manufacturing microarrays involve taking into consideration a variety of factors, including the chemical nature and function of the protein, the surface type of and material, the different chemistries possible and the printing, storage and assay conditions [179].

The main problems encountered in protein microarray development are related to the poor reproducibility and the lack of homogeneity of the spots, mainly due to the great diversity and complexity of their chemical structures. Thus, biofunctionality depends on its tertiary and quaternary structure which can be at the same time altered by changes in conductivity, pH, and the presence of oxidant agents or loss of humidity.

6.1.2 MULTIPLEXATION FOR CARDIOVASCULAR BIOMARKERS

Several immunochemical assays employing different technologies addressed to the multi-detection of cardiovascular biomarkers have been nowadays reported. For instance, Leung and co-workers developed a semiquantitative lateral flow combining CRP and H-FABP detection in order to notify heart disease at an early stage [192]. This test strip required 80 µL of sample and the total assay time was less than 15 min, employing nitrocellulose membranes and colloidal gold as a label. The number of red lines developed in CRP test zone depends on the CRP concentration in the sample, which, in turn, it predicts the heart attack risk semiquantitatively. Only one line indicates that risk for having a heart attack in the near future is low. Two and three lines mean moderate and high heart attack risk, respectively. Another example is the lab-on-a-disc developed by Park et al. [193]. This centrifugal microfluidic layout was designed to simultaneously detect CRP, cTnI and NT-proBNP based on a polystyrene bead-based sandwich ELISA. The sample volume required was 200 µL and the total process took 20 min. In this work the possibility to measure whole blood and whole saliva was assessed and sensitivities achieved are shown in Table 6.1.

Focused on microarrays, an example of a commercially available electrochemiluminescent microarray is that one from Meso Scale Discovery (MSD) for the simultaneous detection of cTnI, CK-MB and myoglobin (MYO) in serum (see Figure 6.3). It is based on a platform called MSD MULTI-ARRAY™, where all three sandwich assays using electrochemiluminescent-labeled detection antibodies are performed in MSD 96-well 4-spot plates and are read on MSD's SECTOR™ Imager 6000, at a throughput of 80 samples per minute. The assay protocol involves a single 1-hour incubation followed by a wash step and all assays are highly specific and linear over the normal clinical ranges,

sensitivities of these assays are shown in Table 6.1. This multiplexed panel demonstrates the ability to perform multiplexed measurement for analytes with different concentration ranges, that differ by ~100-fold in abundance.

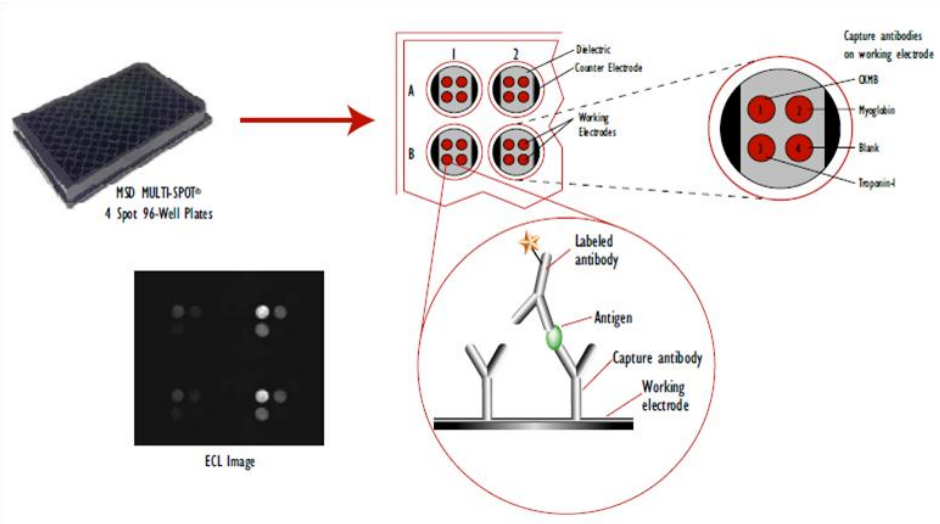

Figure 6.3. Schematic representation of the multiplexed assay developed by Meso Scale Discovery. All three assays are formatted as sandwich immunoassays, using MAb pairs. A 4-spot MULTI-ARRAY plate is used which is pre-coated with three capture antibodies on separate spots within each well. Detection antibodies are labelled with a $Ru(bpy)_3^{2+}$ compound, and electrochemiluminescence is used as the detection technology. Figure copied from the insert of the product.

Another example of CVD biomarkers multi-detection through microarrays is the work of Marquette et al. [194]. They developed a screen-printed (SP) microarray platform able to detect CRP, MYO, cTnI and BNP. It employed highly sensitive chemiluminescence detection, taking advantage of, on the one hand, the amplification reaction catalyzed by the HRP label and, on the other hand, signal enhancement on the gold-plated microelectrodes.

Table 6.1. LOD values assessed for the multiplexed assays described in this section.

		CRP	CK-MB	MYO	cTnI	NT-proBNP	BNP
	Matrix	**LOD, ng mL^{-1}**					
Lab-on-a-disc (ELISA), [193]	Whole blood	0.27	-	-	0.27	0.32	-
Lab-on-a-disc (ELISA), [193]	Whole saliva	0.30	-	-	0.51	0.24	-
MSD MULTI-ARRAY™	Serum	-	0.15	19	0.01	-	-
SP microarray, [194]	1/40 diluted sera	10	-	0.5	1	-	6
Cut-off, ng mL^{-1}		1000-3000[a] >3000[b] ≥10000[c]			>0.06	>0.4	>0.1

SP: screen printed. [a]average risk, [b]high risk, [c]very high risk.

Looking at the LOD values achieved, the difficulties to achieve the required detectability for cTnI and NT-proBNP detection at the basal levels are evident. The MSD MULTI-ARRAY™ is the only device incorporating a high sensitive cTnI assay. Thus, the lab-on-a-disc and the SP microarray systems need to improve the detectability for cTnI, BNP and NT-proBNP.

6.1.3 OBJECTIVE AND SPECIFIC TASKS

Although in vitro diagnostic (IVD) of AMI relies on well-established biomarkers, it is evident the need of a diagnostic platform combining distinct biomarkers which would provide a more complete information of the progression of the disease, the prognosis or allowing a more accurate stratification of the patients to provide a more personalized medicine. Accordingly to several clinical studies and as it has been explained in section 1.5.2 (chapter 1), cTnI, CRP, NT-proBNP, Cys C, H-FABP and Lp(a) were identified as priority biomarkers to assist clinicians in this respect and therefore, we selected them as targets.

The main objective here has been to develop a multiplexed fluorescent microarray device able to analyze simultaneously these biomarkers in plasma and serum samples. For this purpose, the assays developed and optimized first

in microplate ELISA formats for cTnI (chapter 3), NT-proBNP (chapter 4) and CRP, Cys C, Lp(a) and H-FABP (chapter 5) have been implemented on the microarray and further on combined on a multiplexed configuration. Thus, the specific objectives proposed have been:

- Implementation of each individual immunoassay on the microarray, using in this case fluorescent labels
- Development of the multiplexed microarray resulting from the combination of all the immunoreagents
- Evaluation of the microarray performance in clinical samples

Main challenges we had to face have been:

- the differences in the chemical nature between all these target analytes (lipoprotein, proteins and peptide) which require different assay formats (sandwich and competitive formats),
- the target analytes have to be measured at different concentration ranges (see Table 6.1 from the previous section).

6.2 PREVIOUS CONSIDERATIONS

6.2.1 PROPOSED STRATEGY

The proposed strategy for the multiplexed format is schematized in Figure 6.4 and the reagents briefly described in Table 6.2.

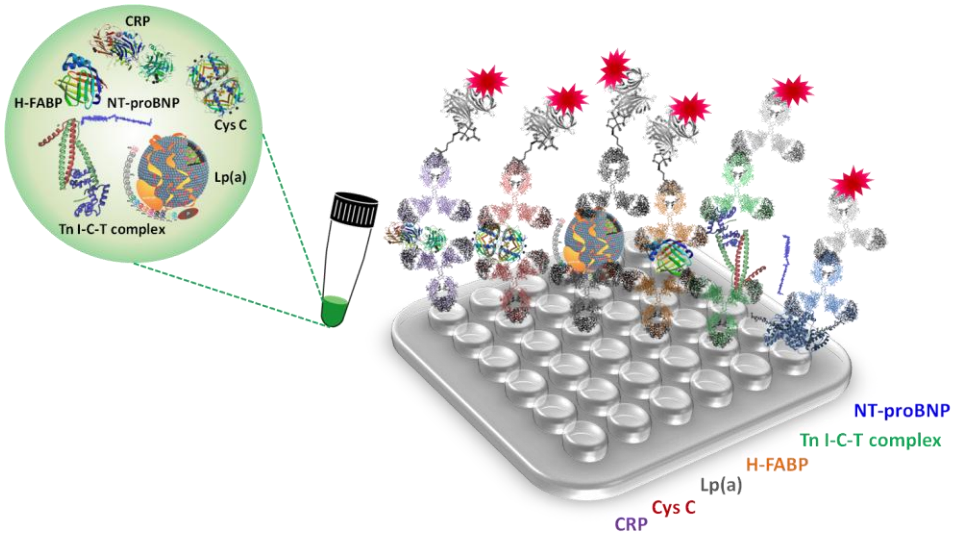

Figure 6.4. Schematic representation of the proposed strategy for the fluorescent multiplexed microarray. From left to right, schematized the corresponding immunoassays for CRP, Cys C, Lp(a), H-FABP, cTnI (sandwich format) and NT-proBNP (competitive format) detection.

The microarray approach would work in the following manner:

1. The microarray would be prepared by immobilizing the different capture antibodies or hapten bioconjugates (for NT-proBNP in a competitive format) in replicates on the glass surface with the aid of a *spotter*.
2. The sample containing the mixture of the target analytes would be added.
3. A cocktail consisting of a mixture of detection Ab (some of them biotinylated: CRP, Cys C, Lp(a) and H-FABP) would be added.
4. Finally, a mixture of fluorescent labelled anti-IgG and streptavidin would be added.

As mentioned above, for the competitive NT-proBNP assay, buffer had to be added in one of the steps (3 or 4) because it has less steps than the other ones.

Attemps to reduce the number of steps by adding simultaneously more than one reagent (i.e. the cocktail of analytes previously mixed with detection antibodies) failed probably due to a blocking of the epitopes by antibody binding, which prevented the analytes from being captured by the immobilized

antibody. A lower signal (RFUs) was recorded in such situation (see the example for CRP in Figure 6.5).

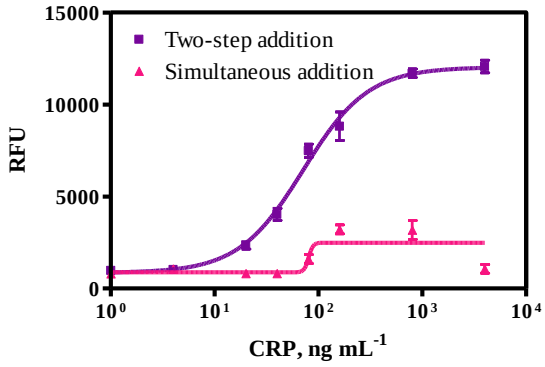

Figure 6.5. CRP immunoassay in buffer when the cocktail of analytes previously mixed with the detection antibodies were added in two different steps and simultaneously (both in the multiplexed format). Each curve was tested once using 6 replicates on every analyte concentration (6 spots per well).

All standards, immunoreagents and conditions were those described in chapter 5 (see Table 6.2), with the only difference of using a fluorophore label for anti-rabbit IgG and streptavidin instead of HRP. Tetramethylrhodamine (TRITC) was selected as label because it could be excited with the green laser (543 nm) available in the scanner for micorarrays we have in our laboratory. It has a reasonable price and it is commercially available with a variety of chemical groups for protein conjugation. Moreover, it has a good quantum yield and sufficient photostability in water.

Table 6.2. Reagents and assay format for the multiplexed microarray development.

Biomarker	Assay format	Biorecognition elements (providers)		Analyte (provider)	Signal
		Capture Ab	Detection Ab		
CRP	Sandwich	Goat PAb (AD): AbCRP2	Goat PAb (AD)-biotin: AbCRP1-biotin	Serum based CRP (AD)	Streptavidin-TRITC
Cys C		Goat PAb (AD): AbCys C	Goat PA (AD)-biotin: AbCys C-biotin	Serum based Cys C (AD)	
Lp(a)		Goat PAb (AD): AbLp(a)3	Goat PAb (AD)-biotin: AbLp(a)1-biotin	Serum based Apo B-100+apo (a) (AD)	
H-FABP		Sheep MAb (R): C3	Sheep PAb (R)-biotin: AbH-FABP-biotin	Human cardiac H-FABP (LD)	
cTnI		Goat PAb (LD): Goat anti-cTnI	Rabbit PAb As 220	Human cardiac Tn I-T-C complex (H)	Anti-IgG-TRITC
NT-proBNP	Competitive	Coating antigen: NB1-CH_2CO-BSA	Rabbit PAb As 251	Recombinant NT-proBNP, aa 1-76 (H)	

AD: Audit Diagnostics, R: Randox, LD: Life Diagnostics, H: Hytest.

6.2.2 WORKING CONDITIONS AND PROTOCOL ESTABLISHMENT

The material used were glass slides (25x75 mm size) were it was possible to print 24 different microarrays. The chemistry selected to immobilize the biomolecules was covalent employing (3-glycidyloxypropyl)trimethoxysilane (GPTMS) to activate the surface. This silanizing agent would allow chemical reaction of the amino groups from the biomolecules with its epoxy groups (see Figure 6.6).

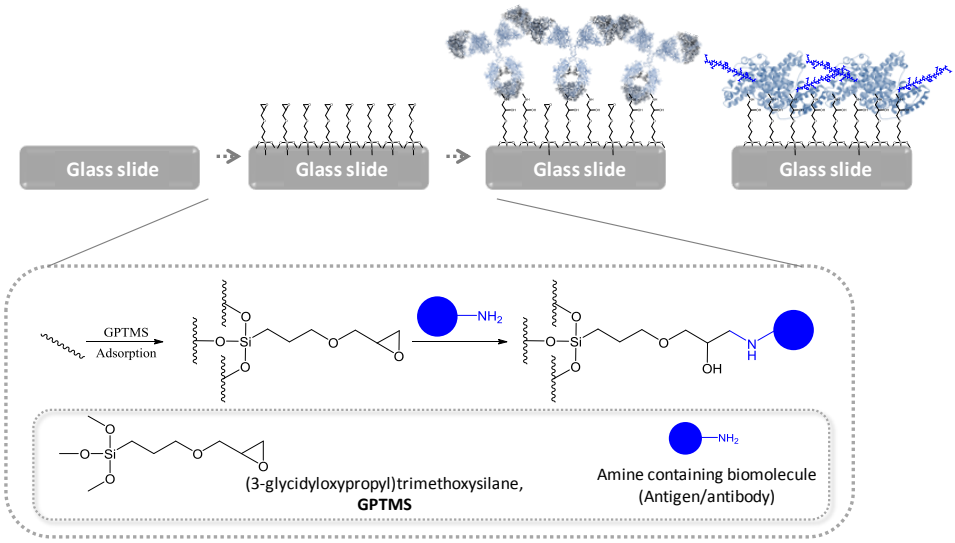

Figure 6.6. Reaction involved in the biofunctionalization of a glass slide. First reaction takes place at room temperature in a fume hood, the second reaction is realized in the spotter chamber where relative humidity and temperature conditions are 60% and 20°C respectively.

Hence, after a washing process of the glass slide and the generation of hydroxyl groups with a 10% (w/v) NaOH solution, the slides were treated with GPTMS dissolved in anhydrous ethanol. Afterwards, the andtibody and/or the bioconjugate were added with the aid of the *spotter* forming micrometric active zones (*spots*). All protocols and procedures related to slides derivatization and functionalization but also related to experiments explained in next section are described in section 8.2. In Table 6.3 the main conditions are described, most of them adapted from the doctoral thesis of Núria Tort.

Table 6.3. Main conditions employed for manufacturing and running the microarray.

		Buffer/solution	Incubation time
Manufacturing	1. Activation of the glass	10% (w/v) NaOH solution	1 h, room T
	2. Silanization	2.5% (v/v) GPTMS in anhydrous ethanol	3 h, room T
	3. Immobilization (printing)	150 mM sodium phosphate pH 8.5, 0.1% sodium dodecyl sulphate 60% relative humidity, 20°C	30 min in spotter (60% humidity, 20°C), room T and desiccant condition until use
Microarray immunochemical assay protocol	1. Washing step	4 washes with PBST	-
	2. Samples or standards/ Competition	0.15% casein in PBST PBST: 0.01 M phosphate buffer pH 7.5, 0.8% saline solution, 0.05% Tween 20	30 min, room T
	3. Washing step	4 washes with PBST	-
	4. Detection antibody	PBST	30 min, room T
	5. Washing step	4 washes with PBST	-
	6. Anti-IgG-TRITC/ Streptavidin-TRITC	PBST	30 min, room T
	7. Final wash	3 washes with PBST and 1 with MilliQ water	-

Once biomolecules were immobilized on the corresponding solid surfaces, these ones were kept at room temperature under desiccant conditions until use. The microarray assay was run by placing the slides in an ArrayIt® multi-well platform (see Figure 6.7). In this manner, each slide was divided in 24 wells; 8 wells in each of the 3 columns. In each well a determined number of spots were printed depending on the experiment. Different configurations are possible which can be programmed in the spotter. Hence, during assay development, microarrays can be manufactured by printing different proteins or the same protein at different concentrations.

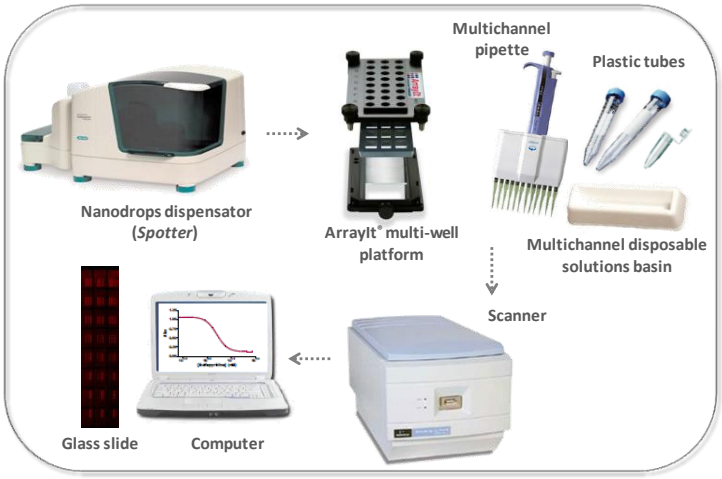

Figure 6.7. All material needed for the different steps involved in fluorescent microarray development: print, assemble, measure, analyze and data treatment.

6.3 INDIVIDUAL ASSAYS ON THE FLUORESCENT MICROARRAY

On a first instance we investigated the possibility of using two different labelled molecules at the same time (anti-IgG-TRITC and streptavidin-TRITC, see Figure 6.8). For this purpose, detection antibodies at three different concentrations were printed in twelve different wells, six for assessing binding of anti-IgG-TRITC and the other six for assessing the binding of streptavidin-TRITC. Dilutions of both were previously optimized, providing similar reactivity at 1/250 and 1/625 respectively. All experimental procedures are described in section 8.2.

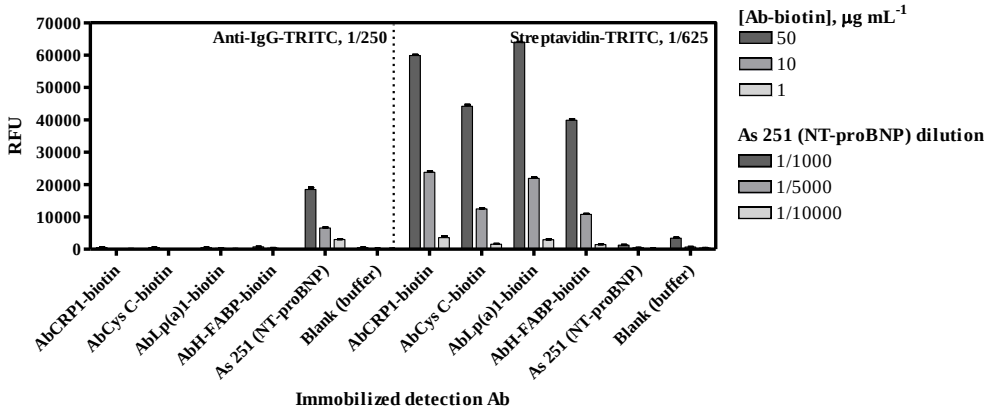

Figure 6.8. Evaluation of the anti-rabbit IgG-TRITC and streptavidin-TRITC assay specificity. The standard deviation shown is the result of analysis made one day using 2 wells with 5 spots per well in each case (10 spots in total).

As it can be observed in the above figure, the anti-rabbit IgG-TRITC only recognized the As 251 developed in rabbit for NT-proBNP while streptavidin-TRITC recognized only the biotinylated antibodies. There was not unspecific recognition at this level. The antibodies for cTnI were not included in this experiment because the need to introduce a blocking agent (see chapter 3, section 3.3) and the effect this would have on the other assays was not yet evaluated on the microarray platform.

Thus, on a second set of experiments the effect of casein as blocking agent on the microarray was studied (see Figure 6.9). The assay was performed by spotting on each microarray (well) four different capture antibodies at the same concentration in four different rows (goat anti-cTnI used in the previous cTnI ELISAs, mouse anti-cTnI, goat anti-CRP and mouse anti-fluoroquinolone in first, second, third and fourth row respectively). After the corresponding incubation and following the protocol described in Table 6.3, analyte (cTnI or Tn I-T-C complex) at different concentrations was added followed by As 220 detection antibody. Finally, anti-IgG-TRITC was added. While the two first rows correspond to specific antibodies, third and fourth rows were used as controls. In the graph below, second and fourth rows are not represented.

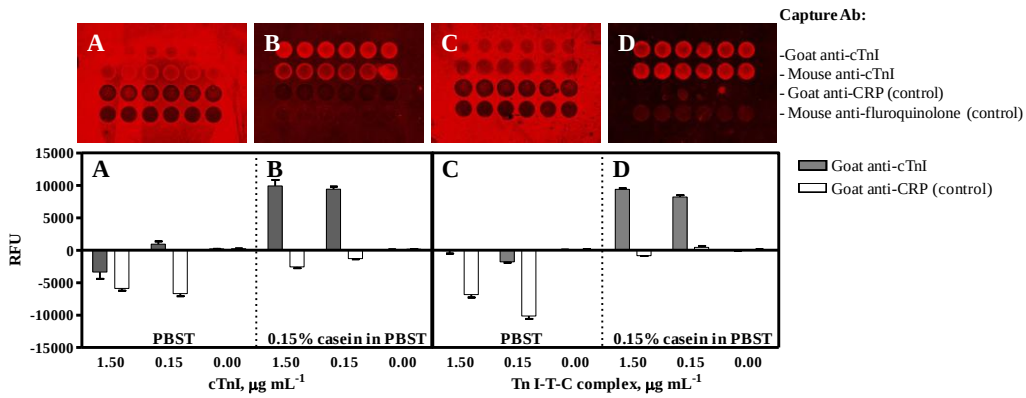

Figure 6.9. Evaluation of the cTnI and cTnI in I-T-C complex non-specific adsorption when 0.15% casein was present in the assay buffer (PBST). Both cTnI forms were assayed at 1.50, 0.15 and 0 µg mL^{-1}. Letters from the pictures above correspond to letters in the graph at 0.15 µg mL^{-1} in each case. The standard deviation shown is the result of analysis made one day using 6 well replicates.

As it can be observed in Figure 6.9, a great reduction of the background could be observed when casein was used as an additive in analyte buffer. Moreover, this background was comparatively lower in Tn I-T-C complex than in cTnI. The scanner where RFU values were obtained provides a value from each spot which is a mean of RFU from the selected area. From this value, the background is subtracted and this explains the negatives values when background is very high. When cTnI was used in a complexed form and casein was added, negative values were corrected which means that casein avoided non-specific adsorptions as it was already observed in chapter 3.

Consequently, and due to the high diagnostic value of troponin I, we decided to incorporate this biomarker to the multiplexed microarray but using 0.15% casein in PBST as assay buffer. Even though, and before moving forward, we tested the effect of casein on the other individual assays in the current platform. For this purpose, we used a single concentration of each analyte but a high concentration to observe the potential effect of this on the signal. Also a lower concentration of each analyte was tested to ensure that the casein did not have a negative effect over the capacity of each assay to discriminate between two different concentrations (see Figure 6.10).

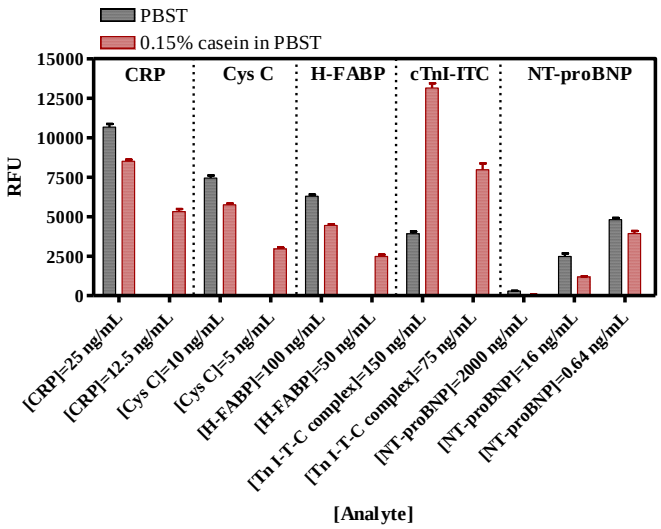

Figure 6.10. Difference in reactivity for the highest analyte concentration in each case when casein was added in analyte buffer. A lower concentration was checked only with casein to compare the behaviour between competitive and sandwich formats. The standard deviation shown is the result of analysis made one day using 20 spots per well in each case.

Although the response of the microarray for the different analytes was slightly reduced when casein was used, the benefit caused over the cTnI assay prompted us to continue using the casein buffer to pursuit with our studies.

After setting up the necessary concentrations of immunoreagents through 2D checkerboard titration experiments, we were able to establish six individual microarray assays for the six target biomarkers selected (see Figure 6.11). The features of those assays are shown in Table 6.4.

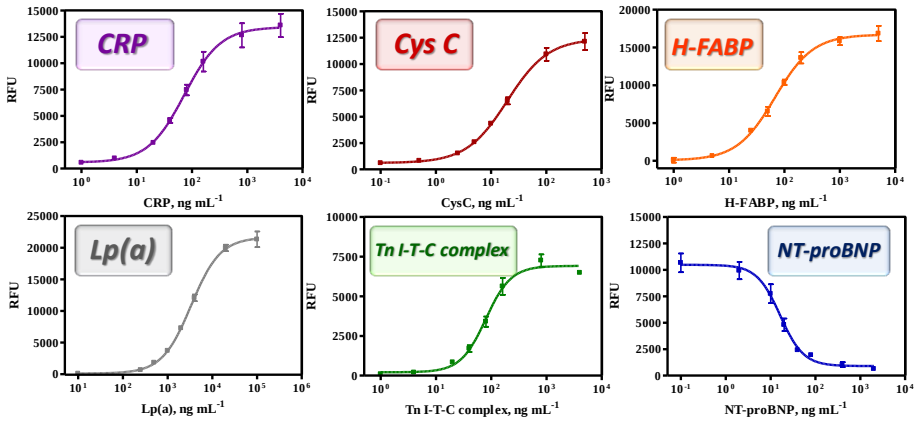

Figure 6.11. Calibration curves for each analyte: CRP, Cys C, H-FABP, Lp(a), Tn I-T-C complex and NT-proBNP, using the blocking buffer in the analyte step for all cases. Calibration curve for CRP was tested 6 times (interday and intraday) using at least 18 replicates on every analyte concentration (18 spots per well). For Cys C, it was tested 7 times (interday and intraday) using at least 18 replicates on every analyte concentration (18 spots per well). For H-FABP and Tn I-T-C complex, it was tested 3 times (interday and intraday) using at least 18 replicates on every analyte concentration (18 spots per well). For NT-proBNP, calibration curve was tested twice (interday and intraday) using at least 12 replicates on every analyte concentration (12 spots per well).

Table 6.4. Microarray features (mean±SD) for each analyte.

	CRP[a]	Cys C[b]	H-FABP[c]	Lp(a)[d]	Tn I-T-C complex[c]	NT-proBNP[c]
	Mean±SD					
RFU_{max}	13453±2731	12559±2163	16750±1417	21668±1634	6937±330	10455±1420
RFU_{min}	564±248	586 ±492	14±567	86±40	202±40	939±217
Slope	1.3±0.2	1.2±0.2	1.3±0.2	1.33±0.09	1.9±0.3	-1.8±0.3
R^2	0.94±0.03	0.96±0.06	0.96±0.02	0.99±0.02	0.92±0.02	0.948±0.006
IC50, ng mL^{-1}	74±15	20±3	68±5	3363±194	82±13	16±4
Working range, ng mL^{-1}	233±63-26±5	62±13-6.0±0.9	220±36-23±4	9122±1520-1161±26	191±23-38±5	7±2-40±6
LOD, ng mL^{-1}	14±3	3.0±0.6	13±3	638±10	24±4	4.1±0.8
Cut-off, ng mL^{-1}	1000-3000[e] >3000[f] ≥10000[g]	>1290	>5.8	$>5 \cdot 10^5$	>0.06	>0.4

[a]Each curve was tested 6 times (interday and intraday) using at least 18 replicates on every analyte concentration (18 spots per well). [b]Each curve was tested 7 times (interday and intraday) using at least 18 replicates on every analyte concentration (18 spots per well). [c]Each curve was tested 3 times (interday and intraday) using at least 18 replicates on every analyte concentration (18 spots per well). [d]Each curve was tested twice (interday and intraday) using at least 12 replicates on every analyte concentration (12 spots per well). [e]average risk, [f]high risk, [g]very high risk.

In comparison to the basal human blood levels of these biomarkers and the recommended cut-off points, it can be observed how, in buffer, the CRP, Cys C and Lp(a) microarrays were able to reach a detectability below the basal levels in healthy patients. However, the necessary detectability for H-FABP, cTnI and NT-proBNP was not accomplished being troponin I assay the worst case. Further attempts to improve the microarray detectability using commercial antibodies (for NT-proBNP) or combinations of home-produced and commercial antibodies (for the case of cTnI) did not succeed in increasing the detectability. Therefore, we moved towards the multiplexation using the originally selected combination of immunoreagents.

6.3.1 SPECIFICITY STUDIES

From the specificity studies performed with all six individual microarrays developed, the most important problem was the cross-recognition the CRP and Cys C microarrays for the Lp(a) (see Figure 6.12). All the other assays did show an excellent specificity recognizing only its target analyte and not showing any kind of signal when the rest of the biomarker targets were added (see Table 6.5).

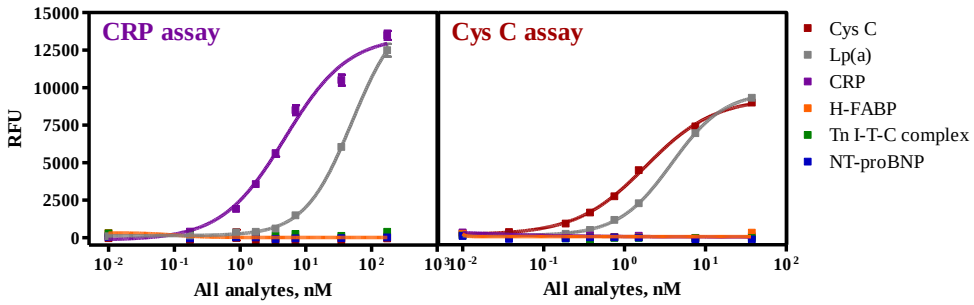

Figure 6.12. Cross-reactivity from Lp(a) on CRP and Cys C microarray. Each curve was tested once using 20 replicates on every analyte concentration (20 spots per well).

Table 6.5. Specificity results obtained for all six individual microarrays: CRP, Cys C, H-FABP, Lp(a), cTnI and NT-proBNP.

	CRP microarray		Cys C microarray	
Analyte	**CRP**	**Lp(a)**	**Cys C**	**Lp(a)**
RFU_{max}	13449	15286	9309	9749
RFU_{min}	-166	129	167	101
Slope	0.90	1.20	1.02	1.32
R^2	0.94	0.98	0.99	0.99
IC50, nM	4.81	50.36	1.82	3.81

	H-FABP microarray	Lp(a) microarray	cTnI microarray	NT-proBNP microarray
Analyte	**H-FABP**	**Lp(a)**	**Tn I-T-C complex**	**NT-proBNP**
RFU_{max}	5780	22833	11200	7405
RFU_{min}	-365	220	4	380
Slope	0.97	1.27	1.18	-2.01
R^2	0.98	0.97	0.95	0.96
IC50, nM	5.78	9.65	5.03	2.15

Each curve was tested once using 20 replicates on every analyte concentration (20 spots per well).

As it can be observed in Figure 6.12 and Table 6.5

Table 6.5, the CRP microarray recognized CRP but also Lp(a) at concentrations higher than 10 nM. In the same way the Cys C microarray recognized Lp(a) at concentrations even lower. The cross-reactivity of Lp(a) on CRP assay was 9.6% while for Cys C was 47.8%. This unexpected behavior could be explained taking into account the complexity of Lp(a) molecule and its considerable high molecular weight (see section 1.6.4). It exists the possibility these proteins would share some epitopes although considering that the antibodies used are polyclonal, the recognition seem too high. Other potential causes could be also its lipophilic character; we should remember that Lp(a) is a lipoprotein. This fact could cause non-specific binding to the surfaces or to the proteins through non-specific interactions. Regarding its size, it is difficult to determine the exact MW of Lp(a) due to the variable number of kringles and the lipidic nature. Thus, for these experiments the Lp(a) MW used was an estimation. Thus, at the light of these results we decided to withdraw Lp(a) from the multiplexed format, even

though the presence of this biomarker would have been interesting since high levels of Lp(a) are associated to a high risk of developing cardiovascular diseases.

6.4 FLUORESCENT MULTIPLEXED MICROARRAY

The conditions established for the individual microarrays were implemented in the multiplexed format. Performance of the multiplexed microarray was first assessed in buffer. A preincubation step of 15 min of the sample (containing all analytes) and As 251 (NT-proBNP) was used as established while developing the NT-proBNP immunochemical assay to improve detectability (see chapter 4, section 4.4.2.3). Results obtained are shown in Table 6.6, where it can be observed that the analytical features are very similar to the individual microarray (see above Table 6.4 for comparison).

Table 6.6. Multiplexed microarray analytical features for the five biomarker targets selected.

	CRP	Cys C	H-FABP	Tn I-T-C complex	NT-proBNP[a]
	Mean±SD				
RFU_{max}	12434±378	8908±1028	7153±896	11186±3273	9223±5229
RFU_{min}	630±162	387±157	159±255	516±247	601±94
Slope	1.5±0.2	1.3±0.2	1.57±0.05	1.9±0.2	-1.3±0.3
R^2	0.97±0.01	0.988±0.004	0.981±0.003	0.97±0.02	0.97±0.02
IC50, ng mL^{-1}	72±11	19±2	100±15	83±13	24±12
Working range, ng mL^{-1}	181±22-27±7	50±10-6±1	252±62-41±6	202±17-40±4	6.9±0.5-85±62
LOD, ng mL^{-1}	15±5	3±1	24±3	25±3	3±1

Each calibration curve was assayed three times in three different days using six replicates for each concentration point in every well (microarray). Each microarray was used to test a determined analyte concentration for all five targets. Thus, a calibration curve was obtained employing 8 different microarrays, each with different concentrations of the target analytes. The biofuncionalized slides used were from three different batches. [a]All parameters were calculated from two replicates in two different days.

From the results shown in the above table, we can conclude that the multiplexed microarray is a robust assay. Hence, the variability observed is not very high considering that the microarray slides were from different batches

and that the assays were run on different days. Only the RFU_{max} showed higher variability but this is quite common on bioanalytical assays and it can be related to changes in the temperature of the laboratory or the buffers as well as the use of new aliquots of immunoreagnets. Unfortunately, as with the individual microarrays, in the multiplexed format the sensitivity for H-FABP, cTnI and NT-proBNP was over the basal levels of the healthy patients. For this reason, an evaluation of the effect of distinct physicochemical parameters was carried out with the aim to improve microarray detectability. Regarding other conditions such as the combination of immunoreagents or their heterology, in the case of the competitive assay, were already evaluated for cTnI and NT-proBNP in chapter 3 and 4 respectively.

6.4.1 EVALUATION OF THE EFFECT OF PHYSICOCHEMICAL PARAMETERS ON THE MULTIPLEXED MICROARRAY

Physicochemical conditions such as conductivity and pH were evaluated in the multiplexed microarray. The results of these studies are shown in Figure 6.13.

The effect of the pH was thought to be essential due to the variety of isoelectric points of the different cardiovascular biomarkers (see Table 6.7). According to it, three different pH values were studied; pHs 6, 7.5 and 9. The pHs of the assay solutions were adjusted after the addition of the casein.

Table 6.7. Isoelectric points (pI) of the selected cardiovascular biomarkers.

	pI
CRP	6.40
Cys C	9.30
H-FABP	6.34
Tn I-T-C complex	9.87
NT-proBNP	8.45

As it can be observed in Figure 6.13, most assays tolerated well this interval of pH values, from 6 to 9. For CRP, Cys C and H-FABP, the detectability improved slightly from pH 6 to pH 7.5 but it remained almost constant between pH 7.5 and 9. For the Tn I-T-C complex, the most significant change was also between

6 and 7, and for NT-proBNP the detectability remained constant in all the intervals. With these results, it was decided to maintain the pH at 7.5 for the subsequent experiments. With these results, it was decided to maintain the pH at 7.5 for the subsequent experiments.

To study the effect of the ionic strength phosphate buffer solutions (0.01 M PB) were prepared with different concentrations of NaCl and KCl in order to accomplish solutions with conductivities of 5.1, 15.1 and 51.0 mS cm^{-1} (corresponding to 0.2, 0.8 and 3.2% NaCl respectively). In each one, 0.15% casein was added, pH was adjusted to pH 7.5 and the percentage of Tween at 0.05%. After adding the casein, conductivity values were again confirmed corresponding to 6.1, 14.2 and 43.9 mS cm^{-1}.

The results shown in Figure 6.13 indicate that each biomarker behaves different in front of the conductivity. While for CRP better detectability was obtained at 6.1 mS cm^{-1}, for Tn I-T-C and H-FABP best conditions were found at 14.2 mS cm^{-1}. Cys C appears to be quite resistant to changes in the conductivity conditions and NT-proBNP seems to reach the best detectability at high (43.9 mS cm^{-1}) or low (6.1 mS cm^{-1}) conductivity values, which is not very common. In any case the differences were not extraordinarily significant (please notice that the scale for the IC50 has been multiplied by 10), for which reason it was decided to continue using the same conductivity as that of the “standard conditions” (0.8% NaCl, 14.2 mS cm^{-1}).

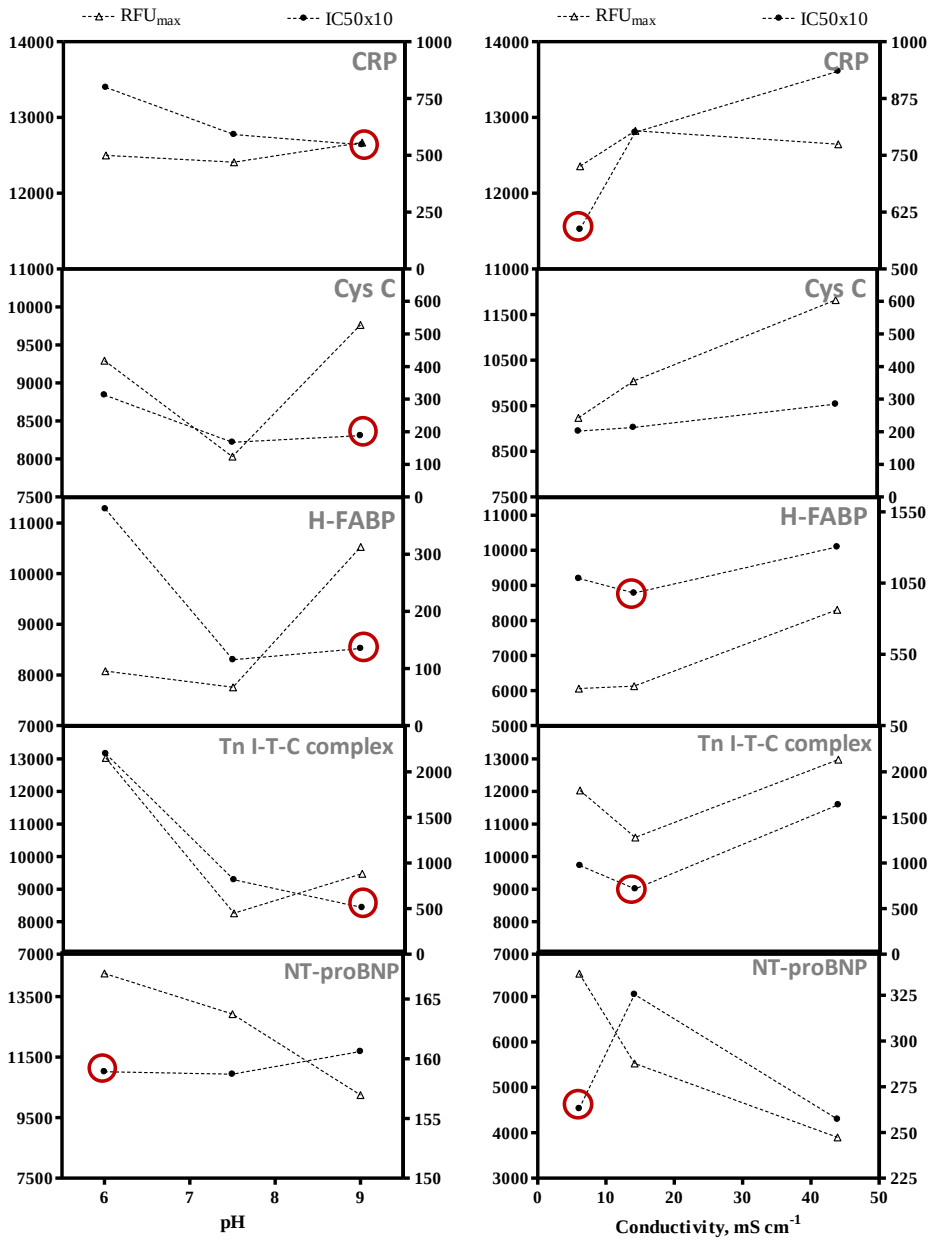

Figure 6.13. On the left, effect of the pH in the analyte buffer and on the right, effect of the conductivity in the analyte buffer. Right axis shows IC50 values while the left axis shows RFU_{max} value.

As result of these studies we were not able to improve the detectabiliy of the H-FABP, cTnI and NT-proBNP assays that was our main objective. Therefore, we

decided to move forward and to investigate the possibility to implement this multiplexed microarray to the analysis of clinical samples.

6.4.2 IMPLEMENTATION OF THE MULTIPLEXED MICROARRAY TO THE ANALYSIS OF HUMAN SERUM AND PLASMA SAMPLES

Assessment of the performance of the multiplexed microarray in clinical samples was made using human plasma and serum provided by Banc de Sang i Teixits de Catalunya. On a first instance, the potential non-specific interferences caused by these sample matrixes were evaluated (matrix effect studies). For this purpose, standard curves were prepared in buffer, plasma and serum and run on the multiplexed microarray to compare the parallelism of the standard curves (see Figure 6.14 and Table 6.8). In order to favor immunochemical reaction kinetics, agitation was introduced during the 15 min preincubation of the standard solutions with the As251. Plasma and serum samples were used undiluted in these experiments, since detectability is much compromised for three of the biomarker targets included in this multiplexed platform.

As it can be observed in Figure 6.14 and Table 6.8, while the response of the microarray for H-FABP, Tn I-T-C complex and NT-proBNP was not significantly affected by the plasma and serum matrixes, the CRP and Cys C response was completely distorted. However, it was very much likely that such effect was specific considering the detectability of our microarray for these biomarker targets and the basal levels which are considerably high; 1000 ng mL^{-1} for CRP (IC50 in buffer is around 70.5 ng mL^{-1}) and between 800-1200 ng mL^{-1} for Cys C approximately (IC50 in buffer is around 9.52 ng mL^{-1}). Therefore, probably the matrix effect could just be removed by previously diluting the sample in the assay buffer. Moreover, the slight matrix effect that could be observed for the rest of the biomarker targets could be avoided by just calibrating the multiplexed microarray in the corresponding sample matrix. With these premises we addressed the investigation of the usefulness of this microarray to at least be used as alarm system to distinguish between healthy and unhealthy patients.

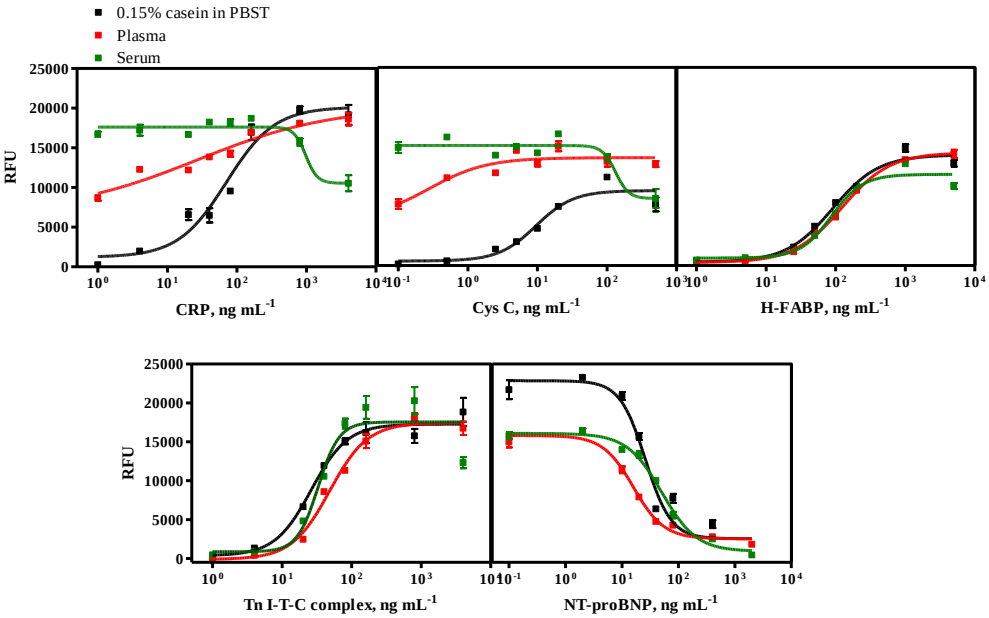

Figure 6.14. Matrix effect caused by human plasma and human serum in each assay from a multiplexed format. Each calibration curve was assayed once using six replicates for each concentration point in every well (microarray). Each microarray was used to test a determined analyte concentration for all five targets.

Table 6.8. Multiplexed microarray analytical features for the five biomarker targets selected in buffer, human plasma and human serum.

	CRP			Cys C			H-FABP		
	Buffer	**Plasma**	**Serum**	**Buffer**	**Plasma**	**Serum**	**Buffer**	**Plasma**	**Serum**
RFU_{max}	20138	20231	17618	9466	13618	15148	13745	14032	11241
RFU_{min}	1204	6717	10536	571.9	5793	8458	-51.42	-105.7	468.6
Slope	1.25	0.45	-5.18	1.61	1.05	-4.57	1.31	1.26	1.93
R^2	0.92	0.87	0.74	0.89	0.67	0.69	0.97	0.99	0.96
IC50,ng mL^{-1}	70.50	26.77	969.40	9.52	0.28	132.20	90.47	122.60	86.99

	Tn I-T-C complex			NT-proBNP		
	Buffer	**Plasma**	**Serum**	**Buffer**	**Plasma**	**Serum**
RFU_{max}	17277	17444	17553	22855	15811	16083
RFU_{min}	357.2	-115.0	866.8	2543	2521	924.6
Slope	1.67	1.59	2.87	-1.92	-1.61	-1.41
R^2	0.91	0.96	0.85	0.93	0.96	0.98
IC50, ng mL^{-1}	26.21	48.09	32.97	26.10	15.96	50.61

Each calibration curve was assayed once using six replicates for each concentration point in every well (microarray). Each microarray was used to test a determined analyte concentration for all five targets.

6.4.3 MODEL STUDY SIMULATING HEALTHY/UNHEALTHY PATIENTS

On a first instance and considering the high concentration values of the CRP and Cys C biomarkers in plasma or serum samples, a pilot study was performed to ensure that these biomarkers at the basal or AMI levels would not interfere in the response of the spots of the rest of biomarkers. With this objective, blind solutions were prepared by spiking 0.15% casein buffer with CRP at their basal and AMI levels and in both cases, solutions were separately spiked with all other analytes at their IC50 concentrations to test the effect of all these circumstances in all assays. The same was also done for Cys C (see Figure 6.15). IC50 concentrations used for CRP, Cys C, H-FABP, troponin complex and NT-proBNP were 61.3, 16.5, 92.8, 84.0 and 31.3 ng mL^{-1}, respectively. In all cases, basal levels are those considered cut-off, while AMI levels are those concentrations where the risk to suffer from CVD is high.

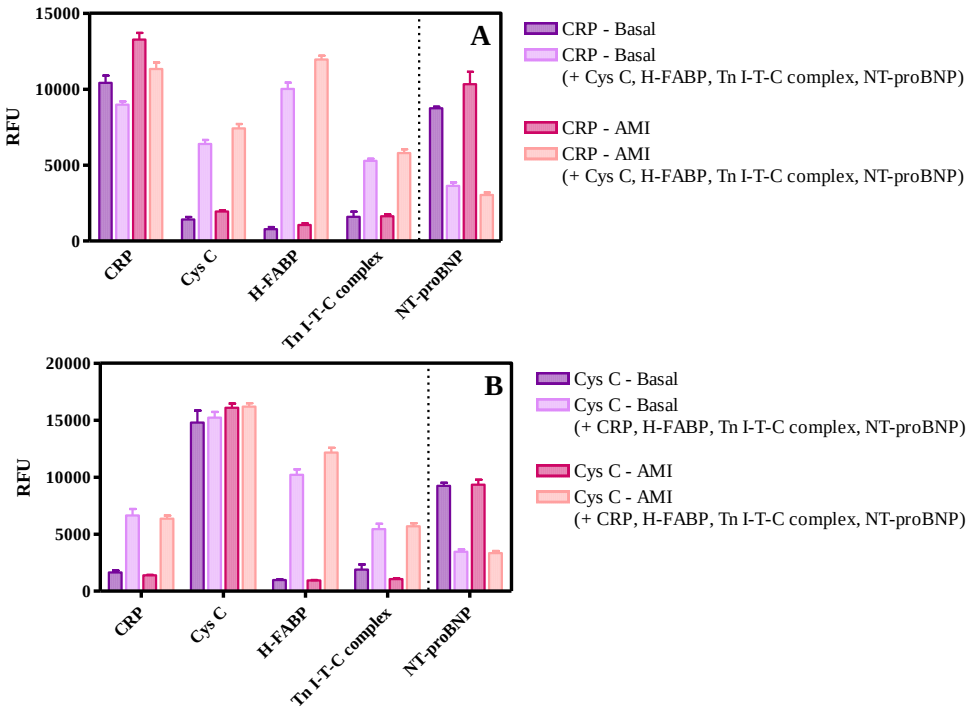

Figure 6.15. A) Response of the multiplexed microarray when sample (casein buffer) contains CRP at its basal level (1000 ng mL^{-1}) and at its AMI level (3000 ng mL^{-1}) and, in both cases, all other analytes at their corresponding IC50. B) Response of the multiplexed microarray when sample (casein buffer) contains Cys C at its basal level (1290 ng mL^{-1}) and its AMI level (2400 ng mL^{-1}) and, in both, all other analytes at their corresponding IC50 concentration. Results shown are the average and standard deviation of assays performed on one slide (one day), where each microarray contained six spots for each analyte.

As it can be observed, when CRP and Cys C are at their basal and AMI levels, do not cause any interference in the response of the spots of the other biomarker targets. For those, response is only observed when samples contained the corresponding biomarker targets at the IC50 values. On the other hand, it was evident that difference between basal and AMI levels for CRP and Cys C was not enough, but this was due to the fact that the signal was saturated, since as mentioned before, the detectability of these assays is too high in respect to the values found in plasma or serum samples. It is clear that to obtain a clinical value from the results of these analysis, the samples will have to be diluted prior to the analysis.

A similar experiment was also done for the H-FABP, Tn I-T-C complex and NT-proBNP biomarkers. In these cases, the sensitivity of the microarray was not

enough to detect these targets at their basal levels occurring on healthy patients, but even though were tested to know about the potential of this microarray to differentiate between healthy patients and those suffering AMI. As before, samples were prepared by spiking these values and the response also compared to that obtained when the other target analytes were present at their IC50 values (see Figure 6.16).

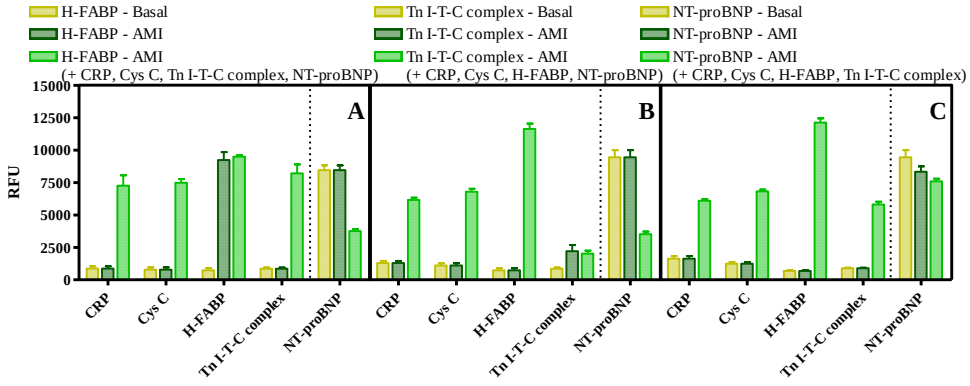

Figure 6.16. A) Response of the multiplexed microarray to samples (prepared in casein buffer) that contains H-FABP at its basal levels (5 ng mL^{-1}) and at its AMI levels (50 ng mL^{-1}); in this last case, also the response obtained when all other biomarker targets are present at their corresponding IC50 concentration values. B) Response of the multiplexed microarray to samples (prepared in casein buffer) that contains Tn I-T-C complex at its basal levels (0.06 ng mL^{-1}) and at its AMI levels (8.8 ng mL^{-1}); in this last case, also the response obtained when all other biomarker targets are present at their corresponding IC50 concentration values. C) Response of the multiplexed microarray to samples (prepared in casein buffer) that contains NT-proBNP at its basal levels (0.4 ng mL^{-1}) and at its AMI levels (2 ng mL^{-1}); in this last case, also the response obtained when all other biomarker targets are present at their corresponding IC50 concentration values. Results shown are the average and standard deviation of assays performed on one slide (one day), where each microarray contained six spots for each analyte.

The results were very good since the response was only observed on the corresponding spots and this was not affected by the presence of the other biomarker targets. For the case of H-FABP, it was possible to clearly distinguish between a healthy and AMI status, but this difference was only small for the case of the NT-proBNP. Even though, the difference was still significant ($p < 0.005$). For the case of the Tn I-T-C complex the difference observed in the graph between the response to the solutions spiked at basal and AMI concentrations was also significant considering this standard deviation of the measurements ($p < 0.03$).

6.4.4 CONVERSION FROM ONE TO TWO MULTIPLEXED ASSAYS FOR THE ANALYSIS OF FIVE BIOMARKERS IN PARALLEL

The results obtained until now clearly indicated that CRP and Cys C could not be measured in the same microarray as the other biomarker targets due to the need to dilute the sample in order to avoid the specific interferences. These interferences are caused by the CRP and Cys C basal levels present in human serum and plasma if these samples are measured undiluted, as it is necessary for the rest of the biomarker targets which are present at much lower concentrations. The different concentration ranges at which important biomarkers are present in biological samples is one of the main challenges of the multiplexed *in vitro* diagnostic. Fortunately, one of the main advantages of the microarray technology is the possibility to run several microarrays in parallel. Thus, as described before, the microarrays prepared in this research work were spotted on glass slides in which is possible to print up to 24 microarrays in a single slide. This allows performing simultaneous measurements of the same sample diluted at different ratios on different microarrays of the same slide. Nevertheless, sometimes the limitation is the sample size, which could not be sufficient to perform analysis on distinct microarrays. In order to establish the appropriate measurement conditions for each group of biomarker targets, slides printed for CRP and Cys C were used to determine the necessary plasma dilution that had to be applied in order to quantify CRP and Cys C. The results are shown in Figure 6.17 and Table 6.9. As it can be concluded, human plasma had to be diluted at least 40 times to measure CRP above the basal levels. Considering the LOD for CRP of the multiplexed microarray (15 ± 5 ng mL^{-1}) and the cut-off of this biomarker (1000 ng mL^{-1}), a 1/40 dilution of the sample would place the CRP basal levels of the samples from healthy patients very close to the LOD (25 ng mL^{-1}), so in case the levels are raised due to an inflammatory process those could be quantified (IC50 is near 75 ng mL^{-1}).

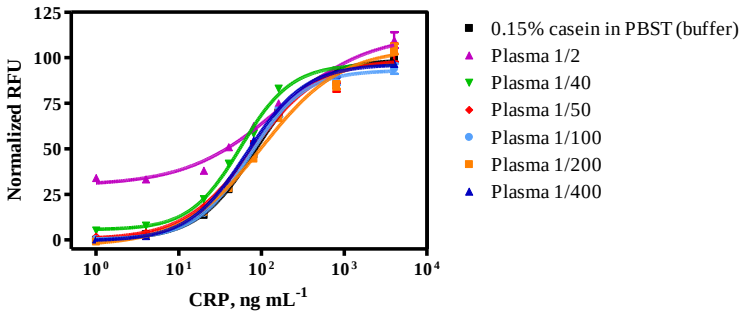

Figure 6.17. Matrix effect caused by diluting human plasma in the CRP individual microarray. Each calibration curve was assayed once, except the one in buffer (reference) that was assayed three times in three different days and all using 18 replicates for each concentration point in every well (microarray).

Table 6.9. Analytical features for the CRP individual microarray in buffer and diluted plasma.

	Buffer	Plasma 1/2	Plasma 1/40	Plasma 1/50	Plasma 1/100	Plasma 1/200	Plasma 1/400
RFU_{max}	98.94	113.00	96.38	98.97	93.08	105.30	96.37
RFU_{min}	0.02	29.73	5.53	0.24	0.21	-3.36	-0.61
Slope	1.24	0.79	1.43	1.07	1.31	0.91	1.23
R^2	0.99	0.89	0.98	0.96	0.96	0.97	0.99
IC50, ng mL^{-1}	84.99	160.20	56.18	77.59	72.43	101.60	66.95

Each calibration curve was assayed once, except the one in buffer (reference) that was assayed three times in three different days and all using 18 replicates for each concentration point in every well (microarray).

Same experiments were performed for Cys C (see Figure 6.18 and Table 6.10). In this case, intrinsic Cys C produced greater interference in the microarray than CRP since the detectability for this biomarker target is also higher. According to the graph, the plasma had to be diluted at least 200 times in order to be able to quantify samples with Cys C values above the basal level.

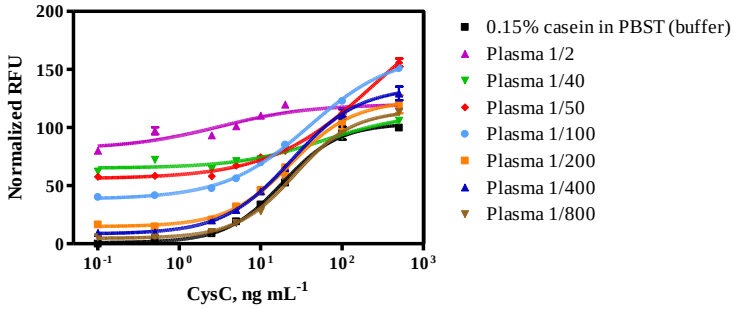

Figure 6.18. Matrix effect caused by diluting human plasma in Cys C individual microarray. Each calibration curve was assayed once, except the one in buffer (reference) that was assayed four times in four different days and all using 18 replicates for each concentration point in every well (microarray).

Table 6.10. Analytical features for the Cys C individual microarray in buffer and diluted plasma.

	Buffer	Plasma 1/2	Plasma 1/40	Plasma 1/50	Plasma 1/100	Plasma 1/200	Plasma 1/400	Plasma 1/800
RFU_{max}	103.40	119.90	113.20	216.10	163.90	123.30	134.8	114.8
RFU_{min}	0.94	81.69	65.05	55.82	38.36	14.72	8.38	4.64
Slope	1.25	0.78	0.80	0.69	0.83	1.12	1.04	1.20
R^2	0.99	0.53	0.81	0.94	0.99	0.89	0.96	0.98
IC50, ng mL^{-1}	18.50	3.11	60.55	238.40	39.32	23.61	23.69	26.38

Each calibration curve was assayed once, except the one in buffer (reference) that was assayed four times in four different days and all using 18 replicates for each concentration point in every well (microarray).

For an accurate quantification of both CRP and Cys C biomarkers it would have been necessary to measure each clinical sample at least at three different dilution factors: i) 1/40 for CRP; ii) 1/200 for Cys C and iii) undiluted for the rest of the biomarker targets. With this scenario, and even the high throughput capabilities of the microarray technology, we thought that we were moving on a direction in which each biomarker would have to be measured on different conditions that is against the multiplexed diagnostic ideal concept. For this reason, we decided to assess the possibility of measuring CRP and Cys C on the same microarray sacrifying accuracy on the quantification of one of these biomarkers. Considering the higher relevance for CRP in cardiovascular diseases, it was decided in this case to sacrify accuracy for Cys C and measuring

both analytes at 1/40 dilution. Although quite unspecific, CRP is a well-recognized biomarker clearly associated to early steps of the CVD. In contrast, Cys C is considered an almost perfect candidate for estimating renal function. The strong correlation between chronic kidney disease (CKD) and CVD along with the growing understanding of the role of cysteinyl cathepsins in the pathophysiology of CVD inspired researchers to explore the potential association of Cys C with CVD. Thus, elevated levels of Cys C are associated to CVD developed due to impaired renal function [195]. In this way, results obtained for Cys C in this microarray would have to be interpreted as qualitative better than quantitative.

As proof-of-concept samples spiked with a mixture of all the biomarkers at different levels (basal and AMI) were measured on two multiplexed microarrays at two different dilutions (1/40 for CRP and Cys C and undiluted for H-FABP, cTnI and NT-proBNP). The results are shown in Figure 6.19. As it can be observed, except for troponin and NT-proBNP where both basal and AMI levels could not be differentiated, for the rest of biomarker targets it was possible to differentiate between both conditions. Even though, it must be noticed that on patients with high probability to suffer from myocardial infarction or heart failure; H-FABP and NT-proBNP, respectively, could be quantified but not when measuring samples from patients with low levels nearer of the cut-off.

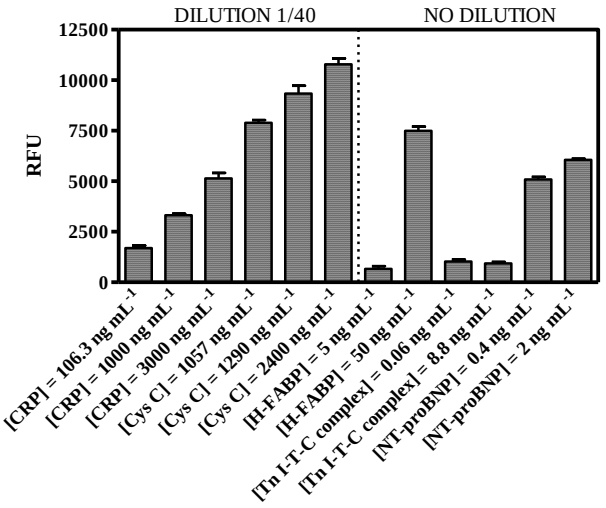

Figure 6.19. Signal comparison in the multiplexed microarray platform employing both levels of each analyte; basal levels and AMI levels with high risk of CVD. For CRP and Cys C where 1/40 dilution of the sample is required, the minimum levels (a mean of 5 values obtained by 5 different measures of non-diluted blank plasma) are tested to compare the difference with the cut-off (1000 ng mL^{-1} for CRP and 1290 ng mL^{-1} for Cys C). The standard deviation shown is the result of analysis made one day using 6 spots per well in each case.

6.4.4.1 Accuracy studies

The accuracy was assessed by measuring plasma samples fortified with all analytes at different concentrations. The samples were splinted in two parts, one of them diluted 1/40 for CRP and Cys C, and the other measured undiluted for the rest of the biomarker targets. Analysis were performed in six different days for CRP and Cys C, while for H-FABP, Tn I-T-C complex and NT-proBNP analyses were done in three different days employing at least 6 spot-replicates per microarray for each target. The results shown in Figure 6.20 correspond to the correlation found between the measured and the fortified concentration values. As can be observed, while for NT-proBNP, H-FABP and CRP the coefficients of correlation were acceptable, for Cys C and troponin complex were lower than 0.8. Moreover, while CRP and Cys C microarray tended to overestimate (slopes 1.5 and 1.2, respectively), for the rest of the targets an underestimation was observed (slopes between 0.8 and 0.9). In spite of these circumstances we consider that the microarray could still be useful for screening and patient stratification, although the accuracy was not great. In

that respect, it should be noticed that most of the POC assays in the market also show important variations and discordances between them as it has been stated in chapter 3 for the cTn assays.

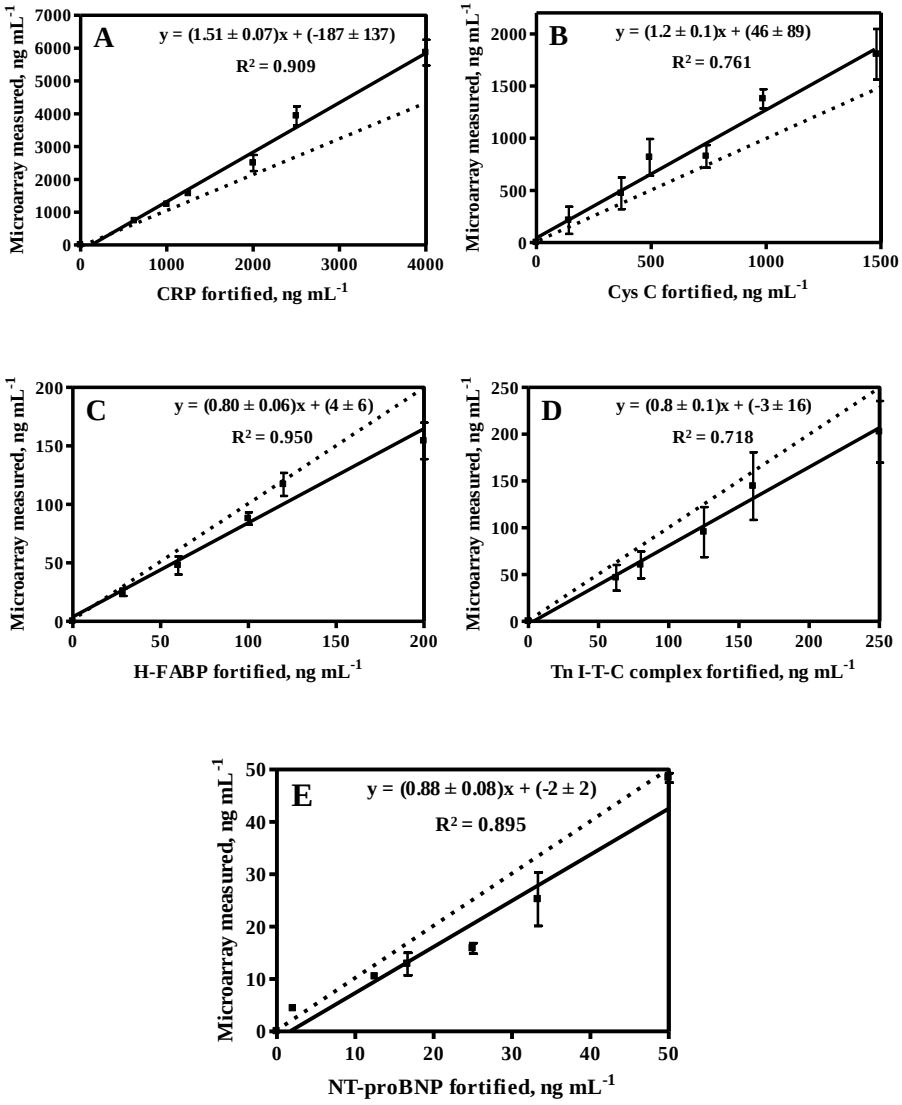

Figure 6.20. Correlation between the fortified and measured concentration values for A) CRP, B) Cys C, C) H-FABP, D) Tn I-T-C complex and E) NT-proBNP assays. CRP and Cys C are performed in one slide with 1/40 sample dilution, while H-FABP, troponin and NT-proBNP are performed in another slide without sample dilution. The dotted line corresponds to a perfect correlation (slope=1).

6.4.4.2 Measurement of real clinical samples

Clinical plasma samples obtained from patients showing different pathologies were provided by Institut d'Investigació Germans Trias i Pujol (IGTP) for the preliminary evaluation of the multiplexed microarray developed. These plasma samples had been already analyzed at the IGTP for cTnI, CK-MB and CRP concentrations using a Siemens Dimension analyzer, for NT-proBNP with a Radiometer AQT 90 FLEX (see Table 6.11). Both equipments are bench-top analyzers that provide data for each biomarker target as result of separate and individual analysis. The Radiometer AQT 90 FLEX is a time-resolved fluorescence immunoassay with europium-chelate labelled fluorescent tracer antibody similar to Roche ECLIA system, while the Siemens Dimension analyzer is based on LOCI® chemiluminescent technology.

Creatine kinase (CK) is an enzyme expressed by various tissues and cell types. CK catalyses the conversion of creatine and utilizes adenosine triphosphate (ATP) to create phosphocreatine and adenosine diphosphate (ADP). Isoenzyme patterns differ in tissues. Although creatine kinase MB isoenzyme (CK-MB) by mass assay is a sensitive marker of myocardial damage, it has inferior myocardial specificity compared to cTnI because it is present in high concentrations in both cardiac and skeletal muscle [196].

Table 6.11. Analysis of several cardiovascular biomarkers from different patient samples with different clinical diagnosis. Data provided by IGTP.

Patient	CK ($U\ L^{-1}$)	MB ($ng\ mL^{-1}$)	cTnI ($ng\ mL^{-1}$)	NT-proBNP ($ng\ mL^{-1}$)	CRP ($ng\ mL^{-1}$)	Clinical diagnosis
1	274	37.4	2.32	-	4200	AMI
2	916	203.4	11.18	-	-	Inferior AMI
3	1217	247.1	20.3	-	-	Inferior AMI
4	107	0.8	0.1	-	-	Pain without ST increase
5	104	12.6	3.52	-	-	AMI
6	54	3.2	0.91	-	-	Pain without ST increase
7	54	3.2	0.92	-	-	Pain without ST increase
8	42	1.4	0.31	-	-	Pain without ST increase

9	-	-	-	-	-	Unknown
10	-	17.2	0.92	-	-	Cardiac arrest
11	-	-	-	0.268	-	Hypertension
12	-	-	-	2.490	-	HF
13	-	-	-	0.371	-	HF
14	-	-	-	14.000	-	Possible Addison illness
15	-	-	-	9.160	-	HF
16	-	-	-	60.200	-	Ischemia and terminal renal insufficiency
17	-	-	-	0.670	-	HF
18	-	-	-	-	79000	Obstetric control
19	-	-	-	-	9800	Obstetric control
20	-	-	-	-	1400	Gastric disorders
21	-	-	-	-	4400	Gastric disorders
22	-	-	-	-	8700	Gastric disorders
23	-	-	-	-	160000	Gastric disorders
24	-	-	-	-	114400	Urinary infection
25	-	-	-	-	35000	Thoracic pain
26	227	32.9	7.9	-	-	Anterolateral AMI
27	414	146.7	-	-	-	Anterolateral AMI
28	372	39.8	-	-	-	Anterolateral AMI
29	201	31.6	11.51	-	-	Anterolateral AMI

Total CK is analyzed in the second column, while in the third only MB subtype is expressed. ST elevations refer to a finding on an electrocardiogram, wherein the trace in the ST segment is abnormally high above the baseline.

The results obtained with the bench-top analyzers are shown in Table 6.11, related to the diagnosed pathology. As it can be observed the samples were obtained from patients with and without symptoms related to CVDs. All samples were analyzed with the multiplexed microarray developed and the results are shown in the graphs from Figure 6.21. H-FABP, Tn I-T-C complex and NT-proBNP were measured undiluted and the data shown is the result of a single measurement on the microarray since the sample size was not sufficient. CRP and Cys C could be measured on different microarrays and distinct slides during three different days since there was more sample available because of the dilution factor that had to be applied. The grey bars correspond to the results obtained with the bench-top analyzers and are shown for comparison to

the results obtained with the microarray. As it can be observed no data could be recorded for cTnI since the detectability of the microarray was insufficient, therefore the data shown correspond only to the data provided by the IGTP At the opposite, bench-top analyzers did not provide data for H-FABP and Cys C.

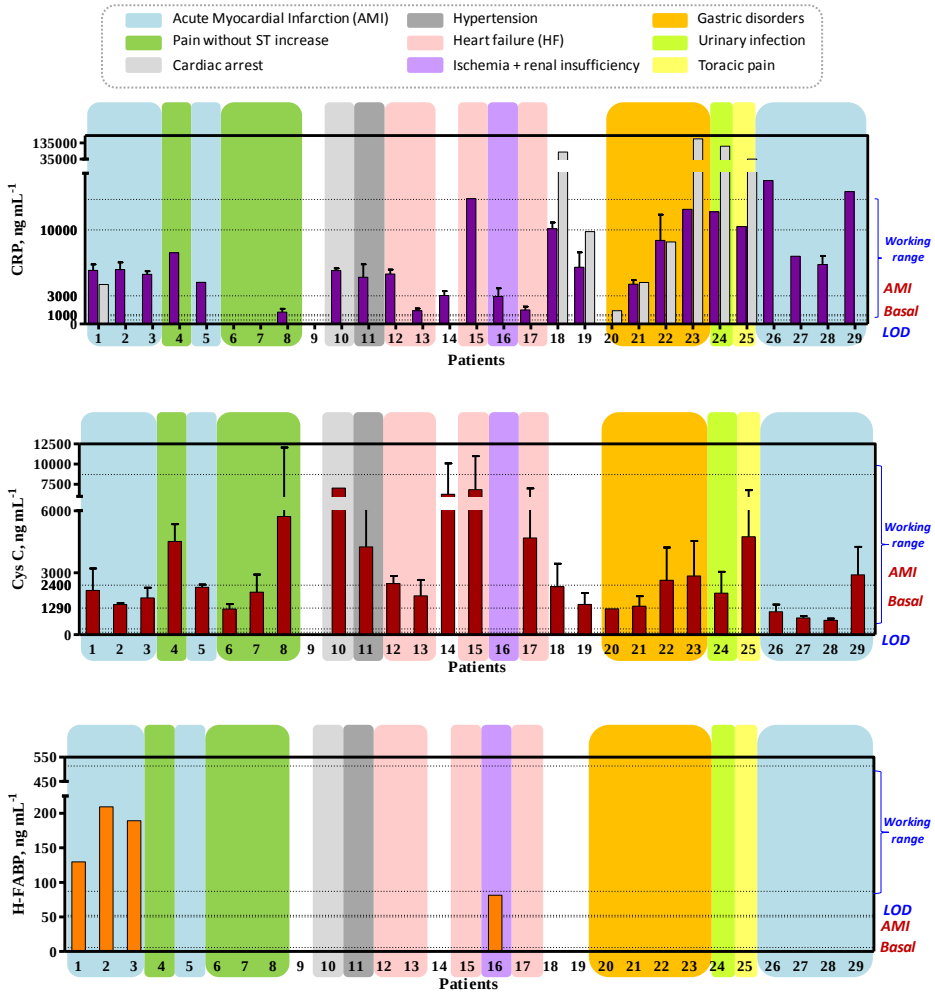

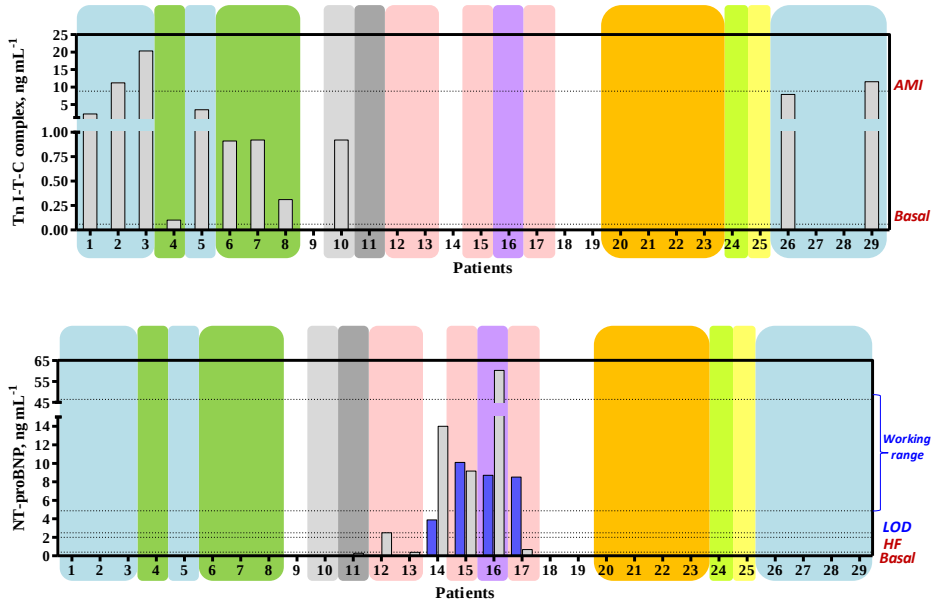

Figure 6.21. Preliminary studies with real clinical samples performed in the two multiplexed platforms developed in this chapter. Grey bars correspond to measurements taken by IGTP. For troponin, any sample could be detected through the methodology here described. For CRP, patients 6, 7, 9 and 20 were not detected because they were lower than the LOD. For Cys C, patients 9 and 16 were not detected because they were above the working range. For H-FABP, Tn I-T-C complex and NT-proBNP, bars not shown correspond to patients with levels below the LOD which could not be detected. For patient 9 no cardiovascular biomarkers were found.

Overall we could say that in fact the microarray was able to give much more information and had superior regarding sample throughput capabilities. Thus, all 29 samples were measured and screened for the five biomarker targets on a short time, while with the bench-top analyzers each sample was measured only for particular biomarkers. For example, no data was collected at all regarding H-FABP and Cys C levels of these patients and CRP levels were found elevated in much more patients that those analyzed with the bench-top equipments. Another important aspect to be noticed is that all the samples that did test positive with the microarray, were also positive with the bench-top analyzers and in most cases a similar profile of response could be observed. Hence, for example, for CRP there exists an agreement between both techniques for the samples that contained the higher or lower levels of CRP. Similarly for NT-proBNP, even if the detectability for this biomarker was questionable during the development. As it can be seen in the graph, the results were negative for all samples, except for those that were measured and did test positive also with

the bench-top analyzer. Only sample 12 did give a positive response with the Radiometer AQT 90 FLEX but the microarray here reported was not able to detect levels over the threshold for this biomarker. On the other hand, sample 17 did test clearly positive with the microarray, but the response was very low with the bench-top analyzer.

Regarding clinical interpretation of these results, the CRP is a biomarker related to inflammatory processes which explains why it was found elevated in many patients even if they did not suffer CVDs. Patients with CRP concentrations lower than 1000 ng mL^{-1} are classified as low risk, moderate for levels in the 1000-3000 ng mL^{-1} range and high risk for concentrations higher than 3000 ng mL^{-1} [22]. In this study many patients had higher levels of CRP but could not be related to CVD because they did suffer other pathologies also involving inflammatory processes. However, based on the clinical history and the data provided by the IGPT, the results obtained with the microarray confirmed that patients 6, 7 and 20 had low risk of suffering CVD since their concentration was below 1000 ng mL^{-1}, which makes sense since they had chest pain but without ST increase and vomits. Otherwise, patients 8, 13, 14, 16 and 17 could have a moderate risk and they were diagnosed to have pain without ST increase, HF, Addison disease, HF and ischemia with renal insufficiency respectively. Addison disease is a rare, chronic endocrine system disorder in which the adrenal glands do not produce sufficient steroid hormones. Those patients diagnosed of AMI did show high levels of CRP and two of them (patients 26 and 29) were in very high risk. Also, according the CRP levels, patients 4, 10 and 11 were in high risk of having cardiovascular disorders, which is in accordance with the information related to their previous story of having chest pain without ST increase, cardiac arrest and hypertension. Patients 12 and 15 diagnosed of HF were in high and very high risk and patients 18 and 19 who were passing the obstetrician control were in the high risk of CVD zone as well. The same situation was for the rest of patients suffering gastric disorders, urinary infection and thoracic pain. In general, CRP measurements correlated quite well with those ran by IGTP (patients 18-25).

As it happened for CRP, patients 6 and 20 had Cys C levels corresponding to the basal levels which pointed out again that both patients had low probability to present cardiac problems. On the contrary, those patients diagnosed from AMI (26, 27 and 28) had similar levels and this fact underlines the doubtfully

cardiovascular specificity of this marker. Even though, those patients suffering from cardiac arrest, HF and thoracic pain (10, 15, 17 and 25) presented high levels of Cys C above 2400 ng mL^{-1} which is the value assigned for high risk of CVD. Finally, patient 16 is the one with the highest level of Cys C and he has ischemia and renal insufficiency. Increased levels of Cys C are associated of kidney function and renal disorders, apart from risk of death and cardiovascular events in elderly persons.

Also in this last patient 16, H-FABP levels found were above the AMI ones which shows some kind of relation. Moreover, patients suffering AMI (1, 2 and 3) were in the same situation. Even though, other patients with also the same diagnostic their levels were not detected. It means they could be below AMI levels but above the basal levels. AMI levels are those ones representing high risk of infarction.

NT-proBNP levels were found elevated in patients suffering from HF and ischemia with renal insufficiency. It should also be noticed that high values of troponin I were assigned to patients without an AMI diagnostic which means that also analyzers provide incoherent results.

6.5 DISCUSSION

The main purpose of this thesis in general was to develop a multiplexed microarray platform as a diagnostic tool for cardiovascular diseases. Relevant biomarker targets were selected to develop the corresponding immunochemical procedures described in the previous chapters, facing important and challenging problems. The difference in the chemical nature between the target analytes (lipoprotein, proteins and peptide) has forced to combine in the same platform different immunochemical formats (sandwich and competitive). Moreover, the fact that biomarkers are present at very different concentration ranges has prevented from obtaining all data in single measurement. Even though, the high throughput capabilities of this technology have allowed obtaining important amount of data by running several microarrays simultaneously.

The lack of commercial devices for multi-analyte measurement of several cardiac markers already pointed to difficulties to accomplish this aim. Moreover, as it has been shown at the beginning of this chapter, the few existing multi-detection methods also showed a lack of the necessary sensitivity. MSD MULTI-ARRAY™ platform sold by Meso Scale Discovery was the unique technology that achieved all required LODs for all analytes (CK-MB, MYO and cTnI). The work of Marquette et al. [194] regarding multiplexed microarrays or the work of Park et al. [193] representing other kind of methodologies, in this case a multiplexed ELISA in a lab-on-a-disc, could not achieve either the sensitivity for cTnI and brain natriuretic peptides (BNP and NT-proBNP).

As it was explained in the discussion of chapter 4, the lack of sensitivity is related to the technology being used and the signal acquisition. For instance, MSD platform employs detection antibodies labelled with $Ru(bpy)_3^{2+}$ compound, and electrochemiluminescence is used as the detection technology. It is different compared to the fluorescent microarray here employed.

In spite of all the efforts, we have not been able to improve the sensitivity for troponin, NT-proBNP and H-FABP until reaching the basal levels. Differences in concentration ranges were solved by splitting the sample in two parts and analyze them simultaneously in two different microarrays. In this manner, real clinical samples have been analyzed and reasonable results were obtained in these preliminary studies. When AMI and HF were diagnosed, H-FABP and NT-proBNP could be detected respectively. What is more and in reference to CRP assay, those patients diagnosed from AMI all were in high risk ([CRP]>3000 ng mL^{-1}) of suffering from cardiac disorders and two of them were in very high risk ([CRP]>10000 ng mL^{-1}). Also patients diagnosed of HF were in high and very high risk. Both CRP and Cys C concentrations were very low for these healthy patients and Cys C presented high specificity for renal disorders also related to cardiovascular diseases at the same time. To sum up, the diagnostic tool developed in this chapter, despite having some limitations in some aspects, could serve as a semi-quantitative tool for an accurate patient risk stratification and suitable treatment.

7 AN OPTICAL IMMUNOSENSOR FOR CRP AND NT-PROBNP DETECTION

7.1 INTRODUCTION

7.1.1 SENSORS AS POC TESTS FOR CVD

Point-of-care testing (POCT) is a laboratory-medicine discipline that is growing fast in the analytical field and clinical application. POC tests are a simple, rapid and relatively inexpensive way for reducing hospital stay, complications and improving adherence to treatment. Their use can lead to a decrease in test ordering, sample transport to laboratories and data reporting. Apart from this, this modern variety of laboratory medicine is characterized by minimizing instrument size and procedures and the increasing use of current information technology [6]. Nowadays, there are analytical devices available to analyze a whole blood sample in a simple manner allowing untrained staff to carry out laboratory diagnostics. An example of this is the blood-sugar test strips and devices for home testing in diabetes. More examples are listed in Table 7.1.

Table 7.1. List of laboratory parameters currently available using point-of-care testing (POCT) [197].

Clinical application	Parameter
Acid-base balance, blood gases	pH, pCO_2, pO_2
Electrolytes	Na^+, K^+, Cl^-, Ca^{2+}, Mg^{2+}
Metabolites	Cholesterol, HDL-cholesterol, triglycerides, creatinine, urea, uric acid, bilirubin, lactate, ammonia
Enzymes	Amylase, alkaline phosphatase, CK, AST, ALT, γ-GT
Coagulation	Activated clotting-time (ACT), activated partial thromboplastin time (aPTT), prothrombin time (PT, INR), D-dimer, platelet function tests, ex-vivo bleeding time
Hematology	Hemoglobin, hematocrit, erythrocytes, leukocytes, thrombocytes
Hemoglobin fractions	CO-Oximetry
Cardiac markers	TnT, cTnI, myoglobin, CK-MB, BNP/NT-proBNP
Diabetes mellitus	Glucose, HbA1c, microalbumin, minimal invasive continuous glucose monitoring
Acute-phase proteins	CRP
Allergy in-vitro diagnostics	Allergy specific IgE

Rheumatology	Antibodies against mutated citrullinated vimentin (anti-MCV)
Therapeutic drug monitoring, drug-of-abuse screening	Therapeutic drugs, alcohol, amphetamines, barbiturates, benzodiazepines, cannabinoids, cocaine, methadone, opiates
Infectious agents	HIV, infectious mononucleosis, Chlamydia trachomatis, Trichomonas vaginalis, Plasmodium falciparum and vivax, Influenza A and B, Streptococcus A and B
Fertility	hCG, LH and FSH, sperm count
Urine diagnostics	Urine strips (pH, protein, glucose, ketones, bilirubin, urobilinogen, nitrite, leukocytes, erythrocytes), microalbumin, NMP22 bladder carcinoma check
Stool diagnostics	Blood

The determination and quantification of blood based cardiac biomarkers are crucial in the triage and management of a range of cardiac related conditions, where time delay has a major impact on short and longer-term outcomes of a patient. POC testing in patients with cardiac disease is therefore driven by the time-critical need for fast, specific and accurate results to initiate therapy instantly. According to current guidelines, the results of the cardiac marker testing should be available to the physician within 30 min (vein-to-brain time) [196] to initiate therapy within 60-90 min (door-to-needle time) after the patient has arrived at the emergency room or intensive care unit.

Due to the fact that the existing POC devices for cardiovascular markers such as TnT, cTnI, myoglobin, CK-MB, BNP and NT-proBNP (Table 7.1) are currently in the market, issues such as time of analysis, volume of sample, pretreatment of the sample have to be competitive. Moreover, multiplexing of different biomarkers has to be the key issue to be competitive with the existing devices. Also, the implementation in this multiplexed device of the golden and four other potential biomarkers chosen and described in section 1.6 and employed in chapter 5 and 6, can help to the prognosis and diagnosis for the medical personal both in hospital as in outpatient services.

The two main types of POC testing formats available for clinical application are small bench-top analyzers and hand-held devices. The first ones are a miniaturized version of the central lab equipment including modifications to

avoid operator error and provide rapid and reproducible results. The second ones are developed using novel microfabrication techniques which incorporate different analytical steps like sample clean-up, separation, analysis and data reporting. Devices for cardiac biomarkers POCT are mainly based upon immunoassay methods which principally use 2-site immunometric methods, lateral-flow technology and flow-through immunoassay systems [6].

POCT devices often employ biosensors and the rapid development in the field of antibody-based biosensors is predicted to lead to a new era in POCT development. Biosensors are analytical devices for the detection of analytes that combine a biological component with a physicochemical-detector component (IUPAC definition, see section 1.4.1.3). This generally occurs through the use of miniaturized analysis systems, where biological components are immobilized on a solid surface which in turn interacts with the analyte. These interactions may be detected by using either electrochemical or optical methods. In the last case, fluorescence or reflection spectroscopy plays an important role [197]. Thus, different parameters being characteristic for a certain disease, in this case cardiovascular disease, can be detected by using specific biomolecules such as antibodies (immunosensor).

The Abbot i-STAT is the only electrochemical POC immunosensor available for the determination of cTnI from whole blood. The system uses disposable plastic cartridges containing all control materials and reagents for a two-step enzyme immunoassay and microfabricated film electrodes. In this case, the analyte is quantitated by a hand-held reader which utilized electrochemical sensor technology [5]. Additionally to other optical POC immunosensors explained in the next section, Resonant Acoustic Profiling™ (RAP™) system for quantification of CRP levels in serum samples was also developed as a piezoelectric sensor. Although not being a prototypical POCT, this system is label-free and has good correlation with a commercial hs-CRP ELISA but with reduced sample analysis time [6, 198]. In addition to these commercial devices, there has been reported a variety of biosensors approaches based on distinct transducing principles for the detection of distinct cardiovascular biomarkers [15, 17, 199]. As an example, the group of Prof. Pingarron has reported two electrochemical magnetoimmunosensors, one for the detection of cTnT and another for the detection of NT-proBNP [200, 201].

7.1.2 MULTIPLEXED DETECTION OF CARDIOVASCULAR BIOMARKERS THROUGH OPTICAL IMMUNOSENSORS

The ideal POC test would be that one available for multi-analyte detection and that could be used for different intentions such as risk identification, early detection disease, emergency or routine follow-up at cardiology units or at home. Thus, the operators of this multiplex test could be physicians, nurses at hospital units or at home or the patients itself. Modalities of use must have a strong impact on the technical characteristics of the final product like blood sampling, time to get results, assay accuracy (qualitative or quantitative values, sensibility, specificity, etc.), results display and results storage. In general, the optical transducers most used in multiple analyte immunoassays are the integrated optical waveguide (IOW) or the internal reflection element (IRE) [202].

Some examples of multiplexed optical immunosensors for cardiovascular biomarkers detection were found and examined. One of them is a POC test commercially available and is called Lifelite assay.

The Lifelite cardiac panel offers a multiplexed immunochip that measures three cardiac markers (myoglobin, CK-MB and cTnI) together with three integrated controls from whole blood. Measurements are carried on simultaneously and results are obtained within 5 min using Evanescent Planar Waveguide™ technology. The tube where the sample is collected already contains fluorophore-labelled antibodies against each biomarker to tag the analyte immediately after the blood addition. After the mixture has been introduced into the test cartridge, the fluorophore-tagged antibody-analyte complexes are bound to specific capture antibodies. A laser source and lens system directs light into the precision-molded plastic biochip which serves as a waveguide. When light passes down the length of the plastic material, differences in refraction indices between the plastic and the sample cause total internal reflection of the light producing an evanescent field over the chip surface. This evanescent field excites the fluorophore molecules bound to the chip and a charge-coupled-device camera/optics system records the intensity of the emitted light, providing then quantitative measurements of the analytes as a result[5].

Although not being POC tests, in the literature there are several examples of multiplexed optical immunosensors for cardiovascular biomarkers. For instance and in chronological order, Plowman et al. first performed an IOW multi-analyte immunoassay for the detection of CK-MB, cTnI and myoglobin. The surface used was an array of 3 mm-sized protein "channels" adsorbed onto a grating coupled SiON IOW transducer operating in an evanescently fluorescence detection format. MAbs were employed in all three sandwich formats since it was previously observed with other systems that multi-analyte immunoassays with MAbs were more selective than PAbs by comparison with single-analyte immunoassays (less cross-reactivity). The capture ones were physically adsorbed on the surface modified with dimethyldichlorosilane (DDS) while the detection antibodies were labeled with Cy5. Final results showed comparable analytical sensitivities for CK-MB whereas for cTnI and myoglobin assays they were affected by the multiplexed format due to the non-specific binding (from 15.9 to 26.9 ng mL^{-1} and from 7.0 and 33.8 ng mL^{-1} respectively) [202].

Mandal et al. developed a label-free multiplexed immunosensor based on a nanoscale optofluidic sensor array (NOSA) architecture for the detection of multiple interleukins (IL-4, IL-6, IL-8). This device consisted of arrays of evanescently coupled 1-D photonic crystals resonators. Thus, the accessible optical field inside the holes of photonic crystal was stronger increasing the light-matter interactions that enhanced sensitivity. The smallest amount of bound mass that could be detected by this sensor was 63 ag corresponding to a surface mass coverage of 7.5 pg mm^2. Later, an SPR fiber-optic sensor for the simultaneous detection of cTnI and myoglobin was developed by Masson et al. [203]. Particularly, a coating based on a self-assembled monolayer (SAM) of N-hydroxysuccinimide activated 16-mercaptohexadecanoic acid (NHS-MHA) was used as a non-fouling coating while also covalently binding the antibodies and minimizing adsorption. Due to the impossibility to use diluted serum of blood because it would decrease the analyte concentrations below the LOD of the SPR sensor, it was observed that with such a coating the error in the signal reproducibility was nearly equivalent to the system noise. Thus, similar LOD for those biomarkers detection in serum were expected when compared to measurement in saline solution. LODs obtained were 0.7 and 0.9 ng mL^{-1} for cTnI and myoglobin respectively, with which patients suffering from a MI could be detected.

Finally, Lu et al. achieved a multiplexed detection of cTnI, CRP and BNP using a photonic suspension array [204] . Different silica colloidal crystal bead (SCCBs) were used with different reflection peak position for each analyte; 465, 502 and 600 nm for cTnI, CRP and BNP. SCCBs were conjugated to the corresponding MAbs and PAbs were labelled with FITC and used as detection antibodies. LODs were 0.01 ng mL^{-1} for cTnI, 360 ng mL^{-1} for CRP and 0.004 ng mL^{-1} for BNP with an assay time of 60 min. In this last case, LOD for cTnI assay was much better compared to the SPR sensor previously explained which could not detect the corresponding basal levels.

7.1.3 IMMUNOSENSORS FOR BNP AND NT-PROBNP

Brain Natriutetic Peptides (BNPs) are the analytes to which the greatest effort have been addressed in this thesis, starting from their hapten design, antibody production, ELISA development and finishing with the implementation of the NT-proBNP immunoassay to a multiplexed platform involving different cardiovascular biomarkers (chapter 6). As an alternative to the classical analytical methods explained in chapter 4 for the detection of NT-proBNP, BNP and their precursor, immunosensors have been developed with the aim to improve analysis time, cost and instrument portability. All immunosensors found in the literature and detailed in Table 7.2 employed immunoassays with sandwich formats except the amperometric magnetoimmunosensor [201] in which an indirect competitive format was used. Polyclonal and monoclonal antibodies were used in these publications and just in few of them the production and the recognized epitopes were specified.

Table 7.2. Analytical characteristics of different brain natriuretic peptides immunosensors reported in the literature.

	Sensor	Analyte, reagents	Sample	LOD (ng mL^{-1})	Working range (ng mL^{-1})	t_{assay} (min)	Ref.
OPTICAL IMMUNOSENSORS	Nanogold-particle fluorescence optical immunosensor (Fiber-optic sensor)	BNP MAb_1 MAb_2-Cy5	Ethanol	-	-	6.5	[205]
	SPR	BNP MAb_1 MAb_2-biotin	Plasma	1 (amplified)	10 - 100	~ 340	[206]

		NP-streptavidin Biotin-Ab(anti-strept.)					
	Diffractive optics technology (dot^{TM}), label-free (streptavidin pattern)	NT-proBNP MAb-biotin Goat PAb Anti-goat PAb-HRP	Plasma	-	0.03 – 2.50	90	[207]
	On-chip ELISA + SPR	BNP PAb-AChE	Serum	$1 \cdot 10^{-3}$	$5 \cdot 10^{-3}$ - 100	30	[208]
ELECTROCHEMICAL IMMUNOSENSORS	Amperometry Magnetoimmunosensor (E_{app} = -0.10 V vs. Ag pseudo-ref. electrode)	NT-proBNP MP-NT-proBNP MAb-HRP	Serum	0.02	0.12 – 42.9	210	[201]
	Cyclic voltammetry (-0.5 to 0.5 V vs. SCE at 50 mV s^{-1})	NT-proBNP MAb_1-DpAu-BSA-CNTs AuNCs-HRP-PAb_2 AuNPs-HRP-PAb_2	-	$6 \cdot 10^{-3}$	0.02 - 100	120	[209]
	Amperometry	NT-proBNP MAb(Fab)-biotin MP-avidin	Serum	0.03	0.04 – 2.5	-	[210]
	Amperometry, microfluidic system (E_{app} = -0.10 V vs. Ag pseudo-ref. electrode)	NT-proBNP MAb_1(Fab)-biotin PPN-MAb_2 MP-avidin	Serum, blood	0.003	0.005 – 1.67 1.67 - 4	18	[211]
	ECL immunoassay (aptasensor, amperometry)	NT-proBNP MAb_1 MAb_2-liposome (cocaine)	-	$7.7 \cdot 10^{-4}$	0.01 - 500	180	[212]
	Amperometry (E_{app} = 0.2 V vs. Ag/AgCl ref. electrode)	BNP scFv recombinant Ab-AP	-	$1 \cdot 10^{-6}$	$1 \cdot 10^{-6}$ – 0.01	180	[213]
	Electrochemical enzyme immunoassay (E_{app} = -0.7 V vs. Ag/AgCl ref. electrode)	BNP PAb-AChE GoldNP-BNP	PB, serum	A) 0.02 B) 0.04	0.02 – 0.1	~ 30	[214]

As can be observed in the above table, different kind of particles were employed in the distinct immunosensors [201, 210, 211] as it was also mentioned in chapter 4 for BNPs immunoassays. They were as well used to increase the sensitivity of the assays, get faster kinetics and decrease matrix effects. Additionally, with magnetic particles, sample pre-treatment can be avoided due to the possibility to isolate the complex antibody-analyte by a magnetic separation.

With the aim to achieve high sensitivities, most assays added an amplification step or combined different techniques with the needed technology. For instance, Hong et al.[205] added nanogold particles in his optical sensor, which when placed at an appropriate distance from a fluorophore can effectively enhance the fluorescence by transferring the free electrons of the fluorophore. In Teramura's work [206], signal was amplified by using streptavidin-conjugated nanobeads although not succeeding in achieving the LOD required and Zhuo et al. [209] used immobilized carbon nanotubes to promote the electron transfer and increase the current response and gold nanochains to have more active places and be able to immobilize more enzyme, thus getting a larger current response. Finally, Mao et al. [212] developed an electrogenerated chemiluminescence (ECL) immunoassay based on the signal changes caused by cocaine previously encapsulated in a liposome conjugated to the detection antibody. The common used biotin-streptavidin amplification strategy was widely used in several cases, which theoretically the 1:4 stoichiometry of the streptavidin-biotin interaction enables more amount of immobilized antibody.

7.1.4 OPTICAL IMMUNOSENSORS FOR OTHER CVD BIOMARKERS

Apart from all the immunosensors developed for BNPs detection already published nowadays in the literature and detailed in the previous section, there is also a great amount of immunosensors for other cardiovascular biomarkers. In the following table (Table 7.3), most examples regarding optical sensors are described and divided in the three main groups: surface plasmon resonance (SPR), evanescent wave and fiber-optic sensors. The differences and main characteristics of these different types of sensors are explained in section 1.4.1.3.

Table 7.3. Analytical characteristics of different optical immunosensors for different cardiovascular biomarkers reported in the literature.

	Sensor, ligand immobilization	Analyte, reagents	Sample	LOD (ng mL^{-1})	Working range (ng mL^{-1})	t_{assay} (min)	Ref.
SPR	Biacore 2000 CM, EDC/NHS	MMP-2 GoldNP-MAb Tissue inhibitor MMPs (TIMP)	Buffer	0.036	0 – 7.2	44	[215]
	Described in [216] MHA, EDC/NHS, protein G	mCRP, pCRP MAb C8, 8D8, 9C9	Buffer	1000 (MAb C8, pCRP)	0 - 25000	~1723	[216]
	Plasmonic® SPR APTES, biotin-NHS	CRP Streptavidin, MAb(C6)-biotin, MAb(C2)	Buffer	1000	2000 - 5000	-	[217]
	Biacore 3000 -	CRP Fab' (MAb) pTHMMAA	Serum (1/100)	1.5	4 - 50000	-	[218]
	SPR_i LAB, K-MAC P3SET polymer	CRP PAb	Buffer	-	-	-	[219]
	Spreeta™ Outer membrane particle with Z-domain	CRP PAb	Buffer	1.5	0.1 - 200	-	[220]
	AutoLab Spirit® CM, EDC/NHS, streptavidin	TnT MAb-biotin	Serum	0.01	0.03 - 6.5	35	[221]
	AutoLab Spirit® CYS, GLUT	TnT MAb	Serum	-	0.05 - 4.5	287	[222]
	SPR (Navi 200, BioNavis) OEG alkanethiolate/MHA	TnT Ab	Buffer	100	0 - 50000	98	[223]
	K-MAC micro SPR NHS-gold chip (K-MAC)	cTnI 2 MAbs	Serum	0.068	0 - 160000	-	[224]
	Biacore 3000 CM, EDC/NHS	MPO scFv-HA, anti-HA (MAb)	Buffer	-	-	51	[225]
	Imaging-SPR (SPRilab,	TNF-α	Buffer	-	-	-	[226]

	Genoptic) MHA-EDC/NHS, PEG-SH	$F(ab')_2$ (PAb)-Qdot®655					
	Planar surface/Fiber-optic SPR. Described in [227] DSP	H-FABP H-FABP, PAb	Buffer	200	200 - 2000	40	[227]
EVANESCENT WAVE	Fluorescence based Eudragit L100, EDC/NHS	CRP MAb(C5), MAb(C7)-DY647	Buffer	4	100 - 50000	121	[228]
	Fluorescence based AMD, GOPTS, glutaric anhydride, DIC/NHS	CRP MAb(C5), MAb(C7)-DY647	Serum (1/100)	1)130 (sandwich) 2)55 (inhibition)	1)44 - 2900 2)130 - 22900	4675	[229]
	Silicon photonic microring resonators DNA-encoded approach	CRP 1)MAb_1-DNA, 2)MAb_2-biotin, 3)streptavidin-beads	Serum/ Plasma (1/1000)	1)10 2)1 3)0.03	1)10 – 10000 2)1 – 1000 3)0.03 – 0.1	>76	[230]
	Grating coupler sensor TSC	H-FABP MAb	Buffer	330	-	1938	[231]
	Optomagnetic (f-TIR) Immobilization by sciFLEXARRAYER	cTnI (ITC complex) PAb, MP-MAb	Plasma	0.03	0.03 – 6.5	1508	[232]
	Optomagnetic (f-TIR) Inkjet printing	cTnI MP-streptavidin, Ab-biotin, Ab	Serum (20%)/ plasma (100%)	$6 \cdot 10^{-3}$ 0.07	0.01 – 11.94 -	>5	[233]
	RIfS GOPTS, AMD, glutaric anhydrite, DIC/NHS	Cys C MAb, Cys C	Serum (1/10)	52	67 - 257	2495	[234]
FIBER-OPTIC	Fluorescence based α,ω-diaminoalkanes, glutaraldehyde	H-FABP MAb, MAb-FITC	Buffer	-	-	916	[235]
	Combination tapered fiber-optic biosensor (CTFOB) dip-probe APTS, sulfo-SMCC	IL-6 MAb_1, MAb_2-Alexa Fluor 488	Buffer	0.12	-	489	[236]

As it can be concluded from the above table, SPR sensors are predominant among the others. They have several advantages in detection applications such as label-free capabilities, real time monitoring of interactions and kinetic detection. Most of the SPR sensors developed used either direct detection of the target or sandwich formats to amplify the signal, except Kunz et al. that developed an inhibition immunoassay for H-FABP detection employing a silver surface in two different configurations and achieving the same LOD for both (200 ng mL^{-1}) [227], above the basal levels.

The specificity and sensitivity of the biosensors are significantly related to the way how antigens or antibodies were produced (although this information rarely is found) and the strategy used for the preparation of the biofunctionalized sensor surface as well as to the stability during the reaction with the analyte. This immobilization can be done by physical adsorption or through a covalent linkage; moreover, it also can be done in a random way or with a certain orientation. Covalent attachment is preferred for sensor stability and regeneration aspects and the control over the orientation of the antibodies increase the availability of the binding sites which leads to higher activity.

Most SPR sensors here detailed employed a covalent immobilization, using a coating with carboxymethyl dextran (CM) that later reacted with the biomolecule through EDC/NHS chemistry [215, 221, 225] or SAMs of activated mercaptohexadecanoic acid (MHA) [216], of cysteamine (CYS) that later reacted with glutaraldehyde (GLUT) in order to couple the bioreceptor [222] or using dithio-bis-succinimidylpropionate (DSP) [227]. Mixed SAMs composed by activated MHA and oligo(ethylene glycol) (OEG) alkanethiolate [223] or activated MHA and thiolated poly(ethylene)glycol (PEG-SH) [226] were also employed as well as a polymer layer of poly(3-(2-((N-succinimidyl)succinyloxy)ethyl)thiophene (P3SET) [219]. Additionally, nearly covalent immobilizations were done through streptavidin and biotin labeled antibodies [217, 221] and with an E.coli outer membrane with autodisplayed Z-domain immobilized presenting IgG-binding activities [220].

An effective approach for immobilizing IgG with a correct orientation is to use binding proteins like protein A or protein G. Both of them have Fc-binding domains and can bind specifically Fc portion of the IgG. Thus, antibodies can be successfully immobilized in a well orientation manner and the sensitivity of the

assay can also improve as a result. An example of this methodology was followed by Hu et al. [216] for CRP SPR biosensing. Another way to achieve an oriented antibody layer is by covalently attach Fab' fragments directly onto the gold supports as it was done by Vikholm-Lundin et al. [218].

Although most of the SPR sensors in Table 7.3 fulfilled the LOD required to detect the basal levels of the corresponding target analytes, some used gold nanoparticles [215], nano-grating surfaces (periodic structures) [226] or used and compared different SPR configurations [227] to try to do so.

In regard to the two other kinds of optical sensors, based on the evanescent wave and optical fiber, again the immobilization and protein orientation are key aspects. In these cases, gold surfaces are not used and often materials such as glass [229, 231, 234, 236] or plastic [228, 232, 233, 235] have been reported. The most employed assay format is the sandwich, although inhibition formats have in few cases been reported, particularly for Cys C and H-FABP [229, 231, 234]. The covalent immobilization is also preferred and the chemical strategies followed depended on the surface or on the polymer used for its functionalization.

Kapoor et al. developed a fiber-optic biosensor for the determination of IL-6 in which the capture antibody was reduced by β-mercaptoethylamine (MEA) in order to expose the sulfhydryl group and react with the maleimide-activated prove in a selective way. This strategy was compared to the one using protein A which was rejected due to the increase of the distance between the dye molecules and probe surface that made the fluorescence generation inefficient. Also in this same work both unwanted non-specific signals were avoided: the autofluorescence signal and the false-fluorescence signal. In the first, the characteristic fluorescence spectral profile was extracted by subtracting the background spectral profile from the total fluorescence signal, while for the second a solution containing egg albumin (1 mg mL^{-1}) in the detection antibody step was employed to successfully reduce the false signal due to non-specific binding of labelled detection antibodies or residual dye molecules. This article is then another example together with those described in [216, 218] for protein orientation when the attachment of the antibodies wants to be controlled and the associated problem of mixed avidity avoided.

Thus, at the light of this literature search we can conclude that research addressed to develop optical immunosensors for cardiovascular biomarkers has been intense during the last decade. Mainly, the immunosensors reported are focused on individual detection of cardiovascular biomarkers including CRP, Cys C, H-FABP, IL-6, MMP-2, MPO, TNF-α, cTnI, cTnT, BNP and NT-proBNP. Between them, CRP is the most frequently addressed target probably due to the easily achievable LOD and the lower cost of analyte and immunoreagents. In spite of employing different methods, surfaces, assay formats, matrixes and protein immobilization or orientation strategies, most of them achieved the required limit of detection for each target analyte except for H-FABP. Finally, assay time can be compared meaning in this case the time from the very beginning, the surface derivatization, to the final signal acquisition. While the analyte (direct assay) or analyte and detection antibody (sandwich and inhibition assay) step/s takes normally few minutes like in ELISAs or even less, the longer and more laborious step is the surface functionalization (chemical derivatization and protein immobilization). This last procedure is normally shorter for SPR sensors since the Au-thiol binding is nearly covalent, selective and easy to achieve compared to other chemical procedures required in other optical sensors.

In summary, in the clinical diagnostic field for cardiovascular diseases, there is a great need for suitable instruments able to provide efficient results both at patient bedside and at the clinical laboratory. Optical biochips can represent an important option for the development of POCT instrumentation with the additional ability to carry on a multiplexed analysis for the optimal prognosis or diagnosis of the disease. A review of the literature has made evident the extraordinary effort made in this respect, but still there are almost no examples of the development of multiplexed biosensors devices. In this sense, a multiplexed optical biochip could be contemplated as an array of biosensors that could be individually monitored. These devices could be able to perform analysis in a more efficient way than the actual laboratory equipment.

7.1.5 GENERAL OBJECTIVE

The final goal of the research made in this chapter was the implementation of the multiplexed fluorescent microarray on a multiplexed optical biochip based on the evanescent wave and the fluorescence anisotropy principle to obtain a

POCT device for CVD. This was an ambitious long term objective, but as proof-of-concept we decided to evaluate performance of this sensor device with at least two of the biomarker targets selected.The realization of this investigation has been possible thanks to the collaboration established with the Chemical and biochemical optical sensor group (IFAC, CNR) at the pre-doctoral stage of three months in their laboratory. The specific objectives addressed were:

1. Realization of a feasibility study with the CRP because it is one of the targets with less requirements regarding detectability and
2. Implementation of the NT-proBNP immunoassay in the optical sensor.

7.2 SENSOR DESCRIPTION

7.2.1 PHYSICAL PRINCIPLE

The optical sensor used in this chapter was developed by the group of the CNR in the framework of an European project called “Health care by biosensor measurements and networking” (CARE-MAN) as an optical diagnostic device for POC.

The sensor here used is an evanescent wave optical sensor (see section 1.4.1.3). The working principle of the optoelectronic platform is based on the fluorescence anisotropy. The fluorescence emitted by a fluorophore located at a distance from a dielectric interface smaller than or comparable with the emitted wavelength is anisotropic, mainly directed towards the denser medium (with higher refractive index) and with well-defined preferential directions [237]. As it can be observed in Figure 7.1, the light that is radiated into the substrate is called supercritical angle fluorescence (SAF) and it propagates at angles above the critical angle corresponding to the environment (e)-substrate (s) interface; $\theta_c^{es}=\arcsin(n_e/n_s)$. Therefore, a great proportion of the fluorescence emitted by the sensing layer, in this case located at the interface between the rarer liquid medium and the denser plastic medium, remains entrapped inside the chip. The particular comb-shape of the top of the chip implies that the fluorescence is guided along plastic waveguides which run side by side to the microchannel.

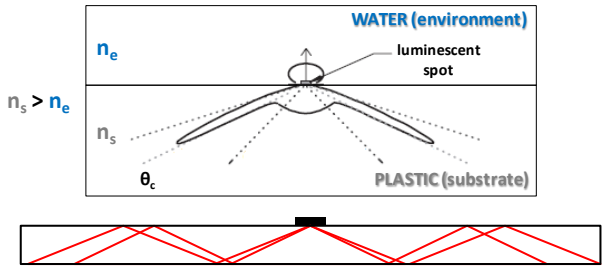

Figure 7.1. Schematic representation of the fluorescence anisotropy optical principle. Electric dipoles exhibit anisotropic emission when the distance from a dielectric interface is small or comparable with the emitted wavelength. n: refractive index, e: environment, s: substrate.

In addition, the platform here employed provides an enhancement of the detected luminescence from the emitting species near the dielectric surface. In conventional techniques, the detector is found above or below the substrate and then the majority of the final signal is waveguided away as substrate-confined (SC) modes and undetected. On the contrary, an array of frustrated cones produced by injection molding is used here. In this way, SC modes radiated undergo total internal reflection at the side-walls of the cone and the redirected SC modes interacts to the bottom interface of the substrate at angles close to 0º, thus transmitting a large fraction of the power to the detector [238]. This can be significant for the application of this kind of chip in high sensitivity assays summed to the possibility that they can be produced using conventional polymer microfabrication techniques.

7.2.2 CHARACTERISTICS OF THE OPTICAL IMMUNOSENSOR

The core of the device is an optical chip based on a polymethylmetacrylate (PMMA) flow-cell with microchannels through which the samples flow. The chip produced by injection molding has 13 channels and the dimension of a single microchannel is 50-100 µm high, 600 µm width and 9.4 mm long. In each channel, 0.01 mM Eudragit L100 in 95% ethanol was deposited until the evaporation of the solvent. Eudragit L100 is an anionic copolymer based on methacrylic acid and methyl methacrylate, thus providing carboxylic groups to be activated and reacted with amino groups from the biomolecules: antibodies, antigens or antigen derivatives. The sensing layer, where the immunochemical

reaction takes place, is located on the upper part of each microchannel (Figure 7.2).

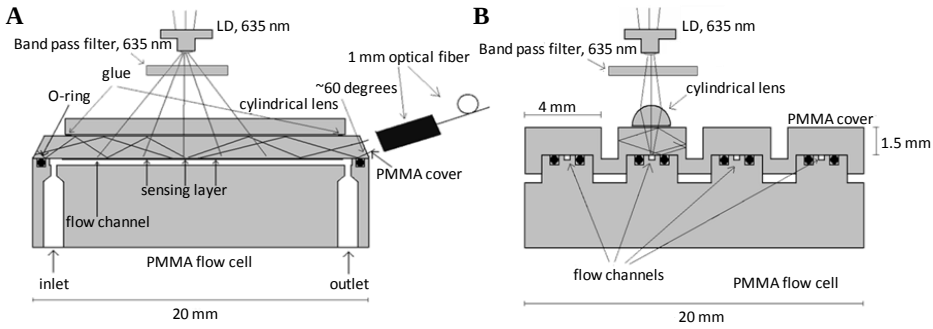

Figure 7.2. A) Longitudinal and B) transversal cross-section of a channel in the PMMA chip.

A line-shaped beam from a 635 nm laser diode (LD) excites perpendicularly the sensing layer, previously filtered by a band pass (BP) filter centered at 635 nm in order to cut the tail of the laser radiation above 650 nm. A plastic cylindrical piano-convex lens located on the cover of the chip leads to an improvement of the excitation efficiency. Thanks to the fluorescence anisotropy, the emitted fluorescence is coupled to the plastic waveguide, collected by a single plastic optical fiber and sent to an amplified photodiode, after a filtering action with the 650 nm high pass (HP) filter that cut all the light coming from the source and scattered by the PMMA chip. Moreover, the end-face of the cover is polished at 50º to facilitate the alignment with the collecting fiber and the particular comb profile of the cover allows a physical separation of the fluorescent signal coming from the different channels, thus each channel is optically separated from the others. Finally, the light is analyzed by the Hamamatsu spectrometer and the spectrum obtained is the average of ten spectra acquired with an interrogation time of 10 s.

Apart from the optical setup and the PMMA-based chip, the sensor system is provided by a peristaltic pump with eight valves and poly(vinyl chloride) (PCV) tubing used for the fluidic system. Although the chip has 13 channels, they had to be used in twice since there are only 8 valves connected to the pump and thus, 8 tubes available. One of these tubes was normally used to collect the solutions once they have already passed through the chip and throw them to the waste, which means that the other 7 valves connected to the chip could be used in each experiment (Figure 7.3).

The samples addressed to the different microchannels are taken one by one instead of all at the same time. Signal acquisition is obtained thanks to a motorized translation stage that allows the automatic scanning of the 13 different channels.

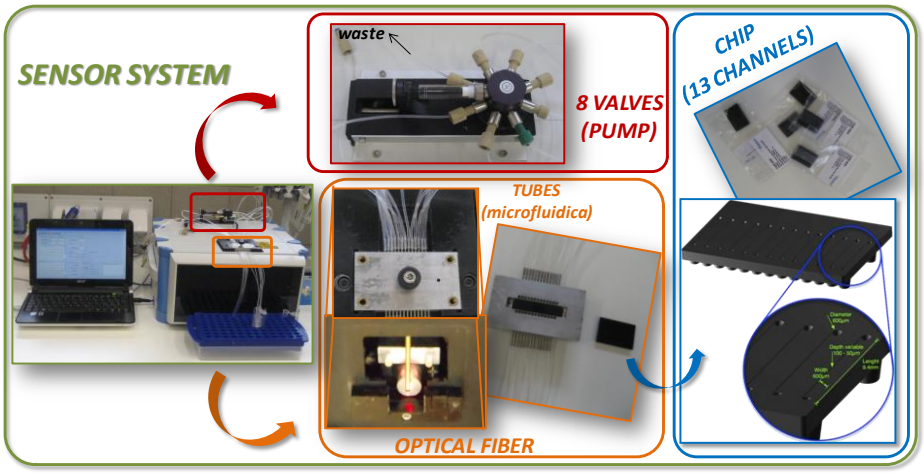

Figure 7.3. Pictures of the different components of the optical sensor system: pump valves, tubing, optical fiber, chips, etc.

A crucial aspect to avoid for optimal fluorescent detection is the autofluorescence. Optical quality plastic materials with low autofluorescence are needed. In Piruska's work [239], the most significant results affirmed that considerable bleaching of the autofluorescence from different plastic chips was achieved under continuous laser illumination. Moreover, it demonstrated that an increase in wavelength meant a decrease in autofluorescence and that plastic chips presented slightly higher autofluorescence than the corresponding materials from which they were made. Thus, although it exist autofluorescence from PMMA which provides and intrinsic background in the detected signals, it is known that PMMA if produced by injection molding has low autofluorescence when excited in the red region.

Apart from the fluorescence coming from the chip, the contribution of the fluorescence coming from the bottom surface of the microchannel can as well interfere and it is important to consider. In spite of all this, autofluorescence is eliminated from the final signal recorded because the background is substracted which eliminates this effect (see section 7.3.2).

7.3 PROPOSED IMMUNOCHEMICAL STRATEGIES

Figure 7.4 shows the immunochemical strategies employed for the optical immunosensor to be developed in this chapter. For CRP determination, strategies A and B were proposed to be compared on a first instance. In both cases are sandwich formats, but while strategy A is the equivalent to that employed in the microarray, strategy B uses detection antibodies directly labelled with the fluorophore. As described before, strategy A involved a four-steps and used two polyclonal antibodies (AbCRP2, AbCRP1) produced in goat. The only difference with the format used in the microarray was the use of neutravidin-Atto 647N instead of streptavidin-TRITC. Also the experimental protocol (immobilization, incubation times, etc.) was different compared to that established for the microarray because the technology also changed, maintaining each step for the addition of each reagent. The strategy B had been previously investigated by Ambra Giannetti from the CNR group in which this work was made. It employed mouse monoclonal antibodies, particularly Clone 5 (C5) as capture antibody and Clone 6 (C6) labelled with DY647 (C6-DY647) as detection antibody. Being monoclonals, this format allowed reducing the number of steps by mixing the detection antibody with the sample prior the injection in the biosensor. Finally, for NT-proBNP determination, the immunochemical format was the strategy C, using anti-IgG-Atto 647N.

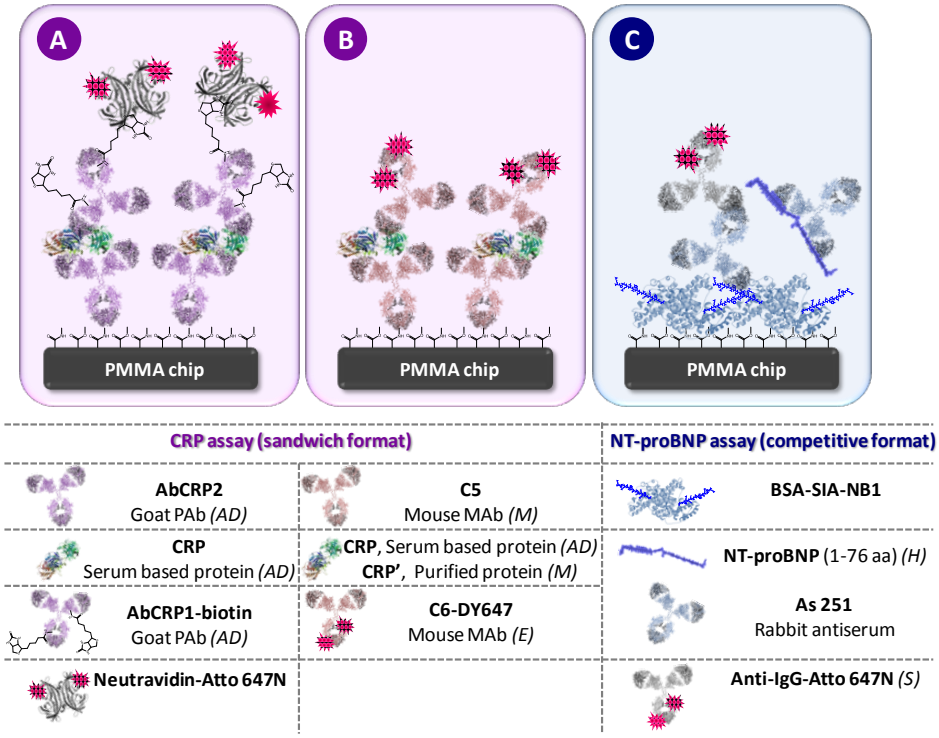

Figure 7.4. Schematic representation of the different strategies used, A, B) for CRP and C) for NT-proBNP detection. Brief description of the immunoreagents used in each strategy and their commercial source. AD: Audit Diagnostics, M: Meridian Life Science, E: Exbio, H: Hytest, S: Sigma-Aldrich.

Both, Atto 647N and DY647 are organic fluorophores that absorb (653 nm and 644 nm, respectively) and emit (672nm and 699 nm, respectively) at the appropriate wavelengths for the light source and detector used. The fact that do absorb and emit high wavelengths (red spectral region) diminished the potential interferences from the sample matrix. Moreover, are characterized by having a strong absorption, high fluorescence quantum yield, high thermal and photostability and, exceptionally, high stability in various media including to the presence of ozone. Both fluorophores can be found commercially available with a wide variety of chemistries for covalent coupling to biomolecules. This better behavior compared to other fluorophores from the same spectrum range may have a high impact on the assay sensitivity bioanalytical assays.

7.4 IMPLEMENTATION OF THE IMMUNOCHEMICAL ASSAYS ON THE OPTICAL SENSOR

7.4.1 BIOFUNCTIONALIZATION OF THE SENSOR SURFACE

This is a crucial step which must provide a stable, homogeneous and bioactive surface and avoid the undesired non-specific adsorptions. Such a step can significantly influence on the selectivity, sensitivity and detectability of the immunosensor. The capture antibody, for CRP, or the bioconjugate, for NT-proBNP, were covalently bound to the poly(methyl methacrylate) (PMMA) chip covered with Eudragit L100 (see Figure 7.5). This immobilization was achieved through the formation of amide bonds after previous activation of the carboxylic acids with N-(3-dimethylaminopropyl)-N'-ethylcarbodiimide (EDC) and N-hydroxysuccinimide (NHS). Once the surface has been functionalized, the remaining reactive groups were blocked with 0.1 % BSA. Once functionalized the chips were washed with PBST and could be immediately used or stored at 4ºC until use.

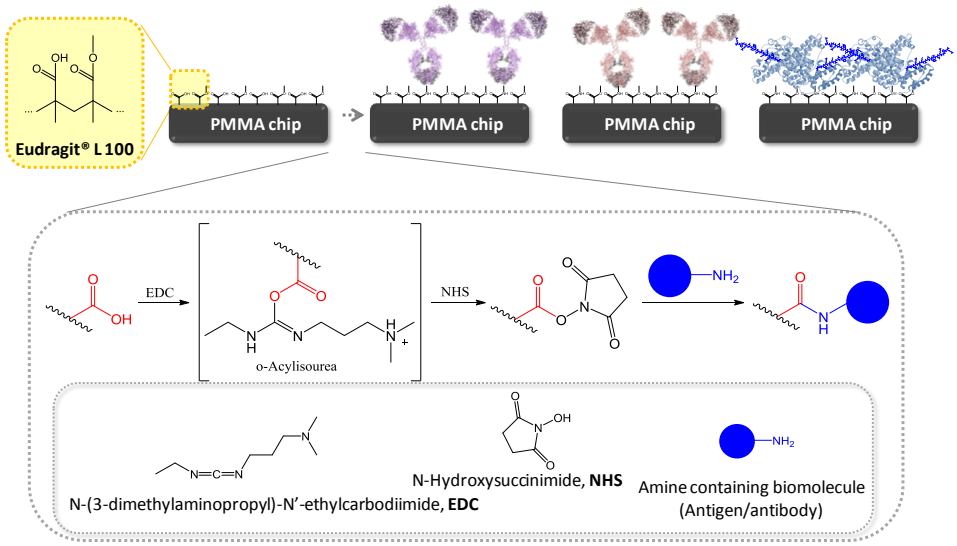

Figure 7.5. Reaction mechanism for the active ester method. EDC and NHS activate the carboxyl that is later reacted with an amino group from the biomolecule (antigen/antibody) forming an amide bond. This reaction takes place at room temperature and in an aqueous media.

7.4.1.1 Establishment of the immunosensor protocol for CRP

The immunosensor procedure for each of the three immunochemical strategies employed for CRP and NT-proBNP determination is shown in Table 7.4. The incubation of all immunoreagents and standards was performed in PBS during 15 min, except the immobilization of the capture antibody or bioconjugate that took 60 min.

The different solutions of the bioreagents were introduced at a constant flow of 50 µL min^{-1} with the aid of a peristaltic pump and the washing steps were performed at 200 µL min^{-1}. Upon binding of the labelled reagent an increase in the signal was observed. Measurements were performed with the channels full of solution, normally PBS or PBST, and with the flow stopped from the corresponding sensograms. As an example, Figure 7.6 (A) shows the sensogram for CRP, when injected a different concentrations on each channel, employing strategy A. The fluorescent signal used for calibration and quantitation was the result of subtracting the background signal recorded previously to the injection of the fluorescent reagent. The bar graph in Figure 7.6 (C) shows the result of such data treatment for the corresponding channels.

Table 7.4. Main conditions employed for CRP (strategy A) and NT-proBNP (strategy C) immunosensors. For strategy B, step 7 is the last step which is the washing after the addition of the sample with C6-DY647.

	Buffer/solution	Flow conditions
1. Activation of the chip surface	EDC/NHS in water	30 min, 50 µL min^{-1}
2. Immobilization (capbture Ab/bioconjugate)	PBS	60 min, 50 µL min^{-1}
3. Washing step	PBS	2.5 min, 200 µL min^{-1}
4. Blocking	0.1% BSA in PBS	15 min, 50 µL min^{-1}
5. Washing step	PBS	2.5 min, 200 µL min^{-1}
6. Samples or standards/Competition	PBS	15 min, 50 µL min^{-1}
7. Washing step	PBST	2.5 min, 200 µL min^{-1}
8. Detection antibody	PBS	15 min, 50 µL min^{-1}
9. Washing step	PBST	2.5 min, 200 µL min^{-1}
10. Neutravidin-Atto 647N	PBS	15 min, 50 µL min^{-1}
11. Final wash	PBST	2.5 min, 200 µL min^{-1}

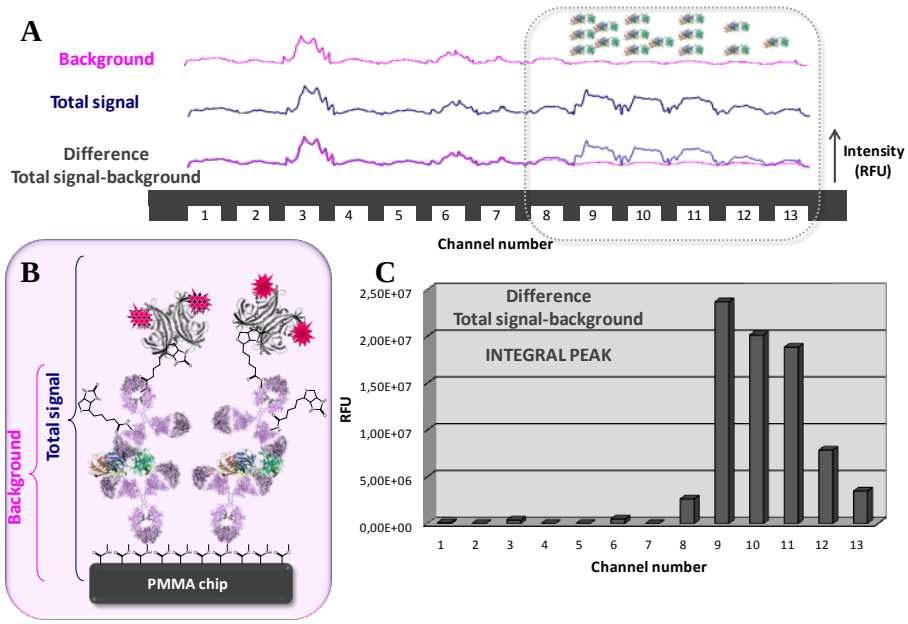

Figure 7.6. A) Sensogram recorded on all chip channels. The figure shows the background signal, the fluorescence recorded in the last step and the resulting signal after subtracting the background. CRP solutions at different concentrations were injected on channels 8 to 13, B) schematic representation of strategy A and the steps where signals were recorded, C) final data represented in a bars graph obtained with the integral peak difference between the final measure and the background.

On a first instance, optimum concentrations of the immunoreagents were established by testing in each sensor channel different concentrations of AbCRP2 (capture antibody; 10, 100 and 1000 µg mL^{-1}) and AbCRP1-biotin (detection antibody, 1 and 10 µg mL^{-1}) keeping constant the concentration of CRP (1 µg mL^{-1}) and neutravidin-Atto 647N (10 µg mL^{-1}). As it can be observed in Figure 7.7, the maximum signal was obtained when using the highest concentration of both, capture and detection antibodies (1000 µg mL^{-1} and 10 µg mL^{-1}, respectively). Using these conditions a calibration curve was run which achieved a LOD of 12.65 ng mL^{-1}, which is good enough to measure CRP over the basal levels (see Table 1.4 in section 1.7).

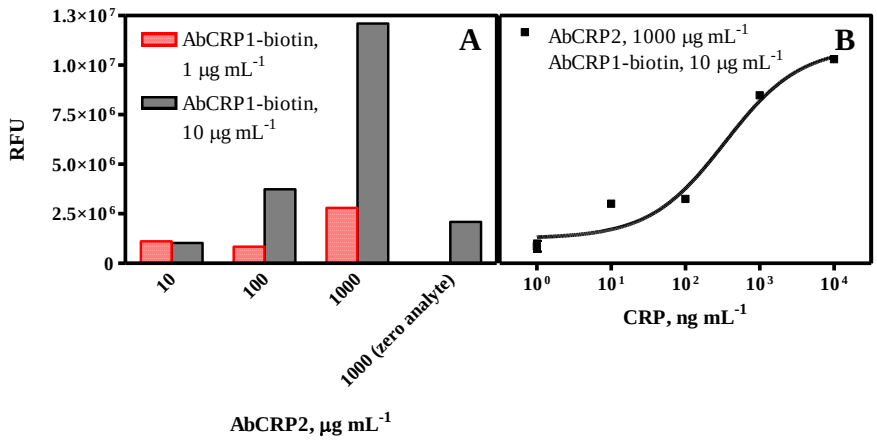

Figure 7.7. A) Study of different concentrations of capture and detection antibodies used in strategy A. Concentration of CRP and neutravidin-Atto 647N were kept constant at 1 µg mL^{-1} and 10 µg mL^{-1} respectively. B) Calibration curve for CRP using capture and detection antibody at 1000 µg mL^{-1} and 10 µg mL^{-1} respectively. The points in the curve correspond to a single run of each concentration.

Table 7.5. Assay features.

RFU_{max}	$1.09 \cdot 10^7$
RFU_{min}	$1.26 \cdot 10^6$
Slope	0.86
R^2	0.97
IC50, ng mL^{-1}	338.8
Working range, ng mL^{-1}	46.38-1147.19
LOD, ng mL^{-1}	12.65

The points in the curve correspond to a single run of each concentration.

Further experiments were addressed to refine conditions by testing different concentrations of AbCRP1-biotin and neutravidin-Atto 647N in different channels. The results of such experiments are shown in Figure 7.8. Surprisingly, at high concentrations of both, AbCRP1-biotin and neutravidin-Atto 647N, the signal diminished as when using the lower concentrations. The excess of both immunoreagents might have caused saturation, hindrance of biotin molecules and of the biotin-binding sites of the neutravidin and, consequently, a decrease in signal. These results were reproduced in subsequent following experiments; therefore, AbCRP1-biotin and neutravidin-Atto 647N at 100 µg mL^{-1} and 10 µg mL^{-1}, respectively, were selected for further experiments. These conditions demonstrated to provide assays with good reproducibility regarding the signals

recorded. On the contrary, in experiments performed using AbCRP1-biotin and neutravidin-Atto 647N at 10 µg mL^{-1} and 100 µg mL^{-1}, respectively (opposite situation), higher variability was observed as well as higher background signal. This was interpreted as potential unspecific adsorption at this high concentration of the labelled neutravidin to the surface of the chip. Therefore, the final concentrations selected for AbCRP2, AbCRP1-biotin and neutravidin-Atto 647N were 1000 µg mL^{-1}, 100 µg mL^{-1} and 10 µg mL^{-1} respectively.

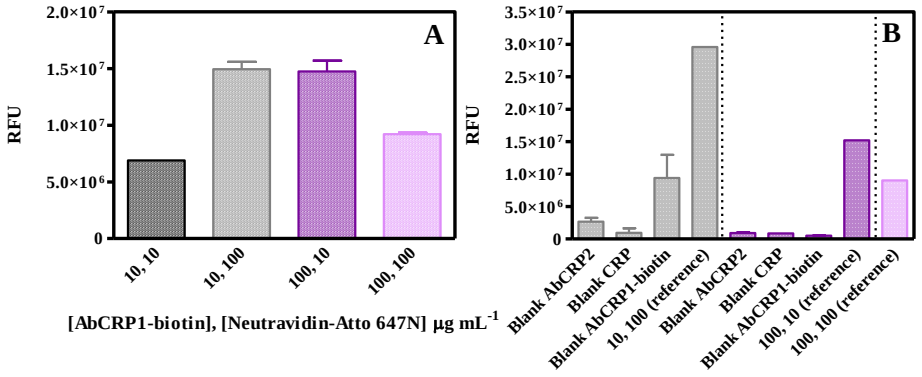

Figure 7.8. A) Study of different concentrations of detection antibody and neutravidin-Atto 647N used in strategy A. Concentration of CRP and AbCRP2 were kept constant at 1 µg mL^{-1} and 1000 µg mL^{-1} respectively. B) All blanks for the combinations studied in A) and the corresponding references. The reference values in B) correspond to the values obtained in A).

With these conditions a calibration curve was run in buffer. Figure 7.9 shows the graph and Table 7.6(strategy A) the parameters resulting from the fitting with a four-parameter equation. The detectability achieved was on the same order as before, but now the data is more representative since it corresponds to the average of assays performed in different days. With a low LOD 16.56 ± 15.26 ng mL^{-1}, the immunosensor in buffer could detect concentrations much below the basal levels of CRP which, as it has been mentioned, in healthy patients is less than 1000 ng mL^{-1}. The high variability observed at the LOD does not affect the robustness of the assay, considering that the results shown correspond to several days. Nevertheless, at this level, the need to calibrate the instrument each day seemed clear.

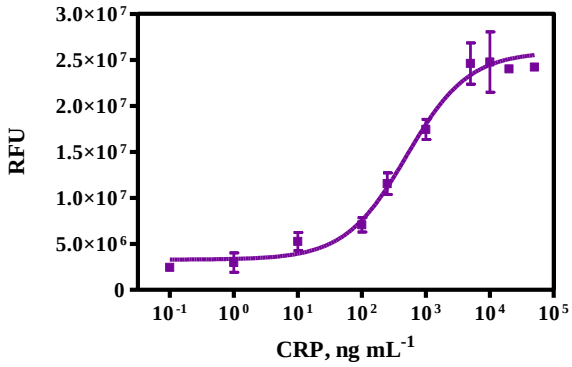

Figure 7.9. Calibration curve for the evaluation of CRP in buffer using strategy A. Each concentration was tested in three days using different channels on the chip for each concentration and each day.

For comparison purposes, strategy B was also run, investigating the effect of the preincubation between the analyte and the detection antibody (C6-DY647). The results are shown in Table 7.6. In these experiments, CRP standards from two different providers were used (AD, Audit Diagnostics and M, Meridian Life Sciences), but the commercial source did not affect the assay.

Table 7.6. Assay features for the evaluation of CRP in buffer using strategy A and B. In strategy B, the 15 min preincubation of CRP and C6-DY647 prior to the analysis was evaluated. When preincubation was not involved, CRP and C6-DY647 were separately flowed into the sensor with a PBST wash between the two steps.

	Strategy A	**Strategy B**			
	CRP (AD)	With preincubation		Without preincubation	
		CRP (AD)	CRP' (M)	CRP (AD)	CRP' (M)
RFU_{max}	$2.68 \cdot 10^7 \pm 5.14 \cdot 10^6$	$1.41 \cdot 10^7$	$1.15 \cdot 10^7$	$9.30 \cdot 10^7$	$8.15 \cdot 10^7$
RFU_{min}	$3.07 \cdot 10^6 \pm 8.99 \cdot 10^6$	$8.80 \cdot 10^4$	$2.85 \cdot 10^4$	$-2.22 \cdot 10^6$	$7.31 \cdot 10^4$
Slope	0.87±0.18	6.68	1.46	0.84	1.06
R^2	0.93±0.10	0.74	1.00	0.97	0.99
IC50, ng mL^{-1}	380.93±179.30	132.00	367.80	1346	2360
Working range, ng mL^{-1}	55.40±18.96-1571.83±387.34	114.43--	143.72-929.96	273.18-4806.04	614.58-7287.05
LOD, ng mL^{-1}	16.56±15.26	100.44	83.95	122.64	291.91
t_{assay} (min)	162.5	127.5		145	

While better sensitivity was obtained when preincubating CRP with C6-DY647, the signal-to-noise ratio was more favourable without preincubation. Although the assay time (t_{assay}) was shorter using strategy B (127.5-145 min *vs*. 162.5 min), the LOD was considerably much better using strategy A. Unfortunately, the maximum/minimum signal ratio was much worse than in strategy B. Maximum RFU values were in the same order of magnitude in all cases, but background noise was higher in strategy A maybe due to unspecific adsorptions from the biotinylated antibody or the neutravidin. Previous experiences in our group have shown that the biotinylated ratio of the antibody has often a great affect on the assay. Over a certain value of biotin residues attached, non-specific interactions are quite strong. On the other hand, it is known that neutravidin yields the lowest non-specific binding in respect to avidin and streptavidin.

The differences in sensitivity can be attributed to the different flurophores used or to the immunochemical format. However, it is very much likely that the most important factors are the antibody source, which is different in both cases, and the amplification provided by the biotin and neutravidin binding.

7.4.1.2 Establishment of the immunosensor protocol for NT-proBNP

Firstly, different concentrations of the competitor NB1-CH_2CO-BSA (from 250 to 1000 µg mL^{-1}) and dilutions of the antiserum (As 251 at 1/10, 1/100 and 1/500) were assayed employing anti-IgG-Atto 647N to generate the signal at 10 and 100 µg mL^{-1} in the absence of analyte. NB1-CH_2CO-BSA was used to biofunctionalized the chip and each of the concentrations were tested on different channels. The results obtained are shown in Figure 7.10 (A) and from these data a concentration of 250 µg mL^{-1} was selected for the NB1-CH_2CO-BSA bioconjugate.

With this concentration fixed, a similar experiment was performed again assessing the response of two dilutions of As 251 (1/10 and 1/100) together with two concentrations of anti-IgG-Atto 647N (10 and 100 µg mL^{-1}), but in this case three different concentrations of NT-proBNP (10000, 100 and 0 ng mL^{-1}) were assayed with the aim to find out the most optimum conditions for the competitive binding of the NT-proBNP biomarker. From these experiments, a dilution factor of 1/10 was chosen for the As 251 and a concentration of 100 µg

mL^{-1} was selected for the anti-IgG-Atto 647N. Thus, as it can be observed in Figure 7.10 (B), a clear dose-dependent decrease of the signal was observed when increasing the concentration of the biomarker.

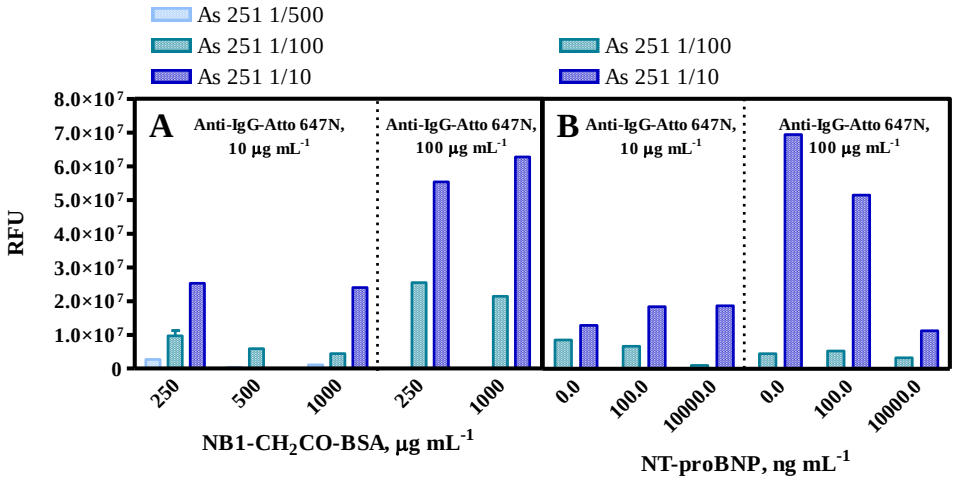

Figure 7.10. A) Study of different concentrations of the competitor, anti-IgG-Atto 647N and dilutions of antiserum used in strategy C. The values obtained corresponds to the zero of the curve, B) Study of different dilutions of antiserum and concentrations of anti-IgG-Atto 647N used in strategy C for different concentrations of NT-proBNP.

Due to the low signal-to-noise ratio observed in these experiments (RFU_{max} $6.94 \cdot 10^7$, RFU_{min} $1.13 \cdot 10^7$) compared to those observed in CRP immunosensors, the effect of different blocking agents were investigated and used them on an additional "blocking step" or as additives in the assay buffer, in the presence (10000 ng mL^{-1}) and absence (0 ng mL^{-1}) of NT-proBNP. As it can be observed in Figure 7.11 the addition of 0.15% casein or 2% Tween 80 in the blocking step caused a considerable decrease in the maximum signal. The use of 0.1% BSA at the blocking step provides a signal-to-noise ratio of 6.1, much better than with the other agents. When this blocking step is combined with the use of additives in the assay buffer, it can be observed that a 2% Tween 20 increases the maximum signal but also the background noise, and the use of 0.15% casein decreases only the maximum signal and not the noise. Similarly for 0.05% BSA, although the reduction in the signal is not so high. Thus, for further studies we continued using just a blocking step with 0.1% BSA.

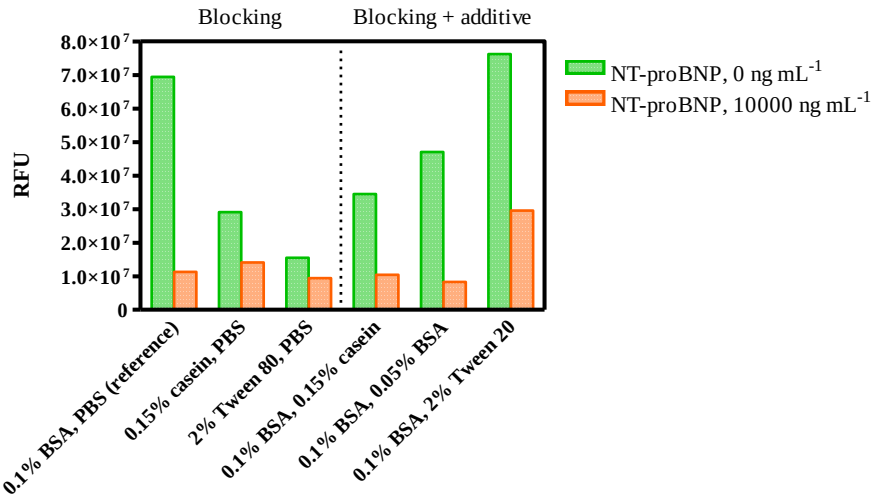

Figure 7.11. Different blocking agents and additives in the assay buffer (competitive step) in order to increase the signal-to-noise ratio.

Using the conditions established, a calibration curve of NT-proBNP was run in buffer (see Figure 7.12). A LOD of 93 ± 5 ng mL^{-1} was reached with a maximum signal/background noise ratio of 4.6. This detectability is very far away from the required values considering the basal levels of this peptide in healthy patients are below 0.4 ng mL^{-1}.

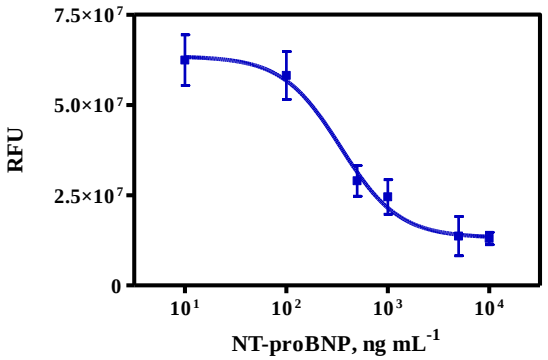

Figure 7.12. Calibration curve and assay features for the evaluation of NT-proBNP in buffer using strategy C. Each concentration was tested in two days using different channels on the chip for each concentration and each day.

Table 7.7. Assay features for the NT-proBNP assay in buffer.

RFU_{max}	$6 \cdot 10^7 \pm 1 \cdot 10^7$
RFU_{min}	$1.3 \cdot 10^7 \pm 3 \cdot 10^6$
Slope	-1.5±0.2
R^2	0.97±0.03
IC50, ng mL^{-1}	350±19
Working range, ng mL^{-1}	149±3-927±95
LOD, ng mL^{-1}	93±5

Each concentration was tested in two days using different channels on the chip for each concentration and each day.

In comparison with the ELISA and the individual and multiplexed microarray assay for NT-proBNP, results reached with this optical sensor were considerably worse regarding sensitivity and variability. However, such results could be improved optimizing different parameters of the assay. Between the potential parameters to be investigated are the syntheses of new bioconjugate competitors with different degrees of heterology or also trying to play with that hapten density of the bioconjugate. However, these features were already deeply investigated during the development of the microplate ELISA (see chapter 4). By doing this we could establish an immunoassay with a detectability close to the basal level, but these conditions have not been reproduced when implemented on the optical sensor described in this chapter. A more drastic decision would be trying to produce new antibodies with a different hapten design or using the monoclonal antibody technology to select a high affinity antibody producing clone. Another possibility would be to move towards a sandwich format, but for this purpose there would be necessary to perform a monoclonal antibody screening addressed to select antibodies against different epitopes of the molecule. On the other hand, additional efforts could be invested trying to improve the actual amplification capabilities of the sensor transducer; however this is far of our expertise and the chances to evaluate this possibility correspond to the Chemical and Biochemical Optical sensor group (IFAC, CNR).

8 MATERIALS AND METHODS

8.1 PREPARATION OF IMMUNOREAGENTS

8.1.1 PREPARATION OF IMMUNOGENS AND COMPETITORS

Chemicals

All peptides used for the preparation of immunoreagents were synthesized by Unitat de Química Combinatòria (UQC, PCB), native TnC was purchased from Life Diagnostics (West Chester, PA, USA) and two monoclonal antibodies (24C5 and 50E1) for BNP were provided by Hytest (Turku, Finland). Horseshoe crab hemocyanin (HCH), bovine serum albumin (BSA) horseradish peroxidase (HRP), ovalbumin (OVA), N-(3-dimethylaminopropyl)-N'-ethylcarbodiimide hydrochloride (EDC·HCl), N-Hydroxysuccinimide (NHS), 4-pentinoic acid, 1,3-dicyclohexylcarbodiimide (DCC), dimethyl pimelimidate dihydrochloride (DMP·2 HCl), benzidine hydrochloride (benzidine·HCl), cysteine (Cys) and 3-(4-hydroxy-3,5-dimethoxyphenyl)prop-2-enoic acid (sinapinic acid) were from Sigma-Aldrich Co. (St. Louis, Missouri). The Bradford solution, ammounium persulfate (APS) and Nupage LDS were purchased from Bio-Rad Laboratories GmbH (Hercules, CA, USA). Sulfosuccinimidyl 4-(N-maleimidomethyl)cyclohexane-1-carboxylate (sulfo-SMCC) was obtained from Pierce (Rockford, Illinois), N,N-dimethylformamide (DMF) form Sharlau (Barcelona, Spain) and acetonitrile (ACN) from Fisher Chemical (Leicestershire, UK). 2-amino-2-hydroxymethyl-propane-1,3-diol (Tris) was from Roche (Basel, Switzerland), glycine and tetramethylethylenediamine (TEMED) from GE Healthcare (Little Chalfont, UK) and acrylamide:bis-acryladmide (37.5:1) 40% solution (A-B mix) and sodium dodecyl sulphate (SDS) from Amresco (Solon, UH, USA). Formic acid and all salts were obtained from Merck (Darmstadt, Germany). N-Succinimidyl 3-maleimidopropionate (SMP) and N-succinimidyl iodoacetate (SIA) were already synthesized and available in the laboratory.

Buffers and solutions

Unless otherwise indicated, phosphate buffered saline (PBS) is 0.01 M phosphate buffer in a 0.8% saline solution (137 mM NaCl, 2.7 mM KCl), pH 7.5.

PBST is PBS with 0.05% Tween 20. Borate buffer is 0.25 M boric acid/sodium borate, pH 8.7. MES buffer is 0.1 M MES, pH 5.1. Coating buffer is 0.05 M carbonate-bicarbonate, pH 9.6. Citrate buffer is a 0.04 M solution of sodium citrate, pH 5.5. The substrate solution contains 0.01% 3,3',5,5'-tetramethylbenzidine (TMB) and 0.004% H_2O_2 in citrate buffer. For non-reducing SDS-PAGE electrophoresis, running buffer is 0.25 M Tris, 1.92 M glycine (pH 8.3-8.7) in a 1% SDS solution, upper buffer is 0.5 M Tris (pH 6.8) in 0.4% SDS solution, lower buffer is 1.5 M Tris (pH 8.8) in 0.4% SDS solution, the stain solution is 0.8% Coomassie Blue in methanol:acetic acid (4:1) and the destain solution is methanol:acetic acid:MilliQ water (30:10:60).

Instrumentation

The MALDI-TOF-MS (matrix assisted laser desorption ionization time-of-flight mass spectrometer) used to characterize the protein conjugates was a Bruker Autoflex Smartbeam-II (Bruker, Kalsruhe, Germany). The pH and the conductivity of all buffers and solutions were measured with a pH meter 540 GLP and a conductimeter LF 340, respectively (WTW, Weilheim, Germany). Polystyrene non-treated microtiter plates were purchased from Daslab (Barcelona, Spain). Absorbances were read on a SpectramaxPlus (Molecular Devices, Sunnyvale, CA, USA) and electrophoresis was realized with the equipment provided by Bio-Rad Laboratories GmbH (Hercules, CA, USA).

Procedures

For all calculations it was assumed that BSA has 30 accessible lysines whereas HRP has 2 accessible lysines. For HCH conjugates preparation, the same protocol, calculations and characterization done for BSA conjugates were used supposing a similar behavior.

- **NB1-CH_2CO-BSA, NB1-CH_2CO-HCH, TI1-CH_2CO-BSA, TI1-CH_2CO-HCH, TI2-CH_2CO-BSA, TI2-CH_2CO-HCH, TC1-CH_2CO-BSA, TC1-CH_2CO-HCH, TI3-CH_2CO-BSA, TI3-CH_2CO-HCH, TI4-CH_2CO-BSA, TI4-CH_2CO-HCH, TC2-CH_2CO-BSA, TC2-CH_2CO-HCH** (molar ratio peptide:SIA:Lys = 2:2:1)

A solution of SIA (3.9 mg) in anhydrous DMF (500 µL) was added dropwise to a protein solution (HCH or BSA, 15 mg each) in borate buffer (4.5 mL). The mixture was kept under stirring 4 h at RT. The activated protein was purified by size-exclusion chromatography using a HiTrap desalting Sephadex G-25 Superfine column (Amersham Biosciences) and borate buffer as eluent. The eluted fractions (0.5 mL) were collected in eppendorfs tubes and those tested positive in the qualitative Bradford protein test were combined (2 mL from 1 initial mL). A part of this solution (5 µL) was reserved for MALDI-TOF-MS analysis.

Peptides (2.8 µmol) dissolved in H_2O/ACN 50:50 (150 µL) were added dropwise to the purified activated protein solutions (3 mg, 2 mL). The mixture was kept under stirring overnight at 4°C to obtain the corresponding conjugates. Capping of the remained unreacted iodine atoms was performed by adding a solution of Cys·HCl (35.7 mM, 350µL) and stirring the mixture for 2 h more at RT. Finally the conjugates were purified by dialysis against 0.5 mM PBS (4 x 5 L) and Milli-Q water (1 x 5 L), lyophilized and stored freeze-dried at -20°C.

- **BNP1-T(4)$(CH_2)_2$CO-BSA, BNP1-T(4)$(CH_2)_2$CO-HCH , BNP1-T(4)$(CH_2)_2$CO-OVA** (molar ratio BNP1:alkyl:Lys = 0.06:2.17:1)

The conjugation of BSA, HCH and OVA to the azide-containing BNP peptide took place in two steps. In the first one, proteins were modified in order to introduce an alkyne group using the active ester method. In the second step, the peptide was covalently coupled to the modified protein through a 1,3-cicloaddition or also so-called *Click* reaction.

4-Pentinoic acid (10 µmol), N-hydroxysuccinimide (NHS) (25 µmol) and 1,3-dicyclohexylcarbodiimide (DCC) (50 µmol) were left to react in 200 µL of anhydrous DMF at RT for 1 h, with constant agitation. The suspension was centrifuged for 10 min at 10000 rpm, and the supernatant (12 µL) was added to both protein solutions (10 mg, 1.988 mL of borate buffer). The mixture was left to react for 4 h at RT with agitation. The conjugates were purified by dialysis against 0.5 mM PBS (5 x 5 L).

Peptide (0.93 mg) dissolved in 50 mM phosphate buffer (PB, pH 7.5) (1.25 mL) was added to the purified modified protein solutions (10 mg, 2 mL), followed by

the addition of $CuSO_4$ (0.1 M, 32.5 µL) and L-ascorbic dissolved both dissolved in H_2O (0.2 M, 32.5 µL). The mixture was kept under stirring overnight at RT to obtain the corresponding conjugates. Finally the conjugates were purified by dialysis (2 mM EDTA, 20 mM PB and 2 mM β-mercaptoethanol, 1 x 5 L) in order to remove the Cu^+ in excess and another against 0.5 mM PBS (4 x 5 L). Both BSA and HCH solutions were aliquoted and stored freeze-dried at -20°C.

The alkyne density of the (4-pentinoic acid)-BSA conjugate was assessed by MALDI-TOF-MS by comparing the molecular weight of the bioconjugates with that intact protein. For the final conjugates, it was not possible its characterization through MALDI-TOF-MS. Thus, it was assessed on a non-competitive indirect ELISA by measuring the binding of serial dilutions of commercial BNP antibodies (MAb 24C5 and 50E1) to microtiter plates coated with BNP1-T(4)$(CH_2)_2$CO-BSA, BNP1-T(4)$(CH_2)_2$CO-OVA and BNP1-T(4)$(CH_2)_2$CO-HCH . Further on, a solution of anti-IgG-HRP 1/6000 diluted in PBST was added before the substrate solution. Signal appeared affirming the obtention of the desired conjugate. The assay procedure is better explained in detail in section 9.1.2.

- **NB1-CH_2CO-BSA** (molar ratio peptide:SIA:Lys = 0.2:2:1, 0.1:2:1)

A solution of SIA (1.3 mg) in anhydrous DMF (166.7 µL) was added dropwise to a protein solution (HCH or BSA, 5 mg each) in borate buffer (1.5 mL). The mixture was kept under stirring 4 h at RT. The activated protein was purified by size-exclusion chromatography using a HiTrap desalting Sephadex G-25 Superfine column (Amersham Biosciences) and borate buffer as eluent. The eluted fractions (0.5 mL) were collected in eppendorfs tubes and those tested positive in the Bradford protein test were combined (2 mL from 1 initial mL). A part of this solution (5 µL) was reserved for MALDI-TOF-MS analysis, and the rest was used for conjugation as it is described in next step.

Peptides (0.37, 0.19 µmol) dissolved in H_2O/ACN 50:50 (100 µL) were added dropwise to the purified activated protein solutions (2 mg, 1.33 mL). The mixture was kept under stirring overnight at 4°C to obtain the corresponding conjugates. Capping of the remained unreacted iodine atoms was performed by adding a solution of Cys·HCl (90.7 mM, 100 µL) and stirring the mixture for 2 h

more at RT. Finally the conjugates were purified by dialysis against 0.5 mM PBS (4 x 5 L) and Milli-Q water (1 x 5 L), lyophilized and stored freeze-dried at -20°C.

- **NB1-EDC-BSA** (molar ratio peptide:EDC:Lys = 0.20:46:1)

The peptide (0.33 mg) dissolved in milliQ water (200 µL) was added to a solution of BSA (2 mg) in PBS (500 µL, pH 6.5). The conjugation was done by adding dropwise a solution EDC·HCl (52.3 mM) dissolved in PBS (100 µL, pH 6.5) and kept under stirring 2 h at RT. Final conjugate was purified by dialysis against 0.5 mM PBS (4 x 5 L) and Milli-Q water (1 x 5 L), lyophilized and stored freeze-dried at -20°C.

- **NB1-DMP-BSA** (molar ratio peptide:DMP:Lys = 0.20:0.67:1)

A solution of DMP·2HCl (0.16 mg) dissolved in borate buffer (66 µL) in an ice bath was added to the peptide solution (0.33 mg) in milliQ water (100 µL) also in ice. The mixture was then added dropwise to a solution of BSA (2 mg) in borate buffer (500 µL) submerged in ice and kept under stirring 10 min and 60 min at RT. The reaction was stopped by adding Tris base (20 mM) in borate buffer (134 µL). Final conjugate was purified by dialysis against 0.5 mM PBS (4 x 5 L) and Milli-Q water (1 x 5 L), lyophilized and stored freeze-dried at -20°C.

- **NB1-SMP-BSA** (molar ratio peptide:SMP:Lys = 0.32:0.32:1)

SMP (0.97 mg) dissolved in anhydrous DMF (113.8 µL) was added to a solution of BSA (3 mg) in PBS (225 µL). The reaction mixture was kept under stirring for 2 h at RT. The activated protein was purified by size-exclusion chromatography using a HiTrap desalting Sephadex G-25 Superfine column (Amersham Biosciences) and PBS as eluent. The eluted fractions (0.5 mL) were collected in eppendorfs tubes and those tested positive in the Bradford protein test were combined (2 mL from 1 initial mL). A part of this solution (5 µL) was reserved for MALDI-TOF-MS analysis, and the rest was used for conjugation as it is described in next step.

Peptide (0.8 mg) dissolved in H_2O/ACN 50:50 (200 µL) was added dropwise to the purified activated protein solution (3 mg, 2 mL). The mixture was kept

under stirring 2h at RT to obtain the corresponding conjugate. Finally it was purified by dialysis against 0.5 mM PBS (4 x 5 L) and Milli-Q water (1 x 5 L), lyophilized and stored freeze-dried at -20°C.

- **NB1-SMCC-BSA, NB1-SMCC-HCH** (molar ratio peptide:SMCC:Lys = 0.32:0.32:1)

Sulfo-SMCC (0.19 mg) dissolved in milliQ water (27.6 µL) was added to a solution of BSA (3 mg) in PBS (225 µL). The reaction mixture was kept under stirring for 2 h at RT. The activated protein was purified by size-exclusion chromatography using a HiTrap desalting Sephadex G-25 Superfine column (Amersham Biosciences) and PBS as eluent. The eluted fractions (0.5 mL) were collected in eppendorfs tubes and those tested positive in the Bradford protein test were combined (2 mL from 1 initial mL). A part of this solution (5 µL) was reserved for MALDI-TOF-MS analysis, and the rest was used for conjugation as it is described in next step.

Peptide (0.8 mg) dissolved in H_2O/ACN 50:50 (200 µL) was added dropwise to the purified activated protein solution (3 mg, 2 mL). The mixture was kept under stirring 2h at RT to obtain the corresponding conjugate. Finally it was purified by dialysis against 0.5 mM PBS (4 x 5 L) and Milli-Q water (1 x 5 L), lyophilized and stored freeze-dried at -20°C.

This procedure was followed for the competitor preparation for NT-proBNP immunoassay but also for the second antibody production in parallel with HCH. In this last conjugation, double quantities of all reagents were used to also obtain a doubled amount of the final product.

- **NB1-BDB-BSA** (molar ratio $Tyr_{NT\text{-}proBNP}$:BDB:Tyr_{BSA} = 1.44:5:1)

Sodium nitrite (3.5 mg) was added to a solution of benzidine·HCl (5 mg) already dissolved in HCl 0.2 M (1 mL). Benzidine is a carcinogen compound and must be manipulated with extreme caution. The mixture was stirred during 1 h at 4°C and protected from the light in order to give the bis-diazotized benzidine (BSB) in a yellow colored solution. BSA (2.5 mg) dissolved in borate buffer (4 mL, pH 9) was mixed with the peptide (1 mg) also in borate buffer (1 mL, pH 9). BDB solution (50 µL) was added with the protein and peptide and the solution

turned to a more brownish color. The coupling reaction was left for 2 h at 4°C. The final product was purified by dialysis against 0.5 mM PBS (4 x 5 L) and Milli-Q water (1 x 5 L), lyophilized and stored freeze-dried at -20°C.

- **NB1-SMCC-HRP** (molar ratio peptide:SMCC:Lys = 4:4:1)

Sulfo-SMCC (0.26 mg) dissolved in PBS (200 µL) was added to a solution of HRP (3 mg) in PBS (800 µL). The reaction mixture was kept under stirring for 2 h at RT. The activated protein was purified by size-exclusion chromatography using a HiTrap desalting Sephadex G-25 Superfine column (Amersham Biosciences) and PBS as eluent. The eluted fractions (0.5 mL) were collected in eppendorfs tubes and those tested positive in the Bradford protein test were combined (2 mL from 1 initial mL). A part of this solution (5 µL) was reserved for MALDI-TOF-MS analysis, and the rest was used for conjugation as it is described in next step.

Peptide (1.07 mg) dissolved in Milli-Q water (200 µL) was added dropwise to the purified activated protein solution (3 mg, 2 mL). The mixture was kept under stirring 2h at RT to obtain the corresponding conjugate. Finally it was purified by dialysis against 0.5 mM PBS (4 x 5 L) and Milli-Q water (1 x 5 L), lyophilized and stored freeze-dried at -20°C.

- **BNP-EDC-BSA, BNP-EDC-OVA (molar ratio BNP:EDC:Lys_{BSA} = 0.3:4.6:1 and BNP:EDC:Lys_{OVA} = 0.2:3.1:1)**

Amino groups of BNP (0.57 µmol) reacted with BSA or OVA (5 mg) by the activation of carboxylic groups using EDC (10.4 µmol) in MES buffer 0.1M pH=5.1.

- **TnC-DMP-BSA** (molar ratio TnC:DMP:BSA = 1.6:47:1)

A solution of DMP·2HCl (0.17 mg) dissolved in borate buffer (17 µL) in an ice bath was added to the commercial peptide solution (0.41 mg, 260 µL) also in ice. The mixture was then added dropwise to a solution of BSA (0.91 mg) in borate buffer (72.9 µL) submerged in ice and kept under stirring 60 min and 4 h

at RT. Final conjugate was purified by dialysis against 0.5 mM PBS (4 x 5 L) and Milli-Q water (1 x 5 L), lyophilized and stored freeze-dried at -20°C.

For the final conjugate, it was not possible its characterization through MALDI-TOF-MS. Thus, it was assessed on a non-reducing SDS polyacrylamide gel electrophoresis (SDS-PAGE).

A-B mix (2.4 mL), lower buffer (2.5 mL), MilliQ water (4.35 mL), TEMED (10 µL) and 10% APS solution (100 µL) were mixed to obtain the separator gel and it was immediately added between the two crystals of the setting up avoiding bubbles. Isopropanol (200 µL) was added on the gel and left for 30 min for polymerization. Once isopropanol had been removed, A-B mix (0.3 mL), upper buffer (1 mL), MilliQ water (2.6 mL), TEMED (10 µL) and 10% APS solution (100 µL) were mixed to provide the concentrator gel and immediately added on the separator gel. A comb was located on the upper part to create the different channels. It was left for polymerization during 30 min.

Once the running buffer was added in the electrophoresis tray and the comb removed, samples (1 µg mL^{-1} in PBS) and Kalidoscope (MW reference) were mixed with Nupage LDS (3:1) and the mixtures (15 µL) were added dropwise in the different channels. The electrophoresis gel was runned at 120 V until bromophenol blue arrived at the end of the gel. The gel was dismounted and dyed with stain solution for 20 min. Several washings with destain solution were carried on until bands could be visualized.

MALDI-TOF-MS

Peptide densities of all bioconjugates were estimated by measuring the molecular weight of the native proteins to that of the conjugates by MALDI-TOF-MS. Thus, MALDI spectra were carried on by adding on the plate 2 µL of the prepared matrix (*trans*-3,5-dimethoxy-4-hydroxycinnamic acid or sinapinic acid, 10 mg/mL in ACN/H_2O 70:30, 0.1% HCOOH) until dryness, followed by 2 µL of the aliquot taken during the conjugation procedure or 2 µL of the reference protein (BSA or HRP, 5 mg mL^{-1} in ACN/H_2O 50:50, 0.1% HCOOH). Finally and after dryness, 2 µL more of the prepared matrix are added. The peptide density (δ peptide) was calculated according to the following equation: {MW (conjugate) – MW (protein)}/MW (peptide). Coupling efficiency evaluated by

MALDI-TOF-MS of the corresponding haptenized BSA and HRP immunoreagents is shown in Table 8.1.

Table 8.1. Linker and peptide densities of BSA or HRP conjugates. Peptide conjugation is calculated assuming that BSA has 30 accessible lysines whereas HRP has 2 accessible lysines.

Immunoreagent	δ linker	δ peptide	%conjugation
NB1-CH_2CO-BSA (1:2:2)	17	17	57
TI1-CH_2CO-BSA (1:2:2)	17	15	50
TI2-CH_2CO-BSA (1:2:2)	17	14	47
TI3-CH_2CO-BSA (1:2:2)	17	2	7
TC1-CH_2CO-BSA (1:2:2)	17	3	10
TI4-CH_2CO-BSA (1:2:2)	18	11	37
TC2-CH_2CO-BSA (1:2:2)	18	12	40
(4-pentinoic acid)-BSA	5	-	-
NB1-CH_2CO-BSA (1:2:0.2)	19	5	17
NB1-CH_2CO-BSA (1:2:0.1)	19	3	10
NB2-CH_2CO-BSA (1:2:0.1)	19	3	10
NB3-CH_2CO-BSA (1:2:0.1)	19	3	10
NB4-CH_2CO-BSA (1:2:0.1)	19	4	13
NB1-EDC-BSA	11	1	3
NB1-DMP-BSA	8	1	3
NB1-SMP-BSA (1:0.32:0.32)	10	3	10
NB1-SMCC-BSA (1:0.32:0.32)	9	3	10
NB1-BDB-BSA (1:5:1.44)	-	8	27
NB1-SMCC-HRP (1:4:4)	1	1	50
BNP-EDC-BSA	-	1	-
BNP-EDC-OVA	-	1	-

Some of the bioconjugates (TI1-CH_2CO-HCH, NB1-CH_2CO-HCH and NB1-CH_2CO-BSA and BNP1-T(4)$(CH_2)_2$CO-HCH) in the above table presented low solubilities being necessary the filtration to obtain working aliquots with a determined concentration. This concentration was then estimated by using the quantitative Bradford test.

- **Quantitative Bradford test**

Calibration curves were prepared with the proteins of the corresponding bioconjugates, starting at 50-100 μg mL^{-1} in 0.01 M PBS depending on the protein. These concentrations as well as the samples (bioconjugates) were added to the non-treated microplate (320 μL/well) in triplicates and 1/2 diluted until reaching a final volume of 160 μL/well. Next, 40 μL/well of Bradford solution was added and incubated for 5 min at RT. Absorbances were read at 595 nm.

- **Qualitative Bradford test**

8 μL from the eluted fractions were mixed with 2 μL of Bradford test on a plastic film. Those drops that turned from red to blue contained protein and the content of their corresponding eppendorfs were combined and used for the conjugation.

8.1.2 ANTIBODY PRODUCTION

Chemicals and immunoreagents

Immunoreagents used were prepared as explained previously, native cTnI and TnC were purchased from Life Diagnostics (West Chester, PA) and two monoclonal antibodies for BNP (24C5 and 50E1) were provided by Hytest (Turku, Finland). Complete and incomplete Freud's adjuvants, other chemicals were obtained from Sigma Chemical Co. (St. Louis, Missouri) and all salts were obtained from Merck (Darmstadt, Germany).

Buffers and solutions

PBS is 0.01 M phosphate buffer 0.8% saline solution. Coating buffer is 0.05 M carbonate-bicarbonate pH = 9.6. PBST is PBS with 0.05% Tween 20. Citrate buffer is a 0.04 M solution of sodium citrate pH = 5.5. The substrate solution contains 0.01% 3,3',5,5'-tetramethylbenzidine (TMB) and 0.004% H_2O_2 in citrate buffer.

Instrumentation

The pH and the conductivity of all buffers and solutions were measured with a pH meter 540 GLP and a conductimeter LF 340, respectively (WTW, Weilheim, Germany). Polystyrene microtiter plates were purchased from Nunc (Maxisorp, Roskilde, Denmark). Washing steps were performed on a SLY96 PW microplate washer (SLT Labinstruments GmbH, Salzburg, Austria). Absorbances were read on a SpectramaxPlus (Molecular Devices, Sunnyvale, CA, USA).

Procedures

- **Production of polyclonal antibodies**

All polyclonal antisera were obtained by immunizing female white New Zealand rabbits with the corresponding immunogen.

Each immunogen was used to immunize three rabbits weighting around 1–2 kg once in a month during five months (six inoculations in total) in order to get three different final antisera for one immunogen. The immunogens (100 µg mL^{-1}) were inoculated for the first time in each rabbit dissolved in PBS/complete Freud's adjuvant 50:50 (1 mL) in ten injections well distributed around the left and right part of the spine. The following immunizations were equally done but dissolved in PBS/incomplete Freud's adjuvant except for NB1-CH_2CO-HCH, TI3-CH_2CO-HCH that fifth inoculation and second inoculation for NB1-SMCC-HCH were realized with complete Freud's adjuvant in order to increase the antibody titer signal.

Antibody production for native cTnI and TnC was achieved by inoculating 80 µg mL^{-1} of the native protein instead of 100 µg mL^{-1} and using two rabbits for each protein instead of three.

For all cases, preimmune or first bleed was obtained before any inoculation while the second bleed was obtained ten days after the second inoculation. Next ones were extracted ten days after the corresponding inoculations until reaching the 6^{th} inoculation and the 6^{th} or final bleed.

The evolution of the antibody titer was assessed on a non-competitive indirect ELISA by measuring the binding of serial dilutions of each antiserum to microtiter plates coated with the corresponding antigen, competitor (i.e. peptide-BSA) or the native protein (1 μg mL^{-1}, 100 μL/well), overnight at 4°C or 4 h at RT. Next day, plates were washed four times with PBST (300 μL/well) and seven consecutive 1/2 antiserum dilutions and a blank starting at 1/1000 in PBST were added to the wells (100 μL/well) and incubated for 30 min at room temperature. The plates were washed as before, and a solution of anti-IgG-HRP (1/6000 in PBST) was added to the wells (100 μL/well) and washed again, and the substrate solution was added (100 μL/well). Color development was stopped after 30 min at room temperature with 4 N H_2SO_4 (50 μL/well), and absorbances were read at 450 nm.

After obtaining the 6^{th} bleed was when in all cases an acceptable antibody titer was observed and animals were exsanguinated. The blood was collected on vacutainer tubes provided with a serum separation gel. Antisera were obtained by centrifugation at 4°C, 4000 rpm during 10 min and store at -80°C in the presence of 0.02% NaN_3.

- **Production of monoclonal antibodies**

All monoclonal antisera were obtained by immunizing four Balb/c mice with the corresponding immunogen, peptide-HCH or peptide-BSA.

Immunizations were done within an interval of four weeks. The immunogens (100 μg) were inoculated in each mouse dissolved in PBS/complete Freud's adjuvant 50:50. The following immunizations were equally done but dissolved in PBS/incomplete Freud's adjuvant.

For all cases, preimmune or first bleed was obtained before any inoculation while the second bleed was obtained ten days after the third inoculation. Next ones were extracted ten days after the corresponding inoculations.

The evolution of the antibody titer was assessed on a non-competitive indirect ELISA by measuring the binding of serial dilutions of each antiserum to microtiter plates coated with the corresponding antigen; BSA, HCH or OVA conjugated with the peptide (1 μg mL^{-1}, 100 μL/well), overnight at 4°C or 4 h at RT. Next day, plates were washed four times with PBST (300 μL/well) and seven

consecutive 1/2 antiserum dilutions and a blank starting at 1/1000 in PBST were added to the wells (100 µL/well) and incubated for 30 min at room temperature. The plates were washed as before, and a solution of anti-IgG-HRP (1/6000 in PBST) was added to the wells (100 µL/well) and washed again, and the substrate solution was added (100 µL/well). Color development was stopped after 30 min at room temperature with 4 N H_2SO_4 (50 µL/well), and absorbances were read at 450 nm.

After obtaining the desired bleed, the blood was collected on microtubes and antisera were obtained by centrifugation at 4°C, 4000 rpm during 10 min and store at -80°C in the presence of 0.02% NaN_3.

- **Antibody purification by ammonium sulfate precipitation**

A saturated ammonium sulfate solution was prepared at least 24h before used. The sample serum to be purified was placed into a centrifuge tube, which was filled below half of the maximum volume. Thus, it was cooled to 4°C in an ice bath and while being slowly stirred, the saturated ammonium sulfate solution was added dropwise to produce around 35% final saturation.

Mixture was stirred 4h at 4°C and centrifuged at 10000 G for 10 minat 4°C. Later, the supernatant was discarded and the pellet was completely dispersed with PBS using half volume of the initial serum sample. Once the pellet was dissolved, the final solution was dialyzed against 0.5 mM PBS (4 x 5 L) and Milli-Q water (1 x 5 L), lyophilized and stored freeze-dried at -20°C.

8.1.3 ANTIBODY AND NEUTRAVIDIN LABELLING

Chemicals and immunoreagents

Polyclonal goat antibodies for CRP, Cys C and Lp(a) were provided by Audit Diagnostics (Cork, Ireland) and polyclonal sheep anti-H-FABP from Randox (Crumlin, United Kingdom). EZ-link sulfo-NHS-LC-LC-biotin was obtained from Pierce (Rockford, Illinois), Atto 647N NHS ester was purchased from Sigma-Aldrich Co. (St. Louis, Missouri) and neutravidin from Thermo Scientific (Rockford, Illinois). Ultrafree-MC centrifugal filters were obtained from Merck

Millipore (Billerica, Massachusetts) and all salts were provided by Merck (Darmstadt, Germany).

Buffers and solutions

PBS is 0.01 M phosphate buffer 0.8% saline solution, pH 7.5. Borate buffer is 0.25 M boric acid/sodium borate, pH 8.7 and coating buffer is 0.1 M carbonate-bicarbonate pH 9.

Instrumentation

The spectrophotometer was a Lambda 19 purchased from Perkin Elmer (Waltham, Massachusetts). The pH and the conductivity of all buffers and solutions were measured with a pH meter 540 GLP and a conductimeter LF 340, respectively (WTW, Weilheim, Germany).

Procedures

- **Antibody biotinylation**

A solution of EZ-link sulfo-NHS-LC-LC-biotin (0.34 mg) in Milli-Q water (200 µL) was added dropwise to an antibody solution (4 mg) in borate buffer (2 mL) already incubated in an ice bath at 4°C. The mixture was stirred in the ice bath for 30 min and then at RT for 4 h. Final conjugates were purified by dialysis against PBS 0.5 mM (4 x 5 L) and Milli-Q water (1 x 5 L), lyophilized and stored at -20°C. Working aliquots (1 mg mL^{-1}, PBS 10 mM) were kept at 4°C.

- **Neutravidin-Atto 647N**

Atto 647N NHS ester (1 mg) was dissolved in dry DMSO (500 µL) and 30 µL of this solution were immediately added to neutravidin (2 mg) previously dissolved in coating buffer (1 mL). The reaction was incubated at RT for 60 min under stirring. The labeled protein solution was divided in two Ultrafree-MC filters (500 µL each) and separated from unreacted dye by centrifugation at RT, 5000 rpm during 20 min. The conjugate in each filter was then washed with

coating buffer (400 µL) and centrifugated again. The purification procedure was repeated twice with coating buffer and three times with PBS with a total of seven centrifugations. Labeled protein from both filters was joined together obtaining a final conjugate dissolved in PBS (1 mL). Aliquots were stored frozen at -20°C except the working aliquot that was kept at 4°C and protected from light in both cases.

Fluorophore density of the bioconjugate was estimated by measuring the absorbance of the protein and the conjugate at 282 nm and at 647 nm which are the λ_{max} of the protein and the dye (Atto 647N) (see Figure 8.1). Thus, a spectrophotometer cuvette of 1 cm path length and the following formulas were used.

Protein concentration (M)={[Abs_{282}-(Abs_{647}·CF)]/ε}·dilution factor
Moles dye per mol protein={Abs_{647}labelled protein/[ε'·protein concentration (M)]}·dilution factor
Where,
ε=Neutravidin molar extinction coefficient (101640 M^{-1} cm^{-1})
ε'=Atto 647N molar extinction coefficient (150000 M^{-1} cm^{-1})
CF=Correction factor, adjust for the amount of absorbance at 282 nm caused by Atto 647N.

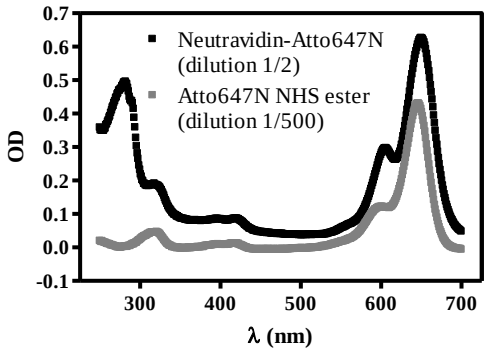

Figure 8.1. Absorbance spectra for the labeled protein and the dye. OD: optical density.

Table 8.2. [a]Dye conjugation yield is calculated with the difference between the final and initial moles dye per mol protein.

Immunoreagent	δ dye	%conjugation[a]
Neutravidin-Atto 647N	0.84	39.3

8.2 IMMUNOASSAY PROTOCOLS

8.2.1 SANDWICH IMMUNOASSAY: ELISA, MICROARRAY AND OPTICAL SENSOR

Chemicals and immunochemicals

Polyclonal goat antibodies for CRP, Cys C and Lp(a) and the corresponding standards were provided by Audit Diagnostics (Cork, Ireland). Polyclonal sheep and monoclonal sheep anti-H-FABP were obtained from Randox (Crumlin, United Kingdom). Polyclonal goat anti-cTnI, native cTnI and human cardiac H-FABP were provided by Life Diagnostics (West Chester, Pennsylvania). Human cardiac troponin I-T-C complex was obtained from Hytest (Turku, Finland) and all salts were provided by Merck (Darmstadt, Germany). Antisera 220 (As 220) was produced in-house by immunizing native cardiac troponin I. Monoclonal mouse antibody for CRP (clone 5, C5) and the purified CRP were purchased from Meridian Life Science (Memphis, Tennessee). Monoclonal mouse anti-CRP (clone 6, C6) labeled with DY647 was obtained from Exbio (Prague, Czech Republic). Neutravidin, N-(3-dimethylaminopropyl)-N'-ethylcarbodiimide hydrochloride (EDC·HCl), N-hydroxysuccinimide (NHS), streptavidin-TRITC were purchased from Thermo Scientific (Rockford, Illinois) and the poly(methyl methacrylate) (PMMA) chips from Chip Shop (Jena, Germany). Bovine serum albumin (BSA), Atto 647N NHS ester, anti-rabbit IgG-HRP, anti-rabbit IgG-TRITC, streptavidin-HRP and other chemicals were from Sigma Chemical Co. (St. Louis, Missouri).

Buffers and solutions

PBS is 0.01 M phosphate buffer 0.8% saline solution, pH 7.5. Coating buffer is 0.05 M carbonate-bicarbonate, pH 9.6. PBST is PBS with 0.05% Tween 20. The blocking buffer is PBS with 0.15% casein dissolved in 0.1 M NaOH and 0.05% Tween 20, pH 7.5. Citrate buffer is a 0.04 M solution of sodium citrate, pH 5.5. The substrate solution contains 0.01% 3,3',5,5'-tetramethylbenzidine (TMB) and 0.004% H_2O_2 in citrate buffer. Printing buffer consisted of 150mM sodium phosphate (pH 8.5) with 0.01% sodium dodecyl sulphate (SDS).

Instrumentation

Polystyrene microtiter plates were purchased from Nunc (Maxisorp, Roskilde, Denmark). Washing steps were performed on a SLY96 PW microplate washer (SLT Labinstruments GmbH, Salzburg, Austria). Absorbances were read on a SpectramaxPlus (Molecular Devices, Sunnyvale, CA, USA). Plain microscope glass slides used to prepare the microarrays were from CORNING (Tewksbury, USA). Immobilization on the glass slides in spots was performed with a BioOdissey Calligrapher MiniArrayer (Bio-Rad Laboratories, Inc. USA). Fluorescent measurements were recorded on a ScanArray® Gx PLUS (Perkin Elmer, USA) using a green laser with an optical emission filter at 543 nm with 10 µm resolution. The laser power and PMT were set to 90% and 60%, respectively. The spots were measured by F543_Mean-B543 (Mean TRITC foreground intensity minus mean TRITC background intensity). For the sensor, the optical source used was a laser diode (LD) emitting at 635 nm with 3 mW output power (Hitachi HL6314MG). A band-pass (BP) filter, at 635 nm (Thorlabs FL635-10), with 10-nm full width at half maximum, and a high-pass (HP) filter, cut-on at 650 nm (Thorlabs FEL0650) were purchased from Thorlabs GMBH (Dacahau, Germany). An optical fiber, 1 mm in core diameter, was obtained from Polymicro Technologies, (Phoenix, Arizona). An optical spectrum analyzer Hamamatsu TG-SWNIR CCD (C9405CA) was provided by Hamamatsu Photonics Italia S.R.L. (Arese, Italy) and was used as a detector system. A peristaltic pump Minipulse 3-Gilson and poly(vinyl chloride) (PCV) tubing (i.d. 0.76 mm – Gilson) used for the fluidic system were from Gilson Inc., (Middleton, Wisconsin). The pH and the conductivity of all buffers and solutions were measured with a pH

meter 540 GLP and a conductimeter LF 340, respectively (WTW, Weilheim, Germany).

Procedures

ELISA

- **Checkerboard titration ELISA experiments**

Every three columns of a microtiter plate were coated with different concentrations of capture antibody in coating buffer (100 µL/well), the last three ones were filled with coating buffer (100 µL/well) in order to assess the corresponding blanks. The coating was done for 4 h at RT. After that, the plate was washed four times with PBST (300 µL/well). Analyte solution in PBST (100 µL/well) was added in three different concentrations: a high (H), a low concentration (L) and a blank without analyte (O), in this order and repetitively along the different concentrations of capture antibody. The plate was incubated for 30 min at RT and washed as before. Different concentrations of detection biotinylated antibody or dilutions of antiserum in PBST (100 µL/well) were added in each two rows, except for the last two ones that were filled with PBST (100 µL/well). The plate was then incubated for 30 min at RT and washed. A solution of streptavidin-HRP (1/10000 in PBST) or anti-IgG-HRP (1/6000 in PBST) was added to wells (100 µL/well), incubated during 30 min at RT and washed again. The substrate solution was added (100 µL/well) and plate was again incubated 30 min protected from light at RT before the enzymatic reaction was stopped by adding H_2SO_4 4N (50 µL/well). The absorbances were read at 450 nm.

The antibodies combination chosen were those in which the capture antibody covers all well surface and the signal does not increase when increasing its concentration and the detection antibody gives an absorbance value around 1.0 in the high concentration (H) of analyte and is the first concentration already in the saturation. This analyte concentration will be the highest concentration in the calibration curve.

- **Sandwich ELISA (calibration curve)**

The microtiter plate was coated with capture antibody appropriately diluted in coating buffer (100 µL/well) 4 h at RT. Then, the plate was washed four times with PBST (300 µL/well) and the corresponding analyte standard solutions and a zero in PBST (100 µL/well) were added. The plate was then incubated for 30 min at RT and washed. Detection biotinylated antibody or antiserum appropriately diluted in PBST (100 µL/well) were added, incubated for 30 min at RT and washed again with PBST (300 µL/well). A solution of streptavidin-HRP (1/10000 in PBST) or anti-IgG-HRP (1/6000 in PBST) was added to wells (100 µL/well), incubated during 30 min at RT and washed again. The substrate solution was added (100 µL/well) and plate was again incubated 30 min protected from light at RT before the enzymatic reaction was stopped by adding H_2SO_4 4N (50 µL/well). The absorbances were read at 450 nm. The standard curves were fitted to a four-parameter equation according to the following formula: $y = [(A-B)/1-(x/C)^D]+B$, were A is the maximal absorbance, B is the minimum absorbance, C is the concentration producing 50% of the maximal absorbance, and D is the slope at the inflexion point of the sigmoid curve. Unless otherwise indicated, data presented correspond to the average of at least two well replicates. The IC_{10} (the concentration producing 10% of the maximal signal) value was used to assess the detectability of the assay.

Conditions used in all sandwich assays such as capture antibody concentration, detection antibody concentration or antiserum dilution and analyte step conditions are shown in Table 8.3.

MICROARRAY

Epoxysilane activated slides were prepared in the laboratory by deeping the slides on a 10% (w/v) NaOH solution for 1h at RT, followed by derivatization with a 2.5% (v/v) (3-glycidyloxypropyl)trimethoxysilane (GPTMS) solution in anhydrous ethanol for 3h at RT. Before and after derivatization, slides were washed several times with water and ethanol and dried. From then and until their use, they were kept in dried conditions and at room temperature.

Immobilization of the corresponding proteins and/or antibodies was done through the BioOdissey Calligrapher MiniArrayer (also called spotter),

employing the printing buffer and under 60% humidity and 20°C. Functionalized slides were kept under these conditions 30 min before assay performance.

- **Sandwich immunoassay**

  Once slides were assembled in the Array-It® platform and washed four times with PBST, analytes dissolved in 0.15% casein PBST were added to the corresponding wells of the slide (100 µL/well), incubated for 30 min at RT and washed four times with PBST. Then, a PBST solution with detection antibody and/or antibodies (100 µL/well) was added and incubated for 30 min at RT. Slides were washed four times with PBST before adding anti-IgG-TRITC and/or streptavidin-TRITC solution (100 µL/well). After an incubation step of 30 min at RT, slides were washed three times with PBST, once with MilliQ water, dried with nitrogen and read with the scanner.

  Fluorescence intensity values are expressed in relative fluorescence units (RFUs) as average of a determined number of replicate spots. Calibration curves were all adjusted with a four-parameter logistic equation according to the following formula: $y = [(A-B)/1-(x/C)^{D}]+B$, were A is the maximal RFU, B is the minimum RFU, C is the concentration producing 50% of the maximal absorbance, and D is the slope at the inflexion point of the sigmoid curve. The IC_{10} (the concentration producing 10% of the maximal signal) value was used to assess the detectability of the microarray.

  Conditions used in all sandwich assays such as capture antibody concentration, detection antibody concentration or antiserum dilution and analyte step conditions are shown in Table 8.3.

OPTICAL SENSOR

Biofunctionalization of the poly(methyl methacrylate) (PMMA) chips as well as the other steps in the protocol were performed under flow conditions at 50 µL min^{-1}, except for the washings that were performed at 200 µL min^{-1}. First, carboxyl groups on the PMMA chip covered with Eudragit L100 were activated

by passing through the EDC/NHS solution (30 min), containing EDC (38.3 mg mL^{-1}) and NHS (5.8 mg mL^{-1}) in water prepared prior to use. Immediately, a solution of capture antibody dissolved in PBS at a certain concentration was flowed (60 min). After the chip had been washed with PBS (2.5 min), a solution of BSA was passed (1 mg mL^{-1} in PBS, 15 min) to block the remaining surface. The chip was washed again with PBST (2.5 min).

Strategy A

The CRP standards prepared in PBS were flowed into the sensor for 15 min and the chip was then washed with PBST (2.5 min). AbCRP1-biotin dissolved in PBS was introduced in the chip for 15 min and after washing with PBST (2.5 min), a solution of neutravidin-Atto 647N in PBS was passed through (15 min). A final wash with PBST (2.5 min) was performed and the signal was acquired while channels remained filled of PBST.

Strategy B

Prior to analysis, the CRP standards prepared in PBS were mixed with the labeled detection antibody C6-DY647 solution (1 µg mL^{-1} in PBS) in a 1:1 volume ratio an incubated for 15 min at RT. Afterward, the mixture was flowed into the sensor for 15 min and the chip was then washed with PBST (2.5 min). The signal acquisition was performed while channels remained filled of PBST.

This same protocol was realized adding CRP standards and C6-DY647 in different steps with a PBST wash (2.5 min) between them instead of a unique addition of the mixture being previously incubated for 15 min at RT.

After optimizing the conditions of all immunoreagents, calibration curves were all adjusted with a four-parameter logistic equation according to the following formula: $y = [(A-B)/1-(x/C)^D]+B$, were A is the maximal absorbance, B is the minimum absorbance, C is the concentration producing 50% of the maximal absorbance, and D is the slope at the inflexion point of the sigmoid curve. Unless otherwise indicated, data presented correspond to the average of at least two well replicates. The IC_{10} (the concentration producing 10% of the maximal signal) value was used to assess the detectability of the sensor method.

Table 8.3. Immunoreagent conditions for each sandwich immunoassay.

Assay	Capture antibody, µg mL^{-1}	Detection antibody, µg mL^{-1}/dilution	Analyte step conditions
Assay cTnI, additives in analyte buffer (Figure 3.6)	Ab220, 1	Ab221-biotin, 1	2% different additives in PBST, 30 min
Assay cTnI, percentage of casein in analyte buffer (Figure 3.7)	Ab220, 1	Ab221-biotin, 1	different % casein in PBST, 30 min
Assay cTnI and Tn I-T-C complex, different plates (Figure 3.8)	Ab220, 2	Ab221-biotin, 4	0.15% casein in PBST 30 min
Assay cTnI and Tn I-T-C complex, different strategies (Figure 3.10)	*(A)* As 220, 1/8000 *(B)* Mouse anti-cTnI, 2 *(C)* Goat anti-cTnI, 1 *(D)* Goat anti-cTnI, 5	*(A)* Ab221-biotin, 2 *(B)* As 221, 1/2000 *(C)* Mouse anti-cTnI, 0.5 *(D)* As 220, 1/12000	0.15% casein in PBST 30 min
Assay CRP (Figure 5.3)	AbCRP2, 10	AbCRP1-biotin, 0.05	0.15% casein in PBST 30 min
Assay Cys C (Figure 5.3)	AbCys C, 15	AbCys C, 0.05	0.15% casein in PBST 30 min
Assay Lp(a) (Figure 5.3)	AbLp(a)3, 0.5	AbLp(a)1-biotin, 0.1	PBST
Assay H-FABP (Figure 5.3)	C3 (MAb), 5	AbH-FABP-biotin, 5	0.15% casein in PBST 30 min
Assay Tn I-C-T complex (Figure 5.3)	Goat anti-cTnI, 5	As 220, 1/12000	0.15% casein in PBST 30 min
Assay CRP. Two steps/simultaneous addition (Figure 6.5)	AbCRP2, 200	AbCRP1-biotin, 2	PBST and 0.15% casein in PBST 30 min
Anti-IgG-TRITC and streptavidin-TRITC specificity (Figure 6.8)	AbCRP1-biotin, 50, 10, 1 AbCysC-biotin, 50, 10, 1	Anti-IgG-TRITC, 1/250 Streptavidin-TRITC, 1/625	-

	AbLp(a)-biotin, 50, 10, 1 AbH-FABP-biotin, 50, 10, 1		
Casein effect on cTnI and Tn I-C-T complex (Figure 6.9)	Goat anti-cTnI, 125 Goat anti-CRP, 125	As 220, 1/1000	PBST and 0.15% casein in PBST 30 min
Casein effect in all assays (Figure 6.10)	AbCRP2, 200 AbCysC, 200 C3, 100 Goat anti-cTnI, 125	AbCRP1-biotin, 2 AbCysC-biotin, 20 AbH-FABP-biotin, 150 As220, 1/1000	PBST and 0.15% casein in PBST 30 min
Individual assays (Figure 6.11)	AbCRP2, 200 AbCysC, 200 C3, 100 AbLp(a)3, 100 Goat anti-cTnI, 125	AbCRP1-biotin, 2 AbCysC-biotin, 20 AbH-FABP-biotin, 150 AbLp(a)1-biotin, 10 As220, 1/1000	0.15% casein in PBST 30 min
Cross-reactivity, CRP and Cys C assays (Figure 6.12, Table **6.5**)	AbCRP2, 200 AbCysC, 200 C3, 100 Goat anti-cTnI, 125	AbCRP1-biotin, 2 AbCysC-biotin, 20 AbH-FABP-biotin, 150 As220, 1/1000	0.15% casein in PBST 30 min
Multiplexed assays (Table 6.6, Figure 6.13, Figure 6.14, Figure 6.15, Figure 6.16)	AbCRP2, 200 AbCysC, 200 C3, 100 Goat anti-cTnI, 125	AbCRP1-biotin, 2 AbCysC-biotin, 20 AbH-FABP-biotin, 150 As220, 1/1000	0.15% casein in PBST 30 min
Matrix effect, CRP assay (Figure 6.17)	AbCRP2, 200	AbCRP1-biotin, 2	0.15% casein in PBST 30 min
Matrix effect, Cys C assay (Figure 6.18)	AbCysC, 200	AbCysC-biotin, 20	0.15% casein in PBST 30 min
Basal and AMI levels, accuracy and real samples (Figure 6.19, Figure **6.20**, Figure **6.21**)	(Slide 1) AbCRP2, 200 AbCysC, 200 (Slide 2) C3, 100 Goat anti-cTnI, 125	(Slide 1) AbCRP1-biotin, 2 AbCysC-biotin, 20 (Slide 2) AbH-FABP, 150 As220, 1/1000	0.15% casein in PBST 30 min

Study of different concentrations of capture and detection antibodies (Figure 7.7)	*(A)* 10 *(A)* 100 *(A)* 1000 *(A)* 1000 *(B)* 1000	*(A)* 1, 10[a] *(A)* 1, 10[a] *(A)* 1, 10[a] *(A)* 10 *(B)* 10	PBS, 15 min, RT
Study of different concentrations of detection antibody and neutravidin-Atto 647N (Figure 7.8)	*(A, B)* 1000	(A) 10 (A) 10 (A) 100 (A) 100 (B) 10 (B) 100 (B) 100	PBS, 15 min, RT
Calibration curve, strategy A (Figure 7.9)	1000	100	PBS, 15 min, RT
Calibration curves, strategy B (Table 7.6)	1000	1	PBS, 15 min, RT

8.2.2 COMPETITIVE IMMUNOASSAY: ELISA, MICROARRAY AND OPTICAL SENSOR

Chemicals and immunoreagents

Immunoreagents used were prepared as explained previously (see section 8.1). Human recombinant NT-proBNP and BNP, NT-proBNP free plasma and two monoclonal antibodies for BNP (24C5 and 50E1) were provided by Hytest (Turku, Finland) and human plasma was obtained from Banc de Sang i Teixits (Barcelona, Spain). N-(3-dimethylaminopropyl)-N'-ethylcarbodiimide hydrochloride (EDC·HCl), N-hydroxysuccinimide (NHS) were purchased from Thermo Scientific (Rockford, Illinois) and the poly(methyl methacrylate) (PMMA) chips from Chip Shop (Jena, Germany). Bovine serum albumin (BSA), Atto 647 goat anti-rabbit IgG, anti-rabbit IgG-HRP, anti-rabbit IgG-TRITC and other chemicals were from Sigma Chemical Co. (St. Louis, Missouri) and all salts were provided by Merck (Darmstadt, Germany).

Buffers and solutions

PBS is 0.01 M phosphate buffer 0.8% saline solution. Coating buffer is 0.05 M carbonate-bicarbonate pH = 9.6. PBST is PBS with 0.05% Tween 20. Citrate buffer is a 0.04 M solution of sodium citrate pH = 5.5. The substrate solution contains 0.01% 3,3',5,5'-tetramethylbenzidine (TMB) and 0.004% H_2O_2 in citrate buffer. Printing buffer consisted of 150mM sodium phosphate (pH 8.5) with 0.01% sodium dodecyl sulphate (SDS).

Instrumentation

The pH and the conductivity of all buffers and solutions were measured with a pH meter 540 GLP and a conductimeter LF 340, respectively (WTW, Weilheim, Germany). Polystyrene microtiter plates were purchased from Nunc (Maxisorp, Roskilde, Denmark). Washing steps were performed on a SLY96 PW microplate washer (SLT Labinstruments GmbH, Salzburg, Austria). Absorbances were read on a SpectramaxPlus (Molecular Devices, Sunnyvale, CA, USA). Plain microscope glass slides used to prepare the microarrays were from CORNING (Tewksbury, USA). Immobilization on the glass slides in spots was performed with a BioOdissey Calligrapher MiniArrayer (Bio-Rad Laboratories, Inc. USA). Fluorescent measurements were recorded on a ScanArray® Gx PLUS (Perkin Elmer, USA) using a green laser with an optical emission filter at 543 nm with 10 µm resolution. The laser power and PMT were set to 90% and 60%, respectively. The spots were measured by F543_Mean-B543 (Mean TRITC foreground intensity minus mean TRITC background intensity). For the sensor, the optical source used was a laser diode (LD) emitting at 635 nm with 3 mW output power (Hitachi HL6314MG). A band-pass (BP) filter, at 635 nm (Thorlabs FL635-10), with 10-nm full width at half maximum, and a high-pass (HP) filter, cut-on at 650 nm (Thorlabs FEL0650) were purchased from Thorlabs GMBH (Dacahau, Germany). An optical fiber, 1 mm in core diameter, was obtained from Polymicro Technologies, (Phoenix, Arizona). An optical spectrum analyzer Hamamatsu TG-SWNIR CCD (C9405CA) was provided by Hamamatsu Photonics Italia S.R.L. (Arese, Italy) and was used as a detector system. A peristaltic pump Minipulse 3-Gilson and poly(vinyl chloride) (PCV) tubing (i.d. 0.76 mm – Gilson) used for the fluidic system were from Gilson Inc., (Middleton, Wisconsin).

Procedures

ELISA

- **Two-dimensional checkerboard titration ELISA experiments (2D)**

  Direct format: The first column of a microtiter plate was coated with an antiserum (1/1000 diluted in coating buffer, 100 µL/well) and successive dilutions 1/2 were added in the following columns, except for the last one that was filled with coating buffer (100 µL/well). The coating was done overnight at 4°C and plates were covered with adhesives plate sealers. The next day, the plate was washed four times with PBST (300 µL/well). A solution of enzyme tracer was added in the first row (2 µg mL^{-1}, PBST, 100 µL/well) and successive dilutions 1/2 were added in the following rows, except for the last one that was filled with PBST (100 µL/well) and incubated for 30 min at RT. The plate was washed as before and the substrate solution was added (100 µL/well). Color development was stopped after 30 min at RT with 4 N H_2SO_4 (50 µL/well), and the absorbances were read at 450 nm.

  Indirect format: The first column of a microtiter plate was coated with an antigen (from 10 to 1 µg mL^{-1} depending on the case, coating buffer, 100 µL/well) and successive dilutions 1/2 were added in the following columns, except for the last one that was filled with coating buffer (100 µL/well). The coating was done overnight at 4°C and plates were covered with adhesives plate sealers. The next day, the plate was washed four times with PBST (300 µL/well). A solution of antiserum was added in the first row (1/1000 diluted in PBST, 100 µL/well) and successive dilutions 1/2 were added in the following rows, except for the last one that was filled with PBST (100 µL/well) and incubated for 30 min at RT. The plate was washed as before and a solution of anti-IgG-HRP (1/6000 in PBST) was added to the wells (100 µL/well) and incubated for 30 min at RT. The plate was washed again and the substrate solution was added (100 µL/well). Color development was stopped after 30 min at RT with 4 N H_2SO_4 (50 µL/well), and the absorbances were read at 450 nm.

In both cases, the combinations chosen were those that gave absorbance values from 0.7 to 1.0 and were around 70–80% of saturation.

- **Competitive ELISA (calibration curve)**

  Direct format: The microtiter plate was coated with the antisera appropriately diluted in coating buffer (100 µL/well) overnight at 4°C and covered with an adhesive plate sealer. The next day, the plate was washed four times with PBST (300 µL/well) and NT-proBNP standard solutions (2000 ng mL^{-1}–0.128 ng mL^{-1} and zero in PBST, 50 µL/well) followed by HRP-SMCC-NT-proBNP$_1$ appropriately diluted in PBST (50 µL/well) were added. The plate was then incubated for 30 min at RT and washed. The substrate solution was added (100 µL/well) and plate was again incubated 30 min protected from light at RT before the enzymatic reaction was stopped by adding H_2SO_4 4 N (50 µL/well). The absorbances were read at 450 nm. The standard curves were fitted to a four-parameter equation according to the following formula: $y = [(A – B)/1 – (x/C)^D] + B$, were A is the maximal absorbance, B is the minimum absorbance, C is the concentration producing 50% of the maximal absorbance, and D is the slope at the inflexion point of the sigmoid curve. Unless otherwise indicated, data presented correspond to the average of at least two well replicates.

  Indirect format: The microtiter plate was coated with the antigen appropriately diluted in coating buffer (100 µL/well) overnight at 4°C and covered with an adhesive plate sealer. The next day, the plate was washed four times with PBST (300 µL/well) and NT-proBNP standard solutions (2000 ng mL^{-1}–0.128 ng mL^{-1} and zero in PBST, 50 µL/well) followed by the corresponding antiserum appropriately diluted in PBST (50 µL/well) were added. The plate was then incubated for 30 min at RT and washed. A solution of anti-IgG-HRP (1/6000 in PBST) was added to the wells (100 µL/well), incubated during 30 min at RT and washed again. The substrate solution was added (100 µL/well) and plate was again incubated 30 min protected from light at RT before the enzymatic reaction was stopped by adding H_2SO_4 4 N (50 µL/well). The

absorbances were read at 450 nm. The standard curves were fitted to a four-parameter equation according to the following formula: $y = [(A – B)/1 – (x/C)^D] + B$, were A is the maximal absorbance, B is the minimum absorbance, C is the concentration producing 50% of the maximal absorbance, and D is the slope at the inflexion point of the sigmoid curve. Unless otherwise indicated, data presented correspond to the average of at least two well replicates.

Conditions used in all competitive assays such as coating antigen concentration, antiserum dilution and competition conditions are shown in Table 8.4.

MICORARRAY

Epoxysilane activated slides were prepared in the laboratory by deeping the slides on a 10% (w/v) NaOH solution for 1h at RT, followed by derivatization with a 2.5% (v/v) (3-glycidyloxypropyl)trimethoxysilane (GPTMS) solution in anhydrous ethanol for 3h at RT. Before and after derivatization, slides were washed several times with water and ethanol and dried. From then and until their use, they were kept in dried conditions and at room temperature.

Immobilization of the corresponding proteins was done through the BioOdissey Calligrapher MiniArrayer (also called spotter), employing the printing buffer and under 60% humidity and 20°C. Functionalized slides were kept under these conditions 30 min before assay performance.

- **Optimization of NB1-CH_2CO-BSA and As 251 concentrations (2D)**

  Every column of a slide was spotted with different concentrations of NB1-CH_2CO-BSA. Once slides were assembled in the Array-It® platform and washed four times with PBST, different dilutions of As251 dissolved in 0.15% casein in PBST were added (100 µL/well) in different rows, incubated for 30 min in RT and washed four times with PBST. A PBST solution (100 µL/well) was added and incubated for 30 min at RT. Slides were washed four times with PBST before adding anti-IgG-TRITC solution (100 µL/well). After an incubation step of 30 min at RT, slides

were washed three times with PBST, once with MilliQ water, dried with nitrogen and read with the scanner.

The combination chosen for the competitive immunoassay was that around 70–80% of saturation and above 10000 RFUs.

- **Competitive immunoassay (calibration curve)**

  Once slides were assembled in the Array-It® platform and washed four times with PBST, analyte dissolved in 0.15% casein PBST were added with the antiserum (100 µL/well) to the corresponding wells of the slide, incubated for 30 min at RT and washed four times with PBST. Then, a PBST solution (100 µL/well) was added and incubated for 30 min at RT. Slides were washed four times with PBST before adding anti-IgG-TRITC and/or streptavidin-TRITC solution (100 µL/well). After an incubation step of 30 min at RT, slides were washed three times with PBST, once with MilliQ water, dried with nitrogen and read with the scanner.

  Fluorescence intensity values are expressed in relative fluorescence units (RFUs) as average of a determined number of replicate spots. Calibration curves were all adjusted with a four-parameter logistic equation according to the following formula: $y = [(A-B)/1-(x/C)^D]+B$, were A is the maximal RFU, B is the minimum RFU, C is the concentration producing 50% of the maximal absorbance, and D is the slope at the inflexion point of the sigmoid curve.

  Conditions used in all competitive assays such as coating antigen concentration, antiserum dilution and competition conditions are shown in Table 8.4.

OPTICAL SENSOR

Strategy C

Biofunctionalization of the poly(methyl methacrylate) (PMMA) chips as well as the other steps in the protocol were performed under flow conditions at 50 µL min^{-1}, except for the washings that were performed at 200 µL min^{-1}. First, carboxyl groups on the PMMA chip covered with Eudragit L100 were activated by passing through the EDC/NHS solution (30 min), containing EDC (38.3 mg mL^{-1}) and NHS (5.8 mg mL^{-1}) in water prepared prior to use. Immediately, a solution of antigen NB1-CH_2CO-BSA dissolved in PBS at a certain concentration was flowed (60 min). After the chip had been washed with PBS (2.5 min), a solution of BSA was passed (1 mg mL^{-1} in PBS, 15 min) to block the remaining surface. The chip was washed again with PBST (2.5 min).

- **Optimization of NB1-CH_2CO-BSA, As 251 and anti-IgG-Atto 647N concentrations**

  Indirect format: As 251 diluted in PBS was flowed into the sensor for 15 min and the chip was then washed with PBST (2.5 min). Anti-IgG-Atto647N dissolved in PBS was introduced in the chip for 15 min and after washing with PBST (2.5 min), a solution of neutravidin-Atto 647N in PBS was passed through (15 min). A final wash with PBST (2.5 min) was performed and the signal was acquired while channels remained filled of PBST.

- **Competitive immunoassay (calibration curve)**

  Indirect format: Prior to analysis, the NT-proBNP standards prepared in PBS were mixed with the As 251 diluted in PBS in a 1:1 volume ratio an incubated for 15 min at RT. Afterward, the mixture was flowed into the sensor for 15 min and the chip was then washed with PBST (2.5 min). A solution of anti-IgG-Atto 647N in PBS was passed through (15 min) and the chip was finally washed with PBST (2.5 min). The signal acquisition was performed while channels remained filled of PBST.

After optimizing the conditions of all immunoreagents, calibration curves were all adjusted with a four-parameter logistic equation according to the following formula: $y = [(A-B)/1-(x/C)^{D}]+B$, were A is the maximal absorbance, B is the minimum absorbance, C is the concentration producing 50% of the maximal absorbance, and D is the slope at the inflexion point of the sigmoid curve. Unless otherwise indicated, data presented correspond to the average of at least two well replicates. The IC_{90} (the concentration producing 90% of the maximal signal) value was used to assess the detectability of the sensor method.

Table 8.4. Immunoreagent conditions for each competitive immunoassay.

Assay	Coating antigen, µg mL^{-1}	Antiserum, final dilution	Competition conditions
Indirect - direct format (Figure 4.14)	NB1-CH_2CO-BSA, 0.0625	As 251, 1/8000	PBST 30 min, RT
	NB1-CH2CO-BSA, 0.0625	As 252, 1/16000	
	NB1-CH2CO-BSA-, 0.0625	As 253, 1/32000	
	NB1-SMCC-HRP, 2 [a]	As 251, 1/16000 [a]	
	NB1-SMCC-HRP, 2 [a]	As 252, 1/8000 [a]	
	NB1-SMCC-HRP, 2 [a]	As 253, 1/16000 [a]	
Hapten density (Figure 4.15)	NB1-CH_2CO-BSA (δ=5), 0.0625 NB1-CH2CO-BSA (δ=3), 0.125	As 251, 1/8000	PBST 30 min, RT
Heterology studies (Figure 4.17)	NB1-CH2CO-BSA, 0.125	As 251, 1/5000	PBST 30 min, RT
	NB1-EDC-BSA, 0.25	As 251, 1/6000	
	NB1-DMP-BSA, 0.25	As 251, 1/6000	
	NB1-SMP-BSA, 0.0625	As 251, 1/6000	
	NB1-SMCC-BSA, 0.125	As 251, 1/6000	
	NB1-BDB-BSA, 0.5	As 251, 1/1000	

Heterology studies (Figure 4.19)	*(B)* NB1-CH_2CO-BSA, 0.125	As 251, 1/5000	PBST 30 min, RT
	(B) NB2-CH_2CO-BSA, 0.75	As 251, 1/1000	
	(B) NB2-CH_2CO-BSA, 0.75	As 252, 1/2000	
	(B) NB3-CH_2CO-BSA, 0.75	As 252, 1/2000	
	(B) NB4-CH_2CO-BSA, 0.2813	As 252, 1/8000	
	(B) NB2-CH_2CO-BSA, 0.75	As 253, 1/8000	
	(B) NB3-CH_2CO-BSA, 0.5625	As 253, 1/2000	
	(B) NB4-CH_2CO-BSA, 0.75	As 253, 1/12000	
	(C) NB1-CH_2CO-BSA, 0.125	As 251, 1/5000	
	(C) NB2-CH_2CO-BSA, 1.5	As 252, 1/4000	
Physicochemical parameters (Figure 4.20, Figure **4.21**, Figure **4.22**, Figure **4.23**)	NB1-CH_2CO-BSA, 0.125	As 251, 1/5000	Described in section 4.4.2.3
Physicochemical parameters (Figure 4.24)	NB1-CH_2CO-BSA, 0.125	As 251, 1/5000	Described in section 4.4.2.3
	NB1-CH_2CO-BSA, 0.125	As 251, 1/10000	
Matrix effect (Figure 4.26)	NB1-CH_2CO-BSA, 0.125	As 251, 1/5000	Buffer 1 / Buffer 1[b] Plasma / Buffer 2[b]
	NB1-CH_2CO-BSA, 0.5	As 251, 1/2000	
Matrix effect (Figure 4.27)	NB1-CH_2CO-BSA, 0.125	As 251, 1/10000	Buffer 1 / Buffer 1[c] Plasma / Buffer 2[c]
	NB1-CH_2CO-BSA, 0.5	As 251, 1/4000	
Accuracy studies (Figure 4.28)	NB1-CH_2CO-BSA, 0.125	As 251, 1/10000	Buffer 1 / Buffer 1[c] Plasma / Buffer 2[c]
	NB1-CH_2CO-BSA, 0.5	As 251, 1/4000	
Antibody production 2nd generation (Figure 4.30)	NB1-SMCC-BSA, 0.156	As 321, 1/6000	PBST 30 min, RT
	NB1-SMCC-BSA, 0.156	As 322, 1/6000	
	NB1-SMCC-BSA, 0.078	As 323, 1/8000	
	NB1-SIA-BSA, 0.125	As 251, 1/5000	
	NB1-SIA-BSA, 0.156	As 321, 1/8000	
	NB1-SIA-BSA, 0.156	As 322, 1/4000	
	NB1-SIA-BSA, 0.078	As 323, 1/12000	

Antibody production for BNP (Figure 4.35)	BNP1-T(4)(CH_2)$_2$CO-OVA, 0.5 BNP-EDC-OVA, 0.5 BNP-EDC-OVA, 0.25	As 329, 1/8000 MAb 24C5, 1/128000 MAb 50E1, 1/256000	PBST 30 min, RT
Assay NT-proBNP (Figure 5.3)	0.125	1/2000	(15 min preincubation analyte-As 251) 0.15% casein in PBST 30 min[d]
Anti-IgG-TRITC and streptavidin-TRITC specificity (Figure 6.8)	As 251, 1/1000, 1/5000, 1/1000	Anti-IgG-TRITC, 1/250	-
Casein effect in all assays (Figure 6.10)	NB1-CH_2CO-BSA, 100	As 251, 1/400	0.15% casein in PBST 30 min
Individual assays (Figure 6.11)	NB1-CH_2CO-BSA, 100	As 251, 1/400	0.15% casein in PBST 30 min
Cross-reactivity, (Table 6.5)	NB1-CH_2CO-BSA, 100	As251, 1/400	0.15% casein in PBST 30 min
Multiplexed assays (Table 6.6, Figure 6.13, Figure 6.15,Figure 6.16)	NB1-CH_2CO-BSA, 100	As 251, 1/400	0.15% casein in PBST 30 min

levels, accuracy and real samples (Figure 6.19, Figure **6.20**, Figure	NB1-CH_2CO-BSA, 100	As 251, 1/400	0.15% casein in PBST 30 min
Study of different assay conditions (Figure 7.10)	(A) 250, 500, 1000 (B) 250	(A) 1/10, 1/100, 1/500 (B) 1/10, 1/100	PBS, 15 min, RT
Study of blocking agents and additives (Figure 7.11)	250	1/10	PBS, 15 min, RT
Calibration curve (Figure 7.12)	250	1/10	PBS, 15 min, RT

[a]For direct format, anibody was immobilized while the enzyme tracer (NB1-SMCC-HRP) was added together with the analyte in the competition step. [b]For the assay in buffer, the analyte and antiserum were both diluted in the same buffer 1 (0.01 M phosphate buffer in a 0.4% saline solution, 0.05% Tween 20, pH 7.5), while in plasma assay the analyte was diluted in plasma and the antiserum in buffer 2 (0.01 M phosphate buffer solution without salt, 0.1% Tween 20, pH 7.5). For both assays, the competition step was done during 30 min at RT with a previous preincubation during 15 min at RT. [c]The physicochemical conditions were the same than before, except the Tween 20 that was used 10 times diluted in both cases and the competition step was run at 40°C. [d]A preincubation analyte-antiserum (As 251) was carried on during 15 min at RT, previous to the competitive step. After the competitive step and before the addition of anti-IgG-HRP solution, an incubation with PBST during 30 min was done in order to evaluate the performance on the multiplexed microarray.

9 CONCLUSIONS AND CONTRIBUTIONS OF THIS THESIS

9.1 CONCLUSIONS

- In the course of this thesis, the optimal epitopes for the subsequent polyclonal rabbit antibody production for cTnI and NT-proBNP have been studied and chosen. cTnI and NT-proBNP are the most relevant cardio-specific biomarkers for the diagnosis of cardiovascular diseases. With these antibodies, a sandwich ELISA for the detection of cTnI has been developed together with a competitive ELISA for the detection of NT-proBNP, both in a microplate format.

- It has been observed that cTnI has an extraordinary tendency to non-specifically adsorb itself onto surfaces and other biomolecules. This with the inability to achieve the required detectability for this biomarker have been the main problems to face with. Regarding the non-specific adsorption, different additives in the analyte or sample buffer have been evaluated. Thus, 0,15% casein in PBST combined with the use of low adsorption microplates (Immulon^{TM} 2HB) helps considerably to solve this problem. However, the sensitivity obtained for this assay in aqueous buffer is much lower than that required corresponding to the basal levels of cTnI in the blood.

- For the NT-proBNP ELISA development, the required limit of detection was achieved after studying various parameters related to heterology and other physicochemical parameters. Moreover, a good accuracy with NT-proBNP fortified plasma samples was obtained.

- It has been possible to develop a multiplexed microarray for the simultaneous detection of 5 biomarkers (cTnI, NT-proBNP, very important in the process of developing cardiovascular diseases, CRP, Cys C and H-FABP). Once the microarray is biofunctionalized using a spatial encoding with the corresponding bioconjugates or capture antibodies, immunoreagents and other biomarkers can be used in a cocktail. Neither cooperativity phenomena (union of immunoreagents that are in solution in sites where there are other biomarkers immobilized) nor cross-reactivity (recognition of different biomarkers from those for which immunoreagents have been developed) have been observed in any case.

Only Lp(a) immunoreagents produced such interferences and therefore they were discarded.

- It has been highlighted the fact that the biomarkers present in different concentration ranges remains one of the main challenges for the multiplexed diagnosis when simultaneous measurements are desired. In this research, it was impossible to quantify the CRP and Cys C in the same microarray than H-FABP, cTnI and NT-proBNP employing direct samples. Fortunately, the fact of using glass surfaces in which 24 microarrays can be printed, has allowed to make these measurements in a simultaneous and parallel way.

- With the multiplexed microarray, it has been possible to measure samples from patients with different pathologies. The results show that the efficiency of this microarray is much higher than that of analyzers currently used in clinical laboratories, regarding the ability to measure multiple biomarkers in a large number of samples in a short time and the coherence of the results. Thus, the microarray developed in this PhD thesis has been able to measure all the biomarkers from all patient samples, while analyzers only analyzed some of them, depending on the pathology, due to the cost (financial and time). The microarray was then able to detect high levels of CRP from patient samples that were not analyzed in clinical laboratory. Additionally, the microarray results are coherent with those obtained with analyzers for those cases in which measures had been made, and the disease had been diagnosed. The results have been satisfactory even in the case of NT-proBNP, which had not reached the detectability baseline even though it was very close. Unfortunately, it was not possible to measure cTnI levels with the microarray as it was expected according to previous studies done with the same immunoreagents. Thus, we can consider this multiplexed microarray as a semi-quantitative method useful for improving the diagnosis of cardiovascular disease for patients who are at different stages of the disease.

- Finally, preliminary studies have been realized to implement the multiplexed immunochemical system in a fluorescent optical sensor

based on the evanescent wave. This was done with the aim to achieve a POC (point-of-care) device suitable to be used outside hospital premises, adapted to non-specialist users, and facilitate the diagnosis of cardiovascular diseases. Unfortunately, the results obtained point to the need to make greater efforts to increase the detectability of the system, since the LOD values obtained are worse than those achieved with the ELISA or the microarray, far from the basal levels in the case of NT-proBNP.

The main problem in this thesis has been to reach the detection limits required by some biomarkers. Although in the literature and in the market there are assays that have achieved it, this fact mainly lies in the signal acquisition method as well as in the intrinsic sensitivity of the instrument addressed to do so.

9.2 CONTRIBUTIONS

A great part of this research has not been published yet. Until this moment, part of it is reflected in the following publication and congress participation:

Llibertat Abad, Francisco Javier del Campo, Francesc Xavier Muñoz, Luis J. Fernández, Daniel Calavia, **Gloria Colom**, Juan Pablo Salvador, M. Pilar Marco, Vanessa Escamilla-Gómez, Berta Esteban-Fernández de Ávila, Susana Campuzano, María Pedrero, José Manuel Pingarrón, Neus Godino, Robert Gorkin III, Jens Ducrée.
Design and fabrication of a COP-based microfluidic chip: Chronoamperometric detection of Troponin T. *Electrophoresis*, 33(21), 3187-3194., 2012.

Bioselect Bioscience. June 2013, Barcelona, Spain **(Best-Poster Prize awarded)**
Poster: Development of a multiplexed fluorescent microarray for cardiovascular biomarker detection
Glòria Colom, J.-Pablo Salvador, M.-Pilar Marco

10 RESUM

(Aquest apartat està redactat en català d'acord amb un dels requisits establerts en l'article 37 de la normativa reguladora del doctorat a l'empara del RD 99/2011 i de la Comissió de Doctorat de la Facultat de Química. "Quan la totalitat de la tesi es presenta en una llengua diferent de les especificades al programa de doctorat, s'exigeix que es presenti un resum que no sigui inferior a un 10% del volum redactat en l'altra llengua").

10.1 INTRODUCCIÓ

Les malalties cardiovasculars són un grup de trastorns del cor i els vasos sanguinis que inclouen: la malaltia cardíaca coronària, cerebrovascular, arterial perifèrica, la cardiopatia reumàtica, la malaltia cardíaca congènita, la trombosi venosa profunda i l'embòlia pulmonar [1]. Totes elles són causades per l'aterosclerosi, una acumulació de dipòsits grassos a les parets internes dels vasos sanguinis, excepte la cardiopatia reumàtica i la congènita. Els infarts de miocardi, comunament anomenats atacs cardíacs, i els accidents cerebrovasculars són esdeveniments causats per un bloqueig que impedeix que la sang flueixi cap al cor o al cervell respectivament. L'aterosclerosi és la raó més comuna d'aquests fets [2].

L'any 2012, del total de 56 milions de morts al món; 38 milions van ser degudes a malalties no contagioses, principalment malalties cardiovasculars (17.5 milions, 31% del total), càncer i malalties respiratòries cròniques. En el futur, es preveu que el nombre total anual de morts degudes a aquest tipus de malalties augmenti fins a 52 milions l'any 2030 i la mortalitat deguda a malalties cardiovasculars (MCV) augmenti de 17.5 milions al 2012 a 22.2 milions al 2030.

A causa de la rellevància de les MCV, hi ha una gran necessitat de proves que ajudin els metges en la seva detecció precoç en persones que presenten molèsties al pit i electrocardiogrames poc concloents. El protocol d'admissió s'inicia amb l'entrada d'un pacient que pateix dolor al pit a la unitat d'emergència. Després d'una primera avaluació mitjançant l'historial clínic i l'exploració física, es realitza un electrocardiograma (ECG). Si la senyal és clara i hi ha elevació del segment ST infart de miocardi (STEMI), el pacient és admès. Si la senyal no és concloent (sense elevació del segment ST síndromes coronàries agudes, NSTEACS), es demana un test per a la detecció d'un o varis biomarcadors per tal d'aclarir si el pacient ha de ser admès o no. Per tant, es necessiten les eines apropiades per a una estratificació del risc òptima i els biomarcadors cardiovasculars estan dirigits a fer-ho.

Actualment, ja hi ha al mercat molts tests per a la detecció d'aquests biomarcadors, la majoria d'ells són immunoassajos (mètodes analítics basats en anticossos) i poden ser analitzadors de sobretaula (BTA, *bench top analyzers*) o dispositius POC (*point-of-care*) (veure Taula 10.1).

Taula 10.1. Característiques d'alguns tests per marcadors cardíacs.

Nom del test (analit), Tipus d'immunoassaig	Empresa	POC/ BTA	LOD/LOQ (pg mL^{-1})	Volum mostra (µL)	Temps d'assaig (min)
Elecsys® proBNP, ECLIA	Roche	BTA	LOQ: 5	20	18
Cardiac® mioglobina / CK-MB / cTnT / dímer D / NT-proBNP, Immunocromatografia	Roche	POC	LOQ: $3{\cdot}10^4$ / $1{\cdot}10^3$ / 100 / $1{\cdot}10^5$ / 60	150	8 / 12 / 12 / 8 / 12
Triage® cTnI / CK-MB / mioglobina / BNP / dímer-D, Assaig immunocromatogràfic fluorescent	Biosite	POC	LOD: 50 / $1{\cdot}10^3$ / $5{\cdot}10^3$ / 5 / $1{\cdot}10^5$	250	20
ADVIA® Centaur® BNP / CK-MB / Mioglobina / cTnI, CLIA	Siemens	BTA	LOD: 2 / 180 / $3{\cdot}10^3$ / 8	100 / 100 / - / 100	18
H-FABP / CRP / cTnI / MPO / CK-MB ELISA	Percipio Bioscience	BTA	LOD: - / $1{\cdot}10^5$ / 480[a] / $2.5{\cdot}10^4$ / $2.5{\cdot}10^3$	100 / 5 / 100 / 5 / 20	80 / 65 / 110 / 200 / 80
PATHFAST® cTnI / NT-proBNP / dímer D / CRP / Mioglobina / CK-MB massa, CLIA	Mitsubishi Chemical	BTA	LOQ: 1 / 15/ $5{\cdot}10^3$ / $5{\cdot}10^4$ / $5{\cdot}10^3$ / $2{\cdot}10^3$	100	15

LOD: límit de detecció, LOQ: límit de quantificació, ECLIA: assaig electroquimiluminescent, CLIA: assaig quimiluminescent, ELISA: assaig per immunoadsorció lligat a enzims, cTnI: troponina cardíaca I, cTnT: troponina cardíaca T, CRP: proteïna C reactiva; H-FABP: proteïna cardíaca transportadora d'àcids grassos, BNP: pèptid natriurètic cerebral, CK-MB: creatina quinasa MB, MPO: mieloperoxidasa. [a]No assoleix el cut-off requerit (0.06 ng mL^{-1} [19]).

Com es pot observar a la taula anterior, hi ha una gran quantitat de tests per a la detecció de marcadors cardíacs. La majoria d'aquests tests tenen un temps d'assaig curt, necessiten poc volum de mostra i assoleixen excel·lents límits de detecció. En general, la mateixa empresa té tests per a diferents analits sense capacitats de multiplexació. A part d'això, la cTnI, la CK-MB i la mioglobina són detectades per la majoria d'assajos comercials i alguns incorporen marcadors addicionals com la CRP, el dímer D, els pèptids natriurètics cerebrals (BNP o NT-proBNP però no ambdós al mateix temps) i, excepcionalment, la H-FABP o la mieloperoxidasa. La multi-detecció, encara una mica escassa, de diferents marcadors característics de diferents etapes de la malaltia permetria una estratificació del risc més precisa. És aquest, doncs, el principal objectiu d'aquesta tesi.

Els corresponents estudis clínics estan en curs i és difícil en aquests moments identificar la millor combinació de biomarcadors per ajudar els metges en la

millora del diagnòstic de MCV. Per tant, tot i que certs biomarcadors semblen proporcionar una millor predicció de l'infart agut de miocardi (IAM), fins ara cap ha demostrat alterar el resultat d'una teràpia en particular o d'una estratègia de gestió. Cal continuar en la investigació per facilitar el tractament després d'un esdeveniment coronari agut. No obstant això, sembla bastant clara la millora en l'estratificació del pacient i el pronòstic quan s'utilitza la combinació de diferents biomarcadors [19, 29-33]. En conseqüència, a partir d'aquests estudis i tenint en compte la disponibilitat dels immunoreactius corresponents, s'han identificat la CRP, la cistatina C (Cys C), la lipoproteïna (a) (Lp (a)) i la H-FABP juntament amb la cTnI i l'NT-proBNP com a biomarcadors prioritaris que s'inclouen en la palataforma multiplexada d'aquesta tesi.

Aquests biomarcadors pertanyen a diferents naturaleses químiques i també són indicatius de diferents etapes de la progressió de la malaltia. La cTnI, el marcador més cardio-específic i també conegut com a marcador "daurat", és un biomarcador de necrosi miocàrdica. Tant, la CRP com la Lp (a) poden augmentar en les etapes primerenques de la malaltia (inflamació, formació de plaques i desestabilització), però els nivells elevats de CRP també s'observen després d'un IAM. El mateix passa per la H-FABP, els nivells de la qual poden augmentar poc abans de l'IAM, a l'oclusió del vas sanguini, però també durant i després de l'esdeveniment. La H-FABP s'ha assenyalat com un excel·lent biomarcador per al diagnòstic i pronòstic a llarg termini si es combina amb la troponina. Finalment, l'NT-proBNP és un clar indicador de risc de mort cardíaca, ajudant així al pronòstic [27, 28].

Per tenir èxit en la mesura adequada dels marcadors cardíacs seleccionats i la correcta interpretació dels resultats proporcionats és important tenir en compte la regulació establerta per les guies corresponents i considerar els paràmetres analítics de la següent taula referent a les concentracions de tall (*cut-off*) (veure Taula 10.2), a partir de les quals es diferencia un pacient sa d'aquell que pateix algun tipus de malaltia cardíaca.

Taula 10.2. Nivells basals i nivells MCV per sobre del *cut-off* dels diferents biomarcadors cardiovasculars seleccionats.

Biomarcador	Nivells basals, ng mL^{-1}	Nivells MCV, ng mL^{-1}
CRP[a]	<1000 risc baix	1000-3000 risc mitjà >3000 risc alt ≥10000 risc molt alt
Cys C[b]	~800-1200	≥1290
Lp(a)[c]	$<14 \cdot 10^5$	$>5 \cdot 10^5$
H-FABP[d]	≤ 5.8	>5.8
cTnI[d]	≤ 0.06	>0.06
NT-proBNP[e]	<0.4	>0.4

[a]NACB [22], [b][35], [c] [48], [d]Kilcullen, 2007 #5}, [e]Guies ESC [23].

10.2 OBJECTIUS

L'objectiu general d'aquest treball ha estat el desenvolupament d'una plataforma multiplexada capaç de detectar diferents biomarcadors cardiovasculars involucrats en les diferents etapes de la malaltia. En particular, els anticossos per a les troponines i els pèptids natriurètics cerebrals s'han produït en aquesta tesi, mentre que la resta d'immunoreactius van ser cedits per Audit Diagnostics (Cork, Irlanda), un membre del projecte europeu Cajal4EU, o d'altres fonts comercials. Els assajos ELISA es va utilitzar per caracteritzar tots els immunoreactius, optimitzar els assajos, descobrir els problemes i dificultats i investigar les solucions més adequades abans de la seva integració en un xip de micromatrius fluorescent.

Els objectius específics abordats van ser:

1. Selecció dels biomarcadors més rellevants

Aquest objectiu va requerir una revisió exhaustiva de la literatura per obtenir coneixements sobre els passos més rellevants de la malaltia, els biomarcadors implicats i el valor clínic de cada un d'ells. D'altra banda, també es van identificar els assajos que hi ha disponibles al mercat per tal de conèixer el seu comportament amb mostres clíniques.

2. Establiment d'assajos immunoquímics pels biomarcadors cardiovasculars

L'objectiu era establir les condicions immunoquímiques per a la detecció dels biomarcadors seleccionats i caracteritzar el seu comportament amb mostres clíniques en termes de sensibilitat, especificitat, així com altres paràmetres analítics (robustesa, exactitud, precisió, etc.). Per a dur a terme això, va ser necessari tenir accés a anticossos específics pels marcadors elegits. En aquest context, i degut a la seva rellevància, ens vam dirigir a la producció d'anticossos contra les troponines i els pèptids natriurètics. Els anticossos contra la CRP, la Cys C i la Lp (a) van ser cedits per Audit Diagnostics, mentre que la H-FABP i els anticossos per a la seva detecció van ser obtinguts de fonts comercials (Randox Laboratories).

3. Desenvolupament d'un assaig multiplexat per a la multi-detecció

Amb les condicions immunoquímiques d'anàlisi establertes i coneixent el comportament dels immunoreactius en qüestió, el següent pas va consistir en la seva implementació en una plataforma multiplexada. Amb aquest objectiu, es va decidir el desenvolupament d'una micromatriu (a partir d'ara ho anomenarem *microarray*) fluorescent. Per tant, el format multiplexat permetria la determinació simultània de diversos biomarcadors cardiovasculars, en aquest cas CRP, Cys C, H-FABP, Lp (a), cTnI i NT-proBNP, provinents d'una mateixa mostra. Els objectius específics abordats aquí van ser:

3.1. Investigació de possibles reactivitats creuades i fenòmens de cooperació entre els diferents inmunoreactius
3.2. Desenvolupament i caracterització analítica del microarray fluorescent multiplexat
3.3. Implementació del microarray fluorescent per a l'anàlisi de plasma i sèrum humà

4. Desenvolupament d'un dipositiu POC

Per tal de reduir el temps d'anàlisi, facilitar l'ús i millorar la portabilitat, es va desenvolupar un dispositiu POC (immunosensor). Aquest objectiu es va abordar en el context d'una col·laboració entre el grup Chemical and Biochemical Optical sensor group de l'Instituto di Fisica Applicata "Nello Carrara" a Florència (Itàlia) formant part d'una estada pre-doctoral de 3 mesos. El sensor utilitzat va

ser un sensor òptic d'ona evanescent basat en l'anisotropia de la fluorescència. Com a prova de concepte, la potencialitat d'aquest dispositiu es va avaluar per a la detecció de la CRP i l'NT-proBNP com a assajos individuals.

10.3 RESULTATS

10.3.1 DESENVOLUPAMENT D'ANTICOSSOS I TÈCNIQUES IMMUNOQUÍMIQUES PER A TROPONINES

La cTnI i TnC natives es van utilitzar per a immunitzar conills de Nova Zelanda per a l'obtenció d'anticossos policlonals. Es van utilitzar dos conills per a cada immunògen, l'antisèrum dels quals es va anomenar As 220 i 221 pels de la cTnI i As 222 i 223 pels de la TnC. L'evolució del títol dels anticossos es va avaluar mitjançant un ELISA indirecte no competitiu. Els anticossos específics per a la cTnI es van detectar des del principi amb una bona evolució del títol. En canvi, per la TnC, no es van poder obtenir anticossos immunitzant la proteïna nativa (segon sangrat) ni quan es va immunitzar el conjugat TnC-DMP-HCH (tercer sangrat). Aquests resultats ens van portar a la caracterització de la proteïna comercial mitjançant MALDI-TOF-MS on es van observar dos pics, un amb un pes molecular corresponent a la TnC (pic a m/z 18.568,32) i un altre amb un pes molecular més baix corresponent a alguna impuresa o un fragment de la TnC (pic a m/z 16.893,82). El proveïdor no va poder donar cap explicació a aquests resultats i va assegurar que la proteïna que servien era pura. Tot i això, aquest fet no explica la manca de resposta immune. Una possible hipòtesi podria estar relacionada amb la homologia amb altres proteïnes de l'animal hoste, però aquest fet no s'ha comprovat. No s'ha trobat cap explicació racional per explicar aquest fet fins al moment.

Amb els anticossos obtinguts per a la cTnI, es va voler desenvolupar un ELISA per a la seva detecció. El primer problema observat va ser la senyal no específica probablement deguda l'adsorció no específica de la cTnI a la superfície de les microplaques o fins i tot a l'anticòs. Es van dedicar molts esforços a solucionar aquest problema i, finalment, es va poder minimitzar utilitzant PBST amb 0.15% de caseïna a l'etapa de l'analit. A més a més, es va

veure que fent servir les plaques Immulon™ 2HB enlloc de les MaxiSorp™ es minimitzava encara més aquest efecte amb la cTnI. Tot i això, les senyals inespecíficques no van ser eliminades completament i, en alguns experiments, s'ha uilitzat el complex de troponina I-T-C enlloc de la cTnI seguint les recomanacions de la casa comercial Hytest i sent aquest el material de referència establert per l'AACC cTnI Standardization Subcommitee (SRM® 2921).

En la primera estratègia que es va investigar, es van emprar els anticossos produïts inicialment (veure Figura 10.1, estratègia A). Desafortunadament, tot i els intents de millorar l'assaig canviant un gran nombre de condicions, el LOD aconseguit (16,4 ng mL^{-1}) per a l'assaig en tampó estava molt per sota de la línia de tall establerta per a la cTnI (0,06 ng mL^{-1}). Veient aquests resultats desencoratjadors, es va adquirir de fonts comercials (Life Diagnostics) un anticòs monoclonal (MAb) i un anticòs policlonal de cabra (PAb cabra) contra cTnI per provar diferents combinacions i intentar millorar la detectabilitat obtinguda (veure Figura 10.1 i Taula 10.3).

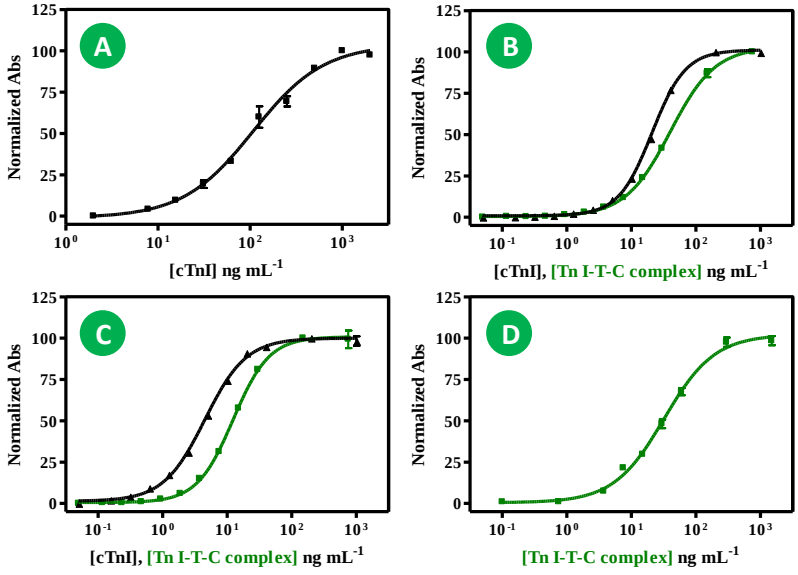

Figura 10.1. Corbes de calibració obtingudes per a les quatre estratègies utilitzant els diferents calibradors I immunoreactius. A, B, C) Cada corba es va realitzar una vegada utilitzant dues rèpliques a l'assaig. D) La corba es va realizar tres vegades (inter-dia i intra-dia) utilitzant almenys dues rèpliques en cada cas.

Taula 10.3. Característiques de l'ELISA per a les quatre combinacions.

	A	B		C		D
	cTnI[a]	cTnI[a]	Complex Tn I-T-C[a]	cTnI[a]	Complex Tn I-T-C[a]	Complex Tn I-T-C[b]
Ab captura	Ab220	MAb		PAb cabra		PAb cabra
Ab detecció	Ab221-B	As221		MAb		As220
Abs_{max}	103.90	101.2	103.00	100.00	100.80	102.03
Abs_{min}	-1.08	0.89	0.45	1.32	0.52	0.71
Pendent	1.13	1.68	1.25	1.36	1.55	1.14
R^2	0.99	1.00	1.00	1.00	1.00	0.98
IC50, ng mL^{-1}	107.90	20.93	40.16	4.51	12.39	33.09
Rang de treball, ng mL^{-1}	31.91-316.99	8.83-46.00	12.60-108.61	1.54-12.41	4.96-29.37	9.10-101.62
LOD, ng mL^{-1}	16.38	5.29	6.48	0.80	2.90	4.29

Ab: anticòs, As: antisèrum, B:biotina. [a]Cada corba es va realitzar una vegada utilitzant dues rèpliques a l'assaig. [b]La corba es va realitzar tres vegades (inter-dia i intra-dia) utilitzant almenys dues rèpliques en cada cas. Tots els càlculs referents al compex Tn I-T-C estan fets tenint en compte una concentració de cTnI de 1.5 mg mL^{-1} en la solució inicial, segons dades del proveedor.

Com a resultat d'aquests estudis, sembla clar que, en qualsevol cas no hem estat capaços d'arribar a la detectabilitat desitjada, ni amb els anticossos produïts en aquesta tesi ni amb els anticossos comercials o una combinació dels dos. En aquesta etapa, vam començar a reconsiderar la idoneïtat de l'immunògen utilitzat. Per tant, tot i que els anticossos contra tota la cTnI nativa s'han reportat o es poden trobar disponibles comercialment, podria ser que aquests haguessin d'estar purificats per immunoafinitat per aïllar les fraccions que reconeixen els epítops no bloquejats per la interacció amb les altres unitats del complex, no fosforilats o no units a l'heparina o a autoanticossos. Alternativament, es va decidir dur a terme una nova generació d'anticossos contra immunògens ben dissenyats basats en seqüències peptídiques (d'uns 10-20 aa) seleccionades i no afectades per totes aquestes possibles interferències. Tots dos enfocaments requerien el disseny i la síntesi de seqüències de pèptids apropiats.

Mentre es realitzava aquesta segona generació d'anticossos, es va seguir endavant amb els experiments destinats al desenvolupament del microarray utilitzant l'estratègia D per a la cTnI, basada en l'ús d'un dels anticossos produïts (As 220) i el PAb comercial de cabra. Aquesta combinació, encara que

no fos l'òptima, permetria la realització d'un estudi de viabilitat de la plataforma multiplexada a un cost raonable.

10.3.2 DESENVOLUPAMENT D'ANTICOSSOS I TÈCNIQUES IMMUNOQUÍMIQUES PER A PÈPTIDS NATRIURÈTICS CEREBRALS

El disseny d'haptens es va realitzar per als tres pèptids natriurètics cerebrals (BNPs): BNP, NT-proBNP i el precursor proBNP, degut a la rellevància clínica que implica l'anàlisi dels tres. Tot i això, l'NT-proBNP és el que proporcionaria una informació més específica i útil de la mort cardíaca. En aquest cas, la reactivitat creuada amb el seu precursor (proBNP) pot evitar-se amb el disseny d'hapté, escollint un epítop només present a l'NTproBNP. Pel contrari, el BNP i el proBNP comparteixen exactament la mateixa seqüència de 32 aa.

Així doncs, per l'NT-proBNP es va escollir com a hapté el fragment comprés entre l'aa 63 i 76. Aquest pèptid (a partir d'ara s'anomenarà NB1) conté una treonina a la posició 71 (T_{71}) que a diferència de l'NT-proBNP, en el proBNP està glicosilada. Addicionalment, l'NB1 va ser sintetitzat amb una cisteïna a l'extrem N-terminal per tal d'utilitzar el seu grup tiol per a l'acoblament covalent a HCH i a BSA utilitzant N-succinimidil iodoacetat (SIA) com a espaiador (veure Figura 10.2).

L'hapté dissenyat per a la immunització del BNP es va basar en la seqüència sencera del pèptid amb l'addició d'una lisina en l'extrem N-terminal amb un grup azida en la cadena variable en lloc d'un grup amino (BNP1), per tal de realitzar una química ortogonal a través d'una 1,3-cilcoaddició amb una proteïna alquinilada [154 95]. Pel proBNP es va proposar produir anticossos contra el lloc d'escissió ja que és un epítop que només existeix en el proBNP [116 22]. Per tant, l'hapté es va basar en una seqüència que contenia els últims set aa de la seqüència de l'NT-proBNP seguit de setze aa corresponents al BNP (aa 70-92). En aquest cas, a l'extrem C-terminal, es va afegir una cisteïna per dur a terme la química ortogonal durant la conjugació amb la proteïna i mig bucle del BNP va ser simulat amb un poli(etilenglicol) (PEG) diamina amb tres unitats de glicol per tal d'augmentar l'afinitat en comparació amb el proBNP. La presència d'un bucle era necessària per poder adoptar la conformació original.

L'ús d'una cadena de PEG hidròfil per assolir aquest objectiu assegura la manca d'immunogenicitat d'aquesta estructura. La col·locació de la Cys en l'extrem C-terminal maximitza el reconeixement de la seqüència d'aa que conté la part més específica pel que fa a BNP i NT-proBNP i minimitzat el reconeixement de la resta que és més semblant al BNP.

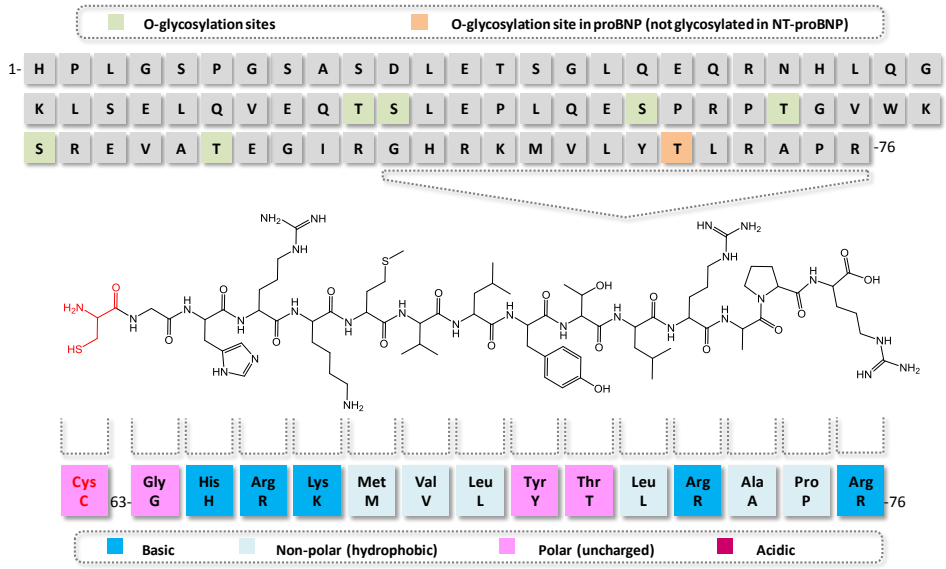

Figura 10.2. Esquema de la seqüència de l'NT-proBNP (aa 1-76) i el fragment escollit (aa 63-76) per a la preparació de l'immunògen (NB1) amb les seves propietats. En vermell, la cisteïna (Cys) que s'afegeix amb la finalitat de realitzar l'acoblament a una proteïna.

Tot el treball relacionat amb la síntesi d'haptens de l'NT-proBNP (NB1), BNP (BNP1) i proBNP va ser realitzat per la Unitat de Química Combinatòria (UQC, PCB), sota la responsabilitat de la Dr. Míriam Royo en el context de la col·laboració dins el projecte Nanocardiococo.

La síntesi de l'hapté del proBNP va plantejar moltes dificultats. En el moment d'acabar aquesta tesi doctoral, l'hapté proposat seguia sent sintetitzat i s'estaven buscant noves estratègies. Les dificultats provenien principalment de la introducció de la cadena de PEG i la forma en com es ciclava. Pel cas del BNP, les dificultats van aparèixer en la producció dels anticossos, fet que va impedir la obtenció del corresponent immunoassaig. Per tant, la major part de la feina que es descriu pels BNPs es centra en la determinació immunoquímica de l'NT-proBNP.

Els primers assajos competitius desenvolupats per a l'NT-proBNP no assolien la detectabilitat requerida. Per aquest motiu es va realitzar una optimització de l'assaig tant pel que fa a aspectes d'heterologia, disminució de la densitat d'haptens com de paràmetres fisicoquímics. Després de trobar les condicions òpimes, es va aconseguir el següent assaig (Figura 10.3 i Taula 10.4)

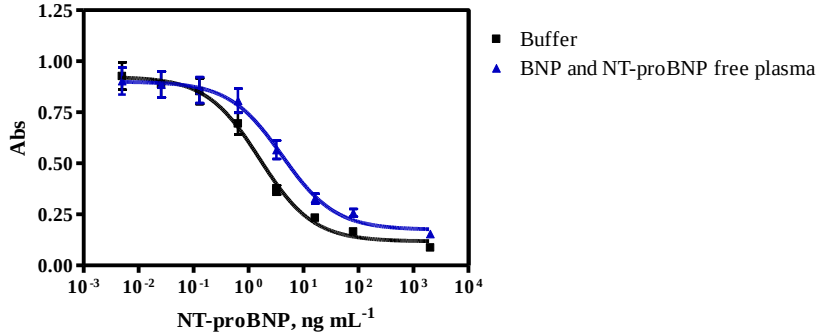

Figura 10.3. Corbes de calibració per a l'avaluació de l'NT-proBNP en tampó i en plasma humà. Cada corba es va realizar quatre dies utilitzant tres replicats en cada assaig (n=12).

Taula 10.4. Característiques de l'ELISA per a l'avaluació de l'NT-proBNP en tampó i plasma humà.

	Buffer		**BNP and NT-proBNP free plasma**	
	Mitjana±SD	**CV (%)**	**Mitjana±SD**	**CV (%)**
Abs_{max}	0.93±0.25	26.86	0.9±0.3	27.6
Abs_{min}	0.12±0.03	21.15	0.2±0.1	26.0
Pendent	-0.9±0.1	13.1	-0.92±0.07	7.36
R^2	0.990±0.001	0.118	0.990±0.002	0.228
IC50, ng mL^{-1}	1.6±0.4	24.0	4±2	41
Rang de treball, ng mL^{-1}	0.4±0.1-10±2	31.9, 21	1.0±0.4-23±10	39.5, 41
LOD, ng mL^{-1}	0.15±0.05	36.04	0.4±0.2	39.0

Cada corba es va realitzar quatre dies utilitzant tres replicats en cada assaig (n=12).

Com es pot observar, l'assaig mostra paràmetres acceptables respecte l'Abs_{max}, la pendent i el LOD està en el *cut-off*. La variació de les condicions de l'assaig va tenir una influència significativa en la detectabilitat. Tot i que no hem aconseguit l'objectiu d'obtenir un assaig amb un límit de detecció per sota del llindar, en aquest punt considerem aquestes característiques suficients per continuar amb els nostres estudis. Els nivells entre 0,4 i 2 ng mL^{-1} indiquen poca

probabilitat de mort cardíaca (diagnòstic incert) i més de 2 ng mL^{-1} indicaria mort cardíaca. Amb les característiques actuals de l'assaig desenvolupat seríem capaços de distingir entre aquests dos grups.

La precisió de l'assaig desenvolupat es va avaluar mitjançant la mesura de 8 mostres fortificades, preparades en tampó i en plasma lliure de BNP i NT-proBNP, durant 4 dies diferents. En cada assaig les mostres es van mesurar utilitzant tres rèpliques. Els resultats obtinguts es mostren a la Figura 10.4. Com es pot observar, hi ha una bona correlació entre la mesura i els valors de concentració fortificats. Els resultats obtinguts coincideixen molt bé amb els valors fortificats. Es va obtenir una pendent prop d'1 (1,06 i 0,91 per tampó i plasma) amb un coeficient de correlació de 0,978 i 0,933, respectivament.

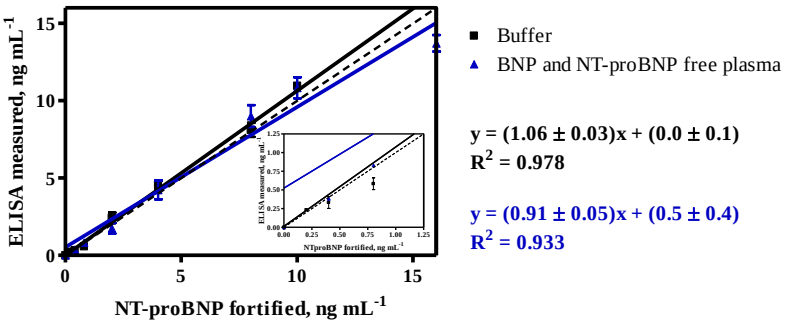

Figura 10.4. Correlació entre les valors de concentració mesurats i fortificats. La línea de punts correspon a una correlació perfecta (pendent=1).

En aquest punt, es va discutir la manera d'augmentar la detectabilitat de l'assaig, tenint en compte l'interés de poder mesurar en l'interval de 0,1-0,4 ng mL^{-1}, on els nivells comencen a augmentar al començament de la malaltia. Una de les hipòtesis era que el SIA utilitzat en la preparació de l' immunògen sigués un espaiador massa curt, i que part de l'estructura del pèptid quedés amagada per la proteïna HCH. Per aquesta raó, es va decidir produir una segona generació d'anticossos utilitzant aquesta vegada un braç espaiador (sulfo-SMCC) més llarg esperant millorar el reconeixement. L'intent no va tenir èxit i no es va aconseguir millorar la detectabilitat.

10.3.3 ASSAJOS INDIVIDUALS PER A LA DETERMINACIÓ DE CRP, CYS C, H-FABP I LP(a)

Es van desenvolupar ELISAs per a tots els analits seleccionats tenint en compte les condicions establertes per als assajos de cTnI i NT-proBNP. Així, el tampó de bloqueig (0,15% de caseïna en PBST) utilitzat per a reduir l'adsorció no específica de la troponina I i el seu complex terciari es va utilitzar per a la etapes d'incubació de la resta d'analits. A més a més, atès que els assaigs de tipus sandvitx (CRP, Cys C, Lp (a), H-FABP i cTnI) tenen un pas addicional (anticòs de detecció) comparat amb l'immunoassaig competitiu (NT-proBNP), en aquest últim es va introduir una etapa addicional d'incubació amb PBST durant 30 min abans de l'addició d'anti-IgG-HRP. Això es va fer per simular l'addició dels anticossos de detecció requerits en els assajos sandvitx i comparar tots els assajos que més tard s'implementaran en el microarray de forma multiplexada.

El LOD que es va aconseguir per la CRP, la Cys C, la Lp (a) i la H-FABP va ser suficient. No obstant això, en aquestes condicions, els assajos de cTnI i NT-proBNP no van arribar a la detectabilitat necessària. Tot i que anteriorment s'ha demostrat que l'assaig de l'NT-proBNP va ser capaç de detectar 0,15 ng mL^{-1} en tampó i 0,4 ng mL^{-1} en plasma lliure de BNP i NT-proBNP, les principals diferències entre el protocol utilitzat llavors i aquí rau en el tampó d'assaig utilitzat en l'etapa de l'analit (competència).

10.3.4 MULTI-DETECCIÓ DE BIOMARCADORS CARDIOVASCULARS MITJANÇANT UN MICROARRAY FLUORESCENT

L'estratègia proposada per al desenvolupament del microarray multiplexat es pot veure a la següent Figura 10.5.

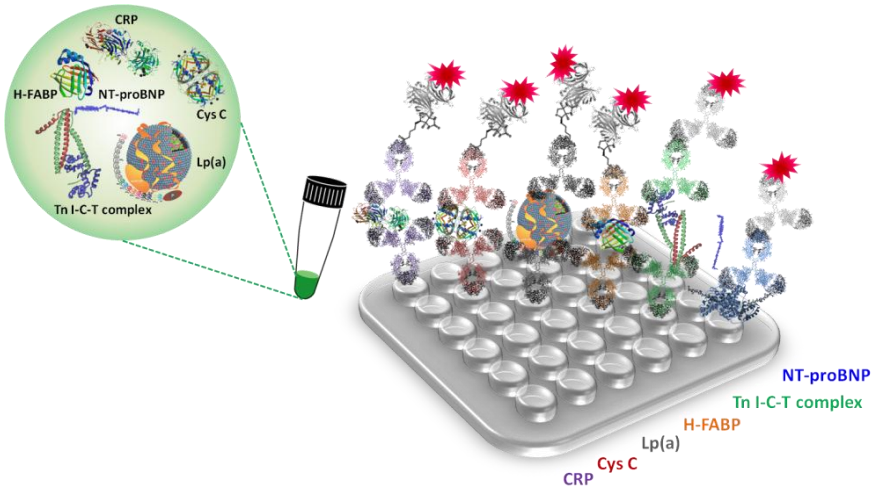

Figura 10.5. Representació esquemàtica de l'estratègia proposada pel microarray multiplexat fluorescent. D'esquerra a dreta, esquematitzat els corresponents immunoassaigs per a la detecció de CRP, Cys C, Lp (a), H-FABP, cTnI (format sandvitx) i NT-proBNP (format competitiu).

L'aproximació del microarray funcionaria de la següent manera:

1. Preparació del microarray mitjançant la immobilització dels diferents anticossos de captura o bioconjugats (per l'NT-proBNP en un format competitiu) en replicats damunt la superfície de vidre amb l'ajuda d'un *spotter*. La superfície de vidre ha estat prèviament activada amb una solució de NaOH al 10% (w/v) i derivatitzada amb grups epoxi mitjançant una solució de GPTMS al 2.5% (v/v) en etanol anhidre.

2. Addició de la mostra que conté la barreja dels analits diana.

3. Addició d'un còctel que consisteix en una barreja de anticossos de detecció (alguns d'ells biotinilats: CRP, Cys C, la Lp (a) i H-FABP).

4. Addició d'una barreja d'anti-IgG i streptavidina marcats amb un fluoròfor.

Com s'ha comentat prèviament, per a l'assaig de l'NT-proBNP, és necessari afegir tampó en el pas 3 ja que té menys etapes que la resta d'assajos.

Abans d'implementar tots els immunoassajos de forma multiplexada en aquest plataforma, es van realitzar els assajos de forma individual i es van dur a terme els corresponents estudis d'especificitat. Es va veure que la micromatriu de CRP reconeixia també la Lp (a) a concentracions superiors a 10 nM. De la mateixa

manera, el microarray de Cys C reconeixia la Lp (a) a concentracions encara més baixes. La reactivitat creuada de la Lp (a) en l'assaig de la CRP era del 9,6%, mentre que en el de la Cys C era del 47,8%. Aquest comportament inesperat podria ser explicat tenint en compte la complexitat de la Lp (a) i el seu considerable alt pes molecular. Hi ha la possibilitat que aquestes proteïnes puguin compartir alguns epítops encara que tenint en compte que els anticossos utilitzats són policlonals, el reconeixement sembla massa alt. Una altra causa podria ser el seu caràcter lipofílic; hem de recordar que la Lp (a) és una lipoproteïna. Aquest fet podria provocar la unió no específica a superfícies o a proteïnes a través d'interaccions inespecífiques. A la llum d'aquests resultats, es va decidir retirar la Lp (a) del format multiplexat, tot i que la presència d'aquest biomarcador hagués sigut interessant ja que els alts nivells de Lp (a) s'associen a un risc elevat de desenvolupar malalties cardiovasculars

Una vegada realitzats aquests estudis i havent descartat la Lp(a) del sistema, es va passar al desenvolupament de l'assaig en format multiplexat obtenint els següents paràmetres per a cada un dels analits diana (veure Taula 10.5).

Taula 10.5. Característiques analítiques del microarray multiplexat per cada un dels cinc de biomarcadors seleccionats.

	CRP	Cys C	H-FABP	Tn I-T-C complex	NT-proBNP[a]
	Mitjana±SD				
RFU_{max}	12434±378	8908±1028	7153±896	11186±3273	9223±5229
RFU_{min}	630±162	387±157	159±255	516±247	601±94
Pendent	1.5±0.2	1.3±0.2	1.57±0.05	1.9±0.2	-1.3±0.3
R^2	0.97±0.01	0.988±0.004	0.981±0.003	0.97±0.02	0.97±0.02
IC50, ng mL^{-1}	72±11	19±2	100±15	83±13	24±12
Rang de treball, ng mL^{-1}	181±22-27±7	50±10-6±1	252±62-41±6	202±17-40±4	6.9±0.5-85±62
LOD, ng mL^{-1}	15±5	3±1	24±3	25±3	3±1

Cada corba de calibració es va assajar tres vegades en tres dies diferents utilitzant 6 rèpliques per a cada punt de concentració en cada pou (microarray). Cada microarray es va utilitzar per provar una concentració determinada d'analit pels cinc analits. Així, es va obtenir una corba de calibració emprant 8 microarrays diferents, cadascun amb diferents concentracions dels analits diana. Les làmines de vidre funcionalitzades provenen de tres lots diferents. [a]Tots els paràmetres es van calcular a partir de dues repeticions fetes en dos dies diferents.

A partir dels resultats mostrats a la taula anterior, es pot concloure que el microarray multiplexat és un assaig robust. Per tant, la variabilitat observada no és molt alta tenint en compte que les làmines de vidres (a partir d'ara anomenarem slides) eren de diferents lots i que els assaigs es van realitzar en diferents dies. Només les RFU_{max} van mostrar més variabilitat però això és bastant comú en els assaigs bioanalítics i pot estar relacionat amb els canvis de temperatura del laboratori, els tampons, així com l'ús de noves alíquotes de immunoreactius. Desafortunadament, i com en els microarrays individuals, en el format multiplexat la sensibilitat per a la H-FABP, cTnI i NT-proBNP estava sobre els nivells basals dels pacients sans. Per aquesta raó, es va estudiar l'efecte dels diferents paràmetres fisicoquímics (pH i conductivitat) amb l'objectiu de millorar la detectabilitat del microarray.

Com a resultat d'aquests estudis, no vam ser capaços de millorar la detectabilitat dels assaigs d'H-FABP, cTnI i NT-proBNP que era el nostre principal objectiu. Per tant, es va decidir seguir endavant i investigar la possibilitat d'aplicar aquest microarray multiplexat per a l'anàlisi de mostres clíniques. Per aquest objectiu es va utilitzar plasma i sèrum humà del Banc de Sang i Teixits de Catalunya. En una primera instància, es van avaluar les interferències no específiques causades per aquestes matrius (estudis de l'efecte matriu). Per a aquest propòsit, les corbes de calibració es van preparar en tampó, plasma i sèrum sense diluir ja que la detectabilitat és molt compromesa per a tres dels cinc biomarcadors inclosos en aquesta plataforma multiplexada. Així es va poder comparar el paral·lelisme de les tres corbes estàndard (veure Figura 10.6 i Taula 10.6).

Mentre que la resposta dels microarrays d'H-FABP, del complex de troponin I-T-C i NT-proBNP no es va veure afectada significativament per les matrius de plasma i sèrum, les senyals de la CRP i la Cys C van ser completament distorsionades . No obstant això, aquest fet era molt probable tenint en compte la detectabilitat del microarray per a aquests biomarcadors i els seus nivells basals que són considerablement alts; 1000 ng mL^{-1} per CRP (IC50 en tampó és al voltant de 70,5 ng mL^{-1}) i entre 800 a 1200 ng mL^{-1} per a Cys C aproximadament (IC50 en tampó és al voltant de 9,52 ng mL^{-1}). Per tant, probablement l'efecte matriu podria ser solucionat simplement diluint prèviament la mostra en el tampó d'assaig. En la resta de marcadors, l'efecte matriu podria evitar-se simplement calibrant el microarray multiplexat amb la

matriu de la mostra corresponent. Amb aquestes premisses vam dirigim la investigació cap a la utilitat d'aquest microarray per almenys ser utilitzat com a sistema d'alarma per a distingir entre pacients sans i malalts.

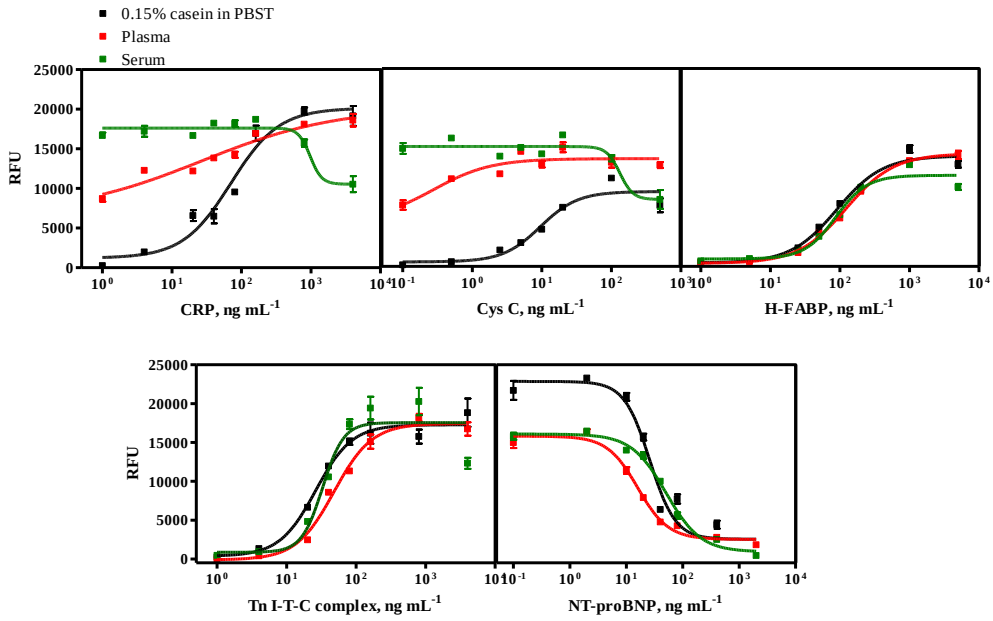

Figura 10.6. Efecte matriu causat pel plasma humà i sèrum humà en cada assaig en un format multiplexat. Cada corba de calibració es va assajar una vegada utilitzant 6 rèpliques per a cada concentració en cada pou (microarray). Cada microarray es va utilitzar per provar una determinada concentració d'analit pels 5 biomarcadors.

Taula 10.6. Característiques analítiques del microarray multiplexat per als cinc biomarcadors seleccionats en tampó, plasma humà i sèrum humà.

	CRP			Cys C			H-FABP		
	Buffer	**Plasma**	**Serum**	**Buffer**	**Plasma**	**Serum**	**Buffer**	**Plasma**	**Serum**
RLU_{max}	20138	20231	17618	9466	13618	15148	13745	14032	11241
RLU_{min}	1204	6717	10536	571.9	5793	8458	-51.42	-105.7	468.6
Pendent	1.25	0.45	-5.18	1.61	1.05	-4.57	1.31	1.26	1.93
R^2	0.92	0.87	0.74	0.89	0.67	0.69	0.97	0.99	0.96
IC50,ng mL^{-1}	70.50	26.77	969.40	9.52	0.28	132.20	90.47	122.60	86.99

	Tn I-T-C complex			NT-proBNP		
	Buffer	**Plasma**	**Serum**	**Buffer**	**Plasma**	**Serum**
RLU_{max}	17277	17444	17553	22855	15811	16083
RLU_{min}	357.2	-115.0	866.8	2543	2521	924.6
Pendent	1.67	1.59	2.87	-1.92	-1.61	-1.41
R^2	0.91	0.96	0.85	0.93	0.96	0.98
IC50, ng mL^{-1}	26.21	48.09	32.97	26.10	15.96	50.61

Cada corba de calibració es va assajar una vegada utilitzant 6 rèpliques per a cada concentració en cada pou (microarray). Cada microarray es va utilitzar per provar una determinada concentració pels 5 biomarcadors.

Després d'observar l'efecte matriu de diferents dilucions del plasma humà en els assajos individuals de la CRP i la Cys C, es va veure que per a una quantificació exacta de tots dos biomarcadors seria necessari mesurar cada mostra clínica almenys en tres factors de dilució diferents: i) 1/40 per a la CRP; ii) 1/200 per a la Cys C i iii) sense diluir per a la resta dels biomarcadors. Veient que ens estàvem movent en una direcció en la qual hauríem de mesurar cada biomarcador en diferents condicions i que això anava en contra del concepte ideal de diagnòstic multiplexat, es va decidir avaluar la possibilitat de mesurar la CRP i la Cys C en el mateix microarray sacrificant exactitud en la quantificació d'un d'aquests biomarcadors. Tenint en compte la major rellevància de la CRP en les malalties cardiovasculars, es va decidir en aquest cas sacrificar l'exactitud per a la Cys C i mesurar els dos analits amb una dilució 1/40. Encara que bastant inespecífica, la CRP és un marcador biològic ben reconegut clarament associat als primers passos de les MCV. De manera contrària, la Cys C es considera una candidata gairebé perfecta per a l'estimació de la funció renal. La forta correlació entre la malaltia renal crònica i les malalties cardiovasculars, va inspirar als investigadors a explorar la possible associació de la Cys C amb les MCV. Per tant, els nivells elevats de Cys C estan associats a malalties cardiovasculars desenvolupades a causa del deteriorament de la funció renal [195 22]. D'aquesta manera, els resultats obtinguts per la Cys C en aquest microarray haurien de ser interpretats d'una manera qualitativa més que quantitativa.

Seguidament, es va avaluar la precisió mitjançant l'anàlisis de mostres de plasma enriquides amb tots els analits a diferents concentracions. Les mostres es van dividir en dues parts, una d'elles diluïda 1/40 per la CRP i la Cys C, i l'altra

es va mesurar sense diluir per a la resta de biomarcadors. L'anàlisis es va realitzar en sis dies diferents per a la CRP i la Cys C, mentre que per la H-FABP, el complex de troponina I-T-C i l'NT-proBNP l'anàlisi es va fer en tres dies diferents emprant almenys 6 rèpliques per microarray per a cada analit. Mentre que per l'NT-proBNP, la H-FABP i la CRP els coeficients de correlació van ser acceptables, per la Cys C i el complex de troponina van ser inferiors a 0,8. D'altra banda, mentre que el microarray de la CRP i la Cys C mostraven una clara tendència a sobreestimar (pendents 1,5 i 1,2, respectivament), per a la resta de biomarcadors es va observar una subestimació (pendents entre 0,8 i 0,9). Malgrat aquestes circumstàncies, considerem que el microarray encara podria ser útil per al cribatge i l'estratificació dels pacients, encara que l'exactitud no fos massa bona. Referent a això, cal fer notar que la majoria dels assajos POC disponibles al mercat també tenen discordances importants entre ells.

Finalment, l'Institut de Recerca Germans Trias i Pujol (IGTP) ens va proporcionar mostres de plasma obtingudes de pacients amb diferents patologies per a l'avaluació preliminar del microarray multiplexat desenvolupat. Aquestes mostres de plasma ja havien estat analitzades a l'IGTP per la cTnI, CK-MB i CRP utilitzant un analitzador Siemens Dimension i per l'NT-proBNP un Radiometer AQT 90 FLEX. Tots dos equips són analitzadors de sobretaula que proporcionen les dades per a cada biomarcador com un resultat d'una anàlisis separada i individual.

Les mostres es van obtenir de pacients amb i sense símptomes relacionats amb malalties cardiovasculars. Totes elles es van analitzar amb el microarray multiplexat desenvolupat i els resultats es mostren en els gràfics de la Figura 10.7. El complex de troponina I-T-C, la H-FABP, i l'NT-proBNP es van mesurar sense diluir i les dades mostrades són el resultat d'una sola mesura en el microarray ja que el volum de mostra no va ser suficient. La CRP i la Cys C es van poder mesurar en diferents microarrays i diferents slides durant tres dies diferents ja que hi havia més mostra disponible degut al factor de dilució que s'havia d'aplicar. Les barres grises corresponen als resultats obtinguts amb els analitzadors de sobretaula i es mostren per a la comparació amb els resultats obtinguts amb el microarray. Com es pot observar, no es van poder obtenir dades per a la cTnI ja que la detectabilitat no era suficient. Per tant, les dades que es mostren d'aquest analit corresponen només a les dades proporcionades

per l'IGTP. Contràriament, els analitzadors de sobretaula no van proporcionar dades d'H-FABP ni de Cys C.

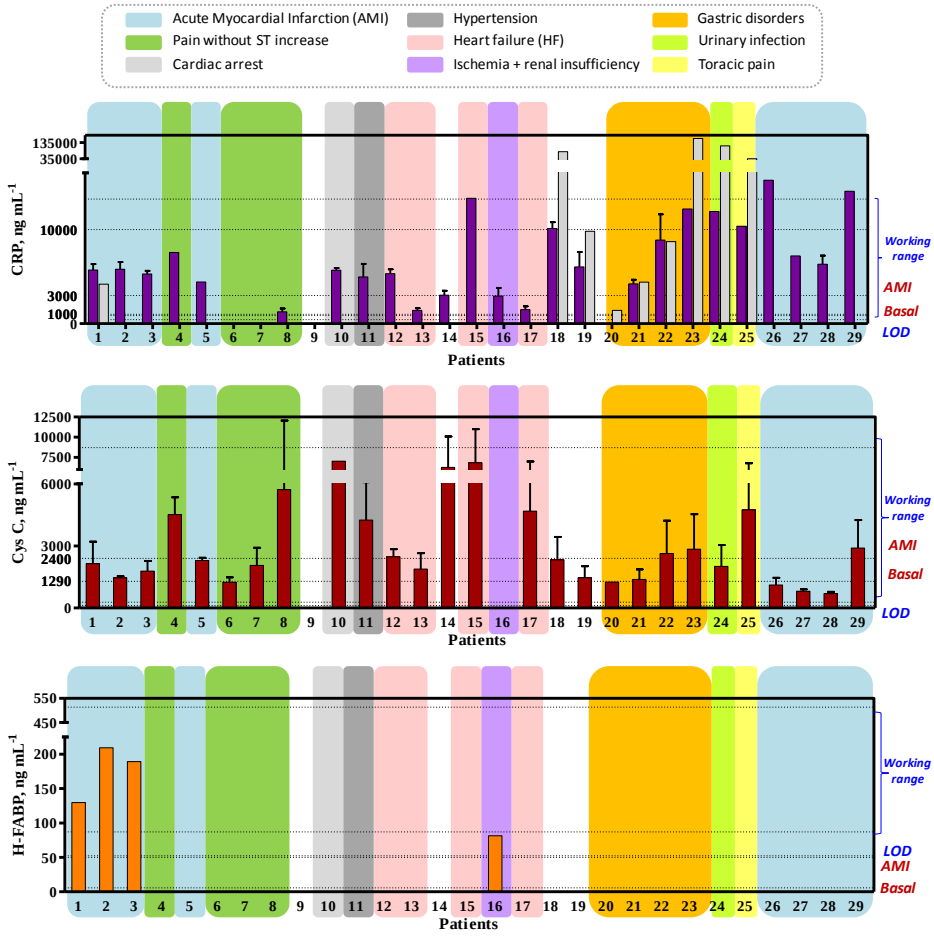

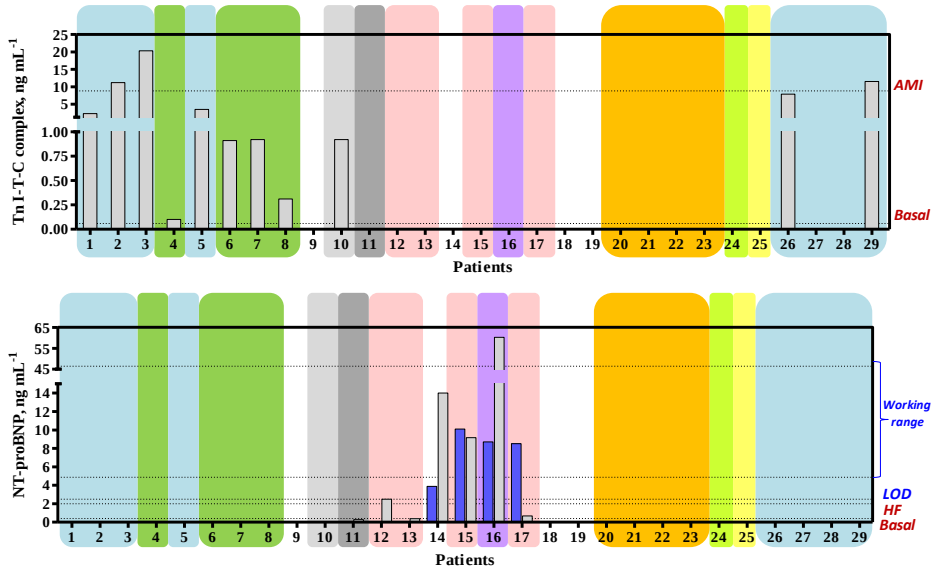

Figura 10.7. Estudis preliminars amb mostres clíniques reals realitzats en les dues plataformes multiplexades desenvolupades en aquesta tesi. Les barres grises corresponen als anàlisi realitzats per l'IGTP. Per la troponina, no es va poder detectar cap mostra amb el microarray. Per a la CRP, els pacients 6, 7, 9 i 20 no es van detectar perquè eren inferiors al límit de detecció. Per la Cys C, els pacients 9 i 16 no es van detectar perquè estaven per sobre del rang de treball. Per la H-FABP, el complex de troponina I-T-C i l'NT-proBNP, les barres que no es mostren corresponen a pacients amb nivells per sota del límit de detecció que no van poder ser detectats. Pel pacients 9 no es van detectar biomarcadors cardiovasculars.

En general, podríem dir que el microarray va ser capaç de donar molta més informació i té major capacitat per analitzar un major nombre de mostres que els analitzadors de sobretaula. Per tant, totes les 29 mostres es van mesurar pels cinc biomarcadors en un període curt de temps, mentre que amb els analitzadors de sobretaula cada mostra es va analitzar només per a uns determinats biomarcadors. Per exemple, no hi ha dades de H-FABP ni de Cys C per cap d'aquests pacients i els nivells de CRP es van trobar elevats en molts més pacients que els analitzats amb els equips de sobretaula. Un altre aspecte important a considerar és que totes les mostres que van donar positives amb el microarray, també van ser positives amb els analitzadors i en la majoria dels casos es va observar un perfil de resposta semblant. Per tant, per exemple, per la CRP hi ha un acord entre les dues tècniques per a les mostres amb els nivells més alts i més baixos. De la mateixa manera passa per l'NT-proBNP, encara que la detectabilitat d'aquest biomarcador era qüestionable durant el desenvolupament. Com es pot observar en el gràfic, els resultats van ser

negatius per a totes les mostres, excepte per a aquelles que es van mesurar i van donar positives amb l'analitzador. Només la mostra 12 va donar una resposta positiva amb el Radiometer AQT 90 FLEX però el microarray no va ser capaç de detectar-ho. D'altra banda, la mostra 17 es va veure clarament positiva amb el microarray, però la resposta va ser molt baixa amb l'analitzador de sobretaula.

Pel que fa a la interpretació clínica d'aquests resultats, en els casos en els que es va diagnosticar infart agut de miocardi (IAM) o mort cardíaca, la H-FABP i l'NT-proBNP es van poder detectar respectivament. A més a més, i en referència a l'assaig per a CRP, els pacients diagnosticats de IAM tots estaven en risc elevat ([CRP] >3000 ng mL^{-1}) de patir trastorns cardíacs i dos d'ells estaven en risc molt elevat ([CRP] > 10.000 ng mL^{-1}). També els pacients diagnosticats de mort cardíaca estaven en zona de risc elevat i molt elevat. Tant les concentracions de CRP com de Cys C eren molt baixes per als pacients sans i la Cys C va presentar una alta especificitat pels trastorns renals també relacionats amb les malalties cardiovasculars, al mateix temps. En resum, l'eina de diagnòstic desenvolupada en aquesta tesi, tot i tenir algunes limitacions en alguns aspectes, podria servir com a eina semi-quantitativa per a una estratificació del risc del pacient precisa i un tractament adequat.

10.3.5 IMMUNOSENSORS PER A LA DETECCIÓ DE CRP I NT-PROBNP

L'objectiu final d'aquesta investigació va ser la implementació del microarray fluorescent multiplexat en un biosensor òptic basat en l'ona evanescent i en el principi d'anisotropia de la fluorescència per tal d'obtenir un dispositiu POC per a MCV. Aquest va ser un objectiu ambiciós a llarg termini, però com a prova de concepte es va decidir avaluar el rendiment d'aquest sensor amb almenys dos dels biomarcadors seleccionats (CRP i NT-proBNP). La realització d'aquesta investigació va ser possible gràcies a la col·laboració establerta amb Chemical and Biochemical sensor group (IFAC, CNR) en una estada pre-doctoral de tres mesos al seu laboratori.

Així doncs, es van poden realitzar les corbes de calibració en tampó tant per la CRP com per l'NT-proBNP, assolint LOD de 16.56 ng mL^{-1} i 93 ng mL^{-1}, respectivament. En comparació amb l'ELISA i el microarray individual i

multiplexat, per l'NT-proBNP, els resultats assolits amb aquest sensor òptic van ser considerablement pitjors pel que fa a la sensibilitat i la variabilitat. No obstant això, aquests resultats poden millorar-se optimitzant els diferents paràmetres de l'assaig i les capacitats d'amplificació del sensor.

10.4 CONCLUSIONS

- En el transcurs d'aquesta tesi s'han estudiat en detall i s'han escollit els epítops òptims per a la conseqüent producció d'anticossos policlonals de conill per a cTnI i NT-proBNP, dos dels biomarcadors més cardio-específics i rellevants pel diagnòstic de malalties cardiovasculars. Amb aquests anticossos, s'ha desenvolupat, per un costat, un ELISA sandvitx per a la detecció de cTnI i, per l'altre, un ELISA competitiu per a la detecció de NT-proBNP, tots dos en format de microplaca.

- S'ha observat que la cTnI te una extraordinària tendència a adsorbir-se de forma inespecífica a superfícies i també a altres biomolècules. Aquest fet, juntament amb la impossibilitat d'assolir la detectabilitat necessària per aquest biomarcador, han estat els principals problemes que hem hagut d'abordar. Pel que fa a l'adsorció inespecífica s'han avaluat diferents additius en el tampó de la mostra o analit veient-se que la caseïna al 0.15% en PBST combinat amb l'ús de microplaques de baixa adsorció (Immulon^{TM} 2HB) ajuda considerablement a solucionar aquest problema. Tot i això, la sensibilitat obtinguda per aquest assaig en tampó aquós és molt inferior a la requerida corresponent als nivells basals d'aquest analit a la sang.

- En el desenvolupament de l'ELISA per NT-proBNP, després d'estudiar diferents paràmetres relacionats amb l'heterologia i altres paràmetres físico-químics, s'ha aconseguit assolir el límit de detecció necessari obtenint una bona exactitud amb mostres de plasma fortificades amb l'analit en qüestió.

- Ha estat possible desenvolupar un microarray multiplexat per a la detecció de 5 biomarcardors (cTnI, NT-proBNP, molt rellevants en el procés de desenvolupament de malalties cardiovasculars, CRP, Cys C i H-FABP). Un cop biofuncionalitzat el microarray mitjançant una codificació espaial amb els corresponents bioconjugats o anticossos de captura, la resta d'immunoreactius i biomarcadors poden ser utilitzats en forma de còctel sense que en cap cas s'hagin observat fenòmens de cooperativitat (unió dels immunoreactius en solució a llocs del microarray a on es troben immobilitzats altres biomarcadors) ni de reactivitat creuada (reconeixement de biomarcadors diferents d'aquells pels quals s'han desenvolupat els immunoreactius). Tant sols els immunoreactius de Lp(a) van produir aquestes interferències i per aquest motiu es van descartar.

- S'ha posat en evidència que el fet de que els diferents biomarcadors estiguin presents a diferents rangs de concentració segueix sent un dels principals reptes del diagnòstic multiplexat quan aquestes mesures es volen fer de forma simultània. En aquest treball de recerca va ser impossible quantificar la CRP i Cys C en el mateix microarray que la H-FABP, cTnI i NT-proBNP de mostres directes. Afortunadament, el fet d'utilitzar superfícies de vidre en les quals es podien imprimir fins a 24 microarrays ha permès poder fer aquestes mesures de forma simultània i paral·lela.

- Amb el microarray multiplexat ha estat possible mesurar mostres de pacients amb diferents patologies. El resultats obtinguts mostren que l'eficiència d'aquest microarray és molt superior a la dels analitzadors actualment emprats als laboratoris clínics, tant pel que fa a la capacitat de mesurar múltiples biomarcadors en un nombre elevat de mostres en poc temps, com pel que referència a la coherència dels resultats obtinguts. Així doncs, el microarray desenvolupat en aquesta tesi doctoral ha estat capaç de mesurar tots els biomarcadors de les mostres tots els malalts, metre que amb els analitzadors, degut al cost que suposa (econòmic i de temps) tant sols s'han analitzat alguns d'ells en cada cas, depenent de la patologia. El microarray ha estat doncs capaç de detectar nivells alts de CRP en mostres de malalts no

analitzades al laboratori clínic. Addicionalment, els resultats obtinguts amb el microarray són coherents amb els obtinguts amb els analitzadors per aquells casos en els que s'havien fet mesures, i també amb la patologia que havia estat diagnosticada. Els resultats han estat satisfactoris inclús pel cas de l'NT-proBNP, pel qual la detectabilitat no havia arribat al valor basal tot i que era molt propera. Malauradament, no va ser possible mesurar els nivells de cTnI amb aquest microarray, tal com era de preveure d'acord amb els estudis previs fets amb els immunoreactius utilitzats. Així doncs, podem considerar aquest microarray com un mètode semi-quantitatiu multiplexat útil per a la millora del diagnòstic de malalties cardiovasculars per a pacients que es troben en les diferents fases de la malaltia.

- Finalment, s'han realitzat estudis preliminars per implementar el sistema immunoquímic multiplexat en un sensor òptic fluorescent d'ona evanescent amb l'objectiu d'aconseguir un dispositiu POC (point-of-care) i facilitar el diagnòstic de malalties cardiovasculars apte per a ser utilitzat fora de recintes hospitalaris i adaptats a usuaris no especialitzats. Malauradament, els resultats obtingut apunten a que és necessari fer un major esforç per a incrementar la detectabilitat d'aquest sistema, donat que els valors de LOD assolits són pitjors que els aconseguits amb l'ELISA o el microarray i, per casos com l'NT-proBNP, es troben molt allunyats dels valors basals.

El problema principal en aquesta tesi ha estat assolir els límits de detecció necessaris per alguns biomarcadors. Encara que tant en la literatura com en el mercat hi ha assajos que ho han aconseguit, aquest fet rau principalment en el mètode d'adquisició de la senyal així com en la sensibilitat intrínseca de l'instrument destinat a dur-ho a terme.

11 BIBLIOGRAPHY

1. http://www.who.int/mediacentre/factsheets/fs317/en/.
2. Mendis, S., P. Puska, and B. Norrving, *Global Atlas on cardiovascular disease prevention and control*. 2011, Geneva: World Health Organization.
3. Mathers, C.D. and D. Loncar, *Projections of global mortality and burden of disease from 2002 to 2030.* Plos Medicine, 2006. 3(11).
4. Mendis, S., et al., *Global status report on noncommunicable diseases 2014*. 2014, Geneva: World Health Organization.
5. Friess, U. and M. Stark, *Cardiac markers: a clear cause for point-of-care testing.* Analytical and Bioanalytical Chemistry, 2009. 393(5): p. 1453-1462.
6. McDonnell, B., et al., *Cardiac biomarkers and the case for point-of-care testing.* Clinical Biochemistry, 2009. 42(7-8): p. 549-561.
7. Yalow, R.S. and S.A. Berson, *Assay of Plasma Insulin in Human Subjects by Immunological Methods.* Nature, 1959. 184(4699): p. 1648-1649.
8. Marco, M.P., S. Gee, and B.D. Hammock, *IMMUNOCHEMICAL TECHNIQUES FOR ENVIRONMENTAL-ANALYSIS .2. ANTIBODY-PRODUCTION AND IMMUNOASSAY DEVELOPMENT.* Trac-Trends in Analytical Chemistry, 1995. 14(8): p. 415-425.
9. Kohler, G. and C. Milstein, *Continuous cultures of fused cells secreting antibody of predefined specificity.* Nature, 1975. 256(5517): p. 495-497.
10. Winter, G., et al., *MAKING ANTIBODIES BY PHAGE DISPLAY TECHNOLOGY.* Annual Review of Immunology, 1994. 12: p. 433-455.
11. Marco, M.P. and D. Barcelo, *Environmental applications of analytical biosensors.* Measurement Science & Technology, 1996. 7(11): p. 1547-1562.
12. Rinken, T. and H. Riik, *Determination of antibiotic residues and their interaction in milk with lactate biosensor.* Journal of Biochemical and Biophysical Methods, 2006. 66(1-3): p. 13-21.
13. Ricardo Romero, M., et al., *Amperometric Biosensor for Direct Blood Lactate Detection.* Analytical Chemistry, 2010. 82(13): p. 5568-5572.
14. Shao, C.Y., et al., *Novel cyanobacterial biosensor for detection of herbicides.* Applied and Environmental Microbiology, 2002. 68(10): p. 5026-5033.
15. Qureshi, A., Y. Gurbuz, and J.H. Niazi, *Biosensors for cardiac biomarkers detection: A review.* Sensors and Actuators B-Chemical, 2012. 171: p. 62-76.
16. Sharma, H. and R. Mutharasan, *Review of biosensors for foodborne pathogens and toxins.* Sensors and Actuators B-Chemical, 2013. 183: p. 535-549.
17. Pedrero, M., S. Campuzano, and J.M. Pingarron, *Electrochemical Biosensors for the Determination of Cardiovascular Markers: a Review.* Electroanalysis, 2014. 26(6): p. 1132-1153.
18. Verma, N. and A. Bhardwaj, *Biosensor Technology for Pesticides-A review.* Applied Biochemistry and Biotechnology, 2015. 175(6): p. 3093-3119.
19. Kilcullen, N., et al., *Heart-type fatty acid-binding protein predicts long-term mortality after acute coronary syndrome and identifies high-risk patients across the range of troponin values.* Journal of the American College of Cardiology, 2007. 50(21): p. 2061-2067.
20. Montorsi, P., M. Villa, and M.A. Dessanai, *Temporal profile of protein release in myocardial infarction.* Heart and metabolism, 2009. 43: p. 31-35.

21. Christenson, R.H., *Biomarkers of acute coronary syndromes and heart failureI*. 2007 Washington: The American Association for Clinical Chemistry.
22. Myers, G.L., et al., *National Academy of Clinical Biochemistry Laboratory Medicine Practice Guidelines: Emerging Biomarkers for Primary Prevention of Cardiovascular Disease.* Clinical Chemistry, 2009. 55(2): p. 378-384.
23. Dickstein, K., et al., *ESC Guidelines for the diagnosis and treatment of acute and chronic heart failure 2008.* European Heart Journal, 2008. 29(19): p. 2388-2442.
24. Yancy, C.W., et al., *2013 ACCF/AHA Guideline for the Management of Heart Failure: Executive Summary A Report of the American College of Cardiology Foundation/American Heart Association Task Force on Practice Guidelines.* Circulation, 2013. 128(16): p. 1810-1852.
25. Jaffe, A.S. and J. Ordonez-Llanos, *High Sensitivity Troponin in Chest Pain and Acute Coronary Syndromes. A Step Forward?* Revista Espanola De Cardiologia, 2010. 63(7): p. 763-769.
26. Jaffe, A.S., L. Babuin, and F.S. Apple, *Biomarkers in acute cardiac disease - The present and the future.* Journal of the American College of Cardiology, 2006. 48(1): p. 1-11.
27. Lopez Haldon, J., et al., *Value of NT-ProBNP Level and Echocardiographic Parameters in ST-Segment Elevation Myocardial Infarction Treated by Primary Angioplasty: Relationships Between These Variables and Their Usefulness as Predictors of Ventricular Remodeling.* Revista Espanola De Cardiologia, 2010. 63(9): p. 1019-1027.
28. Carreiro-Lewandowski, E., *Update on Cardiac Biomarkers.* Lab Medicine, 2006. 37(10): p. 597-605.
29. Tello-Montoliu, A., et al., *A multimarker risk stratification approach to non-ST elevation acute coronary syndrome: implications of troponin T, CRP, NT pro-BNP and fibrin D-dimer levels.* Journal of Internal Medicine, 2007. 262(6): p. 651-658.
30. Cameron, S.J., et al., *A multi-marker approach for the prediction of adverse events in patients with acute coronary syndromes.* Clinica Chimica Acta, 2007. 376(1-2): p. 168-173.
31. James, S.K., et al., *N-terminal pro-brain natriuretic peptide and other risk markers for the separate prediction of mortality and subsequent myocardial infarction in patients with unstable coronary artery disease - A Global Utilization of Strategies to Open occluded arteries (GUSTO)-IV substudy.* Circulation, 2003. 108(3): p. 275-281.
32. Sabatine, M.S., et al., *Multimarker approach to risk stratification in non-ST elevation acute coronary syndromes - Simultaneous assessment of troponin I, C-reactive protein, and B-type natriuretic peptide.* Circulation, 2002. 105(15): p. 1760-1763.
33. Zethelius, B., et al., *Use of multiple biomarkers to improve the prediction of death from cardiovascular causes.* New England Journal of Medicine, 2008. 358(20): p. 2107-2116.
34. Chan, D. and L.L. Ng, *Biomarkers in acute myocardial infarction.* Bmc Medicine, 2010. 8.

35. Shlipak, M.G., et al., *Cystatin-C and mortality in elderly persons with heart failure.* Journal of the American College of Cardiology, 2005. 45(2): p. 268-271.
36. Sarnak, M.J., et al., *Cystatin C Concentration as a Risk Factor for Heart Failure in Older Adults.* Annals of Internal Medicine, 2005. 142(7): p. 497-505.
37. Jernberg, T., et al., *Cystatin C - A novel predictor of outcome in suspected or confirmed non-ST-elevation acute coronary syndrome.* Circulation, 2004. 110(16): p. 2342-2348.
38. Xie, P.-Y., et al., *A ONE-STEP IMMUNOTEST FOR RAPID DETECTION OF HEART-TYPE FATTY ACID-BINDING PROTEIN IN PATIENTS WITH ACUTE CORONARY SYNDROMES.* Journal of Immunoassay & Immunochemistry, 2010. 31(1): p. 24-32.
39. Xu, Q., et al., *Cardiac multi-marker strategy for effective diagnosis of acute myocardial infarction.* Clinica Chimica Acta, 2010. 411(21-22): p. 1781-1787.
40. Dellas, C., et al., *Elevated Heart-Type Fatty Acid-Binding Protein Levels on Admission Predict an Adverse Outcome in Normotensive Patients With Acute Pulmonary Embolism.* Journal of the American College of Cardiology, 2010. 55(19): p. 2150-2157.
41. Pepys, M.B. and M.L. Baltz, *ACUTE PHASE PROTEINS WITH SPECIAL REFERENCE TO C-REACTIVE PROTEIN AND RELATED PROTEINS (PENTAXINS) AND SERUM AMYLOID A-PROTEIN.* Advances in Immunology, 1983. 34: p. 141-212.
42. Thompson, D., M.B. Pepys, and S.P. Wood, *The physiological structure of human C-reactive protein and its complex with phosphocholine.* Structure with Folding & Design, 1999. 7(2): p. 169-177.
43. Black, S., I. Kushner, and D. Samols, *C-reactive Protein.* Journal of Biological Chemistry, 2004. 279(47): p. 48487-48490.
44. Ridker, P.M., *Clinical application of C-reactive protein for cardiovascular disease detection and prevention.* Circulation, 2003. 107(3): p. 363-369.
45. Lequin, R.M., *Enzyme Immunoassay (EIA)/Enzyme-Linked Immunosorbent Assay (ELISA).* Clinical Chemistry, 2005. 51(12): p. 2415-2418.
46. Shlipak, M.G., et al., *Cystatin C and the Risk of Death and Cardiovascular Events among Elderly Persons.* New England Journal of Medicine, 2005. 352(20): p. 2049-2060.
47. Dominiczak, M.H. and M.J. Caslake, *Apolipoproteins: metabolic role and clinical biochemistry applications.* Annals of Clinical Biochemistry, 2011. 48: p. 498-515.
48. Nordestgaard, B.G., et al., *Lipoprotein(a) as a cardiovascular risk factor: current status.* European Heart Journal, 2010. 31(23): p. 2844-U14.
49. McCormick, S.P.A., *Lipoprotein(a): biology and clinical importance.* The Clinical biochemist. Reviews / Australian Association of Clinical Biochemists, 2004. 25(1): p. 69-80.
50. Marcovina, S.M., et al., *EFFECT OF THE NUMBER OF APOLIPOPROTEIN(A) KRINGLE-4 DOMAINS ON IMMUNOCHEMICAL MEASUREMENTS OF LIPOPROTEIN(A).* Clinical Chemistry, 1995. 41(2): p. 246-255.
51. Labugger, R., et al., *Extensive troponin I and T modification detected in serum from patients with acute myocardial infarction - Response.* Circulation, 2001. 104(5): p. E26-E27.

52. Marston, S.B. and C.S. Redwood, *Modulation of thin filament activation by breakdown or isoform switching of thin filament proteins - Physiological and pathological implications.* Circulation Research, 2003. 93(12): p. 1170-1178.
53. Sarko, J. and C.V. Pollack, *Cardiac troponins.* Journal of Emergency Medicine, 2002. 23(1): p. 57-65.
54. Katrukha, A.G., et al., *Troponin I is released in bloodstream of patients with acute myocardial infarction not in free form but as complex.* Clinical Chemistry, 1997. 43(8): p. 1379-1385.
55. Gomes, A.V., J.D. Potter, and D. Szczesna-Cordary, *The role of troponins in muscle contraction.* Iubmb Life, 2002. 54(6): p. 323-333.
56. Reiffert, S.U., et al., *Stepwise subunit interaction changes by mono- and bisphosphorylation of cardiac troponin I.* Biochemistry, 1998. 37(39): p. 13516-13525.
57. Katrukha, A.G., et al., *Degradation of cardiac troponin I: implication for reliable immunodetection.* Clinical Chemistry, 1998. 44(12): p. 2433-2440.
58. Wu, A.H.B., et al., *Characterization of cardiac troponin subunit release into serum after acute myocardial infarction and comparison of assays for troponin T and I.* Clinical Chemistry, 1998. 44(6): p. 1198-1208.
59. Vittorini, S., et al., *Cardiac natriuretic hormones: methodological aspects.* Immuno-Analyse & Biologie Specialisee, 2007. 22(4): p. 236-246.
60. Zois, N.E., et al., *Natriuretic peptides in cardiometabolic regulation and disease.* Nature Reviews Cardiology, 2014. 11(7): p. 403-412.
61. Schellenberger, U., et al., *The precursor to B-type natriuretic peptide is an O-linked glycoprotein.* Archives of Biochemistry and Biophysics, 2006. 451(2): p. 160-166.
62. Seferian, K.R., et al., *The brain natriuretic peptide (BNP) precursor is the major immunoreactive form of BNP in patients with heart failure.* Clinical Chemistry, 2007. 53(5): p. 866-873.
63. Seferian, K.R., et al., *Immunodetection of glycosylated NT-proBNP circulating in human blood.* Clinical Chemistry, 2008. 54(5): p. 866-873.
64. Semenov, A.G., et al., *Processing of Pro-Brain Natriuretic Peptide Is Suppressed by O-Glycosylation in the Region Close to the Cleavage Site.* Clinical Chemistry, 2009. 55(3): p. 489-498.
65. Tonne, J.M., et al., *Secretion of Glycosylated Pro-B-Type Natriuretic Peptide from Normal Cardiomyocytes.* Clinical Chemistry, 2011. 57(6): p. 864-873.
66. Weber, M. and C. Hamm, *Role of B-type natriuretic peptide (BNP) and NT-proBNP in clinical routine.* Heart, 2006. 92(6): p. 843-849.
67. Alpert, J.S., et al., *Myocardial infarction redefined - A consensus Document of the Joint European Society of Cardiology/American College of Cardiology Committee for the Redefinition of Myocardial Infarction.* Journal of the American College of Cardiology, 2000. 36(3): p. 959-969.
68. Apple, F.S., A.H.B. Wu, and A.S. Jaffe, *European Society of Cardiology and American College of Cardiology guidelines for redefinition of myocardial infarction: How to use existing assays clinically and for clinical trials.* American Heart Journal, 2002. 144(6): p. 981-986.

69. Thygesen, K., et al., *Universal Definition of Myocardial Infarction.* Circulation, 2007. 116(22): p. 2634-2653.
70. Braunwald, E., et al., *ACC/AHA 2002 guideline update for the management of patients with unstable angina and non-ST-Segment elevation myocardial infarction - Summary article - A report of the American College of Cardiology/American Heart Association Task Force on Practice Guidelines (Committee on the Management of Patients with Unstable Angina).* Journal of the American College of Cardiology, 2002. 40(7): p. 1366-1374.
71. Morrow, D.A., et al., *National Academy of Clinical Biochemistry Laboratory Medicine Practice Guidelines: Clinical characteristics and utilization of biochemical markers in acute coronary syndromes.* Clinical Chemistry, 2007. 53(4): p. 552-574.
72. Apple, F.S., et al., *National Academy of Clinical Biochemistry and IFCC Committee for Standardization of Markers of Cardiac Damage Laboratory Medicine Practice Guidelines: Analytical issues for biochemical markers of acute coronary syndromes.* Clinical Chemistry, 2007. 53(4): p. 547-551.
73. Apple, F.S., et al., *National Academy of Clinical Biochemistry and IFCC committee for standardization of markers of cardiac damage laboratory medicine practice guidelines: Analytical issues for biomarkers of heart failure.* Clinical Biochemistry, 2008. 41(4-5): p. 222-226.
74. Filatov, V.L., et al., *Troponin: Structure, properties, and mechanism of functioning.* Biochemistry-Moscow, 1999. 64(9): p. 969-985.
75. Li, M.X., X. Wang, and B.D. Sykes, *Structural based insights into the role of troponin in cardiac muscle pathophysiology.* Journal of Muscle Research and Cell Motility, 2004. 25(7): p. 559-579.
76. Ferrieres, G., et al., *Human cardiac troponin I: precise identification of antigenic epitopes and prediction of secondary structure.* Clinical Chemistry, 1998. 44(3): p. 487-493.
77. Morjana, N. and R. Tal, *Expression and equilibrium denaturation of cardiac troponin I: stabilization of a folding intermediate during denaturation by urea.* Biotechnology and Applied Biochemistry, 1998. 28(1): p. 7-17.
78. Eriksson, S., et al., *Negative interference in cardiac troponin I immunoassays from a frequently occurring serum and plasma component.* Clinical Chemistry, 2003. 49(7): p. 1095-1104.
79. Eriksson, S., et al., *Negative interference in cardiac troponin I immunoassays by circulating troponin autoantibodies.* Clinical Chemistry, 2005. 51(5): p. 839-847.
80. Hyytia, H., et al., *A comparison of capture antibody fragments in cardiac troponin I immunoassay.* Clinical Biochemistry, 2013. 46(12): p. 963-968.
81. Le Moal, E., et al., *Earlier detection of myocardial infarction by an improved cardiac TnI assay.* Clinical Biochemistry, 2007. 40(13-14): p. 1065-1073.
82. Bodor, G.S., et al., *Development of monoclonal antibodies for an assay of cardiac troponin-I and preliminary results in suspected cases of myocardial infarction.* Clinical Chemistry, 1992. 38(11): p. 2203-14.

83. Penttil, et al., *Comparison of the troponin T and troponin I ELISA tests, as measured by microplate immunoassay techniques, in diagnosing acute myocardial infarction*. 1997, Berlin, ALLEMAGNE: De Gruyter. A 125-A 160.
84. Filatov, V.L., et al., *Epitope mapping of anti-troponin I monoclonal antibodies.* Biochemistry and Molecular Biology International, 1998. 45(6): p. 1179-1187.
85. Larue, C., et al., *CARDIAC-SPECIFIC IMMUNOENZYMOMETRIC ASSAY OF TROPONIN-I IN THE EARLY PHASE OF ACUTE MYOCARDIAL-INFARCTION.* Clinical Chemistry, 1993. 39(6): p. 972-979.
86. Adams, J.E., et al., *CARDIAC TROPONIN-I - A MARKER WITH HIGH SPECIFICITY FOR CARDIAC INJURY.* Circulation, 1993. 88(1): p. 101-106.
87. Christenson, R.H., et al., *Toward standardization of cardiac troponin I measurements part II: Assessing commutability of candidate reference materials and harmonization of cardiac troponin I assays.* Clinical Chemistry, 2006. 52(9): p. 1685-1692.
88. Tate, J.R., *Troponin revisited 2008: assay performance.* Clinical Chemistry and Laboratory Medicine, 2008. 46(11): p. 1489-1500.
89. Aakre, K.M., et al., *The quality of laboratory aspects of troponin testing in clinical practice guidelines and consensus documents needs to be improved.* Clinica Chimica Acta, 2014. 437: p. 58-61.
90. Andersson, P.O., et al., *Consequences of high-sensitivity troponin T testing applied in a primary care population with chest pain compared with a commercially available point-of-care troponin T analysis: an observational prospective study.* BMC research notes, 2015. 8: p. 210-210.
91. Asselman, V., et al., *Analytical Comparison of three Cardiac Troponin Point-of-Care Testing methods with a Central Laboratory Method.* Acta Clinica Belgica, 2014. 69: p. 6-6.
92. Bair, T.I., et al., *Myocardial Biomarker Testing With Troponin I: Are We Ordering Too Many Studies?* Circulation, 2013. 128(22).
93. Fraga, O.R., et al., *Cardiac Troponin Testing Is Overused after the Rule-In or Rule-Out of Myocardial Infarction.* Clinical Chemistry, 2015. 61(2): p. 436-438.
94. Reiter, M., et al., *Early diagnosis of acute myocardial infarction in patients with pre-existing coronary artery disease using more sensitive cardiac troponin assays.* European Heart Journal, 2012. 33(8): p. 988-997.
95. Reichlin, T., et al., *Early Diagnosis of Myocardial Infarction with Sensitive Cardiac Troponin Assays.* New England Journal of Medicine, 2009. 361(9): p. 858-867.
96. Rubini Gimenez, M., et al., *Rapid rule out of acute myocardial infarction using undetectable levels of high-sensitivity cardiac troponin.* International journal of cardiology, 2013. 168(4): p. 3896-901.
97. Jin, J.-P., *Troponin. Informative diagnostic marker*, ed. NOVA. 2014, New York.
98. Manson, M.M., *Immunochemical protocols*. Methods in Molecular Biology, ed. M.M. Manson. Vol. 10. 1992, Totawa: Humana.
99. Wild, D., *The immunoassay handbook*. Third edition ed, ed. D. Wild. 2005, Amsterdam: Elsevier Science.
100. Adrian, J., et al., *Preparation of Antibodies and Development of an Enzyme-Linked Immunosorbent Assay (ELISA) for the Determination of Doxycycline*

Antibiotic in Milk Samples. Journal of Agricultural and Food Chemistry, 2012. 60(15): p. 3837-3846.
101. Hermanson, G.T., *Bioconjugate techniques*. 2nd edition ed, ed. A. Press. 2008, London (etc.).
102. Cushley, W. and M.M. Harnett, *CELLULAR SIGNALING MECHANISMS IN B-LYMPHOCYTES.* Biochemical Journal, 1993. 292: p. 313-332.
103. Kim, D.-H., et al., *Performance characteristics of monoclonal antibodies as recyclable binders to cardiac troponin I.* Analytical Biochemistry, 2012. 431(1): p. 11-18.
104. http://www.vivo.colostate.edu/molkit/hydropathy/index.html.
105. http://tools.immuneepitope.org/tools/bcell/iedb_input.
106. https://npsa-prabi.ibcp.fr/cgi-bin/secpred_gor4.pl.
107. Lee, N., D.P. McAdam, and J.H. Skerritt, *Development of immunoassays for type II synthetic pyrethroids. 1. Hapten design and application to heterologous and homologous assays.* Journal of Agricultural and Food Chemistry, 1998. 46(2): p. 520-534.
108. Goodrow, M.H. and B.D. Hammock, *Hapten design for compound-selective antibodies: ELISAS for environmentally deleterious small molecules.* Analytica Chimica Acta, 1998. 376(1): p. 83-91.
109. Marco, M.P., B.D. Hammock, and M.J. Kurth, *HAPTEN DESIGN AND DEVELOPMENT OF AN ELISA (ENZYME-LINKED-IMMUNOSORBENT-ASSAY) FOR THE DETECTION OF THE MERCAPTURIC ACID CONJUGATES OF NAPHTHALENE.* Journal of Organic Chemistry, 1993. 58(26): p. 7548-7556.
110. Kramer, P.M., M.P. Marco, and B.D. Hammock, *DEVELOPMENT OF A SELECTIVE ENZYME-LINKED-IMMUNOSORBENT-ASSAY FOR 1-NAPHTHOL - THE MAJOR METABOLITE OF CARBARYL (1-NAPHTHYL N-METHYLCARBAMATE).* Journal of Agricultural and Food Chemistry, 1994. 42(4): p. 934-943.
111. Yancy, C.W., et al., *2013 ACCF/AHA Guideline for the Management of Heart Failure: A Report of the American College of Cardiology Foundation/American Heart Association Task Force on Practice Guidelines.* Circulation, 2013. 128(16): p. e240-e327.
112. Gruson, D., et al., *Value of proBNP(1-108) testing for the risk stratification of patients with systolic heart failure.* Peptides, 2013. 50: p. 125-128.
113. Yeo, K.-T.J., et al., *Multicenter evaluation of the Roche NT-proBNP assay and comparison to the Biosite Triage BNP assay.* Clinica Chimica Acta, 2003. 338(1â€“2): p. 107-115.
114. Jungbauer, C.G., et al., *Equal performance of novel N-terminal proBNP (Cardiac proBNP (R)) and established BNP (Triage BNP (R)) point-of-care tests.* Biomarkers in Medicine, 2012. 6(6): p. 789-796.
115. Liu, R., et al., *A fast and sensitive enzyme immunoassay for brain natriuretic peptide based on micro-magnetic probes strategy.* Talanta, 2010. 81(3): p. 1016-1021.
116. Giuliani, I., et al., *Assay for measurement of intact B-type natriuretic peptide prohormone in blood.* Clinical Chemistry, 2006. 52(6): p. 1054-1061.

117. Kakuta, M., et al., *Development of the microchip-based repeatable immunoassay system for clinical diagnosis.* Measurement Science & Technology, 2006. 17(12): p. 3189-3194.
118. Ala-Kopsala, M., et al., *Single assay for amino-terminal fragments of cardiac A- and B-type natriuretic peptides.* Clinical Chemistry, 2005. 51(4): p. 708-718.
119. Goetze, J.P., et al., *Quantification of pro-B-type natriuretic peptide and its products in human plasma by use of an analysis independent of precursor processing.* Clinical Chemistry, 2002. 48(7): p. 1035-1042.
120. Hunt, P.J., et al., *THE AMINO-TERMINAL PORTION OF PRO-BRAIN NATRIURETIC PEPTIDE (PRO-BNP) CIRCULATES IN HUMAN PLASMA.* Biochemical and Biophysical Research Communications, 1995. 214(3): p. 1175-1183.
121. Hunt, P.J., et al., *Immunoreactive amino-terminal pro-brain natriuretic peptide (NT-PROBNP): A new marker of cardiac impairment.* Clinical Endocrinology, 1997. 47(3): p. 287-296.
122. Hunt, P.J., et al., *The role of the circulation in processing pro-brain natriuretic peptide (proBNP) to amino-terminal BNP and BNP-32.* Peptides, 1997. 18(10): p. 1475-1481.
123. Campbell, D.J., et al., *Plasma amino-terminal pro-brain natriuretic peptide: A novel approach to the diagnosis of cardiac dysfunction.* Journal of Cardiac Failure, 2000. 6(2): p. 130-139.
124. Katrukha, A., et al., *ProBNP is a major form of BNP immunoreactivity in blood of patients with heart failure.* Clinical Chemistry, 2007. 53(6): p. A6-A6.
125. Tamm, N.N., et al., *Novel immunoassay for quantification of brain natriuretic peptide and its precursor in human blood.* Clinical Chemistry, 2008. 54(9): p. 1511-1518.
126. Liu, R., et al., *Combining Magnetic Beads and Chemiluminescence for Rapid Detection of Brain Natriuretic Peptide.* Sensor Letters, 2011. 9(2): p. 725-727.
127. Hughes, D., et al., *An immunoluminometric assay for N-terminal pro-brain natriuretic peptide: development of a test for left ventricular dysfunction.* Clin. Sci., 1999. 96(4): p. 373-380.
128. Nishikimi, T., et al., *Direct Immunochemiluminescent Assay for proBNP and Total BNP in Human Plasma proBNP and Total BNP Levels in Normal and Heart Failure.* Plos One, 2013. 8(1).
129. Wei, J.S., et al., *B-type natriuretic peptide as a biomarker for essential hypertension.* Clinical Chemistry, 2007. 53(6): p. A3-A3.
130. Clerico, A., et al., *Analytical performance and diagnostic accuracy of immunometric assays for the measurement of plasma B-type natriuretic peptide (BNP) and N-terminal proBNP.* Clinical Chemistry, 2005. 51(2): p. 445-447.
131. Prontera, C., et al., *Proficiency testing project for brain natriuretic peptide (BNP) and the N-terminal part of the propeptide of BNP (NT-proBNP) immunoassays: the CardioOrmocheck study*, in *Clinical Chemistry and Laboratory Medicine*. 2009. p. 762.
132. Lewis, L.K., et al., *Comparison of immunoassays for NTproBNP conducted on three analysis systems: Milliplex, Elecsys and RIA.* Clinical Biochemistry, 2013. 46(4-5): p. 388-390.

133. Gruson, D., et al., *Measurement of NT-proBNP with LOCI (R) technology in heart failure patients.* Clinical Biochemistry, 2012. 45(1-2): p. 171-174.
134. Kurihara, T., et al., *Evaluation of cardiac assays on a benchtop chemiluminescent enzyme immunoassay analyzer, PATHFAST.* Analytical Biochemistry, 2008. 375(1): p. 144-146.
135. Foo, J.Y.Y., et al., *NT-ProBNP Levels in Saliva and Its Clinical Relevance to Heart Failure.* Plos One, 2012. 7(10).
136. Di Serio, F., et al., *Analytical evaluation of the Dade Behring Dimension RxL automated N-Terminal proBNP (NT-proBNP) method and comparison with the Roche Elecsys 2010*, in *Clinical Chemical Laboratory Medicine*. 2005. p. 1263.
137. Hickey, G., et al., *Development of a monoclonal antibody based immunoassay for NT-proBNP on the dade behring stratus (R) CS acute care (TM) diagnostic system.* Clinical Chemistry, 2007. 53(6): p. A2-A3.
138. Ullman, E.F., et al., *Luminescent oxygen channeling immunoassay: measurement of particle binding kinetics by chemiluminescence.* Proceedings of the National Academy of Sciences, 1994. 91(12): p. 5426-5430.
139. Kelley, W.E., et al., *Cardiovascular disease testing on the Dimension Vista (R) system: Biomarkers of acute coronary syndromes.* Clinical Biochemistry, 2009. 42(13-14): p. 1444-1451.
140. Beaudet, L., et al., *AlphaLISA immunoassays: the no-wash alternative to ELISAs for research and drug discovery.* Nature Methods, 2008. 5.
141. Obata, K., et al., *Development of a novel method for operating magnetic particles, magtration technology, and its use for automating nucleic acid purification.* Journal of Bioscience and Bioengineering, 2001. 91(5): p. 500-503.
142. Hammerer-Lercher, A., et al., *Clinical value of a competitive NT-proBNP enzyme immunoassay compared to the Roche NT-proBNP platform*, in *Clinical Chemistry and Laboratory Medicine*. 2009. p. 1305.
143. Apple, F.S., et al., *Quality specifications for B-type natriuretic peptide assays.* Clinical Chemistry, 2005. 51(3): p. 486-493.
144. Prontera, C., et al., *Analytical performance and diagnostic accuracy of a fully-automated electrochemiluminescent assay for the N-terminal fragment of the pro-peptide of brain natriuretic peptide in patients with cardiomyopathy: comparison with immunoradiometric assay methods for brain natriuretic peptide and atrial natriuretic peptide*, in *Clinical Chemistry and Laboratory Medicine*. 2004. p. 37.
145. Chien, T.-I., H.-h. Chen, and J.-T. Kao, *Comparison of Abbott AxSYM and Roche Elecsys 2010 for measurement of BNP and NT-proBNP.* Clinica Chimica Acta, 2006. 369(1): p. 95-99.
146. Franzini, M., et al., *Systematic differences between BNP immunoassays: Comparison of methods using standard protocols and quality control materials.* Clinica Chimica Acta, 2013. 424: p. 287-291.
147. Bingisser, R., et al., *Measurement of natriuretic peptides at the point of care in the emergency and ambulatory setting: Current status and future perspectives.* American Heart Journal, 2013. 166(4): p. 614-+.
148. Ng, L.L., et al., *Diagnosis of heart failure using urinary natriuretic peptides.* Clinical Science, 2004. 106(2): p. 129-133.

149. Cortés, R., et al., *Variability of NT-proBNP plasma and urine levels in patients with stable heart failure: a 2-year follow-up study.* Heart, 2007. 93(8): p. 957-962.
150. Ng, L.L., et al., *Community screening for left ventricular systolic dysfunction using plasma and urinary natriuretic peptides.* Journal of the American College of Cardiology, 2005. 45(7): p. 1043-1050.
151. Song, J., et al., *The clinical significance of a urinary B-type natriuretic peptide assay for the diagnosis of heart failure.* Clinica Chimica Acta, 2011. 412(17-18): p. 1632-1636.
152. Michielsen, E.C.H.J., et al., *The diagnostic value of serum and urinary NT-proBNP for heart failure.* Annals of Clinical Biochemistry, 2008. 45: p. 389-394.
153. Lipman, N.S., et al., *Monoclonal versus polyclonal antibodies: Distinguishing characteristics, applications, and information resources.* Ilar Journal, 2005. 46(3): p. 258-268.
154. Xiao, J. and T.J. Tolbert, *Synthesis of N-Terminally Linked Protein Dimers and Trimers by a Combined Native Chemical Ligation-CuAAC Click Chemistry Strategy.* Organic Letters, 2009. 11(18): p. 4144-4147.
155. Deshpand, S., *Enzyme Immunoassays from concept to product development*, ed. C. Hall. 1996, New York.
156. McKimmbreschkin, J.L., *THE USE OF TETRAMETHYLBENZIDINE FOR SOLID-PHASE IMMUNOASSAYS.* Journal of Immunological Methods, 1990. 135(1-2): p. 277-280.
157. Oubiña, A., et al., *Chapter 7 Immunoassays for environmental analysis*, in *Techniques and Instrumentation in Analytical Chemistry*. 2000, Elsevier. p. 287-339.
158. Shu, J., et al., *Synthesis of furaltadone metabolite, 3-amino-5-morpholinomethyl-2-oxazolidone (AMOZ) and novel haptens for the development of a sensitive enzyme-linked immunosorbent assay (ELISA).* Analytical Methods, 2014. 6(7): p. 2306-2313.
159. Nichkova, M., R. Galve, and M.P. Marco, *Biological monitoring of 2,4,5-trichlorophenol (I): Preparation of antibodies and development of an immunoassay using theoretical models.* Chemical Research in Toxicology, 2002. 15(11): p. 1360-1370.
160. Galve, R., et al., *Development and evaluation of an immunoassay for biological monitoring chlorophenols in urine as potential indicators of occupational exposure.* Analytical Chemistry, 2002. 74(2): p. 468-478.
161. Pinacho, D.G., F. Sanchez-Baeza, and M.P. Marco, *Molecular Modeling Assisted Hapten Design To Produce Broad Selectivity Antibodies for Fluoroquinolone Antibiotics.* Analytical Chemistry, 2012. 84(10): p. 4527-4534.
162. Ballesteros, B., et al., *Influence of the Hapten Design on the Development of a Competitive ELISA for the Determination of the Antifouling Agent Irgarol 1051 at Trace Levels.* Analytical Chemistry, 1998. 70(19): p. 4004-4014.
163. Harrison, R.O., M.H. Goodrow, and B.D. Hammock, *COMPETITIVE-INHIBITION ELISA FOR THE S-TRIAZINE HERBICIDES - ASSAY OPTIMIZATION AND ANTIBODY CHARACTERIZATION.* Journal of Agricultural and Food Chemistry, 1991. 39(1): p. 122-128.

164. Abad, A., M.J. Moreno, and A. Montoya, *Hapten synthesis and production of monoclonal antibodies to the N-methylcarbamate pesticide methiocarb.* Journal of Agricultural and Food Chemistry, 1998. 46(6): p. 2417-2426.
165. Galve, R., et al., *Indirect competitive immunoassay for trichlorophenol determination - Rational evaluation of the competitor heterology effect.* Analytica Chimica Acta, 2002. 452(2): p. 191-206.
166. Lee, N.J., J.H. Skerritt, and D.P. McAdam, *HAPTEN SYNTHESIS AND DEVELOPMENT OF ELISAS FOR DETECTION OF ENDOSULFAN IN WATER AND SOIL.* Journal of Agricultural and Food Chemistry, 1995. 43(6): p. 1730-1739.
167. Sanvicens, N., B. Varela, and M.P. Marco, *Immunochemical determination of 2,4,6-trichloroanisole as the responsible agent for the musty odor in foods. 2. Immunoassay evaluation.* Journal of Agricultural and Food Chemistry, 2003. 51(14): p. 3932-3939.
168. Zeravik, J., et al., *Development of direct ELISA for the determination of 4-nonylphenol and octylphenol.* Analytical Chemistry, 2004. 76(4): p. 1021-1027.
169. Manclus, J.J. and A. Montoya, *Development of enzyme-linked immunosorbent assays for the insecticide chlorpyrifos .2. Assay optimization and application to environmental waters.* Journal of Agricultural and Food Chemistry, 1996. 44(12): p. 4063-4070.
170. Abad, A. and A. Montoya, *Development of an enzyme-linked immunosorbent assay to carbaryl .2. Assay optimization and application to the analysis of water samples.* Journal of Agricultural and Food Chemistry, 1997. 45(4): p. 1495-1501.
171. Sanvicens, N., et al., *Preparation of antibodies and development of an enzyme-linked Immunosorbent assay for determination of dealkylated hydroxytriazines.* Journal of Agricultural and Food Chemistry, 2003. 51(1): p. 156-164.
172. Putnam, F.W., *The plasma proteins*. 2nd edition ed, ed. A. Press. Vol. Volume IV. 1984, London.
173. Patton, K.T., G.A. Thibodeau, and M.M. Douglas, *Essentials of Anatomy and Physiology*. 2011: Elsevier.
174. Ekins, R., F. Chu, and E. Biggart, *DEVELOPMENT OF MICROSPOT MULTI-ANALYTE RATIOMETRIC IMMUNOASSAY USING DUAL FLUORESCENT-LABELED ANTIBODIES.* Analytica Chimica Acta, 1989. 227(1): p. 73-96.
175. Ekins, R.P. and F.W. Chu, *MULTIANALYTE MICROSPOT IMMUNOASSAY - MICROANALYTICAL COMPACT-DISK OF THE FUTURE.* Clinical Chemistry, 1991. 37(11): p. 1955-1967.
176. Pease, A.C., et al., *LIGHT-GENERATED OLIGONUCLEOTIDE ARRAYS FOR RAPID DNA-SEQUENCE ANALYSIS.* Proceedings of the National Academy of Sciences of the United States of America, 1994. 91(11): p. 5022-5026.
177. Schena, M., et al., *QUANTITATIVE MONITORING OF GENE-EXPRESSION PATTERNS WITH A COMPLEMENTARY-DNA MICROARRAY.* Science, 1995. 270(5235): p. 467-470.
178. Hartmann, M., et al., *Protein microarrays for diagnostic assays.* Analytical and Bioanalytical Chemistry, 2009. 393(5): p. 1407-1416.
179. Angenendt, P., *Progress in protein and antibody microarray technology.* Drug Discovery Today, 2005. 10(7): p. 503-511.

180. Jonkheijm, P., et al., *Chemical Strategies for Generating Protein Biochips.* Angewandte Chemie-International Edition, 2008. 47(50): p. 9618-9647.
181. Sassolas, A., B.D. Leca-Bouvier, and L.J. Blum, *DNA biosensors and microarrays.* Chemical Reviews, 2008. 108(1): p. 109-139.
182. Wittmann, C., *Immobilisation of DNA on CHIPS II*, in *Immobilisation of DNA on CHIPS II*. 2005.
183. Sobek, J., et al., *Microarray technology as a universal tool for high-throughput analysis of biological systems.* Combinatorial Chemistry & High Throughput Screening, 2006. 9(5): p. 365-380.
184. Arenkov, P., et al., *Protein microchips: Use for immunoassay and enzymatic reactions.* Analytical Biochemistry, 2000. 278(2): p. 123-131.
185. Rubina, A.Y., et al., *Hydrogel-based protein microchips: Manufacturing, properties, and applications.* Biotechniques, 2003. 34(5): p. 1008-+.
186. Afanassiev, V., V. Hanemann, and S. Woelfl, *Preparation of DNA and protein micro arrays on glass slides coated with an agarose film.* Nucleic Acids Research, 2000. 28(12).
187. Kersten, B., et al., *Protein microarray technology and ultraviolet crosslinking combined with mass spectrometry for the analysis of protein-DNA interactions.* Analytical Biochemistry, 2004. 331(2): p. 303-313.
188. Angenendt, P., et al., *Toward optimized antibody microarrays: a comparison of current microarray support materials.* Analytical Biochemistry, 2002. 309(2): p. 253-260.
189. Angenendt, P., et al., *Next generation of protein microarray support materials: Evaluation for protein and antibody microarray applications.* Journal of Chromatography A, 2003. 1009(1-2): p. 97-104.
190. Kusnezow, W., et al., *Antibody microarrays: An evaluation of production parameters.* Proteomics, 2003. 3(3): p. 254-264.
191. Wu, P. and D.W. Grainger, *Comparison of hydroxylated print additives on antibody microarray performance.* Journal of Proteome Research, 2006. 5(11): p. 2956-2965.
192. Leung, W.M., et al., *Novel "digital-style" rapid test simultaneously detecting heart attack and predicting cardiovascular disease risk.* Analytical Letters, 2005. 38(3): p. 423-439.
193. Park, J., et al., *Lab-on-a-Disc for Fully Integrated Multiplex Immunoassays.* Analytical Chemistry, 2012. 84(5): p. 2133-2140.
194. Marquette, C.A., et al., *Disposable screen-printed chemiluminescent biochips for the simultaneous determination of four point-of-care relevant proteins.* Analytical and Bioanalytical Chemistry, 2009. 393(4): p. 1191-1198.
195. Angelidis, C., et al., *Cystatin C: An Emerging Biomarker in Cardiovascular Disease.* Current Topics in Medicinal Chemistry, 2013. 13(2): p. 164-179.
196. Christenson, R.H. and H.M.E. Azzazy, *Cardiac point of care testing: A focused review of current National Academy of Clinical Biochemistry guidelines and measurement platforms.* Clinical Biochemistry, 2009. 42(3): p. 150-157.
197. Luppa, P.B., et al., *Point-of-care testing (POCT): Current techniques and future perspectives.* Trac-Trends in Analytical Chemistry, 2011. 30(6): p. 887-898.

198. McBride, J.D. and M.A. Cooper, *A high sensitivity assay for the inflammatory marker C-reactive protein employing acoustic biosensing.* Journal of Nanobiotechnology, 2008. 6: p. 5-Article No.: 5.
199. Lee, W., et al., *A centrifugally actuated point-of-care testing system for the surface acoustic wave immunosensing of cardiac troponin I.* Analyst, 2013. 138(9): p. 2558-2566.
200. Esteban-Fernandez de Avila, B., et al., *Disposable Electrochemical Magnetoimmunosensor for the Determination of Troponin T Cardiac Marker.* Electroanalysis, 2013. 25(1): p. 51-58.
201. Esteban-Fernandez de Avila, B., et al., *Disposable amperometric magnetoimmunosensor for the sensitive detection of the cardiac biomarker amino-terminal pro-B-type natriuretic peptide in human serum.* Analytica Chimica Acta, 2013. 784: p. 18-24.
202. Plowman, T.E., et al., *Multiple-analyte fluoroimmunoassay using an integrated optical waveguide sensor.* Analytical Chemistry, 1999. 71(19): p. 4344-4352.
203. Masson, J.-F., et al., *Quantitative measurement of cardiac markers in undiluted serum.* Analytical Chemistry, 2007. 79(2): p. 612-619.
204. Lu, W., et al., *Multiplex Detection of B-Type Natriuretic Peptide, Cardiac Troponin I and C-Reactive Protein with Photonic Suspension Array.* Plos One, 2012. 7(7).
205. Hong, B. and K.A. Kang, *Biocompatible, nanogold-particle fluorescence enhancer for fluorophore mediated, optical immunosensor.* Biosensors & Bioelectronics, 2006. 21(7): p. 1333-1338.
206. Teramura, Y., Y. Arima, and H. Iwata, *Surface plasmon resonance-based highly sensitive immunosensing for brain natriuretic peptide using nanobeads for signal amplification.* Analytical Biochemistry, 2006. 357(2): p. 208-215.
207. Borisenko, V., et al., *Diffractive optics technology: A novel detection technology for immunoassays.* Clinical Chemistry, 2006. 52(11): p. 2168-2170.
208. Kurita, R., et al., *On-chip enzyme immunoassay of a cardiac marker using a microfluidic device combined with a portable surface plasmon resonance system.* Analytical Chemistry, 2006. 78(15): p. 5525-5531.
209. Zhuo, Y., et al., *Ultrasensitive electrochemical strategy for NT-proBNP detection with gold nanochains and horseradish peroxidase complex amplification.* Biosensors and Bioelectronics, 2011. 26(5): p. 2188-2193.
210. Yi, W., et al., *Application of a Fab fragment of monoclonal antibody specific to N-terminal pro-brain natriuretic peptide for the detection based on regeneration-free electrochemical immunosensor.* Biotechnology Letters, 2011. 33(8): p. 1539-43.
211. Liang, W., et al., *A novel microfluidic immunoassay system based on electrochemical immunosensors: An application for the detection of NT-proBNP in whole blood.* Biosensors and Bioelectronics, 2012. 31(1): p. 480-485.
212. Mao, L., et al., *Signal-enhancer molecules encapsulated liposome as a valuable sensing and amplification platform combining the aptasensor for ultrasensitive ECL immunoassay.* Biosensors and Bioelectronics, 2011. 26(10): p. 4204-4208.
213. Maeng, B.H., et al., *Functional expression of recombinant anti-BNP scFv in methylotrophic yeast Pichia pastoris and application as a recognition molecule*

in electrochemical sensors. World Journal of Microbiology and Biotechnology, 2012. 28(3): p. 1027-34.
214. Matsuura, H., et al., *Electrochemical enzyme immunoassay of a peptide hormone at picomolar levels.* Analytical Chemistry, 2005. 77(13): p. 4235-4240.
215. Pieper-Furst, U., et al., *Detection of subicomolar concentrations of human matrix metalloproteinase-2 by an optical biosensor.* Analytical Biochemistry, 2004. 332(1): p. 160-167.
216. Hu, W.P., et al., *Immunodetection of pentamer and modified C-reactive protein using surface plasmon resonance biosensing.* Biosensors & Bioelectronics, 2006. 21(8): p. 1631-1637.
217. Meyer, M.H.F., M. Hartmann, and M. Keusgen, *SPR-based immunosensor for the CRP detection - A new method to detect a well known protein.* Biosensors & Bioelectronics, 2006. 21(10): p. 1987-1990.
218. Vikholm-Lundin, I. and W.M. Albers, *Site-directed immobilisation of antibody fragments for detection of C-reactive protein.* Biosensors & Bioelectronics, 2006. 21(7): p. 1141-1148.
219. Kim, H.-C., et al., *Detection of C-reactive protein on a functional poly(thiophene) self-assembled monolayer using surface plasmon resonance.* Ultramicroscopy, 2008. 108(10): p. 1379-1383.
220. Jose, J., M. Park, and J.-C. Pyun, *E-coli outer membrane with autodisplayed Z-domain as a molecular recognition layer of SPR biosensor.* Biosensors & Bioelectronics, 2010. 25(5): p. 1225-1228.
221. Dutra, R.F. and L.T. Kubota, *An SPR immunosensor for human cardiac troponin T using specific binding avidin to biotin at carboxymethyldextran-modified gold chip.* Clinica Chimica Acta, 2007. 376(1-2): p. 114-120.
222. Dutra, R.F., et al., *Surface plasmon resonance immunosensor for human cardiac troponin T based on self-assembled monolayer.* Journal of Pharmaceutical and Biomedical Analysis, 2007. 43(5): p. 1744-1750.
223. Liu, J.T., et al., *Surface plasmon resonance biosensor with high anti-fouling ability for the detection of cardiac marker troponin T.* Analytica Chimica Acta, 2011. 703(1): p. 80-86.
224. Kwon, Y.-C., et al., *Development of a surface plasmon resonance-based immunosensor for the rapid detection of cardiac troponin I.* Biotechnology Letters, 2011. 33(5): p. 921-927.
225. McDonnell, B., et al., *A high-affinity recombinant antibody permits rapid and sensitive direct detection of myeloperoxidase.* Analytical Biochemistry, 2011. 410(1): p. 1-6.
226. Hoa, X.D., A.G. Kirk, and M. Tabrizian, *Enhanced SPR response from patterned immobilization of surface bioreceptors on nano-gratings.* Biosensors & Bioelectronics, 2009. 24(10): p. 3043-3048.
227. Kunz, U., et al., *Sensing fatty acid binding protein with planar and fiber-optical surface plasmon resonance spectroscopy devices.* Sensors and Actuators B-Chemical, 1996. 32(2): p. 149-155.
228. Baldini, F., et al., *An optical PMMA biochip based on fluorescence anisotropy: Application to C-reactive protein assay.* Sensors and Actuators B-Chemical, 2009. 139(1): p. 64-68.

229. Albrecht, C., N. Kaeppel, and G. Gauglitz, *Two immunoassay formats for fully automated CRP detection in human serum.* Analytical and Bioanalytical Chemistry, 2008. 391(5): p. 1845-1852.
230. Luchansky, M.S., et al., *Sensitive on-chip detection of a protein biomarker in human serum and plasma over an extended dynamic range using silicon photonic microring resonators and sub-micron beads.* Lab on a Chip, 2011. 11(12): p. 2042-2044.
231. Kroeger, D., et al., *Surface investigations on the development of a direct optical immunosensor.* Biosensors and Bioelectronics, 1998. 13(10): p. 1141-1147.
232. Dittmer, W.U., et al., *Rapid, high sensitivity, point-of-care test for cardiac troponin based on optomagnetic biosensor.* Clinica Chimica Acta, 2010. 411(11-12): p. 868-873.
233. Bruls, D.M., et al., *Rapid integrated biosensor for multiplexed immunoassays based on actuated magnetic nanoparticles.* Lab on a Chip, 2009. 9(24): p. 3504-3510.
234. Bleher, O., M. Ehni, and G. Gauglitz, *Label-free quantification of cystatin C as an improved marker for renal failure.* Analytical and Bioanalytical Chemistry, 2012. 402(1): p. 349-356.
235. Lin, C.-H., et al., *Quantitative measurement of binding kinetics in sandwich assay using a fluorescence detection fiber-optic biosensor.* Analytical Biochemistry, 2009. 385(2): p. 224-228.
236. Kapoor, R. and C.-W. Wang, *Highly specific detection of interleukin-6 (IL-6) protein using combination tapered fiber-optic biosensor dip-probe.* Biosensors & Bioelectronics, 2009. 24(8): p. 2696-2701.
237. Polerecki, L., J. Hamrle, and B.D. MacCraith, *Theory of the radiation of dipoles placed within a multilayer system.* Applied Optics, 2000. 39(22): p. 3968-3977.
238. Blue, R., et al., *Platform for enhanced detection efficiency in luminescence-based sensors.* Electronic letters, 2005. 41(12).
239. Piruska, A., et al., *The autofluorescence of plastic materials and chips measured under laser irradiation.* Lab on a Chip, 2005. 5(12): p. 1348-1354.

12 ACRONYMS, ABBREVIATIONS AND TABLES

12.1 ACRONYMS AND ABBREVIATIONS

aa	Amino Acid
AACC	American Association for Clinical Chemistry
Ab	Antibody
Abs	Absorbance
ACC	Academy of Clinical Biochemistry
ACN	Acetonitrile
ACS	Acute Coronary Syndrome
ADP	Adenosine DiPhosphate
AE	Acridinium Ester
Ag	Antigen
AHA	American Heart Association
ALPHA	Amplified Luminescence Proximity Homogenous Assays
AMI	Acute Myocardial Infarction
ANP	Atrial Natriuretic Peptide
AP	Alkaline Phosphatase
Apo(a)	Apolipoprotein (a)
ApoB	Apolipoprotein B
APS	Ammounium PerSulfate
As	Antiserum
ATP	Adenosine TriPhosphate
AuNP	Gold nanoparticle
BA	Bulk Acoustic
BDB	Bis-Diazotized Benzidine
BNP	Brain Natriuretic Peptide
BP	Band Pass filter
BR	BioReceptor
BSA	Bovine Serum Albumin
BST	Banc de Sang i Teixits
BTA	Bench-Top Analyzer
cGMP	Cyclic Guanosine MonoPhosphate
CK	Creatine Kinase
CKD	Chronic Kidney Disease
CK-MB	Creatine Kinase MB isoenzyme
CLEIA	ChemiLuminescent Enzyme ImmunoAssay

CLIA	ChemiLuminescent ImmunoAssay
CM	Carboxymethyl
CNP	C-type Natriuretic Peptide
CNR	National Research Council of Italy
COPD	Chronic Obstructive Pulmonary Disease
CRP	C-Reactive Protein
CSIC	Spanish Council for Scientific Research
cTn	Cardiac Troponin
cTnI	Cardiac Troponin I
cTnT	Cardiac Troponin T
CV	Coefficient of Variation
CVD	CardioVascular Diseases
Cys C	Cystatin C
Da	Dalton
DCC	N-dicyclohexylcarbodiimide
DDS	Dimethyldichlorosilane
DEAE	Diethylaminoethanol
DMF	N-dimethylformamide
DMP	Dimethyl pimelimidate
DNA	DeoxyriboNucleic Acid
DSP	Dithio-bis-SuccinimidylPropionate
ECG	ElectroCardioGram
ECL	ElectroChemiLuminescence
ECLIA	ElectroChemiLuminescent Assay
ED	Emergency Departments
EDC	1-Ethyl-3-(3-dimethylaminopropyl)carbodiimide
EDC-HCl	1-Ethyl-3-(3-dimethylaminopropyl)carbodiimide hydrochloride
EDTA	EthyleneDiamineTetraacetic Acid
EIA	Enzyme ImmunoAssay
ELFA	Enzyme-Linked Fluorescent ImmunoAssay
ELISA	Enzyme-Linked ImmunoSorbent Assay
ENIAC	European Nanoelectronics Initiative Advisory Council
ESC	European Society of Cardiology
Fab	Antibody binding fraction
Fc	Fragment crystallisable
FIA	FluoroImmunoAssay

FITC	Fluorescein isothiocyanate
Fv	Fragment variable
GFR	Glomerular Filtration Rate
GLUT	Glutaraldehyde
GPTMS	(3-Glycidyloxypropyl)trimethoxysilane
HCH	Horseshoe Crab Hemocyanin
HCl	HydroChloride
HF	Heart Failure
H-FABP	Heart Fatty Acid Binding Protein
HP	High Pass filter
HPLC	High Performance Liquid Chromatography
HRP	HorseRadish Peroxidise
hs	High-sensitivity
hs- cTnI	High-sensitivity assay for Cardiac Troponin I
HTS	High-Throughput Screening
IA	ImmunoAssay
IC10	Concentration in which the signal is 90 % inhibited
IC20	Concentration in which the signal is 80 % inhibited
IC50	Concentration in which the signal is 50 % inhibited
IC80	Concentration in which the signal is 20 % inhibited
IC90	Concentration in which the signal is 10 % inhibited
ICAM	Intracellular Cell Adhesion Molecules
IFAC-CNR	The “Nello Carrara” Institute of Applied Physics - National Research Council of Italy
IFCC	International Federation of Clinical Chemistry
IgE	Immunoglobulin E
IgG	Immunoglobulin G
IGTP	Institut d’investigació Germans Trias i Pujol
IL-6	InterLeukin-6
IMA	Ischemia-Modified Albumin
IOW	Integrated Optical Waveguide
IQAC	Institute of Advanced Chemistry of Catalonia
IRE	Internal Reflection Element
IRMA	ImmunoRadioMetric Assay
ITC	Troponin complex which consists of three different subunits: TnT, TnI and TnC
IUPAC	International Union of Pure and Applied Chemistry

IVD	In Vitro Diagnostic
KDa	KiloDalton
LD	Laser Diode
LDL	Low-Density Lipoprotein
LFIC	Lateral Flow ImmunoChromatography
LOCI	Luminescent Oxygen Channeling Immunoassay
LOD	Limit Of Detection
LOQ	Limit Of Quantification
Lp(a)	Lipoprotein (a)
LV	Left-Ventricular
MAb	Monoclonal Antibody
MALDI-TOF-MS	Matrix Assisted Laser Desorption Ionization - Time of Flight Mass Spectrometry
MBS	m-maleimidobenzoyl-N-hydroxysuccinimide ester
MEA	β-mercaptoethylamine
MEIA	Microparticle Enzyme ImmunoAssay
MHA	Mercaptohexadecanoic acid
MI	Myocardial Infarction
MIA	Magnetic ImmunoAssay
MMP-2/-9	Matrix MetalloProteinases 2 and 9
MP	MicroParticles
MPO	MyeloPerOxidase
mRNA	Messenger RiboNucleic Acid
MW	Molecular Weight
MYO	Myoglobin
NACB	National Academy of Clinical Biochemistry
Nb4D	Nanobiotechnology for Diagnostics Group
NCD	NonCommunicable Diseases
NHS	N-HydroxySuccinimide
NHS-MHA	N-hydroxysuccinimide-activated 16-mercaptohexadecanoic acid
NOSA	Nanoscale Optofluidic Sensor Array
NPR	Natriuretic Peptide Receptor
NSTEACS	Non-ST segment Elevation Acute Coronary Syndromes
NT-proANP	N-terminal Pro-Atrial Natriuretic Peptide
NT-proBNP	N-terminal Pro-Brain Natriuretic Peptide
OD	Optical Density

OEG	oligo(ethylene glycol)
OVA	Ovalbumin
P3SET	poly(3-(2-((N-succinimidyl)succinyloxy)ethyl)thiophene
PAb	Polyclonal Antibody
PAPP-A	Pregnancy-Associated Plasma Protein A
PBS	Phosphate Buffered Saline solution
PBST	Phosphate Buffered Saline Tween-20 solution
PBT	Standard PBST with the absence of salts
PC	PolyCarbonate
PCR	Polymerase Chain Reaction
PCV	poly(vinyl chloride)
PDMS	Polydimethylsiloxane
PEG	PolyEthylene Glycol
PEG-SH	thiolated poly(ethylene)glycol
PKA	Protein Kinase A
PKC	Protein Kinase C
PlGF	Placental Growth Factor
PMMA	Poly(methyl methacrylate)
POC	Point-Of-Care
POCT	Point-Of-Care Tests
proANP	Pro-Atrial Natriuretic Peptide
proBNP	Pro-Brain Natriuretic Peptide
PS	Polystyrene beads
PVA	PolyVinyl Alcohol
PVP	PolyVinylPyrrolidone
QCM	Quartz Crystal Microbalances
RAAS	Rennin-Angiotensin-Aldosterone System
RAb	Recombinant Antibody
RBD	Red Blood Cells
RFU	Relative Fluorescence Units
RIA	RadioImmunoAssay
RT	Room Temperature
SAF	Supercritical Angle Fluorescence
SAM	Self-Assembled Monolayer
SAW	Surface Acoustic Wave
SC	Substrate-Confined
SCCB	Silica Colloidal Crystal Bead

sCD40L	Soluble CD40 Ligand
SD	Standard Deviation
SDS	Sodium Dodecyl Sulphate
SDS-PAGE	Sodium Dodecyl Sulphate PolyAcrylamide Gel Electrophoresis
SIA	Succinimidyl IodoAcetate
SMCC	Succinimidyl-4-(N-maleimidomethyl) cyclohexane-1-carboxylate
SMP	N- Succinimidyl 3-maleimidopropionate
SP	Screen Printed
SPR	Surface Plasmon Resonance
SRM	Standard Reference Material
STEMI	ST segment Elevation Myocardial Infarction
TAT	TurnAround Time
TEMED	Tetramethylethylenediamine
TIMP	Tissue Inhibitor MMPs
TIRF	Total Internal Reflection Fluorescence
TMB	3,3',5,5'-TetraMethylBenzidine
Tn	Troponin
TnC	Troponin C
TNFα	Tumor Necrosis Factor α
TnT	Troponin T
TRF	Time-Resolved Fluorescence
Tris	2-amino-2-hydroxymethyl-propane-1,3-diol
TRITC	Tetramethylrhodamine
UA	Unstable Angina
uFFA	Unbound Free Fatty Acids
UQC	Unitat de Química Combinatòria
VCAM	Vascular Cell Adhesion Molecules
WHF	World Health Federation
WHO	World Health Organization

Amino acid codes

A	Ala	Alanine	M	Met	Methionine
C	Cys	Cysteine	N	Asn	Asparagine
D	Asp	Aspartic acid	P	Pro	Proline
E	Glu	Glutamic acid	R	Arg	Arginine
F	Phe	Phenylalanine	Q	Gln	Glutamine
G	Gly	Glycine	S	Ser	Serine
H	His	Histidine	T	Thr	Threonine
I	Ile	Isoleucine	V	Val	Valine
K	Lys	Lysine	W	Trp	Tryptophan
L	Leu	Leucine	Y	Tyr	Tyrosine

12.2 TABLE OF FIGURES

12.3 TABLE OF TABLES